APPLICATION OF PLANT SECONDARY METABOLITES TO PAIN NEUROMODULATION, VOLUME II, 2nd Edition

EDITED BY: Adriana Gibara Guimarães, Rajeev K. Singla and Gokhan Zengin

PUBLISHED IN: Frontiers in Pharmacology and Frontiers in Neuroscience

frontiers Research Topics

ISSN 1664-8714
ISBN 978-2-8325-5661-0
DOI 10.3389/978-2-8325-5661-0

About Frontiers

Frontiers is more than just an open-access publisher of scholarly articles: it is a pioneering approach to the world of academia, radically improving the way scholarly research is managed. The grand vision of Frontiers is a world where all people have an equal opportunity to seek, share and generate knowledge. Frontiers provides immediate and permanent online open access to all its publications, but this alone is not enough to realize our grand goals.

Frontiers Journal Series

The Frontiers Journal Series is a multi-tier and interdisciplinary set of open-access, online journals, promising a paradigm shift from the current review, selection and dissemination processes in academic publishing. All Frontiers journals are driven by researchers for researchers; therefore, they constitute a service to the scholarly community. At the same time, the Frontiers Journal Series operates on a revolutionary invention, the tiered publishing system, initially addressing specific communities of scholars, and gradually climbing up to broader public understanding, thus serving the interests of the lay society, too.

Dedication to Quality

Each Frontiers article is a landmark of the highest quality, thanks to genuinely collaborative interactions between authors and review editors, who include some of the world's best academicians. Research must be certified by peers before entering a stream of knowledge that may eventually reach the public - and shape society; therefore, Frontiers only applies the most rigorous and unbiased reviews.
Frontiers revolutionizes research publishing by freely delivering the most outstanding research, evaluated with no bias from both the academic and social point of view. By applying the most advanced information technologies, Frontiers is catapulting scholarly publishing into a new generation.

What are Frontiers Research Topics?

Frontiers Research Topics are very popular trademarks of the Frontiers Journals Series: they are collections of at least ten articles, all centered on a particular subject. With their unique mix of varied contributions from Original Research to Review Articles, Frontiers Research Topics unify the most influential researchers, the latest key findings and historical advances in a hot research area! Find out more on how to host your own Frontiers Research Topic or contribute to one as an author by contacting the Frontiers Editorial Office: frontiersin.org/about/contact

APPLICATION OF PLANT SECONDARY METABOLITES TO PAIN NEUROMODULATION, VOLUME II, 2nd Edition

Topic Editors:
Adriana Gibara Guimarães, Federal University of Sergipe, Brazil
Rajeev K. Singla, Sichuan University, China
Gokhan Zengin, Selcuk University, Turkey

Publisher's note: This is a 2nd edition due to an article retraction.

Citation: Guimarães, A. G., Singla, R. K., Zengin, G., eds. (2024). Application of Plant Secondary Metabolites to Pain Neuromodulation, Volume II, 2nd Edition. Lausanne: Frontiers Media SA. doi: 10.3389/978-2-8325-5661-0

Table of Contents

04 ***Editorial: Application of Plant Secondary Metabolites to Pain Neuromodulation, Volume II***
Rajeev K. Singla, Adriana Gibara Guimarães and Gokhan Zengin

09 ***Metformin Attenuates Bone Cancer Pain by Reducing TRPV1 and ASIC3 Expression***
He-Ya Qian, Fang Zhou, Rui Wu, Xiao-Jun Cao, Tao Zhu, Hao-Dong Yuan, Ya-Nan Chen and Ping-An Zhang

17 ***Tannins in the Treatment of Diabetic Neuropathic Pain: Research Progress and Future Challenges***
Norsuhana Omar, Che Aishah Nazariah Ismail and Idris Long

26 ***Proanthocyanidins Inhibit the Transmission of Spinal Pain Information Through a Presynaptic Mechanism in a Mouse Inflammatory Pain Model***
Hongwei Fan, Zhenyu Wu, DaYu Zhu, Junxiang Gu, Mang Xu, Mingzhe Zhang, Haokai Duan, Yunqing Li and Tao Chen

40 ***Transformation of Stilbene Glucosides From* Reynoutria multiflora *During Processing***
Junqi Bai, Wanting Chen, Juan Huang, He Su, Danchun Zhang, Wen Xu, Jing Zhang, Zhihai Huang and Xiaohui Qiu

56 ***Natural Therapeutics in Aid of Treating Alzheimer's Disease: A Green Gateway Toward Ending Quest for Treating Neurological Disorders***
Basharat Ahmad Bhat, Abdullah Almilaibary, Rakeeb Ahmad Mir, Badr M. Aljarallah, Wajahat R. Mir, Fuzail Ahmad and Manzoor Ahmad Mir

79 ***Myrtenol Reduces Orofacial Nociception and Inflammation in Mice Through p38-MAPK and Cytokine Inhibition***
Janaíne P. Oliveira, Fabíula F. Abreu, José Marcos M. Bispo, Anderson R. A. Cerqueira, José Ronaldo dos Santos, Cristiane B. Correa, Soraia K. P. Costa and Enilton A. Camargo

87 ***Gingerol-Enriched Ginger Supplementation Mitigates Neuropathic Pain* via *Mitigating Intestinal Permeability and Neuroinflammation: Gut-Brain Connection***
Chwan-Li Shen, Rui Wang, Vadim Yakhnitsa, Julianna Maria Santos, Carina Watson, Takaki Kiritoshi, Guangchen Ji, Abdul Naji Hamood and Volker Neugebauer

97 ***Xiongshao Zhitong Recipe Attenuates Nitroglycerin-Induced Migraine-Like Behaviors* via *the Inhibition of Inflammation Mediated by Nitric Oxide Synthase***
Song Yang, Cong Chen, Xiaoyao Liu, Qianjun Kang, Quantao Ma, Pin Li, Yujie Hu, Jialin Li, Jian Gao, Ting Wang and Weiling Wang

116 ***Pristimerin, a Triterpene That Inhibits Monoacylglycerol Lipase Activity, Prevents the Development of Paclitaxel-Induced Allodynia in Mice***
Altaf Al-Romaiyan and Willias Masocha

frontiers | Frontiers in Pharmacology

TYPE Editorial
PUBLISHED 26 September 2022
DOI 10.3389/fphar.2022.1013063

OPEN ACCESS

EDITED AND REVIEWED BY
Nicholas M. Barnes,
University of Birmingham,
United Kingdom

*CORRESPONDENCE
Rajeev K. Singla,
rajeevsingla26@gmail.com
Adriana Gibara Guimarães,
adrianagibara@hotmail.com
Gokhan Zengin,
gokhanzengin@selcuk.edu.tr

SPECIALTY SECTION
This article was submitted to Neuropharmacology, a section of the journal Frontiers in Pharmacology

RECEIVED 06 August 2022
ACCEPTED 15 August 2022
PUBLISHED 26 September 2022

CITATION
Singla RK, Guimarães AG and Zengin G (2022), Editorial: Application of plant secondary metabolites to pain neuromodulation, volume II. *Front. Pharmacol.* 13:1013063. doi: 10.3389/fphar.2022.1013063

Editorial: Application of plant secondary metabolites to pain neuromodulation, volume II

Rajeev K. Singla[1,2]*, Adriana Gibara Guimarães[3]* and Gokhan Zengin[4]*

[1]Institutes for Systems Genetics, Frontiers Science Center for Disease-Related Molecular Network, West China Hospital, Sichuan University, Chengdu, China, [2]School of Pharmaceutical Sciences, Lovely Professional University, Phagwara, India, [3]Federal University of Sergipe, São Cristóvão, Brazil, [4]Selçuk University, Konya, Turkey

KEYWORDS

pain, nociception, natural products, secondary metabolites, phytochemicals, medicinal plants, polyphenol

Editorial on the Research Topic
Application of plant secondary metabolites to pain neuromodulation, volume II

Pain is an uncomfortable condition that is clinically associated with many diseases such as cancer/tumor, metabolic disorders such as diabetes, neurological diseases such as epilepsy and chronic infectious diseases, and functional disorders (Li et al., 2019; Yang, 2019; Singla et al., 2021a; Singla et al., 2021b). The neuromodulation approach has used electrical interfaces to modulate neuronal activity and has proven effective in treating various neurological disorders, including chronic pain (James et al., 2018). It has been adopted and accepted as an alternative techniques because of high attrition rates, costs as well as regulatory conditions in case of pharmacological agents (James et al., 2018). But in order to ascertain the aesthetic and appropriate usage of neurostimulation technique, organizations like "The International Neuromodulation Society (INS)" have framed the practice guidelines (Deer et al., 2014a; Deer et al., 2014b). Even for the cancer pain management, "The Indian Society for Study of Pain (ISSP)" have also prepared guidelines to cover palliative care aspects (Thota et al., 2020). As an alternative to both the synthetic pharmacological agents as well as neurostimulaory techniques, natural products have had a lot of translational potential to reach the bedside (Singla et al., 2021b; Dangar and Patel, 2021; Swarnkar et al., 2021; Rauf et al., 2022). Infact, nature has gifted us with lot of such type of molecules like capsaicin, resinferatoxin, morphine, lipoxin A4, cannabidiol, etc that have a strong potential in pain alleviation (Jin et al., 2020; Singla et al., 2020; Singla et al., 2021b). Nanotechnological approaches further augment the pharmacological properties of the therapeutic agents (Yetisgin et al., 2020; Annaso et al., 2022). Mishra and the team have discussed the clinical translational potential of gold nanoparticles as an effective neuromedicines (Mishra et al., 2022). This Research Topic was thus planned to

cover various aspects related to the plant metabolites for pain neuromodulation to gather further insights in this direction.

Bone cancer pain is unique in that it shares salient characteristics of neuropathic, nociceptive, and inflammatory pain (de Clauser et al., 2020). Metformin is a semi-synthetic analogue of the natural product present there in *Galega officinalis* L. (Hardie, 2022). Qian et al. in their research article entitled "Metformin Attenuates Bone Cancer Pain by Reducing TRPV1 and ASIC3 Expression" studied the effects of metformin in bone cancer pain model of rats and compared with the results of capsazepine, a "transient receptor potential cation channel subfamily V member 1 (TRPV1)" inhibitor and amiloride, an "Acid-sensitive ion channel 3 (ASIC3)" antagonist. They have observed that metformin has a capability to increase the paw withdraw threshold, as well as able to reduce TRPV1 expression in L4-6 dorsal root ganglions (DRG) and L4-6 spinal dorsal horn (SDH), while reducing expression of ASIC3 in L4-6 SDH. This suggested the potential of metformin in alleviating bone cancer pain.

Chinese herbal medicine like *Reynoutria multiflora* Thunb (*Polygonum multiflorum* Thunb.) is well known for multiple therapeutic properties like Cerebral Ischemic Reperfusion Injury (Huang P. et al., 2022), neurodegenerative diseases, and inflammation (Feng and Bounda, 2015). It is officially listed in Chinese Pharmacopoeeia and popularly known as "He shou wu" in China Mainland (Feng and Bounda, 2015; Li et al., 2017). Bai et al. in their research article entitled "Transformation of Stilbene Glucosides From Reynoutria multiflora During Processing" studied the transformation of stilbene glucosides and observed the changes bewteen raw from and the processed form. They have developed a simple and effective protocol using UHPLC-Q-Exactive plus orbitrap MS/MS. They have also observed that the number of transformed compounds are processing time dependent too.

Neuropathic pain and neuroinflammation are often linked with the nerve injuries like scientic nerve injury (Myers et al., 2006; Ellis and Bennett, 2013; Mahmoud et al.). Literature suggested that *Potamogeton perfoliatus* L. inhibiting 5-lipoxygenase and cyclooxygenase-2 enzymes, and thus possessing potential anti-inflammatory and analgesic properties (Rezq et al., 2021). Mahmoud et al. in their research article entitled "Potamogeton perfoliatus L. Extract Attenuates Neuroinflammation and Neuropathic Pain in Sciatic Nerve Chronic Constriction Injury-Induced Peripheral Neuropathy in Rats" has studied the hydroalcholic extract (whole plant) of *Potamogeton perfoliatus* L. on "sciatic nerve chronic constriction injury rat model". They have noticed that the extract was having multitargeted potential and targeting various enzymes/receptors as well as pathways while modulating and attenuating the neuroinflammation and neuropathic pain in the tested animals.

Proanthocyanidin extract was reported to have anti-hyperalgesic and anti-nociceptive potentials when tested in rat model with neuropathic pain (Kaur et al., 2016). El-Shitany and Eid further confirmed the protective effects of proanthocyanidin against cisplatin-induced liver damage through alleviation of inflammation and modulation of NF-κβ/TLR-4 pathway (El-Shitany and Eid, 2017). Fan et al. in their research article "Proanthocyanidins Inhibit the Transmission of Spinal Pain Information Through a Presynaptic Mechanism in a Mouse Inflammatory Pain Model" had found that proanthocyanidin has a potent inflammatory pain relieving ability when studied in mice with Complete Freund's Adjuvant injection. The possible mechanism for this effect is the modulation of PI3K/Akt/mTOR pathway in DRGs.

Diabetic patients are commonly facing complication like diabetic neuropathic pain (Xie et al., 2022). There are various mechnisms channeling diabetic neuropathic pain like WNT-mediated TRPV1 activation (Xie et al., 2022), "thioredoxin-interacting protein (TXNIP)-NOD-like receptor protein 3 (NLRP3)-N-methyl-D-aspartic acid receptor 2B (NR2B) pathway" (Wang J.-W. et al., 2022), $P2Y_{14}$ receptor (Wu et al., 2022), ASK1-MKK3-p38 pathway (Wang F. et al., 2022), NLRP3 (Zhang et al., 2022), P2X7R expression (Hu et al., 2022), along with many others. Omar et al. in their systematic review article entitled "Tannins in the Treatment of Diabetic Neuropathic Pain: Research Progress and Future Challenges" had systematically analyzed the research focused on the tannins for their alleviating effects on diabetic neuropathic symptoms. They concluded that the effects most probably is through the hypoglycaemic effect of these phytochemical tannins.

Alzheimer's disease (AD) is often associated as co-morbid with chronic pain (Cao et al., 2019). Bhat et al. in their review article entitled "Natural Therapeutics in Aid of Treating Alzheimer's Disease: A Green Gateway Toward Ending Quest for Treating Neurological Disorders" has analysed the literature encompassing natural products having anti-alzheimer's potential. In the article, they have discussed various pathologies associated with Alzheimer's disease like that related to cholinergic, tau protein, amyloid-β, neuroinflammation, and oxidative stress. They had further discussed various natural Anti-alzheimer's agents like ellagic acids as having anti-amyloidogenic property, punicalagin as β-secretase inhibitor, curcumin having tau hypophosphorylation effect, along with many other Anti-alzheimer's agents. They had covered literature for around 24 medicinal herbs and 22 phytochemicals having potential to manage Alzheimer's disease.

Orofacial pain primarily affects the head, face, and neck areas and is generally associated with inflammation (Romero-Reyes and Uyanik, 2014). Natural products, especially terpenes are effective in modulating orofacial nociception (Silva et al., 2016; Oliveira et al., 2020). Myrtenol in complex with β-cyclodextrin has been able to elicit anti-nociceptive behavior and cognitive enhancement in a chronic musculoskeletal pain model (Heimfarth et al., 2020). Oliveira et al. in their brief research

report article entitled "Myrtenol Reduces Orofacial Nociception and Inflammation in Mice Through p38-MAPK and Cytokine Inhibition" have evaluated the therapeutic potential of myrtenol in reducing orofacial pain and inflammation in formalin-induced pain model of male Swiss mice. They have further demonstrated possible mechanisms as modulation of IL-1β levels in the trigeminal pathway as well as p38-MAPK modulation in trigeminal ganglia.

Consuming of various forms of ginger (*Zingiber officinale* Roscoe) such as ginger extract, ginger essential oils, etc have tremendous antineuropathic effects including thermal and cold hyperalgesia (Shen et al., 2022a; Shen et al., 2022b). Shen et al. in their original research article entitled "Gingerol-Enriched Ginger Supplementation Mitigates Neuropathic Pain via Mitigating Intestinal Permeability and Neuroinflammation: Gut-Brain Connection" have presented a noteworthy role of gut-brain axis in mitigation of the neuropathic pain that were validated by the *in vivo* experiments on male rats.

Chinese herbs and the traditional Chinese medicines (TCM) are known for their role in modulating of pain and inflammation, and most of them are now experimentally validated (Chen and Zhang, 2014; Du et al., 2016). One such formulation is Xiongshao Zhitong Recipe (XZR, a combination of eight botanical drugs), which is traditionally being indicated for migraine, but mechanisms behind it were not clear (Yang et al., 2022). Keeping this in mind, Yang et al. in their original research article entitled "Xiongshao Zhitong Recipe Attenuates Nitroglycerin-Induced Migraine-Like Behaviors via the Inhibition of Inflammation Mediated by Nitric Oxide Synthase" have done the phytochemical characterization of this TCM using UHPLC-LTQ-Orbitrap MS assay, and validated the antimigraine activity of the aqueous extract obtained from XZR using their own developed rat model with nitroglycerin induced migraine. They have observed that the nitric oxide synthase suppression and NF-κB signaling pathway activation are the possible mechanisms behind the anti-inflammatory activity of XZR.

Previous studies validated the alleviating role of terpenes in neuropathic pain (Bortalanza et al., 2002; Borgonetti et al., 2020; Bilbrey et al., 2021). Earlier studies have indicated that pristimerin is having anti-inflammatory activity and possibly having it by modulation various pathways like NF-κB pathway (Huang D. et al., 2022), PI3K/Akt signalling (Xue et al., 2021), NLRP3 (Zhao et al., 2020), etc. Al-Romaiyan and Masocha in their original research article entitled "Pristimerin, a triterpene that inhibits monoacylglycerol lipase activity, prevents the development of paclitaxel-induced allodynia in mice" have observed that pristimerin is having potent and dose-dependent monoacylglycerol inhibitor when compared with JZL-195, betulinic acid, cucurbitacin B, and euphol. Upregulation of Nrf2 gene expression was also observed.

This Research Topic, thus covered 1 brief research report, 7 original research, 1 review, and 1 systematic review article. As on 4th August, 2022, there were cumulative 10,364 views of the 10 articles published in this Research Topic, with cumulative 2,185 downloads as per Frontiers record. We are highly thankful to all the authors for contributing their scholarly work in our Research Topic and we are indeed grateful to all the reviewers who had spared time from their tight schedule and supported us in processing of these manuscripts. This Research Topic is providing a good overview about the natural products having potential against various types of neuropathic pain and neuroinflammation like bone cancer pain, orofacial pain, diabetic neuropathic pain, spinal pain, etc. It is thus very important to do further translational studies to assess the clinical level application of these natural products.

Author contributions

RS, AG, and GZ have collectively conceived and wrote the text. All authors contributed to the article and approved the submitted version.

Conflict of interest

All authors declare that the research was conducted in the absence of any commercial or financial relationships that could be construed as a potential conflict of interest.

Publisher's note

References

Annaso, P., Dalvi, S., Dhaygude, V., and Shete, D., and , S. (2022). Formulation of silver nanoparticle of Cassia angustifoliaby using green synthesis method and screening for *in-vitro* anti-inflammatory activity. *Indo Glob. J. Pharm. Sci.* 12, 183–188. doi:10.35652/igjps.2022.12022

Bilbrey, J. A., Ortiz, Y. T., Felix, J. S., McMahon, L. R., and Wilkerson, J. L. (2021). Evaluation of the terpenes β-caryophyllene, α-terpineol, and γ-terpinene in the mouse chronic constriction injury model of neuropathic pain: Possible cannabinoid receptor involvement. *Psychopharmacology* 239 (5), 1475–1486. doi:10.1007/s00213-021-06031-2

Borgonetti, V., Governa, P., Biagi, M., Pellati, F., and Galeotti, N. (2020). Zingiber officinale Roscoe rhizome extract alleviates neuropathic pain by inhibiting neuroinflammation in mice. *Phytomedicine* 78, 153307. doi:10.1016/j.phymed.2020.153307

Bortalanza, L. B., Ferreira, J., Hess, S. C., Delle Monache, F., Yunes, R. A., and Calixto, J. B. (2002). Anti-allodynic action of the tormentic acid, a triterpene isolated from plant, against neuropathic and inflammatory persistent pain in mice. *Eur. J. Pharmacol.* 453 (2-3), 203–208. doi:10.1016/s0014-2999(02)02428-7

Cao, S., Fisher, D. W., Yu, T., and Dong, H. (2019). The link between chronic pain and Alzheimer's disease. *J. Neuroinflammation* 16 (1), 204. doi:10.1186/s12974-019-1608-z

Chen, C.-L., and Zhang, D.-D. (2014). Anti-inflammatory effects of 81 Chinese herb extracts and their correlation with the characteristics of traditional Chinese medicine. *Evid. Based. Complement. Altern. Med.* 2014, 985176–985178. doi:10.1155/2014/985176

Dangar, D., and Patel, N. (2021). Anti-inflammatory effect of neuracanthus sphaerostachyus dalz. Leaves on experimental colitis in rats. *Indo Glob. J. Pharm. Sci.* 11 (01), 07–14. doi:10.35652/igjps.2021.111002

de Clauser, L., Luiz, A. P., Santana-Varela, S., Wood, J. N., and Sikandar, S. (2020). Sensitization of cutaneous primary afferents in bone cancer revealed by *in vivo* calcium imaging. *Cancers* 12 (12), E3491. doi:10.3390/cancers12123491

Deer, T. R., Mekhail, N., Petersen, E., Krames, E., Staats, P., Pope, J., et al. (2014a). The appropriate use of neurostimulation: Stimulation of the intracranial and extracranial space and head for chronic pain. Neuromodulation appropriateness consensus committee. *Neuromodulation* 17 (6), 551–570. doi:10.1111/ner.12215

Deer, T. R., Mekhail, N., Provenzano, D., Pope, J., Krames, E., Thomson, S., et al. (2014b). The appropriate use of neurostimulation: Avoidance and treatment of complications of neurostimulation therapies for the treatment of chronic pain. Neuromodulation appropriateness consensus committee. *Neuromodulation* 17 (6), 571–597. doi:10.1111/ner.12206

Du, G.-H., Yuan, T.-Y., Du, L.-D., and Zhang, Y.-X. (2016). "The potential of traditional Chinese medicine in the treatment and modulation of pain," in *Pharmacological mechanisms and the modulation of pain*. Cambridge, MA, United States: Academic Press, 325–361. doi:10.1016/bs.apha.2016.01.001

El-Shitany, N. A., and Eid, B. (2017). Proanthocyanidin protects against cisplatin-induced oxidative liver damage through inhibition of inflammation and NF-κβ/TLR-4 pathway. *Environ. Toxicol.* 32 (7), 1952–1963. doi:10.1002/tox.22418

Ellis, A., and Bennett, D. L. H. (2013). Neuroinflammation and the generation of neuropathic pain. *Br. J. Anaesth.* 111 (1), 26–37. doi:10.1093/bja/aet128

Feng, Y. U., and Bounda, G.-A. (2015). Review of clinical studies of Polygonum multiflorum Thunb. and its isolated bioactive compounds. *Pharmacogn. Res.* 7 (3), 225–236. doi:10.4103/0974-8490.157957

Hardie, D. G. (2022). "A New understanding of metformin," in *Comprehensive Pharmacology*. Amsterdam, Netherlands: Elsevier, 280–300. doi:10.1016/B978-0-12-820472-6.00099-2

Heimfarth, L., dos Anjos, K. S., de Carvalho, Y. M. B. G., dos Santos, B. L., Serafini, M. R., de Carvalho Neto, A. G., et al. (2020). Characterization of β-cyclodextrin/myrtenol complex and its protective effect against nociceptive behavior and cognitive impairment in a chronic musculoskeletal pain model. *Carbohydr. Polym.* 244, 116448. doi:10.1016/j.carbpol.2020.116448

Hu, Q. Q., Ma, Y. Q., Fei, X. Y., Chen, L. H., Kang, Y. R., Li, X., et al. (2022). [Effect of electroacupuncture and pretreatment of electroacupuncture on pain sensitization and expression of P2X7R in spinal dorsal horn in rats with diabetic neuropathic pain]. *Zhongguo Zhen Jiu* 42 (2), 173–178. doi:10.13703/j.0255-2930.20210208-k0004

Huang, D., Su, L., He, C., Chen, L., Huang, D., Peng, J., et al. (2022). Pristimerin alleviates cigarette smoke-induced inflammation in chronic obstructive pulmonary disease via inhibiting NF-κB pathway. *Biochem. Cell Biol.* 100 (3), 223–235. doi:10.1139/bcb-2021-0251

Huang, P., Wan, H., Shao, C., Li, C., Zhang, L., and He, Y. (2022). Recent advances in Chinese herbal medicine for cerebral ischemic reperfusion injury. *Front. Pharmacol.* 12, 688596. doi:10.3389/fphar.2021.688596

James, N. D., McMahon, S. B., Field-Fote, E. C., and Bradbury, E. J. (2018). Neuromodulation in the restoration of function after spinal cord injury. *Lancet. Neurol.* 17 (10), 905–917. doi:10.1016/s1474-4422(18)30287-4

Jin, J., Xie, Y., Shi, C., Ma, J., Wang, Y., Qiao, L., et al. (2020). Lipoxin A4 inhibits NLRP3 inflammasome activation in rats with non-compressive disc herniation through the JNK1/beclin-1/PI3KC3 pathway. *Front. Neurosci.* 14, 799. doi:10.3389/fnins.2020.00799

Kaur, G., Bedi, O., Sharma, N., Singh, S., Deshmukh, R., and Kumar, P. (2016). Anti-hyperalgesic and anti-nociceptive potentials of standardized grape seed proanthocyanidin extract against CCI-induced neuropathic pain in rats. *J. Basic Clin. Physiol. Pharmacol.* 27 (1), 9–17. doi:10.1515/jbcpp-2015-0026

Li, C., Niu, M., Bai, Z., Zhang, C., Zhao, Y., Li, R., et al. (2017). Screening for main components associated with the idiosyncratic hepatotoxicity of a tonic herb, Polygonum multiflorum. *Front. Med.* 11 (2), 253–265. doi:10.1007/s11684-017-0508-9

Li, H., Yang, T., Tang, H., Tang, X., Shen, Y., Benghezal, M., et al. (2019). *Helicobacter pylori* infection is an infectious disease and the empiric therapy paradigm should be changed. *Precis. Clin. Med.* 2 (2), 77–80. doi:10.1093/pcmedi/pbz009

Mishra, N. T. P., Yadav, S., Khantwal, M., Khan, W., and Khan, S. (2022). Clinical translation of gold nanoparticles into effective neuromedicines: Bottlenecks & future prospects. *Indo Glob. J. Pharm. Sci.* 12, 44–52. doi:10.35652/igjps.2022.12005

Myers, R. R., Campana, W. M., and Shubayev, V. I. (2006). The role of neuroinflammation in neuropathic pain: Mechanisms and therapeutic targets. *Drug Discov. Today* 11 (1-2), 8–20. doi:10.1016/s1359-6446(05)03637-8

Oliveira, J. P., Souza, M. T. S., Cercato, L. M., Souza, A. W., Nampo, F. K., and Camargo, E. A. (2020). Natural products for orofacial nociception in pre-clinical studies: A systematic review. *Arch. Oral Biol.* 117, 104748. doi:10.1016/j.archoralbio.2020.104748

Rauf, A., Al-Awthan, Y. S., Khan, I. A., Muhammad, N., Ali Shah, S. U., Bahattab, O., et al. (2022). *Vivo Anti-Inflammatory, Analgesic, Muscle Relaxant, and Sedative Activities of Extracts from Syzygium cumini*, 2022, 1–7. doi:10.1155/2022/6307529(L.) skeels in mice*Evidence-Based Complementary Altern. Med.*

Rezq, S., Mahmoud, M. F., El-Shazly, A. M., El Raey, M. A., and Sobeh, M. (2021). Anti-inflammatory, antipyretic, and analgesic properties of Potamogeton perfoliatus extract: *In vitro* and *in vivo* study. *Molecules* 26 (16), 4826. doi:10.3390/molecules26164826

Romero-Reyes, M., and Uyanik, J. M. (2014). Orofacial pain management: Current perspectives. *J. Pain Res.* 7, 99–115. doi:10.2147/jpr.S37593

Shen, C.-L., Castro, L., Fang, C.-Y., Castro, M., Sherali, S., White, S., et al. (2022a). Bioactive compounds for neuropathic pain: An update on preclinical studies and future perspectives. *J. Nutr. Biochem.* 104, 108979. doi:10.1016/j.jnutbio.2022.108979

Silva, J. C., Almeida, J. R. G. S., Quintans, J. S. S., Gopalsamy, R. G., Shanmugam, S., Serafini, M. R., et al. (2016). Enhancement of orofacial antinociceptive effect of carvacrol, a monoterpene present in oregano and thyme oils, by β-cyclodextrin inclusion complex in mice. *Biomed. Pharmacother.* 84, 454–461. doi:10.1016/j.biopha.2016.09.065

Singla, R. K., Agarwal, T., He, X., and Shen, B. (2021a). Herbal resources to combat a progressive & degenerative nervous system disorder- Parkinson's disease. *Curr. Drug Targets* 22 (6), 609–630. doi:10.2174/1389450121999201013155202

Singla, R. K., Guimarães, A. G., and Zengin, G. (2021b). Editorial: Application of plant secondary metabolites to pain neuromodulation. *Front. Pharmacol.* 11, 623399. doi:10.3389/fphar.2020.623399

Singla, R. K., Sultana, A., Alam, M. S., and Shen, B. (2020). Regulation of pain genes—capsaicin vs resiniferatoxin: Reassessment of transcriptomic data. *Front. Pharmacol.* 11, 551786. doi:10.3389/fphar.2020.551786

Swarnkar, S. K., Khunteta, A., Gupta, M. K., Jain, P., Sharma, S., and Paliwal, S. (2021). Antinociceptive activity shown by Aerva javanica flowering top extract and its mechanistic evaluation. *Indo Glob. J. Pharm. Sci.* 11 (01), 33–41. doi:10.35652/igjps.2021.111005

Thota, R., Salins, N., Bhatnagar, S., Ramanjulu, R., Ahmed, A., Jain, P., et al. (2020). Indian society for study of pain, cancer pain special interest group guidelines on palliative care aspects in cancer pain management. *Indian J. Palliat. Care* 26 (2), 210–214. doi:10.4103/0973-1075.285687

Wang, F., Tang, H., Ma, J., Cheng, L., Lin, Y., Zhao, J., et al. (2022). The effect of yiqi huoxue tongluo decoction on spinal cord microglia activation and ASK1-MKK3-p38 signal pathway in rats with diabetic neuropathic pain. *Evid. Based. Complement. Altern. Med.* 2022, 2408265. doi:10.1155/2022/2408265

Wang, J. W., Ye, X.-Y., Wei, N., Wu, S.-S., Zhang, Z.-H., Luo, G.-H., et al. (2022). Reactive oxygen species contributes to type 2 diabetic neuropathic pain via the thioredoxin-interacting protein-NOD–like receptor protein 3-N-Methyl-D-Aspartic acid receptor 2B pathway. *Anesth. Analg.* doi:10.1213/ane.0000000000006117

Wu, B., Zhou, C., Xiao, Z., Tang, G., Guo, H., Hu, Z., et al. (2022). LncRNA-UC.25 + shRNA alleviates P2Y14 receptor–mediated diabetic neuropathic pain via STAT1. *Mol. Neurobiol.* 59, 5504–5515. doi:10.1007/s12035-022-02925-0

Xie, Y.-K., Luo, H., Zhang, S.-X., Chen, X.-Y., Guo, R., Qiu, X.-Y., et al. (2022). GPR177 in A-fiber sensory neurons drives diabetic neuropathic pain via WNT-mediated TRPV1 activation. *Sci. Transl. Med.* 14 (639), eabh2557. doi:10.1126/scitranslmed.abh2557

Xue, W., Li, Y., and Zhang, M. (2021). Pristimerin inhibits neuronal inflammation and protects cognitive function in mice with sepsis-induced brain injuries by regulating PI3K/Akt signalling. *Pharm. Biol.* 59 (1), 1351–1358. doi:10.1080/13880209.2021.1981399

Yang, P. (2019). Maximizing quality of life remains an ultimate goal in the era of precision medicine: Exemplified by lung cancer. *Precis. Clin. Med.* 2 (1), 8–12. doi:10.1093/pcmedi/pbz001

Yang, S., Chen, C., Liu, X., Kang, Q., Ma, Q., Li, P., et al. (2022). Xiongshao Zhitong Recipe attenuates nitroglycerin-induced migraine-like behaviors via the inhibition of inflammation mediated by nitric oxide synthase. *Front. Pharmacol.* 13, 920201. doi:10.3389/fphar.2022.920201

Yetisgin, A. A., Cetinel, S., Zuvin, M., Kosar, A., and Kutlu, O. (2020). Therapeutic nanoparticles and their targeted delivery applications. *Molecules* 25 (9), E2193. doi:10.3390/molecules25092193

Zhang, Q., Li, Q., Liu, S., Zheng, H., Ji, L., Yi, N., et al. (2022). Glucagon-like peptide-1 receptor agonist attenuates diabetic neuropathic pain via inhibition of NOD-like receptor protein 3 inflammasome in brain microglia. *Diabetes Res. Clin. Pract.* 186, 109806. doi:10.1016/j.diabres.2022.109806

Zhao, Q., Bi, Y., Guo, J., Liu, Y.-x., Zhong, J., Pan, L. R., et al. (2020). Pristimerin protects against inflammation and metabolic disorder in mice through inhibition of NLRP3 inflammasome activation. *Acta Pharmacol. Sin.* 42 (6), 975–986. doi:10.1038/s41401-020-00527-x

frontiers in Pharmacology

ORIGINAL RESEARCH
published: 04 August 2021
doi: 10.3389/fphar.2021.713944

Metformin Attenuates Bone Cancer Pain by Reducing TRPV1 and ASIC3 Expression

He-Ya Qian[1,2†], Fang Zhou[1†], Rui Wu[2], Xiao-Jun Cao[2], Tao Zhu[3], Hao-Dong Yuan[3], Ya-Nan Chen[1] and Ping-An Zhang[2,4]**

[1]Department of Oncology, Affiliated Zhangjiagang Hospital of Soochow University, Zhangjiagang, China, [2]Center for Translational Medicine, Affiliated Zhangjiagang Hospital of Soochow University, Zhangjiagang, China, [3]Department of Laboratory, Affiliated Zhangjiagang Hospital of Soochow University, Zhangjiagang, China, [4]Center for Translational Pain Medicine, Institute of Neuroscience, Soochow University, Suzhou, China

OPEN ACCESS

Edited by:
Rajeev K. Singla,
Sichuan University, China

Reviewed by:
Manoj Kumar Sabnani,
Alloy Therapeutics, Inc., United States
Shikha Joon,
Sichuan University, China
MS Uddin,
Pharmakon Neuroscience Research Network (PNRN), Bangladesh

***Correspondence:**
Ping-An Zhang
pingan@suda.edu.cn
Ya-Nan Chen
chenyanan99@126.com

[†]These authors have contributed equally to this work and share first authorship

Specialty section:
This article was submitted to Neuropharmacology, a section of the journal Frontiers in Pharmacology

Received: 24 May 2021
Accepted: 14 July 2021
Published: 04 August 2021

Citation:
Qian H-Y, Zhou F, Wu R, Cao X-J, Zhu T, Yuan H-D, Chen Y-N and Zhang P-A (2021) Metformin Attenuates Bone Cancer Pain by Reducing TRPV1 and ASIC3 Expression. Front. Pharmacol. 12:713944. doi: 10.3389/fphar.2021.713944

Bone cancer pain (BCP) is a common pathologic pain associated with destruction of bone and pathological reconstruction of nervous system. Current treatment strategies in clinical is inadequate and have unacceptable side effects due to the unclear pathology mechanism. In the present study, we showed that transplantation of Walker 256 cells aggravated mechanical allodynia of BCP rats (**$p < 0.01$ vs. Sham), and the expression of ASIC3 (Acid-sensitive ion channel 3) and TRPV1 was obviously enhanced in L4-6 dorsal root ganglions (DRGs) of BCP rats (**$p < 0.01$ vs. Sham). ASIC3 and TRPV1 was mainly expressed in CGRP and IB4 positive neurons of L4-6 DRGs. While, TRPV1 but not ASIC3 was markedly upregulated in L4-6 spinal dorsal horn (SDH) of BCP rats (**$p < 0.01$ vs. Sham). Importantly, intrathecal injection of CPZ (a TRPV1 inhibitor) or Amiloride (an ASICs antagonist) markedly increased the paw withdraw threshold (PWT) of BCP rats response to Von Frey filaments (**$p < 0.01$ vs. BCP + NS). What's more, intraperitoneally injection of Metformin or Vinorelbine markedly elevated the PWT of BCP rats, but reduced the expression of TRPV1 and ASIC3 in L4-6 DRGs and decreased the TRPV1 expression in SDH (*$p < 0.05$, **$p < 0.01$ vs. BCP + NS). Collectively, these results suggest an effective analgesic effect of Metformin on mechanical allodynia of BCP rats, which may be mediated by the downregulation of ASIC3 and TRPV1.

Keywords: metformin, bone cancer pain, ASIC3, TRPV1, dorsal root ganglions

INTRODUCTION

Pain is a common symptom in cancer patients (Sheng and Zhang, 2020). Previous studies have shown that 85% of patients with lung, breast and prostate cancer appear bone metastasis, and about one-third of them was accompanied with bone cancer pain (BCP) symptoms (Okui et al., 2021). Bone cancer pain (BCP) is a unique pain that includes features of nociceptive, neuropathic, and inflammatory pain (de Clauser et al., 2020). BCP can produce an excruciating pain, but current treatments strategies may be inadequate or have unacceptable side effects (Sindhi and Erdek, 2019; Yu et al., 2020; Chen et al., 2021). Therefore, it is urgent to explore the new mechanisms and develop novel therapeutic targets to relieve BCP. Metformin, serving as an antidiabetic drug (Yu et al., 2019), is recently revealed to exist anti-cancer properties by regulation of cancer-relevant signaling pathways (Cao et al., 2016). Additionally, Metformin was proved to exert analgesic effect in neuropathic pain (Hacimuftuoglu et al., 2020), inflammatory pain (Russe et al., 2013) and

visceral pain (Nozu et al., 2019). However, the effects and mechanism of Metformin in chronic pain induced by cancer bone metastasis remains unknown.

Metabolize of bone cancer cell could produce acidic environment (George et al., 2020). It was reported that the mechanisms of bone cancer pain include tumor cells-induced nerve injury, central sensitization, tumor cells themselves, osteoclast-mediated osteolysis as well as acidic environment of bone tissue (Nagae et al., 2007; Mantyh, 2014; Romero-Morelos et al., 2021). The Acid-sensitive ion channels (ASICs) is one of the most sensitive ion channels in detecting changes in pH (Mir and Jha, 2021). ASIC3 has the highest content in dorsal root ganglions (DRGs) and is sensitive to extracellular acidification. Additionally, transient receptor potential ion channel (TRPV1), a nonselective cation channel, can also be activated by H^+ (Elokely et al., 2016; Wu et al., 2019; Rosenberger et al., 2020). TRPV1 is highly enriched in dorsal root ganglions (DRGs), and its involvement in diverse pain states has been well documented (Sondermann et al., 2019). TRPV1 represents a major player in pathological pain arising from inflamed and injured tissues, i.e., inflammatory pain and cancer pain (Joseph et al., 2019). However, whether ASIC3/TRPV1 is involved in the analgesic effect of Metformin on bone cancer pain remains unclear.

In the present study, we revealed that Metformin exerted therapeutic effects on bone cancer pain. Furthermore, we proved that the mechanism underlying analgesic effect of Metformin was mediated by regulation of TRPV1 and ASIC3 expression.

MATERIALS AND METHODS

Animals

Female Sprague-Dawley (SD) rats (180–220 g) were housed in a temperature- (24 ± 1°C) and light-controlled (12/12-h light-dark cycle) room with free access to food and water. All experimental procedures were approved by the Laboratory Animal Center of Soochow University (Suzhou, Jiangsu, P.R. China).

Generation of the Bone Cancer Pain Model

The BCP model was established according to the method previously reported (Zhou et al., 2015; Hu et al., 2019; Shenoy et al., 2019; Zhang et al., 2020). In detail, the young rat was intraperitoneally injected with 2×10^7 Walker 256 cells. One week later, the ascites fluids were extracted and the cells were collected. After that, the Walker 256 cells were counted and diluted to a final concentration of 1×10^8 cells/ml. The Walker 256 cells (4×10^5) was then slowly injected into the tibia cavity using a microinjection syringe with a 23-gauge needle. In the Sham group, the same volume of normal saline solution was injected into the tibial medullary cavity of rats. In the naïve group, the rats did not suffer any treatment.

Evaluation of Mechanical Allodynia

The "up and down" method was used to evaluate mechanical allodynia (Zhou et al., 2015) and the 50% paw withdrawal threshold (PWT) was determined as previously described methods. In detail, the rats were placed in a transparent box and allowed to acclimate for 30 min. The experiments were performed in a double-blinded manner. A series of standard Von Frey filaments (VFFs) (0.6, 1.0, 1.4, 2.0, 4.0, 6.0, 8.0, 10.0, 15.0 and 26.0 g) were vertically advanced to the plantar surface of the hind paw using sufficient force until the filament bent. The trial began with the filament possessing a buckling weight of 8.0 g. Withdrawal of the hind paw was regarded as a positive response, and a weaker stimulus was presented. In the absence of response, a stronger stimulus was applied.

TABLE 1 | Primers used for real-time PCR.

Name	Forward primer	Reverse primer
TRPV1	GCTCTGGTGCTTGGCTATGA	GGGTCGACCTGATACTTGGC
ASIC3	GTGGTGCTGGCAACGGACTG	GGCTCATCCTGGCTGTGAATCTG
GAPDH	AAGGTGGTGAAGCAGGCGGC	GAGCAATGCCAGCCCCAGCA

Western Blotting

The expressions of TRPV1 and ASIC3 in the dorsal root ganglia (DRGs) and spinal dorsal horn (SDH) were determined using western blotting. After the rats were sacrificed, the L4–L6 spinal dorsal horn and DRGs were collected and lysed. The lysates were centrifuged at 12,000 g at 4°C. The supernatant was collected and the total protein concentration was qualified using a bicinchoninic acid (BCA) protein assay kit (Thermo Scientific, MA, United States). Equal amounts of proteins were separated by 10% polyacrylamide gels (Bio-Rad, CA, United States). Then the proteins were transferred to polyvinyli denedifluoride membranes. The membranes were blocked in a 5% non-fat milk for 2 h at room temperature and incubated with the primary antibodies [anti-TRPV1 (Genetex, United States), anti-ASIC3 (Genetex, United States), and anti-GAPDH (Abcam, Cambridge, United Kingdom)] at 4°C overnight. After washing with TBST (0.5% Tween-20), the membranes were then incubated with peroxidase-conjugated secondary antibodies for 2 h at room temperature. An imaging system (Bio-Rad, CA, United States) was used to examine chemiluminescence. Expression of protein was normalized to that of GAPDH.

Real-Time Quantitative Polymerase Chain Reaction

Total RNA was extracted from the L4-L6 DRGs and SDH using Trizol (Invitrogen, CA) method. cDNA was synthesized from total RNA using an Omniscript RT kit 50 (Qiagen, Valencia, CA) according to the manufacturer's instructions. The primers for TRPV1, ASIC3, and GAPDH (internal control) were used. The primer sequences are showed in **Table 1**. To evaluate the expressions of genes, $2^{-\triangle\triangle Ct}$ values were calculated. The mRNA expression values of TRPV1 and ASIC3 were normalized to that of GAPDH.

Immunofluorescence Assay

The Immunofluorescence assay was conducted as described in previous report (Zhou et al., 2015). In brief, the rats were anesthetized and transcardially perfused with a saline solution

followed by 4% paraformaldehyde (Sinopharm Chemical Reagent Co. Ltd., Shanghai, P.R. China). The L4-6 DRGs were then removed and fixed in paraformaldehyde and dehydrated in 10, 20 and 30% sucrose (Sinopharm Chemical Reagent Co. Ltd.) in succession until sinking. The DRGs were cut at 14 μm thickness using freezing microtome (Leica, Wetzlar, Germany). The sections were incubated with blocking solution, and followed by the primary antibodies [anti-TRPV1 (Genetex, United States), anti-ASIC3 (Genetex, United States), anti-NeuN (Merck Millipore, Germany), anti-GS (Abcam, Cambridge, United Kingdom), anti-calcitonin gene-related peptide (CGRP) (Abcam, Cambridge, United Kingdom), anti-neurofilament (NF)-200 (Abcam, Cambridge, United Kingdom), anti-isolectin B4 (IB4) (Sigma, St. Louis, MO)] at 4°C overnight. After washing with PBS, the secondary antibodies labeled Alexa Fluor 488 and 555 (Molecular Probes, NY, United States) were incubated at room temperature for 1 h. The slides were observed under a fluorescence microscope, and the images were trimmed with AxioVision (Jena, Germany). Negative controls were performed by omitting the primary antibody.

Drug Administration

Capsazepine (HY-15640) was purchased from Medchemexpress (Monmouth Junction, NJ, United States). Amiloride (T0175) and Vinorelbine (T6213) were purchased from TargetMol (Wellesley Hills, MA, United States). Metformin was purchased from Sigma-Aldrich (St. Louis, MO, United States). After acclimatization for 1 week, the rats were injected with Walker 256 cells. After 2 weeks, twenty-four rats were divided into four groups. In group 1, rats were received an intrathecal injection of amiloride (0.1 mg/10 μL), In group 2, rats were received a subcutaneous injection of 15 mg/kg capsazepine (CPZ). In group 3, rats were received an intraperitoneal injection of 3 mg/kg Vinorelbine. In group 4, rats were received an intraperitoneal injection of 200 mg/kg Metformin (Ge et al., 2018; Hacimuftuoglu et al., 2020). The PWT was recorded at 0.5, 1, 2, 4, and 8 h, and 2, 5, 7, 14, and 21 days after the administrations of drugs. To evaluate the long-term effects of Metformin, the rats were received Metformin injections once a day for five consecutive days.

Data Analysis

All data were analyzed using SPSS 17.0 (SPSS, Chicago, IL, United States) and Origin Pro 8 (OriginLab, Northampton, MA). All Data were showed as Mean ± SEM. Statistical analyses were performed by two-way analysis of variance (ANOVA) with multiple comparisons. Normality was verified for all data before analyses. $p < 0.05$ was considered as a statistical significance.

RESULTS

Transplantation of Walker 256 Cells Increased the Expression of Transient Receptor Potential Ion Channel and ASIC3

We evaluated the PWT of rats before transplantation, and no signs of mechanical allodynia were observed in each group (**Figure 1A**, Pre). The result demonstrated that the PWT of BCP rats showed a significant decrease on the 2nd week after transplantation of Walker 256 cells when compared with that of Sham group (**Figure 1A**, $^{**}p < 0.01$ vs. Sham), and the decrease lasted to at least 6 weeks (**Figure 1A**, $^{**}p < 0.01$ vs. Sham). The PWT of rats showed no difference between naïve and Sham group. The result indicates that transplantation of Walker 256 cells aggravated mechanical allodynia of rats.

The mRNA and protein levels of TRPV1 and ASIC3 in the ipsilateral L4-6 DRGs and spinal dorsal horn (SDH) were assessed to determine their role in mechanical allodynia of BCP rats. QPCR results showed that the mRNA levels of TRPV1 and ASIC3 were significantly increased in the ipsilateral DRGs of BCP rats compared with Sham ones (**Figure 1B**, $^{**}p < 0.01$ vs. Sham). Additionally, the mRNA level of TRPV1 but not ASIC3 was markedly increased in the ipsilateral SDH of BCP rats (**Figure 1C**, $^{**}p < 0.01$ vs. Sham). The up-regulation was further confirmed by western blotting (**Figure 1D**). The results showed that the protein levels of TRPV1 and ASIC3 were obviously increased in the ipsilateral DRGs (**Figure 1E**, $^{**}p < 0.01$ vs. Sham). And, the protein level of TRPV1 but not ASIC3 was markedly increased in the ipsilateral SDH of BCP rats compared with Sham ones (**Figure 1F**, $^{**}p < 0.01$ vs. Sham). These results indicate that the expression of TRPV1 and ASIC3 was enhanced in BCP rats.

Transient Receptor Potential Ion Channel and ASIC3 Were Mainly Expressed in the Dorsal Root Ganglions Neurons

We further investigated the distributions of TRPV1 and ASIC3 in the DRG using immunofluorescence assay. As shown in **Figure 2**, TRPV1 was primarily expressed in neurons (labeled by NeuN) but not satellite glial cells (labeled by GS). Furthermore, we co-stained TRPV1 with NF-200 (a marker of large neurons), isolectin B4 (IB4, a marker of non-peptidergic small and medium neurons), and calcitonin gene-related peptide (CGRP, a marker of small and medium peptidergic neurons) by immunofluorescence and the result showed that TRPV1 was mainly expressed in small and medium neurons labeled with IB4 and CGRP. Additionally, we also investigated the distributions of ASIC3 in DRGs. Immunofluorescence assay showed that ASIC3 was mainly co-localized with NeuN, CGRP and IB4, but not with GS and a little with NF200 (**Figure 3**), indicating ASIC3 was mainly expressed in small and medium sensory neurons of L4-6 DRGs.

Injection of Capsazepine or Amiloride Attenuated Mechanical Allodynia of Bone Cancer Pain Rats

To investigate the role of TRPV1 and ASIC3 in the mechanical allodynia, their antagonist CPZ and Amiloride was separately intrathecal injected in BCP rats. As shown in **Figure 4A**, the PWT of BCP rats were markedly increased after CPZ injection from 4 h to 2 days compared with normal saline (NS) treated BCP rats ($^{**}p < 0.01$ vs. BCP + NS). Similarly, the BCP rats treated with Amiloride showed an increase of PWT from 0.5 to 8 h (**Figure 4B**, $^{**}p < 0.01$ vs. BCP + NS). These data suggest that up-regulated TRPV1 and ASIC3 contribute to the mechanical allodynia of BCP rats.

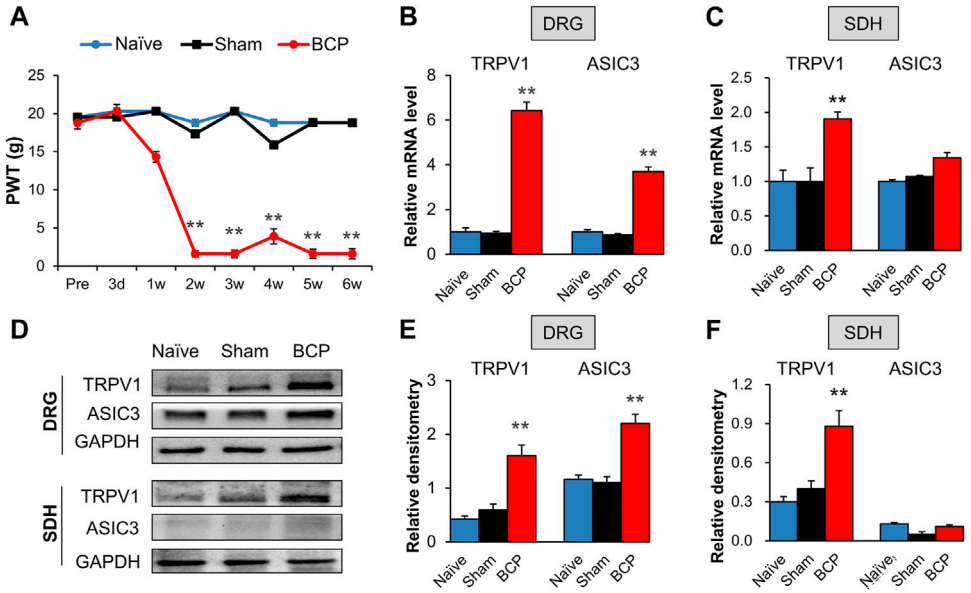

FIGURE 1 | The expression of TRPV1 and ASIC3 was increased in BCP rats. **(A)** PWT was significantly reduced 2 weeks after tumor cell compared with the Naïve group (SD healthy female rats with not any treatment) and Sham group (normal saline injection) (**p < 0.01 vs. Sham, two-way repeated measures ANOVA followed by Tukey's post hoc test). **(B)** Quantification of QPCR assays showing significant up-regulation of TRPV1 and ASIC3 mRNA expression in L4-6 DRGs of BCP rats at 2 weeks after transplantation compared with Sham rats (**p < 0.01 vs. Sham, two-way repeated measures ANOVA followed by Tukey's post hoc test). **(C)** Quantification of QPCR assays showing significant up-regulation of TRPV1 mRNA expression in L4-6 spinal dorsal horn (SDH) of BCP rats at 2 weeks after transplantation compared with Sham rats (**p < 0.01 vs. Sham, two-way repeated measures ANOVA followed by Tukey's post hoc test). While mRNA expression of ASIC3 in L4-6 spinal dorsal horn (SDH) of BCP rats at 2 weeks after transplantation was not altered compared with Sham rats (p > 0.05 vs. Sham, two-way repeated measures ANOVA followed by Tukey's post hoc test). **(D)** Immunoblot showed the protein level of TRPV1 and ASIC3 in DRGs and SDH of Naïve, Sham and BCP rats. **(E)** The protein expression of TRPV1 and ASIC3 in the ipsilateral L4-6 DRGs of BCP rats was significantly increased compared with Sham rats at 2 weeks after transplantation (**p < 0.01 vs. Sham, two-way repeated measures ANOVA followed by Tukey's post hoc test). **(F)** Protein expression of TRPV1 in the ipsilateral L4-6 SDH of BCP rats was significantly increased compared with Sham rats at 2 weeks after transplantation (**p < 0.01 vs. Sham, two-way repeated measures ANOVA followed by Tukey's post hoc test). While protein ASIC3 expression was not altered. (p > 0.05 vs. Sham, two-way repeated measures ANOVA followed by Tukey's post hoc test).

Metformin and Vinorelbine Attenuated Mechanical Allodynia of Bone Cancer Pain Rats

Next, we evaluated the effects of Metformin and Vinorelbine (a clinical chemotherapeutic drugs) on mechanical allodynia of BCP rats. After transplanted cancer cells for 2 weeks, the rats were treated with Metformin or Vinorelbine separately. As shown in **Figure 5A**, the PWT of BCP rats treated with Vinorelbine was continuously increased from 4 h to 7 days, and was most obvious from 5 to 7 days (**p < 0.01 vs. BCP + NS). Similarly, in the Metformin group, the PWT of BCP rats increased from 4 h to 14 days after treatment of Metformin, and the effect lasted to at least 14 days (**Figure 5B**, *p < 0.05, **p < 0.01 vs. BCP + NS).

Metformin or Vinorelbine Injection Reduced ASIC3 and Transient Receptor Potential Ion Channel Expression

To evaluate the effects of Vinorelbine and Metformin on the expression of TRPV1 and ASIC3, qPCR and Western blotting was performed. The results showed that treatment of Vinorelbine or Metformin significantly inhibited the mRNA levels of TRPV1 and ASIC3 in the ipsilateral DRG when compared with those in the BCP + NS group (**Figure 6A**, *p < 0.05, **p < 0.01 vs. BCP + NS). Additionally, treatment of Metformin or Vinorelbine significantly reduced the protein levels of TRPV1 and ASIC3 in the ipsilateral DRG when compared with those in the BCP + NS group (**Figures 6B,C**, **p < 0.01 vs. BCP + NS). Additionally, the mRNA level of TRPV1 but not ASIC3 was obviously reduced in the ipsilateral SDH of BCP rats treated with Metformin or Vinorelbine (**Figure 6D**, **p < 0.01 vs. BCP + NS). Furthermore, the protein level of TRPV1 but not ASIC3 was remarkedly decreased in the ipsilateral SDH of BCP rats treated with Metformin or Vinorelbine (**Figures 6E,F**, **p < 0.01 vs. BCP + NS). The results demonstrate that treatment of Metformin or Vinorelbine decreased the expression of ASIC3 and TRPV1, suggesting a possible involvement of ASIC3 and TRPV1 in Metformin/Vinorelbine-mediated analgesic effect on BCP rats.

DISCUSSION

An important finding in the present study is to reveal the therapeutic potential of Metformin on bone cancer pain (BCP). Although numerous previous studies have demonstrated that Metformin can be used in the treatment of many types of cancers (Al Hassan et al., 2018; Roshan et al., 2019; Xue et al., 2019), the effects of Metformin on bone cancer pain are still unclear. In the

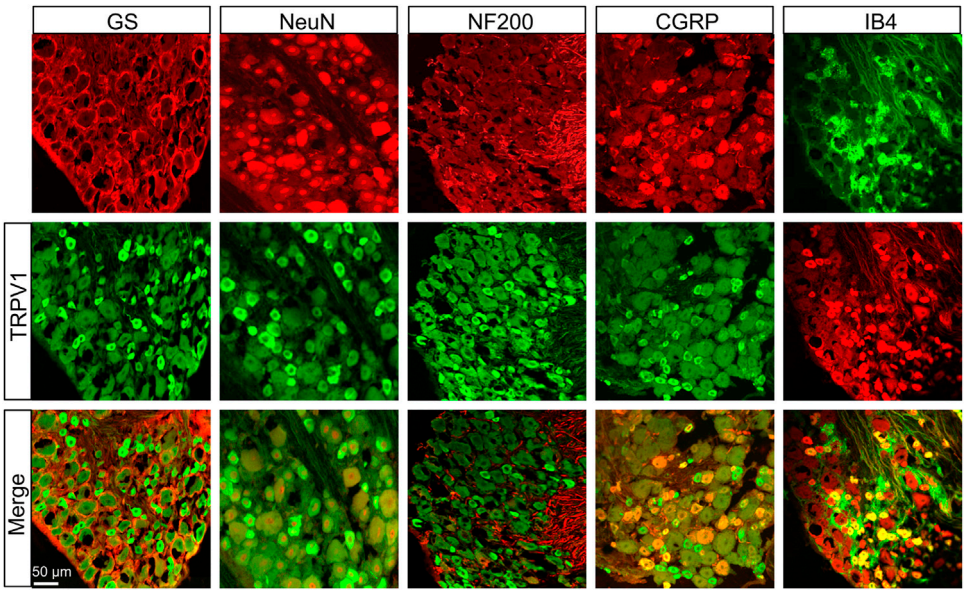

FIGURE 2 | Immunofluorescence assay of TRPV1 in L4-6 DRGs. TRPV1-positive DRG cells (middle row) were co-labeled as neuron-positive (upper left second, red) but not with GS-positive cells (upper left first, red). TRPV1 was co-expressed in IB4-positive (upper right first, green) and CGRP-positive (upper right second, red) DRG neurons. TRPV1 was a few expressed in NF-200-positive (upper middle, red) DRG neurons. Merges of TRPV1 with GS, NeuN, CGRP, NF-200, and IB4 are shown in the lower row. Scale bar, 50 μm. Quantification showing that TRPV1 was mainly located in small and medium sensory neurons labeled with IB4 and CGRP but a few with NF-200.

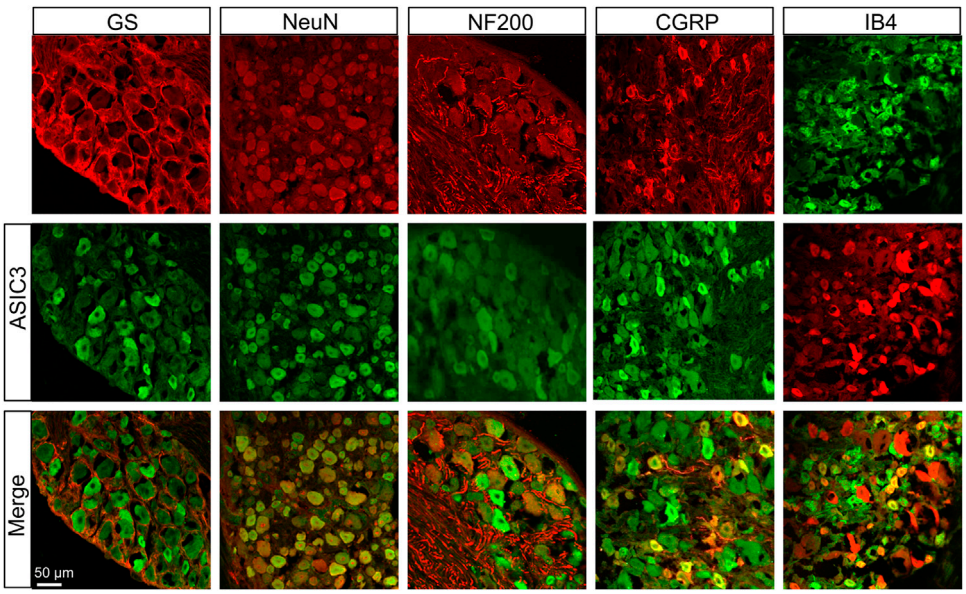

FIGURE 3 | Immunofluorescence assay of ASIC3 in L4-6 DRGs. ASIC3-positive DRG cells (middle row) were co-labeled as neuron-positive (upper left second, red) but not with GS-positive cells (upper left first, red). ASIC3 was co-expressed in IB4-positive (upper right first, green) and CGRP-positive (upper right second, red) DRG neurons. ASIC3 was a few expressed in NF-200-positive (upper middle, red) DRG neurons. Merges of ASIC3 with GS, NeuN, CGRP, NF-200, and IB4 are shown in the lower row. Scale bar, 50 μm. Quantification showing that ASIC3 was mainly located in small and medium sensory neurons labeled with IB4 and CGRP but a few with NF-200.

present study, we found that the PWT of mechanical allodynia in BCP rats continued to increase for at least 14 days after treatment of Metformin, indicating that Metformin therapy could attenuate the bone cancer pain symptoms and the analgesic effect of Metformin was much better than Vinorelbine (last for 7 days). Notably, we revealed that the underlying analgesic mechanisms of Metformin on bone cancer pain are in part *via* reducing the expression of TRPV1 and ASIC3.

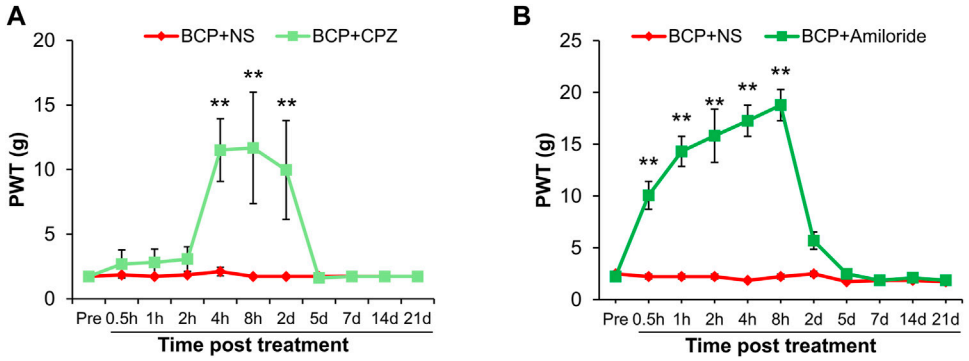

FIGURE 4 | The PWT of BCP rats was increased after Capsazepine (CPZ) or Amiloride injection. **(A)** The PWT of BCP rats (2 weeks after transplantation) subcutaneous injected with TRPV1 inhibitor (CPZ, 15 mg/kg) were significantly increased than in age-matched BCP rats injected with same volume of NS from 4 h to 2 days (**p < 0.01 vs. BCP + NS, two-way repeated measures ANOVA followed by Sidak's post hoc test). **(B)** The PWT of BCP rats (2 weeks after transplantation) intrathecal injected with ASIC3 inhibitor (Amiloride, 0.1 mg/10 μL) were significantly increased than in age-matched BCP rats injected with the same volume of NS from 0.5 to 8 h (**p < 0.01 vs. BCP + NS, two-way repeated measures ANOVA followed by Sidak's post hoc test).

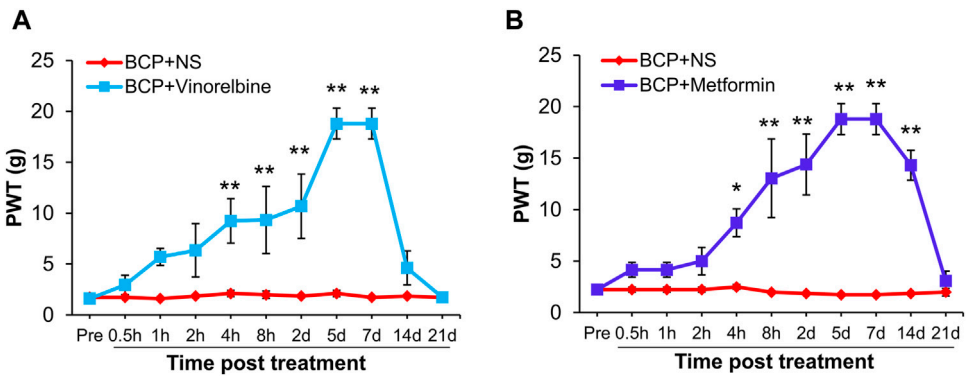

FIGURE 5 | Metformin or Vinorelbine treatment attenuated the mechanical allodynia of BCP rats. **(A)** The PWT of BCP rats (2 weeks after transplantation) treated with Vinorelbine (intraperitoneal injection, 3 mg/kg) was significantly increased than in age-matched BCP rats injected with same volume of NS from 4 h to 7 days (**p < 0.01 vs. BCP + NS, two-way repeated measures ANOVA followed by Sidak's post hoc test). **(B)** The PWT of BCP rats (2 weeks after transplantation) treated with Metformin (intraperitoneal injection, 200 mg/kg) was significantly increased than in age-matched BCP rats injected with same volume of NS from 4 h to 14 days (*p < 0.5, **p < 0.01 vs. BCP + NS, two-way repeated measures ANOVA followed by Sidak's post hoc test).

Firstly, we successfully established a rat model of BCP with the decreased PWT following the up-regulation of TRPV1 in both DRGs and spinal dorsal horn (SDH). Additionally, inhibition of TRPV1 by CPZ was able to ameliorate PWT of BCP rats, and a significant reduction in mechanical allodynia was observed from 8 h to 5 days after CPZ injection. This is consistent with the view that TRPV1 blockage or deletion is proved to be an effective method to attenuate chronic bone pain state (Heo et al., 2017; Hanaka et al., 2018). Importantly, Metformin application could significantly reduce the up-regulated TRPV1 in both DRG and SDH of BCP rats as well as Vinorelbine treatment, suggesting that TRPV1 might mediate the analgesic effect of Metformin and Vinorelbine on BCP. However, the regulation procedure of TRPV1 expression by Metformin and Vinorelbine was unknown and need to be investigated in the future research.

ASIC3 is another important protein that we proved here to contribute to the analgesic effect of Metformin. The increase of ASIC3 in the DRG neuron have been reported in a rat model of cancer-induced pain model (Qiu et al., 2014), and Wu et al. (2004) suggested that ASIC3 expressed little or no expression in rat spinal dorsal horn. Consistent with this, our data showed an increased ASIC3 in DRG neurons but the expression of ASIC3 was not changed in SDH, and the inhibitor Amiloride significantly elevated the PWT of BCP rats. Although inhibitors for ASIC3 showed effectiveness in BCP model, we noticed that the analgesic effect of these inhibitors only lasted for 8 h. Therefore, it is necessary to discover specific agents that are effective with longer-last effects for bone cancer pain such as Metformin. Furthermore, here we provided some evidences to confirm the involvement of ASIC3 in the analgesic effect of Metformin. Metformin treatment obviously reversed the upregulation of ASIC3 in DRGs. However, the regulation mechanism of Metformin in ASIC3 expression was not clear.

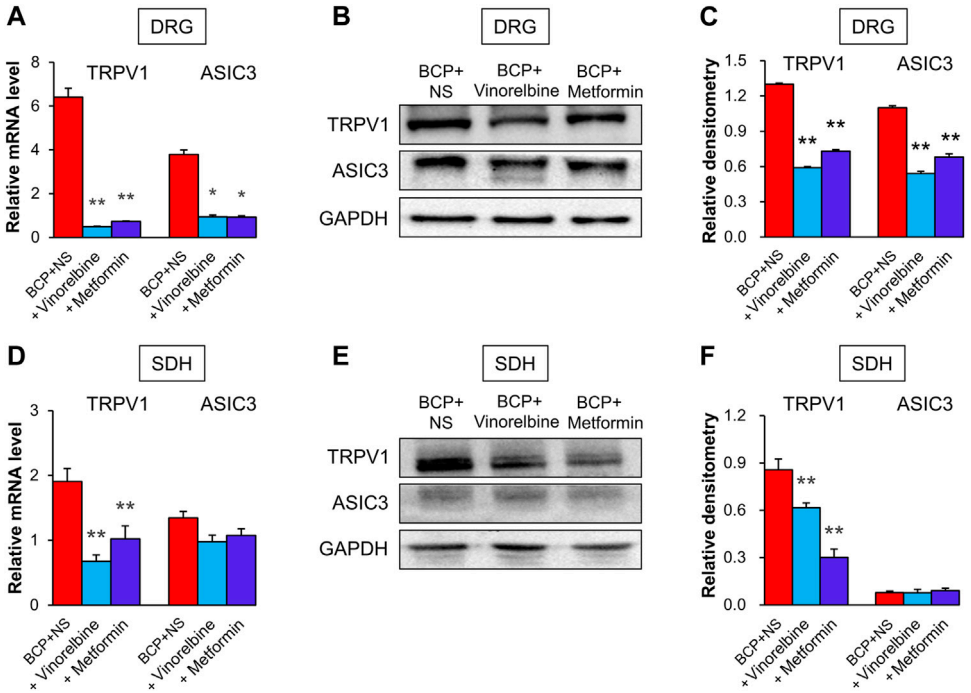

FIGURE 6 | Metformin and Vinorelbine decreased the expressions of TRPV1 and ASIC3. **(A)** Quantification of qPCR assays showed that the mRNA level of TRPV1 and ASIC3 were decreased in the ipsilateral DRGs of BCP rats treated with Vinorelbine or Metformin when compared with BCP + NS rats (*$p < 0.5$, **$p < 0.01$ vs. BCP + NS, two-way repeated measures ANOVA followed by Tukey's post hoc test). **(B)** Immunoblot showed the protein level of TRPV1 and ASIC3 in rat DRGs of BCP + NS, BCP + Vinorelbine, BCP + Metformin group. **(C)** The expression of TRPV1 and ASIC3 at the protein level in the ipsilateral DRGs of BCP rats treated with Vinorelbine or Metformin was greatly decreased when compared with BCP + NS rats (**$p < 0.01$ vs. BCP + NS, two-way repeated measures ANOVA followed by Tukey's post hoc test). **(D)** QPCR assays showed that the mRNA level of TRPV1 was decreased in the ipsilateral SDH of BCP rats treated with Vinorelbine or Metformin when compared with a BCP + NS rats (**$p < 0.01$ vs. BCP + NS, two-way repeated measures ANOVA followed by Tukey's post hoc test). While the mRNA level of ASIC3 was not changed ($p > 0.05$ vs. BCP + NS, two-way repeated measures ANOVA followed by Tukey's post hoc test). **(E)** Immunoblot showed the protein level of TRPV1 and ASIC3 in rat SDH of BCP + NS, BCP + Vinorelbine, BCP + Metformin group. **(F)** The expression of TRPV1 at the protein level was decreased in the ipsilateral SDH of BCP rats treated with Vinorelbine or Metformin when compared with BCP + NS rats (**$p < 0.01$ vs. BCP + NS, two-way repeated measures ANOVA followed by Tukey's post hoc test). While the ASIC3 expression was not changed ($p > 0.05$ vs. BCP + NS, two-way repeated measures ANOVA followed by Tukey's post hoc test).

CONCLUSION

Taken together, in the present study, we revealed that Metformin exerted therapeutic effects on bone cancer pain in a rat model. Treatment of Metformin reduced the mechanical allodynia of BCP rats for 14 days (better than Vinorelbine). Additionally, the mechanisms underlying analgesic effect of Metformin and Vinorelbine on BCP are in part *via* the downregulation of TRPV1 and ASIC3.

DATA AVAILABILITY STATEMENT

The raw data supporting the conclusion of this article will be made available by the authors, without undue reservation.

ETHICS STATEMENT

The animal study was reviewed and approved by the Laboratory Animal Center of Soochow University.

AUTHOR CONTRIBUTIONS

H-YQ and FZ performed experiments, analyzed data and prepared figures and manuscript. RW, X-JC, TZ, and H-DY revised the manuscript. Y-NC and P-AZ designed experiments, supervised the experiments and finalized the manuscript. All the authors have read and approved the paper.

FUNDING

This work was supported by grants from the National Natural Science Foundation of China (No. 81801115), China Postdoctoral Science Foundation Grant (No. 2018M642304), and from the Suzhou Science and Technology Project for Youth (No. KJXW2020059). The funders had no role in the study design, data collection and analysis, decision to publish, or preparation of the manuscript.

REFERENCES

Al Hassan, M., Fakhoury, I., El Masri, Z., Ghazale, N., Dennaoui, R., El Atat, O., et al. (2018). Metformin Treatment Inhibits Motility and Invasion of Glioblastoma Cancer Cells. *Anal. Cell Pathol.* 2018, 1–9. doi:10.1155/2018/5917470

Cao, H., Dong, W., Qu, X., Shen, H., Xu, J., Zhu, L., et al. (2016). Metformin Enhances the Therapy Effects of Anti-IGF-1r mAb Figitumumab to NSCLC. *Sci. Rep.* 6, 31072. doi:10.1038/srep31072

Chen, H.-W., Zhang, X.-X., Peng, Z.-D., Xing, Z.-M., Zhang, Y.-W., and Li, Y.-L. (2021). The Circular RNA circSlc7a11 Promotes Bone Cancer Pain Pathogenesis in Rats by Modulating LLC-WRC 256 Cell Proliferation and Apoptosis. *Mol. Cel Biochem* 476 (4), 1751–1763. doi:10.1007/s11010-020-04020-1

de Clauser, L., Luiz, A. P., Santana-Varela, S., Wood, J. N., and Sikandar, S. (2020). Sensitization of Cutaneous Primary Afferents in Bone Cancer Revealed by *In Vivo* Calcium Imaging. *Cancers* 12 (12), 3491. doi:10.3390/cancers12123491

Elokely, K., Velisetty, P., Delemotte, L., Palovcak, E., Klein, M. L., Rohacs, T., et al. (2016). Understanding TRPV1 Activation by Ligands: Insights from the Binding Modes of Capsaicin and Resiniferatoxin. *Proc. Natl. Acad. Sci. USA* 113 (2), E137–E145. doi:10.1073/pnas.1517288113

Ge, A., Wang, S., Miao, B., and Yan, M. (2018). Effects of Metformin on the Expression of AMPK and STAT3 in the Spinal Dorsal Horn of Rats with Neuropathic Pain. *Mol. Med. Rep.* 17 (4), 5229–5237. doi:10.3892/mmr.2018.8541

George, C. N., Canuas-Landero, V., Theodoulou, E., Muthana, M., Wilson, C., and Ottewell, P. (2020). Oestrogen and Zoledronic Acid Driven Changes to the Bone and Immune Environments: Potential Mechanisms Underlying the Differential Anti-tumour Effects of Zoledronic Acid in Pre- and post-menopausal Conditions. *J. Bone Oncol.* 25, 100317. doi:10.1016/j.jbo.2020.100317

Hacimuftuoglu, A., Mohammadzadeh, M., Taghizadehghalehjoughi, A., Taspinar, N., Togar, B., Nalcı, K. A., et al. (2020). The Analgesic Effect of Metformin on Paclitaxel-Induced Neuropathic Pain Model in Rats: By Considering Pathological Results. *J. Cancer Res. Ther.* 16 (1), 34–39. doi:10.4103/jcrt.JCRT_1455_16

Hanaka, M., Iba, K., Dohke, T., Kanaya, K., Okazaki, S., and Yamashita, T. (2018). Antagonists to TRPV1, ASICs and P2X Have a Potential Role to Prevent the Triggering of Regional Bone Metabolic Disorder and Pain-Like Behavior in Tail-Suspended Mice. *Bone* 110, 284–294. doi:10.1016/j.bone.2018.02.006

Heo, M. H., Kim, J. Y., Hwang, I., Ha, E., and Park, K. U. (2017). Analgesic Effect of Quetiapine in a Mouse Model of Cancer-Induced Bone Pain. *Korean J. Intern. Med.* 32 (6), 1069–1074. doi:10.3904/kjim.2015.377

Hu, X.-M., Yang, W., Du, L.-X., Cui, W.-Q., Mi, W.-L., Mao-Ying, Q.-L., et al. (2019). Vascular Endothelial Growth Factor A Signaling Promotes Spinal Central Sensitization and Pain-Related Behaviors in Female Rats with Bone Cancer. *Anesthesiology* 131 (5), 1125–1147. doi:10.1097/ALN.0000000000002916

Joseph, J., Qu, L., Wang, S., Kim, M., Bennett, D., Ro, J., et al. (2019). Phosphorylation of TRPV1 S801 Contributes to Modality-specific Hyperalgesia in Mice. *J. Neurosci.* 39 (50), 9954–9966. doi:10.1523/JNEUROSCI.1064-1910.1523/jneurosci.1064-19.2019

Mantyh, P. W. (2014). Bone Cancer Pain. *Curr. Opin. Support. Palliat. Care* 8 (2), 83–90. doi:10.1097/SPC.0000000000000048

Mir, F. A., and Jha, S. K. (2021). Locus Coeruleus Acid-Sensing Ion Channels Modulate Sleep-Wakefulness and State Transition from NREM to REM Sleep in the Rat. *Neurosci. Bull.* 37, 684–700. doi:10.1007/s12264-020-00625-0

Nagae, M., Hiraga, T., and Yoneda, T. (2007). Acidic Microenvironment Created by Osteoclasts Causes Bone Pain Associated with Tumor Colonization. *J. Bone Miner Metab.* 25 (2), 99–104. doi:10.1007/s00774-006-0734-8

Nozu, T., Miyagishi, S., Kumei, S., Nozu, R., Takakusaki, K., and Okumura, T. (2019). Metformin Inhibits Visceral Allodynia and Increased Gut Permeability Induced by Stress in Rats. *J. Gastroenterol. Hepatol.* 34 (1), 186–193. doi:10.1111/jgh.14367

Okui, T., Hiasa, M., Ryumon, S., Ono, K., Kunisada, Y., Ibaragi, S., et al. (2021). The HMGB1/RAGE axis Induces Bone Pain Associated with Colonization of 4T1 Mouse Breast Cancer in Bone. *J. Bone Oncol.* 26, 100330. doi:10.1016/j.jbo.2020.100330

Qiu, F., Wei, X., Zhang, S., Yuan, W., and Mi, W. (2014). Increased Expression of Acid-Sensing Ion Channel 3 within Dorsal Root Ganglia in a Rat Model of Bone Cancer Pain. *Neuroreport* 25 (12), 887–893. doi:10.1097/WNR.0000000000000182

Romero-Morelos, P., Ruvalcaba-Paredes, E., Garciadiego-Cázares, D., Pérez-Santos, M., Reyes-Long, S., Alfaro-Rodriguez, A., et al. (2021). Neurophysiological Mechanisms Related to Pain Management in Bone Tumors. *Curr. Neuropharmacol* 19, 308–319. doi:10.2174/1570159X18666201111112748

Rosenberger, D. C., Binzen, U., Treede, R.-D., and Greffrath, W. (2020). The Capsaicin Receptor TRPV1 Is the First Line Defense Protecting from Acute Non Damaging Heat: a Translational Approach. *J. Transl Med.* 18 (1), 28. doi:10.1186/s12967-019-02200-2

Roshan, M. H., Shing, Y. K., and Pace, N. P. (2019). Metformin as an Adjuvant in Breast Cancer Treatment. *SAGE Open Med.* 7, 205031211986511. doi:10.1177/2050312119865114

Russe, O. Q., Möser, C. V., Kynast, K. L., King, T. S., Stephan, H., Geisslinger, G., et al. (2013). Activation of the AMP-Activated Protein Kinase Reduces Inflammatory Nociception. *The J. Pain* 14 (11), 1330–1340. doi:10.1016/j.jpain.2013.05.012

Sheng, H.-Y., and Zhang, Y.-Q. (2020). Emerging Molecular Targets for the Management of Cancer Pain. *Neurosci. Bull.* 36 (10), 1225–1228. doi:10.1007/s12264-020-00526-2

Shenoy, P. A., Kuo, A., Leparc, G., Hildebrandt, T., Rust, W., Nicholson, J. R., et al. (2019). Transcriptomic Characterisation of the Optimised Rat Model of Walker 256 Breast Cancer Cell-Induced Bone Pain. *Clin. Exp. Pharmacol. Physiol.* 46 (12), 1201–1215. doi:10.1111/1440-1681.13165

Sindhi, V., and Erdek, M. (2019). Interventional Treatments for Metastatic Bone Cancer Pain. *Pain Manage.* 9 (3), 307–315. doi:10.2217/pmt-2018-0073

Sondermann, J. R., Barry, A. M., Jahn, O., Michel, N., Abdelaziz, R., Kügler, S., et al. (2019). Vti1b Promotes TRPV1 Sensitization During Inflammatory Pain. *Pain* 160 (2), 508–527. doi:10.1097/j.pain.0000000000001418

Wu, L.-J., Duan, B., Mei, Y.-D., Gao, J., Chen, J.-G., Zhuo, M., et al. (2004). Characterization of Acid-Sensing Ion Channels in Dorsal Horn Neurons of Rat Spinal Cord. *J. Biol. Chem.* 279 (42), 43716–43724. doi:10.1074/jbc.M403557200

Wu, Y., Wang, Y., Wang, J., Fan, Q., Zhu, J., Yang, L., et al. (2019). TLR4 Mediates Upregulation and Sensitization of TRPV1 in Primary Afferent Neurons in 2,4,6-trinitrobenzene Sulfate-Induced Colitis. *Mol. Pain* 15, 174480691983001. doi:10.1177/1744806919830018

Xue, J., Li, L., Li, N., Li, F., Qin, X., Li, T., et al. (2019). Metformin Suppresses Cancer Cell Growth in Endometrial Carcinoma by Inhibiting PD-L1. *Eur. J. Pharmacol.* 859, 172541. doi:10.1016/j.ejphar.2019.172541

Yu, J., Luo, Y., Jin, H., Lv, J., Zhou, T., Yabasin, I. B., et al. (2020). Scorpion Alleviates Bone Cancer Pain through Inhibition of Bone Destruction and Glia Activation. *Mol. Pain* 16, 174480692090999. doi:10.1177/1744806920909993

Yu, X.-J., Zhao, Y.-N., Hou, Y.-K., Li, H.-B., Xia, W.-J., Gao, H.-L., et al. (2019). Chronic Intracerebroventricular Infusion of Metformin Inhibits Salt-Sensitive Hypertension via Attenuation of Oxidative Stress and Neurohormonal Excitation in Rat Paraventricular Nucleus. *Neurosci. Bull.* 35 (1), 57–66. doi:10.1007/s12264-018-0308-5

Zhang, Y., Zhang, X., Xing, Z., Tang, S., Chen, H., Zhang, Z., et al. (2020). circStrn3 Is Involved in Bone Cancer Pain Regulation in a Rat Model. *Acta Biochim. Biophys. Sin (Shanghai)* 52 (5), 495–505. doi:10.1093/abbs/gmaa018

Zhou, Y.-L., Jiang, G.-Q., Wei, J., Zhang, H.-H., Chen, W., Zhu, H., et al. (2015). Enhanced Binding Capability of Nuclear Factor-Kb with Demethylated P2X3 Receptor Gene Contributes to Cancer Pain in Rats. *Pain* 156 (10), 1892–1905. doi:10.1097/j.pain.0000000000000248

Conflict of Interest: The authors declare that the research was conducted in the absence of any commercial or financial relationships that could be construed as a potential conflict of interest.

frontiers in Pharmacology

SYSTEMATIC REVIEW
published: 10 January 2022
doi: 10.3389/fphar.2021.805854

Tannins in the Treatment of Diabetic Neuropathic Pain: Research Progress and Future Challenges

Norsuhana Omar[1], *Che Aishah Nazariah Ismail*[1] *and Idris Long*[2]*

[1]*Department of Physiology, School of Medical Sciences, Health Campus, Universiti Sains Malaysia, Kubang Kerian, Malaysia,* [2]*Biomedical Science programme, School of Health Sciences, Health Campus, Universiti Sains Malaysia, Kubang Kerian, Malaysia*

Diabetes mellitus and its consequences continue to put a significant demand on medical resources across the world. Diabetic neuropathic pain (DNP) is a frequent diabetes mellitus chronic microvascular outcome. Allodynia, hyperalgesia, and aberrant or lack of nerve fibre sensation are all symptoms of DNP. These clinical characteristics will lead to worse quality of life, sleep disruption, depression, and increased mortality. Although the availability of numerous medications that alleviate the symptoms of DNP, the lack of long-term efficacy and unfavourable side effects highlight the urgent need for novel treatment strategies. This review paper systematically analysed the preclinical research on the treatment of DNP using plant phytochemicals that contain only tannins. A total of 10 original articles involved in *in-vivo* and *in-vitro* experiments addressing the promising benefits of phytochemical tannins on DNP were examined between 2008 and 2021. The information given implies that these phytochemicals may have relevant pharmacological effects on DNP symptoms through their antihyperalgesic, anti-inflammatory, and antioxidant properties; however, because of the limited sample size and limitations of the studies conducted so far, we were unable to make definitive conclusions. Before tannins may be employed as therapeutic agents for DNP, more study is needed to establish the specific molecular mechanism for all of these activities along the pain pathway and examine the side effects of tannins in the treatment of DNP.

Keywords: diabetes mellitus, plant phytochemicals, tannins, diabetic neuropathic pain (DNP), preclinical

OPEN ACCESS

Edited by:
Rajeev K. Singla,
Sichuan University, China

Reviewed by:
Santina Chiechio,
University of Catania, Italy
Nisar Ahmad,
University of Peshawar, Pakistan

***Correspondence:**
Idris Long
idriskk@usm.my

Specialty section:
This article was submitted to Ethnopharmacology, a section of the journal Frontiers in Pharmacology

Received: *31 October 2021*
Accepted: *15 December 2021*
Published: *10 January 2022*

Citation:
Omar N, Ismail CAN and Long I (2022) Tannins in the Treatment of Diabetic Neuropathic Pain: Research Progress and Future Challenges. Front. Pharmacol. 12:805854. doi: 10.3389/fphar.2021.805854

INTRODUCTION

Diabetic neuropathic pain (DNP) is the most prevalent diabetes complication, affecting more than half of patients, and is associated with increased morbidity and mortality (Feldman et al., 2017). Tingling, burning, sharp, shooting, and lancinating, as well as electric shock sensations, are all symptoms of DNP. These signs lead to diminished daily routines, higher unemployment rates, sleep disruption, stress and mental health problems, physical co-morbidities, and even amputation (Gylfadottir et al., 2019). The pathogenesis of DNP is not fully understood. Several theories have been proposed to explain the pain associated with diabetic neuropathy, including changes in the blood vessels that supply the peripheral nerves; a neuroinflammation process accompanied by glial cell activation; changes in sodium and calcium channel expression; and, more recently, central pain mechanisms, including increased thalamic vascularity and an imbalance of the facilitatory/inhibitory pathways (Tesfaye et al., 2013).

The molecular mechanism of DNP might also be related to an imbalance in the generation of oxidative stress and antioxidant activity. Prolonged hyperglycemia causes glucotoxicity, which

impairs several biological metabolome pathways such as the polyol, hexosamine, poly (ADP-ribose) polymerase (PARP), protein kinase C (PKC) and generation of the advanced glycation end product (AGE) (Ab Hamid et al., 2021). These processes result in the increased formation of free radicals such as hydrogen peroxide (H_2O_2), nitric oxide (NO), and superoxide anion (O2-), which cause cellular damage (Vincent et al., 2004). Hyperglycemia also activates inflammatory signalling pathways, which excrete a variety of mediators that aggravate the situation and contribute to the development of DNP. Following chronic hyperglycemia, the persistent generation of pro-inflammatory insults such as TNF-α and IL-1β, as well as oxidative stress markers, activates Toll-like receptors (TLRs) (Lawrence, 2009). As a result, these mechanisms translocate Nuclear Factor kappa-light-chain-enhancer β (NF-κβ) into nuclei and activate the expression of NF-κβ-dependent genes such pro-IL-1β, pro-IL-18, and Nod-like receptor protein 3 (NLRP3). Increased NF-κβ activation causes a rise in the creation of additional pro-inflammatory and immunological cells, such as T-cells, which further destroys the cells (Liu et al., 2017). Furthermore, a study has revealed that non-neuronal cells such as microglia and astrocytes have a role in the pathogenesis of DNP in a hyperglycemic environment (Wang et al., 2014). The glial-neuron crosstalk generates pathological pain in DNP, including allodynia and hyperalgesia, by releasing a variety of inflammatory mediators (Ismail et al., 2020).

Only three drugs are currently authorised in the United States by Food and Drug Administration (FDA) to treat DNP, which are duloxetine, a selective serotonin and norepinephrine reuptake inhibitor, pregabalin, an anticonvulsant, and tapentadol, a dual-action opioid receptor agonist and norepinephrine reuptake inhibitor (Freeman, 2013). All these treatments reduce pain by 30–50% but are limitedly prescribed because of their side effects. Therefore, natural products from plant secondary metabolites are now widely used to treat various chronic illnesses due to their low toxicity and high efficacy (Uddin et al., 2020).

Tannins are high-molecular-weight polyphenolic compounds found in a variety of plant species. Tannins bind to proteins and other chemical molecules, such as amino acids and alkaloids, and cause them to precipitate. The two most common tannin types are hydrolysable tannins and condensed tannins. Examples of hydrolysable tannins are gallic and ellagic acid. Whereas condensed tannins are gallocathecin, epigallocathecin, proanthocynidins and procynidin B2 (Laddha and Kulkarni, 2019). Tannins can be found in coffee, tea, wine, grapes, apricot, barley, peaches, dry fruits, mint, basil, rosemary, pomegranate, strawberries, amla, clove, rice, oat, rye, and other foods. Tannins are gaining popularity these days due to the health advantages linked with their antioxidant qualities (Ajebli and Eddouks, 2018).

Despite the health benefits of tannins, there are no systematic evaluations on tannins' potential for treating DNP. Therefore, this study examined and synthesised research on tannins on DNP in *in-vivo* and *in-vitro* experiments to determine their antinociceptive effects in neuropathic pain models.

MATERIALS AND METHODS

For this systematic search, we developed a search strategy to identify relevant works of literature. This search strategy was limited to English articles. It used different combinations of the following keywords: neuropathic pain, plants metabolite, natural product, tannins, gallic acid, ellagic acid, epigallocatechin, and proanthocynidins in three databases: Scopus, PubMed, and Google Scholar.

The databases were combed for studies that took place between 2008 and August 2021. Only DNP studies that included *in-vivo* and *in-vitro* experiments were included, as well as the use of compounds containing only phytochemical tannins (gallic acid, ellagic acid, epigallocatechin, and proanthocynidins) derived from medicinal plants for treatment. Studies were excluded according to the following exclusion criteria: studies in human beings and non-diabetic neuropathic pain, studies using polyphenol that contain another polyphenol such as coumarins and flavonoid, extracts or mixtures (as essential oils), review articles, meta-analyses, abstracts, conference proceedings, editorials/letters and case reports as shown in **Figure 1** (PRISMA statement).

RESULTS

A total of 222 abstracts/citations were identified from the electronic search for preliminary review. After the removal of duplicates and screening for relevant titles and abstracts, a total of 27 articles were submitted for a full-text review. Ten articles fulfilled the inclusion and exclusion criteria established. In most articles analysed, the substances used were purchased commercially (70%). Only three studies were conducted as compounds isolated from plants (30%). **Table 1** and **Table 2** shows the summary of experimental studies using tannins phytochemical in DNP and composition of substances used.

DISCUSSION

Male rats from various species such as Swiss albino (Abo-Salem et al., 2020), Sprague-Dawley (Ding et al., 2014; Addepalli and Suryavanshi, 2018), Wistar (Cui et al., 2008; Piaulino et al., 2013; Raposo et al., 2015) and albino Wistar (Baluchnejadmojarad and Roghani, 2012) were used in the majority of the studies as DNP models. Two more studies used male Swiss Webster (Raafat and Samy, 2014) and C57BL/6J mice (Jin et al., 2013), while two investigations used cell cultures of dorsal root ganglion neuron (Zhang et al., 2018) and RSC96 Schwann cells (Ding et al., 2014) as a model for DNP. The most common technique for inducing diabetes and simulating the DNP is a single dose of streptozotocin (STZ) injection into the intraperitoneal and the tail vein. Other substances, such as alloxan, have also been used to cause diabetes. Mostly the rats or mice induced to be diabetic in these studies were type 1 diabetes. Diabetes can also be generated by changes in diet, such as a high carbohydrate and fat diet, which can lead to type 2 diabetes (Jin et al., 2013; Ding et al., 2014). However, we did

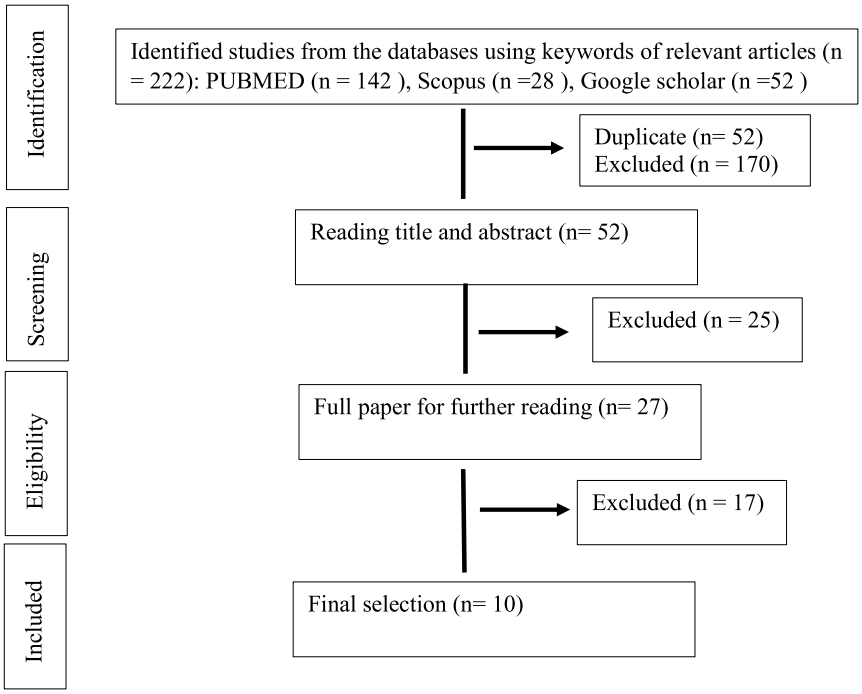

FIGURE 1 | Search and selection results (PRISMA statement).

not find a study to investigate the effects of phytochemical tannins on DNP using genetic modification in rats or mice.

Hyperalgesia and allodynia are symptoms of DNP linked to long-term hyperglycemia, insulin insufficiency or resistance, and dyslipidemia (Kim and Feldman, 2012). Many of the diabetes medications developed aimed to correct these problems and restore the situation by reducing the blood glucose level and increasing body weight. It has been demonstrated that taking (−) -Epigallocatechin-3-O-gallate (EGCG) orally at a dose of 25 mg/kg for 5 weeks can lower serum blood glucose levels, improve serum lipid profiles, and increase body weight (Abo-Salem et al., 2020). Other studies were done by Addepalli and Suryavanshi (2018) used catechin, Raafat and Samy (2014) used *Punica granatum L.* (Lythraceae) extract, and Baluchnejadmojarad and Roghani (2012) used EGCG have validated the benefits of phytochemical tannins in lowering blood glucose and increasing body weight. However, other investigations using EGCC and stem bark extracts of *Cenostigma macrophyllum Tul* (Fabaceae) on male Wistar rats by Raposo et al. (2015) and Piaulino et al. (2013) failed to restore blood glucose levels and body weight gain. A study by Cui et al. (2008) used grape seed proanthocynidins on male Wistar rats and found that they could lower HbA1c and AGEs while increasing body weight but not blood glucose levels. In high glucose dorsal root ganglia (DRG) culture, administration of Proanthocyanidin B2 (10 μg/ml) restored the neurotoxic effect generated by glucose challenge (Zhang et al., 2018). The primary afferent neurons in the DRG are altered by incubated with high glucose concentration. This glucose challenge causes hyperglycemia, which inhibits neuronal development and causes oxidative stress and mitochondrial malfunction, leading to apoptotic cell death in DRG (Chowdhury et al., 2010; Akude et al., 2011).

Furthermore, phytochemical tannin treatment did not much affect blood glucose levels or body weight gain in a type 2 DNP animal model. Ding et al. (2014) observed that grape seed proanthocynidins did not affect blood glucose levels or body weight in male Sprague–Dawley rats fed with a high-carbohydrate, high-fat diet with two injections of 25 mg/kg of STZ. Jin et al. (2013) discovered that providing a high-fat diet to male C57BL/6J mice and given *Vitis vinifera L.* (Vitaceae) grape seed extract (VVE) did not lower blood glucose levels while simultaneously not increasing body weight. Insulin resistance and insulin insufficiency are two characteristics of type 2 diabetes. The natural mechanism of metabolic dysfunctions in human type 2 diabetes would be precisely mimicked by feeding the animal a high carbohydrate and high-fat diet followed by a low-dose STZ injection (Srinivasan et al., 2005). Insulin resistance, one of the critical characteristics of type 2 diabetes, is triggered by a high carbohydrate and fat diet. Low-dose STZ injections can cause a modest decrease in insulin production, similar to the latter stages of type 2 diabetes (Stott and Marino, 2020). However, the benefit of phytochemical tannin treatment on hyperglycemia and body weight in the DNP animal model is equivocal, with findings varying depending on the rat species, types of diabetes, DNP induction techniques, and substances delivery procedures.

Phytochemical tannins have been shown to have neuroprotective benefits in diabetic complications due to their anti-inflammatory and antioxidant characteristics (Meng et al., 2019). When EGCG was given orally at a 25 mg/kg dose for 5 weeks, inflammatory markers such as plasma IL-6, NO NO, and

TABLE 1 | Characteristic of included studies.

Compound, plants species, source, concentration	Tannins constituents	Type of study, animals and diabetic model	Control group and duration of treatment	Daily dose (mg/kg) and routes of administration	Outcomes	References/country
Pure compound (Sigma Aldrich)	(–)-epigallocatechin-3-O-gallate	*In vivo* Male Swiss albino rats Single injection of STZ (55 mg/kg, i.p)	No treatment (–ve control) 5 weeks	25 mg/kg/orally/ once/daily after fourth day diabetes induction	Reduce blood glucose Increase Body weight Improved serum lipids profile Ameliorated plasma level of Nitric oxide (NO), IL-6 and TNF-α level Reduced diabetes-induced hyperalgesia in the behavioural tests (hot plate, formalin, tail immersion and carrageenan-induced oedema model)	Egypt, (Abo-Salem et al., 2020)
Pure compound (Sigma Aldrich)	Catechin	*In vivo* Male Sprague Dawley rats. Single injection of STZ (55 mg/kg, i.p.)	No treatment (–ve control) 28 days	25 mg/kg and 50 mg/kg orally after 6 weeks of diabetes induction	Reduce blood glucose Increased body weight Reduced Malondialdehyde (MDA) Increased glutathione (GSH), catalase, Superoxide dismutase (SOD) Reduced MMP-9	India, (Addepalli and Suryavanshi, 2018)
Pure compound (Sigma Aldrich)	Proanthocyanidin B2	*In-vitro* Dorsal root ganglion neuron culture. Incubated with 45 mM high-glucose	Incubated in neurobasal medium (–ve control) 24 h	10 μg/ml	Decreased Neuronal ROS Increased Neurite outgrowth Decreased apoptosis Increased cell viability increased GAP-43 mRNA	China, (Zhang et al., 2018)
Pure compound (Holliday and Co. Canada)	Epigallocatechin-gallate	*In vivo* Adult male Wistar rats. Intraperitoneal (i.p.) injection of STZ (60 mg/kg body weight	Injected with citrate buffer (–ve control) 10 weeks	2 g/L in drinking water	Not affected blood glucose level Not affected body weight Reduced 8-OHdG immunoreaction Reduced c-Fos IR neurons in the spinal cord Amelioration of tactile allodynia and mechanical hyperalgesia	Portugal, (Raposo et al., 2015)
Punica granatum L. (Lythraceae) extract (Ibn-Al-Nafess herbalist, Beirut, Lebanon)	gallic acid	*In vivo* Male Swiss-Webster mice. Alloxan (180 mg/kg) every 48 h for 3 time	Vehicle (0.9% sterile saline (–ve control) 1 day (acute) and 7 days (subacute)	25, 50, and 100 mg/kg, i.p after fourth day diabetes induction	Reduce blood glucose Increase Body weight Rise serum catalase activity Improvement in hot plate latency Improvement in tail-flick latency	Lebanon, (Raafat and Samy, 2014)

(Continued on following page)

TABLE 1 | (*Continued*) Characteristic of included studies.

Compound, plants species, source, concentration	Tannins constituents	Type of study, animals and diabetic model	Control group and duration of treatment	Daily dose (mg/kg) and routes of administration	Outcomes	References/country
Pure compound Grape seed proanthocyanidins (Jianfeng Natural Product. Co. Ltd. (Tianjin China))	proanthocyanidins	*In vivo* Male Sprague–Dawley rats. Induced diabetes by 8 weeks of the high-carbohydrate/high fat diet and 2 injections of 25 mg/kg BW streptozotocin	Vehicle-treated (–ve control) 24 weeks	250 mg/kg by stomach tube	Blood glucose and body weight are not affected Increased the level of nerve conduction velocity (NCV) Reduced the concentration of free Ca^{2+} and ER stress markers	China, (Ding et al., 2014)
		In vitro RSC96 Schwann cells (SC) Challenged with DMEM containing 10% serum from diabetic rats	Cells treated with 10% serum from healthy rats (–ve control) 48 h	5, 10 and 20 μmol/L	Ameliorated cell injury Decreased cytoplasmic free Ca^{2+} Alleviated ER stress Decreased GRP78 and phospho-JNK expression	
Vitis vinifera L. (Vitaceae) grape seed extract	Proanthocyanidins	*In vivo* Male C57BL/6J mice. High Fat diet.	Normal diet (–ve control) 12 weeks	100 mg/kg and 250 mg/kg dissolved in drinking water, given orally once per day	Not reduced plasma blood glucose Reduced body weight gain Increased IENF (intraepidermal innervation nerve fiber)	Korea, (Jin et al., 2013)
Cenostigma macrophyllum Tul. (Fabaceae) Stem bark extracts	ellagic acid and valoneic acid dilactone	*In vivo* Male Wistar rats. streptozotocin (STZ, 40 mg/kg, i.v.)	No treatment (–ve control) STZ + insulin 2.5U (+ve control) 5 weeks	Ethanol extract (200 and 300 mg/kg, p.o.(chronic)	Not affected blood glucose and body weight	Brazil, (Piaulino et al., 2013)
				Ethyl acetate fraction (250 and 500 mg/kg, p.o.) after 28 days' diabetic induction. (acute)	Increase the pain threshold	
Pure compound [Sigma (St. Louis, MO)]	Epigallocatechin-gallate	*In vivo* Male albino Wistar rats. Single injection of STZ (60 mg/kg, i.p.)	Normal saline (–ve control) 7 weeks	20 and 40 mg/kg orally after 1 week diabetes induction	Reduce blood glucose Increased body weight lower nociceptive scores in both phases of the formalin test Increased tail flick response latency Increased the vocalization threshold in Randall-Selitto test (mechanical hyperalgesia) Reduced MDA, NO and increased SOD activity	Iran, (Baluchnejadmojarad and Roghani, 2012)
Pure compound (Jianfeng Natural Product. Co. Ltd. (Tianjin China))	Grape seed proanthocynidins	Male Wistar rat. Single injection of STZ (55 mg/kg, into tail vein)	Vehicle-treated (–ve control) 24 weeks	250 mg/kg/daily intragastric after 1 week diabetes induction	Reduced HbA1c and AGEs but not plasma blood glucose Increased body weight Increased withdrawal threshold in von Frey test Decreased MDA and increased SOD activity	China, (Cui et al., 2008)

TABLE 2 | The plants botanical and chemical composition.

Study	Compound, concentration	Source	Purity (%) (and grade if applicable)	Quality control reported? (Y/N)
(Abo-Salem et al., 2020)	Pure compound	Sigma Aldrich	≥90%	Y-HPLC
(Addepalli and Suryavanshi, 2018)	Pure compound	Sigma Aldrich	≥90%	Y-HPLC
(Zhang et al., 2018)	Pure compound	Sigma Aldrich	≥90%	Y-HPLC
(Raposo et al., 2015)	Pure compound	Holliday and co. Canada	≥90%	Y-HPLC
(Ding et al., 2014)	Pure compound	Jianfeng Natural Product. Co. Ltd. (Tianjin China)	≥90%	Y-HPLC
(Cui et al., 2008)	Pure compound	Jianfeng Natural Product. Co. Ltd. (Tianjin China)	≥90%	Y-HPLC and GCMS.
(Baluchnejadmojarad and Roghani, 2012)	Pure compound	Sigma (St. Louis, MO)	≥90%	Y-HPLC

Study	Species, source, concentration	Quality control reported? (Y/N)	Chemical analysis reported? (Y/N)
(Raafat and Samy, 2014)	Dried *Punica granatum L.* (Lythraceae) fruit, Ibn-Al-Nafess herbalist, Beirut, Lebanon	Y-Authenticated with reference sample and voucher specimen (PS-13–11) deposited in the faculty herbarium	Y-HPLC
(Jin et al., 2013)	*Vitis vinifera L.* (Vitaceae) grape seed extract, Korea Hanlim Co. (Seoul, Korea)	Y-Prepared according to this protocol. The seeds of ripe grape were separated from pulp and shade-dried. Then the seeds were crushed into a powder. Seed material (1 kg) was extracted with 300 ml distilled water and 200 ml acetone. Then the extract was filtered and concentrated to a volume of 100–150 ml. Chloroform was added and the filtrates were pooled and evaporated below 50°C in a vacuum drier to yield final preparation of 3.5 g	Y-HPLC
(Piaulino et al., 2013)	Stem bark of *Cenostigma macrophyllum Tul.* (Fabaceae) was collected surrounding the Federal University of Piaui, Teresina, Brazil	Y-Authenticated with voucher specimen (TEPB 10.374) deposited in Graziela Barroso herbarium of Federal University of Piaui, Teresina, Brazil	Y- Thin layer chromatography

TNF-α were reduced (Abo-Salem et al., 2020). When given orally at dosages of 25 mg/kg and 50 mg/kg for 28 days, catechin can reduce matrix metalloproteinase-9 (MMP-9) levels (Addepalli and Suryavanshi, 2018). Raposo et al. (2015) discovered that EGCC at a dose of 2 g/L in drinking water for 10 weeks decreased Fos IR neurons in male Wistar rats, a marker for nociceptive response.

In addition to their anti-inflammatory properties, phytochemical tannins play a crucial role in preventing DNP because of their antioxidant activity. Catechin (25 mg/kg and 50 mg/kg orally for 28 days) decreased malondialdehyde (MDA) but raised the reduced glutathione (GSH), catalase, and superoxide dismutase (SOD) levels in STZ-induced diabetic rats (Addepalli and Suryavanshi, 2018). Baluchnejadmojarad and Roghani (2012) and Cui et al. (2008) investigations also revealed comparable impact. In STZ-induced diabetes, in male albino Wistar rats, treatment with EGCG (20 and 40 mg/kg BW orally) for 7 weeks decreased blood MDA and NO levels while increasing SOD level (Baluchnejadmojarad and Roghani, 2012). In STZ-induced diabetic male Wistar rats, grape seed proanthocynidins (250 mg/kg/daily intragastric) therapy for 24 weeks decreased plasma MDA and elevated SOD levels (Cui et al., 2008). Raposo et al. (2015) found that early treatment with EGCG decreased the 8-hydroxy-21-deoxyguanosine (8-OHdG) immunoreaction, preventing oxidative stress damage (Raposo et al., 2015).

In tunicamycin-treated sciatic nerves and rat Schwann cells (RSC cells), administration of proanthocyanidin and its metabolites catechin and epicatechin decreased cell damage. It downregulated the expression level of endoplasmic reticulum (ER) stress proteins (Ding et al., 2014). Schwann cells (SC) create lipid-rich myelin sheaths to extend their plasma membrane to conduct the action potential along axons and maintain axonal integrity (Eckersley, 2002). SC must generate many myelin membrane proteins, cholesterol, and membrane lipids through the secretory route during the active phase of myelination (Clague and Hammond, 2006). Demyelination and axonal degeneration, which are early stages of DNP, can be caused by disruptions in the secretory system, dependent on ER homeostasis (Lin and Popko, 2009).

Treatment with phytochemical tannins has also been shown to help with DNP hyperalgesia and allodynia symptoms. Its anti-inflammatory, antioxidant, and antihyperalgesic properties are thought to be the mechanism for decreasing these symptoms (Stott and Marino, 2020). According to Abo-Salem et al. (2020), treatment with EGCG alleviated hyperalgesia responses indicated

by a hot plate, tail immersion, formalin, and carrageenan-induced oedema tests in STZ-induced diabetic rats. After being treated with EGCG for 10 weeks, STZ-induced diabetics also had a higher paw withdrawal threshold (PWT), indicating that tactile allodynia and mechanical hyperalgesia had improved (Raposo et al., 2015). In diabetic rats, chronic EGCG therapy (40 mg/kg) dramatically reduced hyperalgesia (formalin test, hot tail immersion test, and paw pressure test) as compared to untreated diabetics (Baluchnejadmojarad and Roghani, 2012). In the hot plate and tail-flick tests, *Punica granatum L.* (Lythraceae) extract significantly reduced thermal and tail-flick latency in alloxan-induced diabetic mice (Raafat and Samy, 2014). Piaulino et al. (2013) found that treating diabetic Wistar rats with stem bark extracts of *Cenostigma macrophyllum Tul.*(Fabaceae) raised mechanical nociceptive threshold (MNT) by using von Frey filaments as compared to untreated diabetic rats. In diabetic rats, grape seed proanthocyanidin extract can also reduce mechanical allodynia by the von Frey test (Cui et al., 2008).

STRENGTH AND LIMITATION

This study offers a thorough evaluation of research progress on tannins and their efficacy in the treatment of symptomatic DNP. Tannins have been shown to alleviate the hyperalgesia and allodynia symptoms associated with DNP through their anti-inflammatory, antioxidant, and antihyperalgesic properties. We discovered the most relevant articles since we took a thorough approach with all search keywords. This study can be used as a baseline to offer information regarding the efficacy of tannins as a therapeutic therapy for symptomatic DNP. Phytochemical tannins have anti-inflammatory, antioxidant, and antihyperalgesic properties to help with the hyperalgesia and allodynia symptoms of DNP. However, we could not draw any definitive findings because of the small sample size. Attempts to re-investigate also fell short of including new tannins and DNP treatment data.

There are limitations to the research conducted thus far to examine the potential of tannins in DNP. The drawback of the tannins studies and their efficacy on symptomatic DNP was that some of the models employed did not entirely replicate the DNP condition. Zhang et al. (2018) employed DRG culture in high glucose conditions, which did not accurately imitate the situation of DNP *in vivo*. *In-vivo* trials, on the other hand, lacked a control group that was treated with current medications authorised to treat symptomatic DNP for comparison. Many research intended to lower blood glucose levels and increase body weight, primarily the type 1 diabetes model but did not compare their findings to those treated with metformin and insulin. Metformin and insulin are the medication taken by the diabetic patient to control their glucose level in the blood. Tannins anti-inflammatory, antioxidant, and antihyperalgesic properties are also not comparable to those of other approved drugs such as duloxetine, pregabalin, and tapentadol (Freeman, 2013).

Tannins research as a possible symptomatic DNP therapy has yet to identify a specific molecular basis for its anti-inflammatory, antioxidant, and antihyperalgesic properties. Only Zhang et al. (2018) proposed that the PI3K/Akt signalling pathway was engaged in the neurotoxicity of high glucose conditions in DRG culture. Furthermore, most research concentrates exclusively on behaviour analysis and changes in inflammatory markers, with a little examination into molecular changes in the expression of specific genes, proteins, and receptors along the pain pathway, which begins in the peripheral nervous system and ends in the brain. There is no evidence on whether tannins can modify these specific genes, proteins, and receptors to decrease DNP symptoms. Furthermore, no toxicological studies have been conducted to examine the toxicities of tannins on liver and kidney biochemical markers.

PRIORITIES FOR FUTURE RESEARCH

A future investigation on tannins and their efficacy on DNP symptoms should reveal a precise molecular mechanism for their anti-inflammatory, antioxidant, and antihyperalgesic effects along the pain pathway. To investigate the effectiveness of tannins, a suitable *in vitro* and *in vivo* model to simulate the situation at the periphery, spinal cord, and brain during DNP and changes in particular genes, proteins, and receptors when treated with tannins, is required. In treating DNP symptoms, a specific molecular pathway connected to anti-inflammatory, antioxidant, and antihyperalgesic properties of tannins must be targeted and investigated to elucidate its molecular function better. A comparison of the effects of tannins and approved drugs on DNP symptoms is also required to see whether tannins' results are equal or even superior to all of these treatments. Because the aetiology of DNP includes multiple elements and pathways, a combination of medications may be effective.

CONCLUSION

Tannins, a phytochemical, help to alleviate DNP symptoms. These results are due to its hypoglycaemic effect, most visible in type 1 diabetic rats but not in type 2 diabetic rats. Phytochemical tannins lower blood glucose levels while increasing body weight in insulin insufficiency (type 1 diabetes), but not in insulin resistance or hyperlipidaemia studies (type 2 diabetes). Phytochemical tannins can be used as an anti-inflammatory, antioxidant, and antihyperalgesic to help with the hyperalgesia and allodynia symptoms of DNP. Tannins, a phytochemical, might potentially be used to treat DNP. However, we could not make definitive conclusions because of the limited sample size and limitations of the studies conducted. Before tannins may be employed as

therapeutic agents for DNP, more study is needed to establish the specific molecular mechanism for all of these tannins properties along the pain pathway and examine the side effects of tannins in the treatment of DNP.

DATA AVAILABILITY STATEMENT

The original contributions presented in the study are included in the article/Supplementary Materials, further inquiries can be directed to the corresponding author.

AUTHOR CONTRIBUTIONS

IL provided funding and prepared the manuscript, while CI and NO proofread this manuscript.

FUNDING

This study was supported by the Fundamental Research Grant Scheme (FRGS) Ministry of Higher Education Malaysia (No. FRGS/1/2020/SKK0/USM/03/5).

REFERENCES

Ab Hamid, N., Omar, N., Ismail, C. A. N., and Long, I. (2021). Insight of Mechanism and Signaling Pathway in Pathogenesis of Diabetic Neuropathy: A Review. *IIUM Med. J. Malaysia* 20 (4), 95–103. doi:10.31436/imjm.v20i4.1947

Abo-Salem, O. M., Ali, T. M., Harisa, G. I., Mehanna, O. M., Younos, I. H., and Almalki, W. H. (2020). Beneficial Effects of (-)-Epigallocatechin-3-O-Gallate on Diabetic Peripheral Neuropathy in the Rat Model. *J. Biochem. Mol. Toxicol.* 34 (8), e22508. doi:10.1002/jbt.22508

Addepalli, V., and Suryavanshi, S. V. (2018). Catechin Attenuates Diabetic Autonomic Neuropathy in Streptozotocin Induced Diabetic Rats. *Biomed. Pharmacother.* 108 (July), 1517–1523. doi:10.1016/j.biopha.2018.09.179

Ajebli, M., and Eddouks, M. (2018). The Promising Role of Plant Tannins as Bioactive Antidiabetic Agents. *Curr. Med. Chem.* 26 (25), 4852–4884. doi:10.2174/0929867325666180605124256

Akude, E., Zherebitskaya, E., Chowdhury, S. K., Smith, D. R., Dobrowsky, R. T., and Fernyhough, P. (2011). Diminished Superoxide Generation Is Associated with Respiratory Chain Dysfunction and Changes in the Mitochondrial Proteome of Sensory Neurons from Diabetic Rats. *Diabetes* 60 (1), 288–297. doi:10.2337/db10-0818

Baluchnejadmojarad, T., and Roghani, M. (2012). Chronic Oral Epigallocatechin-Gallate Alleviates Streptozotocin-Induced Diabetic Neuropathic Hyperalgesia in Rat: Involvement of Oxidative Stress. *Iran J. Pharm. Res.* 11 (4), 1243–1253.

Chowdhury, S. K., Zherebitskaya, E., Smith, D. R., Akude, E., Chattopadhyay, S., Jolivalt, C. G., et al. (2010). Mitochondrial Respiratory Chain Dysfunction in Dorsal Root Ganglia of Streptozotocin-Induced Diabetic Rats and its Correction by Insulin Treatment. *Diabetes* 59 (4), 1082–1091. doi:10.2337/db09-1299

Clague, M. J., and Hammond, D. E. (2006). Membrane Traffic: Catching the Lysosome Express. *Curr. Biol.* 16 (11), R416–R418. doi:10.1016/j.cub.2006.05.009

Cui, X. P., Li, B. Y., Gao, H. Q., Wei, N., Wang, W. L., and Lu, M. (2008). Effects of Grape Seed Proanthocyanidin Extracts on Peripheral Nerves in Streptozocin-Induced Diabetic Rats. *J. Nutr. Sci. Vitaminol (Tokyo)* 54 (4), 321–328. doi:10.3177/jnsv.54.321

Ding, Y., Dai, X., Zhang, Z., Jiang, Y., Ma, X., Cai, X., et al. (2014). Proanthocyanidins Protect against Early Diabetic Peripheral Neuropathy by Modulating Endoplasmic Reticulum Stress. *J. Nutr. Biochem.* 25 (7), 765–772. doi:10.1016/j.jnutbio.2014.03.007

Eckersley, L. (2002). Role of the Schwann Cell in Diabetic Neuropathy. *Int. Rev. Neurobiol.* 50 (February), 293–321. doi:10.1016/s0074-7742(02)50081-7

Feldman, E. L., Nave, K. A., Jensen, T. S., and Bennett, D. L. H. (2017). New Horizons in Diabetic Neuropathy: Mechanisms, Bioenergetics, and Pain. *Neuron* 93 (6), 1296–1313. doi:10.1016/j.neuron.2017.02.005

Freeman, R. (2013). New and Developing Drugs for the Treatment of Neuropathic Pain in Diabetes. *Curr. Diab Rep.* 13 (4), 500–508. doi:10.1007/s11892-013-0396-6

Gylfadottir, S. S., Weeracharoenkul, D., Andersen, S. T., Niruthisard, S., Suwanwalaikorn, S., and Jensen, T. S. (2019). Painful and Non-painful Diabetic Polyneuropathy: Clinical Characteristics and Diagnostic Issues. *J. Diabetes Investig.* 10 (5), 1148–1157. doi:10.1111/jdi.13105

Ismail, C. A. N., Suppian, R., Ab Aziz, C. B., and Long, I. (2020). Expressions of Spinal Microglia Activation, BDNF, and DREAM Proteins Correlated with Formalin-Induced Nociceptive Responses in Painful and Painless Diabetic Neuropathy Rats. *Neuropeptides* 79, 102003. doi:10.1016/j.npep.2019.102003

Jin, H. Y., Cha, Y. S., Baek, H. S., and Park, T. S. (2013). Neuroprotective Effects of Vitis vinifera Extract on Prediabetic Mice Induced by a High-Fat Diet. *Korean J. Intern. Med.* 28 (5), 579–586. doi:10.3904/kjim.2013.28.5.579

Kim, B., and Feldman, E. L. (2012). Insulin Resistance in the Nervous System. *Trends Endocrinol. Metab.* 23 (3), 133–141. doi:10.1016/j.tem.2011.12.004

Laddha, A. P., and Kulkarni, Y. A. (2019). Tannins and Vascular Complications of Diabetes: An Update. *Phytomedicine* 56 (August 2018), 229–245. doi:10.1016/j.phymed.2018.10.026

Lawrence, T. (2009). The Nuclear Factor NF-kappaB Pathway in Inflammation. *Cold Spring Harb Perspect. Biol.* 1 (6), a001651–11. doi:10.1101/cshperspect.a001651

Lin, W., and Popko, B. (2009). Endoplasmic Reticulum Stress in Disorders of Myelinating Cells. *Nat. Neurosci.* 12 (4), 379–385. doi:10.1038/nn.2273

Liu, T., Zhang, L., Joo, D., and Sun, S. C. (2017). NF-κB Signaling in Inflammation. *Signal. Transduct Target. Ther.* 2 (March). doi:10.1038/sigtrans.2017.23

Meng, J. M., Cao, S. Y., Wei, X. L., Gan, R. Y., Wang, Y. F., Cai, S. X., et al. (2019). Effects and Mechanisms of tea for the Prevention and Management of Diabetes Mellitus and Diabetic Complications: An Updated Review. *Antioxidants (Basel)* 8 (6), 170. doi:10.3390/antiox8060170

Piaulino, C. A., Carvalho, F. C., Almeida, B. C., Chaves, M. H., Almeida, F. R., and Brito, S. M. (2013). The Stem Bark Extracts of Cenostigma macrophyllum Attenuates Tactile Allodynia in Streptozotocin-Induced Diabetic Rats. *Pharm. Biol.* 51 (10), 1243–1248. doi:10.3109/13880209.2013.786096

Raafat, K., and Samy, W. (2014). Amelioration of Diabetes and Painful Diabetic Neuropathy by Punica Granatum L. Extract and its spray Dried Biopolymeric Dispersions. *Evid. Based Complement. Alternat Med.* 2014, 180495. doi:10.1155/2014/180495

Raposo, D., Morgado, C., Pereira-Terra, P., and Tavares, I. (2015). Nociceptive Spinal Cord Neurons of Laminae I-III Exhibit Oxidative Stress Damage during Diabetic Neuropathy Which Is Prevented by Early Antioxidant Treatment with Epigallocatechin-Gallate (EGCG). *Brain Res. Bull.* 110, 68–75. doi:10.1016/j.brainresbull.2014.12.004

Srinivasan, K., Viswanad, B., Asrat, L., Kaul, C. L., and Ramarao, P. (2005). Combination of High-Fat Diet-Fed and Low-Dose Streptozotocin-Treated Rat: A Model for Type 2 Diabetes and Pharmacological Screening. *Pharmacol. Res.* 52 (4), 313–320. doi:10.1016/j.phrs.2005.05.004

Stott, N. L., and Marino, J. S. (2020). High Fat Rodent Models of Type 2 Diabetes: From Rodent to Human. *Nutrients* 12 (12), 1–19. doi:10.3390/nu12123650

Tesfaye, S., Boulton, A. J., and Dickenson, A. H. (2013). Mechanisms and Management of Diabetic Painful Distal Symmetrical Polyneuropathy. *Diabetes Care* 36 (9), 2456–2465. doi:10.2337/dc12-1964

Uddin, M. S., Mamun, A. A., Rahman, M. A., Kabir, M. T., Alkahtani, S., Alanazi, I. S., et al. (2020). Exploring the Promise of Flavonoids to Combat Neuropathic Pain: From Molecular Mechanisms to Therapeutic Implications. *Front. Neurosci.* 14 (June), 478–518. doi:10.3389/fnins.2020.00478

Vincent, A. M., Russell, J. W., Low, P., and Feldman, E. L. (2004). Oxidative Stress in the Pathogenesis of Diabetic Neuropathy. *Endocr. Rev.* 25 (4), 612–628. doi:10.1210/er.2003-0019

Wang, D., Couture, R., and Hong, Y. (2014). Activated Microglia in the Spinal Cord Underlies Diabetic Neuropathic Pain. *Eur. J. Pharmacol.* 728 (1), 59–66. doi:10.1016/j.ejphar.2014.01.057

Zhang, Y. P., Liu, S. Y., Sun, Q. Y., Ren, J., Liu, H. X., and Li, H. (2018). Proanthocyanidin B2 Attenuates High-Glucose-Induced Neurotoxicity of Dorsal Root Ganglion Neurons through the PI3K/Akt Signaling Pathway. *Neural Regen. Res.* 13 (9), 1628–1636. doi:10.4103/1673-5374.237174

Conflict of Interest: The authors declare that the research was conducted in the absence of any commercial or financial relationships that could be construed as a potential conflict of interest.

Publisher's Note: All claims expressed in this article are solely those of the authors and do not necessarily represent those of their affiliated organizations, or those of the publisher, the editors and the reviewers. Any product that may be evaluated in this article, or claim that may be made by its manufacturer, is not guaranteed or endorsed by the publisher.

frontiers in Neuroscience

ORIGINAL RESEARCH
published: 03 February 2022
doi: 10.3389/fnins.2021.804722

Proanthocyanidins Inhibit the Transmission of Spinal Pain Information Through a Presynaptic Mechanism in a Mouse Inflammatory Pain Model

Hongwei Fan[1,2†], Zhenyu Wu[2,3†], DaYu Zhu[1,2], Junxiang Gu[2,4], Mang Xu[2,5], Mingzhe Zhang[2], Haokai Duan[2], Yunqing Li[1,2] and Tao Chen[1,2]*

[1] Department of Human Anatomy, Xuzhou Medical University, Xuzhou, China, [2] Department of Anatomy, Histology and Embryology, K. K. Leung Brain Research Centre, Fourth Military Medical University, Xi'an, China, [3] Epilepsy Center of Xijing Hospital, Fourth Military Medical University, Xi'an, China, [4] Department of Neurosurgery, The Second Affiliated Hospital of Xi'an Jiaotong University, Xi'an, China, [5] Department of Anatomy, Basic Medical College, Dali University, Dali, China

OPEN ACCESS

Edited by:
Gokhan Zengin, Selcuk University, Turkey

Reviewed by:
Rainer Viktor Haberberger, University of Adelaide, Australia
Ying Huang, Tongji University, China

***Correspondence:**
Tao Chen
chtkkl@fmmu.edu.cn

[†] *These authors share first authorship*

Specialty section:
This article was submitted to Neuropharmacology, a section of the journal Frontiers in Neuroscience

Received: *29 October 2021*
Accepted: *31 December 2021*
Published: *03 February 2022*

Citation:
Fan H, Wu Z, Zhu D, Gu J, Xu M, Zhang M, Duan H, Li Y and Chen T (2022) Proanthocyanidins Inhibit the Transmission of Spinal Pain Information Through a Presynaptic Mechanism in a Mouse Inflammatory Pain Model. Front. Neurosci. 15:804722. doi: 10.3389/fnins.2021.804722

Inflammatory pain is one of the most common symptoms of clinical pain that seriously affects patient quality of life, but it currently has limited therapeutic options. Proanthocyanidins, a group of polyphenols enriched in plants and foods, have been reported to exert anti-inflammatory pain-alleviating effects. However, the mechanism by which proanthocyanidins relieve inflammatory pain in the central nervous system is unclear. In the present study, we observed that intrathecal injection of proanthocyanidins inhibited mechanical and thermal pain sensitivity in mice with inflammatory pain induced by Complete Freund's Adjuvant (CFA) injection. Electrophysiological results further showed that proanthocyanidins inhibited the frequency of spontaneous excitatory postsynaptic currents without affecting the spontaneous inhibitory postsynaptic currents or the intrinsic properties of parabrachial nucleus-projecting neurons in the spinal cord. The effect of proanthocyanidins may be mediated by their inhibition of phosphorylated activation of the PI3K/Akt/mTOR pathway molecules in dorsal root ganglia neurons. In summary, intrathecal injection of procyanidin induces an obvious anti-inflammatory pain effect in mice by inhibiting peripheral excitatory inputs to spinal neurons that send nociceptive information to supraspinal areas.

Keywords: proanthocyanidins, inflammatory pain, spinal cord, excitatory postsynaptic currents, mice

INTRODUCTION

Inflammatory pain is caused by chemical or physical stimulation of damaged tissue (surgery, osteoarthritis or trauma, etc.). In the condition of inflammatory pain, the released chemical mediators act on the receptors located in the peripheral process of dorsal root ganglia (DRG) neurons and increase the afferent firing from their central process to the spinal dorsal horn, leading to the hyperactivity of spinal nociceptive neurons and inducing allodynia and hyperalgesia (Demir et al., 2013; Muley et al., 2016). In the spinal cord, neurons that send nociceptive information to

supraspinal areas are primarily located in lamina I of the dorsal horn, 95% of which project to the parabrachial nucleus (PBN). This type of projection neuron is also an important afferent target for the transmission of enhanced nociceptive information (Todd, 2010).

Proanthocyanidins are oligomers or polymers composed of units of flavanols extracted from cherry, grape seeds, cocoa, and other plants (Chacón et al., 2009). Their protective effects in nervous system diseases have received increasing attention in recent years. In addition to their widely known antioxidant, antiapoptotic, and antiallergic effects (Martinez-Micaelo et al., 2012, 2015), their roles in alleviating inflammatory pain have gradually been recognized. It has been reported that proanthocyanidins reduce the amount of abdominal writhing induced by intraperitoneal (*i.p.*) injection of acetic acid and decrease the duration of formalin-induced paw licking (Cordeiro et al., 2016), by peripherally inhibiting the inflammatory exudation (Sobrinho et al., 2017). Intra-articular injection of proanthocyanidins also inhibits the expression of inflammasomes in macrophages and relieves arthritis (Liu et al., 2017). However, these results primarily indicate that proanthocyanidins have anti-inflammatory effects by acting on peripheral tissues. Although Pan et al. (2018) reported that proanthocyanidins produce behavioral analgesia by inhibiting activated matrix metalloproteinase (MMP)-9 and MMP-2 in the spinal cord of mice with neuropathic pain, whether proanthocyanidins relieve inflammatory pain and the possible mechanism in regulating nociceptive information transmission in the central nervous system remain elusive.

Therefore, in the present study, we investigated whether and how proanthocyanidins induce antinociceptive effects at the spinal cord level in mice with inflammatory pain. We found that intrathecal administration of proanthocyanidins increased the mechanical and thermal pain threshold in mice 7 days after Complete Freund's Adjuvant (CFA) injection. Bath application of proanthocyanidins reduced excitatory peripheral inputs to PBN-projecting spinal cord neurons. Western blotting analysis further revealed that proanthocyanidins may inhibit the phosphorylated activation of PI3K/Akt/mTOR pathway molecules in the DRG neurons. Our work shows for the first time that the anti-inflammatory pain effect and mechanism of proanthocyanidins occur in the spinal cord of mice.

MATERIALS AND METHODS

Animals

The animals used in the experiment were all adult male C57BL/6 mice, 8–12 weeks of age, weighing 18–30 g. Forty mice were used for behavioral tests, 32 mice were used in Western blotting, and 65 mice were used in whole-cell patch experiments. All mice were raised in a pathogen-free environment with a constant temperature of 23°C, humidity of 50 ± 10%, 12 h light/dark cycle, and adequate food and water. The use agreement for experimental animals was approved by the Animal Care and Use Committee for Research and Education of the Fourth Military Medical University (Xi'an, China). All experiments were performed in a single-blind manner. The experimenters who collected the raw data were not aware of group allocation.

Drugs

Proanthocyanidins (natural extracts, CAS number: 4852-22-6, Molecular formula: C30H26O13, Molecular weight: 594.52) were purchased from Shanghai Yuanye Biotechnology (Shanghai Yuanye Biological Technology Co. Ltd.). The solution was dissolved in artificial cerebrospinal fluid (ACSF) to produce the original solution at a concentration of 8.41 mM, that is, 5 mg/ml. The final concentration was diluted in ACSF for behavioral and electrophysiological experiments.

Model of Complete Freund's Adjuvant-Induced Inflammatory Pain

Before the animal model was established, the mice were fully adapted to the environment and were subjected to mechanical pain sensitivity tests 1 day in advance to monitor the baseline pain threshold. After the mice were anesthetized by 1.5% isoflurane in 100% O_2 at 1.5 L/min, 10 μl of CFA (obtained from Sigma, F5881-10 × 10 ml) was injected into the left hind paw of the CFA group using a microinjector, and the needle was left in place for 10 s after injection to prevent CFA overflow. The saline group was injected with the same amount of normal saline, and the needle was kept in place for the same time. From 30 min to 1 h after injection, redness and swelling were observed in the hind feet of the CFA group, while no significant changes were observed in the hind feet of the saline group. After 1 day, mechanical pain sensitivity was tested in both groups. The mechanical pain sensitivity threshold of mice in the CFA group was significantly decreased compared to that before the injection of CFA, while the mechanical pain sensitivity threshold of mice in the saline group was not significantly changed compared to that before the injection of saline, indicating that the inflammatory pain model of CFA was successfully established.

Intrathecal Injection

Mice were placed in open-hole 50-ml centrifuge tubes to limit head movement to the tube, and the tail and waist were exposed. According to Hylden and Wilcox's method (Hylden and Wilcox, 1980), 20 μg of proanthocyanidins dissolved in ACSF was injected into the L5 and L6 regions of mice using an insulin microinjector after removing the hair from the waist and tail, and the saline group was injected with the same amount of ACSF as the control experiment. When the tip of the needle accurately entered the intervertebral space, rapid movement of the mouse tail could be observed to demonstrate the success of needle insertion into the sheath, and clear and colorless cerebrospinal fluid could be seen during withdrawal. The injection speed was slow and uniform, and the needle was kept in place for 10 s after the injection to prevent liquid efflux.

Behavioral Testing

Behavioral testing was performed referring to Yin's method (Yin et al., 2020). Before the mechanical pain sensitivity study, mice were placed in separate plexiglass boxes covered with clear plastic

sheets. After the mice were adapted to the box for 30–60 min, we used a set of calibration intact Von Frey filaments (scale range is 0.04 and 0.07, 0.16 and 0.40, 0.60 and 1.00, and 1.40 and 2.00 g) to stimulate mice using the paw foot measure do determine their paw withdrawal mechanical threshold (PWMT). Von Frey filaments were applied vertically to the plantar surface of the hind paws of mice with sufficient force until the Von Frey filaments bent or the mice exhibited pain manifestations such as paw retraction and foot licking, which were recorded as positive responses. Each grade of Von Frey filament scale was stimulated five times in each hind paw with an interval of 5 min, and three positive responses were observed as the PWMT. If no positive response occurred after >3 times, the next larger Von Frey filament was applied. To prevent injury during the test, the maximum intensity of Von Frey filaments was 2.00 g.

To determine thermal sensitivity in mice, we followed Rashid's method (Rashid et al., 2006). The paw withdrawal thermal latency (PWTL) of the mice was measured. Each mouse was placed in a separate plexiglass box and placed on a thermostatically elevated glass plate upon a thermal radiation stimulator. After the mice were adapted for 30 min–1 h, each hind paw was exposed to constant heat radiation five times at an interval of 10 min, and the average value of the latent time of paw retraction was taken as the heat pain sensitivity value. To prevent injury to the rear paw, each stimulation time was <20 s.

An open field test was performed to determine whether intrathecal injection would affect the locomotor ability of the mice. In a 50 cm × 50 cm square box, the underside is white. Mice were placed in the laboratory in advance and allowed to adapt to the environment for 1 h, and 75% alcohol was used to eliminate the odor of the boxes and environment used in the experiment. Each mouse was placed separately into the center of each square box, and the video recording began for 15 min. Automatic analysis software was used to analyze the locomotor route of the mice.

We performed the rotating rod test in mice to test the motor coordination ability of mice after intrathecal injection of proanthocyanidins. Before the experiment, the mice were placed in the test chamber for 30 min to adapt and then placed on the rotating rod in the opposite direction of rotation. The rotary bar rotates at speeds from 5 to 30 r/min. The time until the mice fell from the bar was recorded. The test was repeated three times for each mouse with an interval of 10 min, and the average of the results was taken.

Brain Stereotaxic Injection

To label the noxiously transmitting neurons in the superficial neurons of the dorsal horn of the spinal cord, we injected the retrograde tracer TMR into the PBN site of the mouse head. After intraperitoneally injecting Ketamine/Xylazine mixture in 100 and 10 mg/kg body weight, respectively, the mice were deeply anesthetized and fixed in the prone position on a stereotaxic apparatus (NARISHIGE Scientific Instrument Las, Tokyo, Japan). The microinjector (1 μl, Hamilton, NV, United States) was introduced into the PBN according to the following coordinates: 5.1 mm after the anterior fontanelle, 1.25 mm outside the midline, and 3.4 mm below the surface of the skull (Bai et al., 2020). A small hole was drilled into the skull above the PBN position, the broken bone was removed, and a hemostatic sponge was used to remove the oozing blood. The trace injector [0.15 μl 10% tetramethylrhodamine (TMR), D3308, 3000 MW, Molecular Probe, Eugene, OR, United States] was injected into the PBN coordinate position. After injection for 15 min, the needle was kept in the original position for another 30 min. After surgery, the mice were placed on a heating pad to keep their body temperature at approximately 37°C until they woke up at which point they were treated with antibiotics in the abdominal cavity and at the site of the head wound. The electrophysiological experiment was started on the seventh day after the surgery was completed.

Immunofluorescent Histochemical Staining

To enable the observation of TMR-labeled PBN projected neurons recorded by whole-cell patch clamp, 1% biocytin was added to the intracellular solution. After recording, the spinal cord sections were fixed in precooled 4% paraformaldehyde for 4–6 h and then washed with 0.01 mol/L PBS solution containing 0.5% Triton X-100 (pH 7.4) three times for 10 min each. In addition, avidin conjugated with Alexa-488 fluorophore (obtained from Invitrogen, S11223) was added to PBS at a dilution ratio of 1:1000 to incubate the sections for 4–6 h. Finally, the slices were washed with PBS three times for 10 min each, fixed on clean slides, and sealed with fluorescent tablets. The sections were then observed under a confocal laser scanning microscope (FV-1000, Olympus, Tokyo, Japan), and an appropriate laser beam [Alexa 488 (excitation at 488 nm; emission 510–530 nm), Alexa 594 (excitation 543 nm; emission 590–615 nm), Fluoview software (Olympus)] was used to capture digital images.

Western Blotting

Under isoflurane anesthesia (1.5% isoflurane in 100% O_2 at 1.5 L/min), mice in the saline, CFA, and proanthocyanidin treatment groups were decapitated and sacrificed in extraction buffer containing 100 mM Tris, pH 7.4, 10 mM EDTA, and 2 mM PMSF. The samples were derived from eight mice and then homogenized and centrifuged. Samples containing 75 μg protein were loaded onto 12% acrylamide gels using a Bio-Rad Mini system. The transfer device was used to electrotransfer gels onto nitrocellulose membranes at 120 V for 1.5 h. Membranes were treated with a blocking solution containing 5% skimmed milk powder at room temperature for 2 h and washed followed by the addition of primary antibody: rabbit anti-PI3K (#4292, RRID:AB_329869), p-PI3K [#17366 (Sun et al., 2020)], PKA (#5842, RRID:AB_10706172), PKC (#9368, RRID:AB_10693777), p-PKC (#9378, RRID:AB_2168217), Akt (#9272, RRID:AB_329827), p-Akt (#9271, RRID:AB_329825), NF-κB (#3035, RRID:AB_330564), p-mTOR (#5536, RRID:AB_10691552), and mouse anti-mTOR (#2927, RRID:AB_2259936) (obtained from Cell Signaling Technology, diluted 1:1000 in PB containing 0.3% Triton X-100, Xi'an Kehao Biological Engineering Co. Ltd.) or mouse-β-actin (#A1978) (obtained from Sigma, diluted 1:5000) overnight

at 4°C. Membranes were then washed and incubated with horseradish peroxidase-conjugated, anti-mouse (#ZB-2305) and anti-rabbit (#ZB-2301) secondary antibody diluted 1:5000 (Beijing Zhongshan Biological Technology Co. Ltd.) at RT for 2 h. Antibodies were detected using a chemiluminescence reagent kit (Xi'an Zhongtuan Biotechnology Co. Ltd.). The optical density of the bands was quantified using Bio-Rad Image Lab 5.1 (ChemiDocMXRS, Bio-Rad, United States). In control groups, all experimental procedures for immunostaining were similar but replaced the primary antibodies with normal serum. We found no immunostaining positive results in those experiments.

Electrophysiological Studies

Spinal Cord Slice Preparation

We used whole-cell patch clamp to record spontaneous EPSCs and IPSCs of labeled PBN projective nociceptive neurons in the superficial dorsal horn in mice with lumbar enlargement. Before the whole-cell patch-clamp experimental study, we prepared mouse spinal cord sections according to Yu's method (Yu et al., 2019). The mice were anesthetized by isoflurane anesthesia (1.5% isoflurane in 100% O_2 at 1.5 L/min). After decapitation, the lumbar spine of the mice was rapidly cut and placed in precooled ASCF containing 95% O2 + 5% CO2. The ACSF for dissection contained the following (in millimolar): 252 sucrose, 2.5 KCl, 6 MgSO4·7H2O, 1.2 NaH2PO4, 26 NaHCO3, 0.5 CaCl2, and 10 D-glucose. Thoracolumbar laminectomy was performed using delicate surgical instruments to remove the L4-5 spinal cord and remove the dura, pia, and arachnoid meninges. A spinal cord vibration microtome (Leica VT1200S, Heidelberg, Nussloch, Germany) tray was used with an amplitude of 0.65 mm/s, speed of 0.20 mm/s, coronary section of the spinal cord, and a slice thickness of 300–400 μm. Then, the sections were incubated in oxygen-containing ACSF at room temperature for at least 1 h (in mmol/L: 124 NaCl, 2 CaCl2·H2O, 2.5 KCl, 1 MgSO4, 1 NaH2PO4, 37 D-glucose). The osmotic pressure was 310 mOsm.

Whole-Cell Patch-Clamp Recordings

Spinal cord sections were continuously infused with oxygen-containing ACSF at room temperature at a rate of 2.5–5 ml/min in a recording chamber, and the experimental operation was performed. Microelectrodes (6–9 Ω) were injected with intracellular fluid for experimental records. The injected intracellular fluid was divided into two types (in mmol/L): (1) a potassium gluconate-based solution containing 120 K^+-glucose, 5 NaCl, 1 $MgCl_2$, 10 HEPES, 0.2 EGTA, 2 MgATP, 0.1 Na_3GTP, 10 phosphocreatine (Adjust pH using KOH to 7.2, 290 mOsm) and (2) a cesium mesylate-based solution containing 122 $CSMeSO_3$, 3.7 NaCl, 20 HEPES, 10 BAPTA, 0.2 EGTA, 0.3 MgATP, 0.3 Na_3ATP, 5 TEA-Cl, 5 QX314-Br (CsOH adjusted pH to 7.2, 290 mOsm). PBN-projecting neurons with TMR labeling were recorded in laminar I of the dorsal horn of the spinal cord. These neurons were visualized using a microscope equipped with infrared differential interference contrast optics. The neurons were voltage-clamped at −60 mV using whole-cell adsorption mode. Spontaneous excitatory postsynaptic currents (sEPSCs) were recorded by holding the cell membrane potential at −60 mV, and spontaneous inhibitory postsynaptic currents (sIPSCs) were recorded when holding at 0 mV. In two consecutive stimuli (interval 50 ms) pair pulse ratio (PPR) experiments, a bipolar stimulation electrode connection isolation current stimulator was used [Natus Medical Incorporated (nasdaq: PCLN – news, L6H5S1, Canada)] at an intensity of 20 μA. The ratio of the EPSC amplitude generated by the second stimulus to the EPSC amplitude generated by the first stimulus was calculated as the PPR value.

The above experiments guaranteed a sealing resistance >2 GΩ and a series resistance <35 MΩ; if series resistance changes during recording by >15%, the record result was discarded. We used a Multiclamp 700B amplifier (Axon Instruments, Foster City, CA, United States) to record all signals. Records and analyses of data used pCLAMP 10.2 (Axon Instruments) and mini-Analysis Program (Synatosoft Inc., NJ, United States). To enable observation of TMR-labeled PBN-projecting neurons, 0.5% biocytin was added to the intracellular solution.

Statistical Analysis

All data are shown as the mean ± SEM. Data were analyzed using paired and unpaired *t*-tests or two-way ANOVA. Unpaired *t*-tests were used for behavior test in **Figure 1** and Western blotting in **Figure 5**. Paired *t*-tests and two-way ANOVA were used for whole-cell patch in **Figures 2–4**. A more detailed description has been carried out in the results section together with the statistical results. For all analyses, the criterion of significance was set at $P < 0.05$. All statistical analyses were performed using GraphPad Prism 8.4.2 software. Figures were made using GraphPad Prism 8.4.2 and OriginPro 9.1.

RESULTS

Intrathecal Application of Proanthocyanidins Induces Analgesic Effects in Mice With Complete Freund's Adjuvant Injection

First, we explored whether intrathecal (*i.t.*) injection of proanthocyanidins should change the mechanical and heat pain responses by testing the PWMT and PWTL in mice administered with CFA or saline injection. We found that the PWMT and PWTL of mice with left paw CFA (10 μl) injection were significantly lower than those of mice with the same amount of saline injection, indicating that mechanical allodynia and thermal hyperalgesia occurred in mice with CFA injection ($P < 0.0001$, $n = 6$ and 10 in the saline and CFA groups, respectively, unpaired *t*-test) (**Figures 1A,B**). However, *i.t.* injection of proanthocyanidins on the third ($P = 0.003$, proanthocyanidins vs. ACSF, $n = 10$ in each group, unpaired *t*-test) and seventh ($P = 0.011$, proanthocyanidins vs. ACSF, $n = 8$ in each group, unpaired *t*-test) days post-surgery significantly increased the PWMT in mice with CFA injection but not in mice with saline injection (third day: $P = 0.56$, seventh day: $P = 0.56$, proanthocyanidins vs. ACSF, $n = 6$ in each group, unpaired *t*-test) (**Figure 1A**). In addition, *i.t.* injection of proanthocyanidins on the third ($P = 0.009$, proanthocyanidins

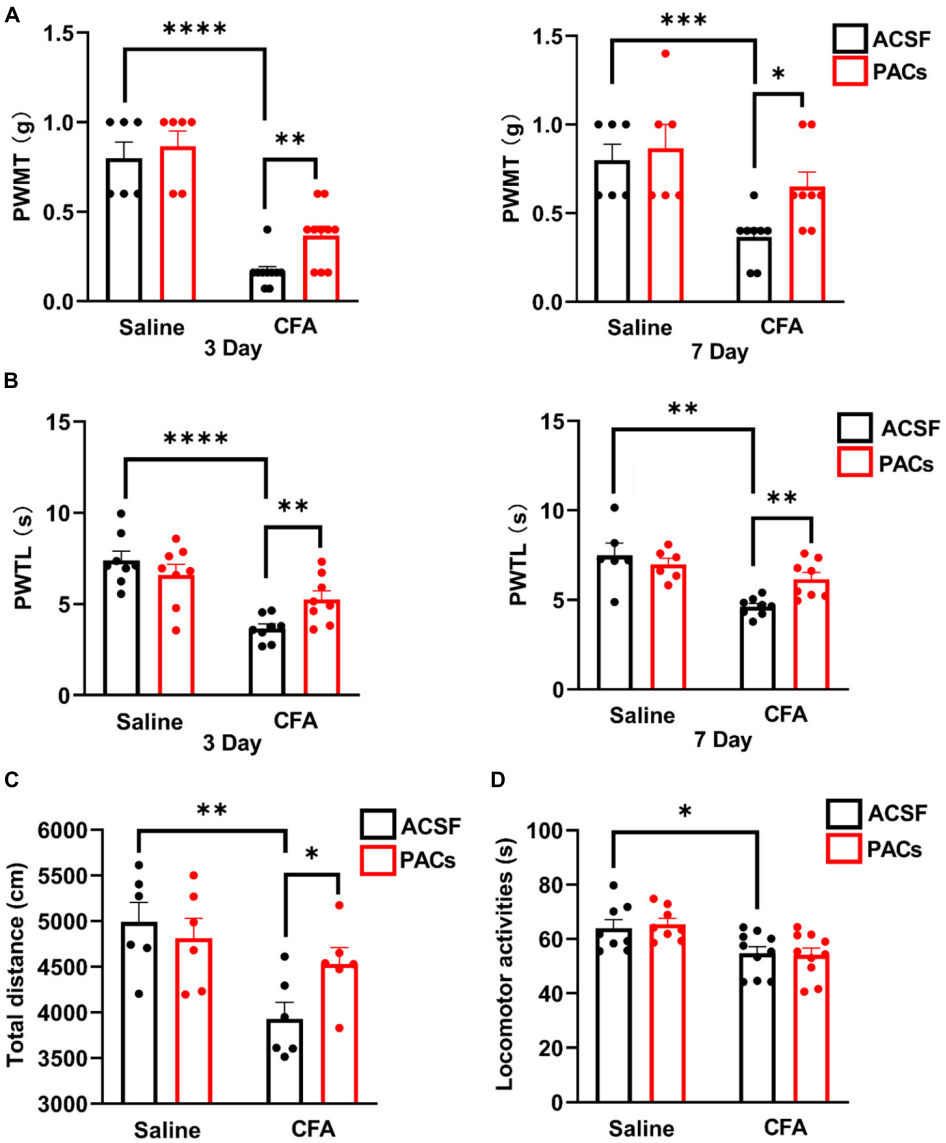

FIGURE 1 | Intrathecal injection of proanthocyanidins increased mechanical and thermal pain thresholds in mice with CFA injection. Intrathecal injection of proanthocyanidins on the third and seventh day post-surgery increased the paw withdrawal mechanical threshold (PWMT) **(A)** and paw withdrawal thermal latency (PWTL) **(B)** of mice in the CFA group. **(C)** Intrathecal injection of proanthocyanidins increased the movement distance of mice in the CFA group. **(D)** Intrathecal injection of proanthocyanidins had no effect on the motor function of mice in either the CFA or saline group in the rotary rod test. $^{*}P < 0.05$; $^{**}P < 0.01$; $^{***}P < 0.001$; $^{****}P < 0.0001$. PWMT, paw withdrawal mechanical threshold; PWTL, paw withdrawal thermal latency; CFA, Complete Freund's Adjuvant; ACSF, artificial cerebrospinal fluid; PACs, proanthocyanidins.

vs. ACSF, $n = 8$ in each group, unpaired t-test) and seventh ($P = 0.002$, proanthocyanidins vs. ACSF, $n = 8$ in each group, unpaired t-test) days post-surgery significantly increased the PWTL in mice with CFA injection but not in mice with saline injection (third day: $P = 0.31$, $n = 8$; seventh day: $P = 0.53$, $n = 6$, proanthocyanidins vs. ACSF, unpaired t-test) (**Figure 1B**). These results indicate that proanthocyanidins at the spinal cord level inhibit both mechanical and thermal pain in a mouse model of inflammatory pain induced by CFA injection.

We then tested the locomotion activities of mice using the open field test and rotary rod test. CFA injection decreased the total moving distance in the open field test ($P = 0.004$, CFA vs. saline, $n = 6$ in each group, unpaired t-test), which was rescued by *i.t.* injection of proanthocyanidins ($P = 0.03$, proanthocyanidins vs. ACSF, $n = 6$ in each group, unpaired t-test) in mice with CFA injection but not in mice with saline injection ($P = 0.57$, proanthocyanidins vs. ACSF, $n = 6$ in each group, unpaired t-test) (**Figure 1C**). Motor coordination and antifatigue ability were decreased in the rotary rod test in mice with CFA compared to those in mice with saline injection ($P = 0.03$, $n = 8$ and 10 in the saline and CFA groups, respectively, unpaired t-test), which were not affected by *i.t.* injection of proanthocyanidins (saline:

$P = 0.85$, CFA: $P = 0.71$; proanthocyanidins vs. ACSF, $n = 8$ and 10 in the saline and CFA groups, respectively, unpaired t-test) (**Figure 1D**). These results suggest that CFA injection decreases mice's desire to move and motor coordination ability. Application of proanthocyanidins rescues the impaired locomotion desire but not motor coordination ability.

Bath Application of Procyanidins Decreases Excitatory Inputs to Parabrachial Nucleus-Projecting Neurons in the Spinal Cord

We next tested whether procyanidins affected the synaptic transmission and intrinsic properties of spinal noxious neurons. Since most of the projecting neurons in the spinal cord send ascending nociceptive information to the contralateral side of the lateral part of the PBN (Todd, 2010), we injected retrograde tracer TMR into the right lateral PBN to label the projecting neurons in the left spinal cord (the ipsilateral side of CFA injection) (**Figure 2A**). TMR retrogradely labeled (TMR^+) neurons were primarily located in lamina I of the left spinal cord, consistent with previous reports (Todd, 2010). We then applied whole-cell patch-clamp recording of the TMR^+ neurons and tested the sEPSC, which represents the probability of presynaptic excitatory neurotransmitter release and postsynaptic responses (Chen et al., 2015). We found that both the frequency ($P < 0.0001$) and amplitude ($P = 0.0119$) of sEPSCs were significantly increased in mice with CFA injection compared to those in mice with saline injection ($n = 20$ cells and 22 cells from 5 mice in the saline and CFA groups, respectively, unpaired t-test), indicating enhanced excitatory synaptic transmission to PBN-projecting spinal neurons in mice with inflammatory pain (**Figures 2B,C,F,G**). Bath application of proanthocyanidins (50 μM) significantly reduced the frequency ($P = 0.005$) but not the amplitude of the sEPSCs ($P = 0.13$) in the CFA group ($n = 22$ cells from 5 mice, paired t-test), nor did the frequency ($P = 0.49$) or amplitude ($P = 0.97$) of the sEPSCs in mice with saline injection ($n = 20$ cells from 4 mice, paired t-test) (**Figures 2B–G**). These results indicate that proanthocyanidins inhibit presynaptic glutamate inputs to PBN-projecting spinal neurons without changing AMPA receptor-mediated postsynaptic responses.

We then recorded the paired-pulse ratio (PPR) of evoked EPSCs (eEPSCs) of PBN-projecting spinal neurons to confirm the presynaptic effect of proanthocyanidins. Paired monosynaptic eEPSCs are induced by electrical stimulation of the dorsal root entry zone (Li et al., 1999) at 50 ms intervals. We found that the PPR was decreased in mice injected with CFA compared to that in mice injected with saline ($P = 0.0091$, $n = 10$ cells from 5 mice in each group, unpaired t-test), indicating increased peripheral inputs to PBN-projecting spinal neurons (**Figures 2H,I,L**). Bath application of procyanidins increased the PPR in mice with CFA injection ($P = 0.0032$, $n = 10$ cells from 5 mice, paired t-test) but not in mice with saline injection ($P = 0.65$, $n = 10$ cells from 5 mice, paired t-test) (**Figures 2H–L**), further confirming the presynaptic inhibitory effect of procyanidins in mice with CFA injection.

Bath Application of Procyanidins Does Not Change the Inhibitory Inputs to Parabrachial Nucleus-Projecting Neurons in the Spinal Cord

We further recorded the sIPSC of TMR^+ spinal neurons to determine whether procyanidins affect inhibitory inputs to PBN-projecting spinal neurons. In mice with CFA injection, the frequency ($P = 0.003$) but not the amplitude ($P = 0.45$) of the sIPSCs was decreased in comparison with those in mice with saline injection ($n = 23$ cells from 5 mice in each group, unpaired t-test) (**Figures 3A,B,E,F**), suggesting decreased inhibitory inputs to PBN-projecting spinal neurons in mice with CFA injection. We found that bath application of proanthocyanidins affected neither the frequency nor the amplitude of sIPSCs in the CFA (frequency: $P = 0.50$; amplitude: $P = 0.82$; $n = 23$ cells from 5 mice, paired t-test) or saline (frequency: $P = 0.51$; amplitude: $P = 0.25$; $n = 23$ cells from 5 mice, paired t-test) group (**Figures 3A–F**), suggesting that proanthocyanidins do not alter inhibitory synaptic transmission into PBN-projecting spinal neurons. These effects were confirmed by testing the PPR of the evoked IPSCs: the PPR was increased in mice with CFA injection compared to that in mice with saline injection ($P = 0.0098$, $n = 11$ and 10 cells from 5 mice in the saline and CFA groups, respectively, unpaired t-test); bath application of procyanidins did not affect the PPR in the CFA ($P = 0.75$, $n = 10$ cells from 5 mice, paired t-test) or saline group ($P = 0.22$, $n = 11$ cells from 5 mice, paired t-test) (**Figures 3G–K**).

Bath Application of Procyanidins Does Not Affect the Kinetic Properties of the Synaptic Transmission of Parabrachial Nucleus-Projecting Neurons in the Spinal Cord

We then recorded the single eEPSCs of PBN-projecting spinal neurons to investigate whether procyanidins affect glutamate release kinetics and the properties of post-synaptic AMPA channels. We found that bath application of proanthocyanidins affected neither the decay time constants [the fast decay (τ_{fast}): $P = 0.87$; the slow decay (τ_{slow}): $P = 0.81$, $n = 10$ cells from 5 mice, paired t-test] nor the fraction constituent [the fast constituent (A_{fast}): $P = 0.82$; the slow constituent (A_{slow}): $P = 0.88$, $n = 10$ cells from 5 mice, paired t-test] in the TMR^+ spinal neurons (**Figures 4A–C**), suggesting that procyanidins do not affect the pre-synaptic glutamatergic vesicle release velocity and their presynaptic inhibitory effect may be mediated by the reduced number of released vesicles. We then applied the non-stationary fluctuation analysis (NSFA) of eEPSCs to compare the unitary conductance and number of active channels in TMR^+ spinal neurons before and after the application of procyanidins. We found that bath application of proanthocyanidins affected neither the unitary conductance ($P = 0.79$, $n = 8$ cells from 5 mice, paired t-test) nor the number of active channels ($P = 0.27$, $n = 8$ cells from 5 mice, paired t-test) (**Figures 4D–F**), which indicate that proanthocyanidins do not affect the number and ion conductance of post-synaptic AMPA receptors and further

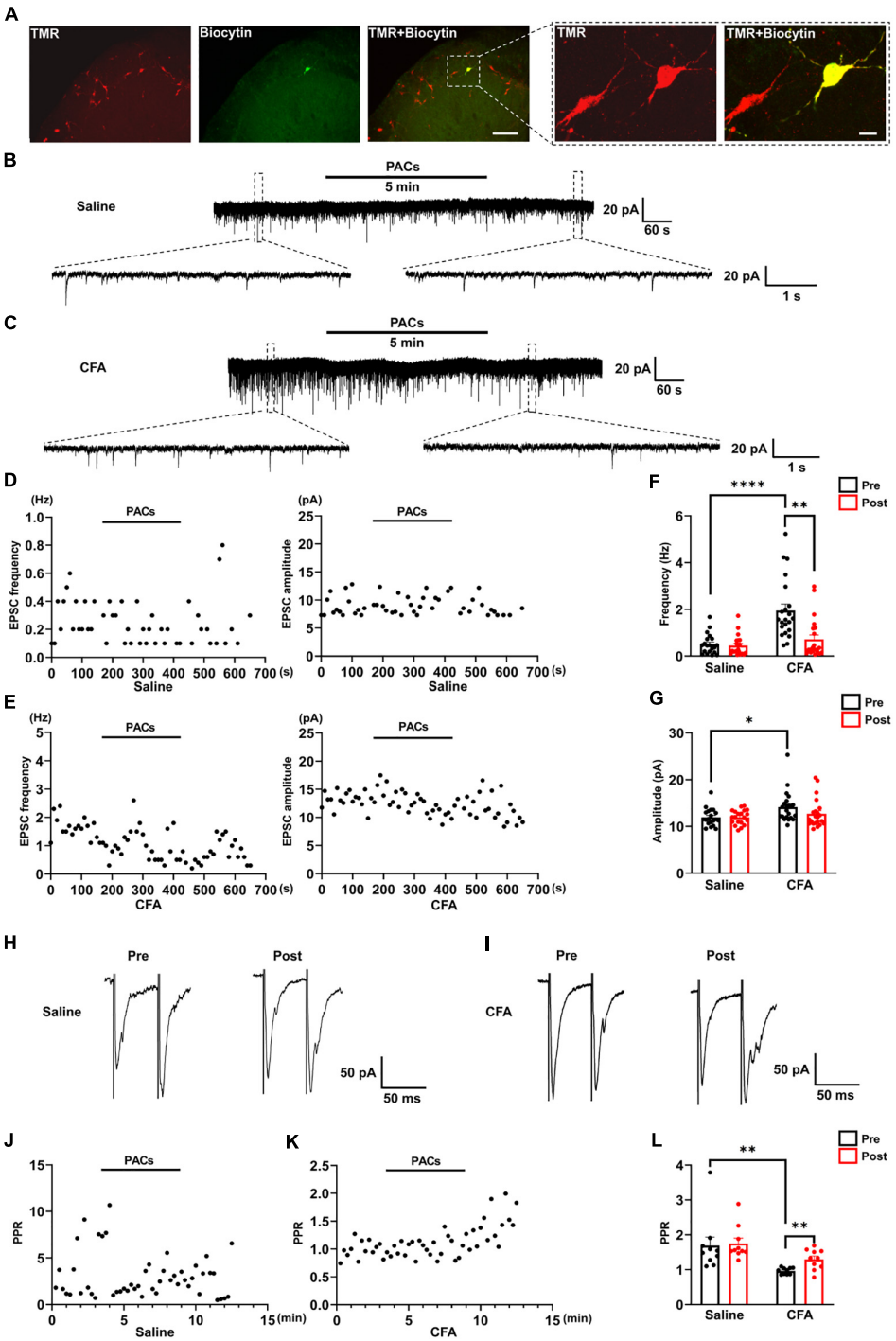

FIGURE 2 | The effect of proanthocyanidins on sEPSCs of PBN-projecting neurons in the spinal dorsal horn. **(A)** Double-labeling immunohistochemistry staining confirmed that all recorded neurons were TMR-positive retrogradely labeled neurons (red) those distributed in laminar I of the left spinal cord. The rectangle area was enlarged in the right panel. The scale bars equal to 150 μm in the left panel images and 30 μm in the right panel images. Representative electrophysiological samples **(B)** and scatter plots **(D)** showing sEPSCs with bath application of proanthocyanidins (50 μM) in the saline group. Representative electrophysiological samples **(C)** and scatter plots **(E)** showing sEPSCs with bath application of proanthocyanidins in the CFA group. **(F)** Application of proanthocyanidins decreased the frequency of sEPSCs in the CFA but not saline group. **(G)** Application of proanthocyanidins had no effect on the amplitude of sEPSCs in the CFA or saline group. Representative electrophysiological samples **(H)** and scatter plots **(J)** showing the PPR with bath application of proanthocyanidins in the saline group. Representative electrophysiological samples **(I)** and scatter plots **(K)** showing the PPR with bath application of proanthocyanidins in the CFA group. **(L)** Application of proanthocyanidins increased the PPR in the CFA but not saline group. $^{*}P < 0.05$; $^{**}P < 0.01$; $^{****}P < 0.0001$. TMR, tetramethylrhodamine; CFA, Complete Freund's Adjuvant; PACs, proanthocyanidins; PPR, paired-pulse ratio.

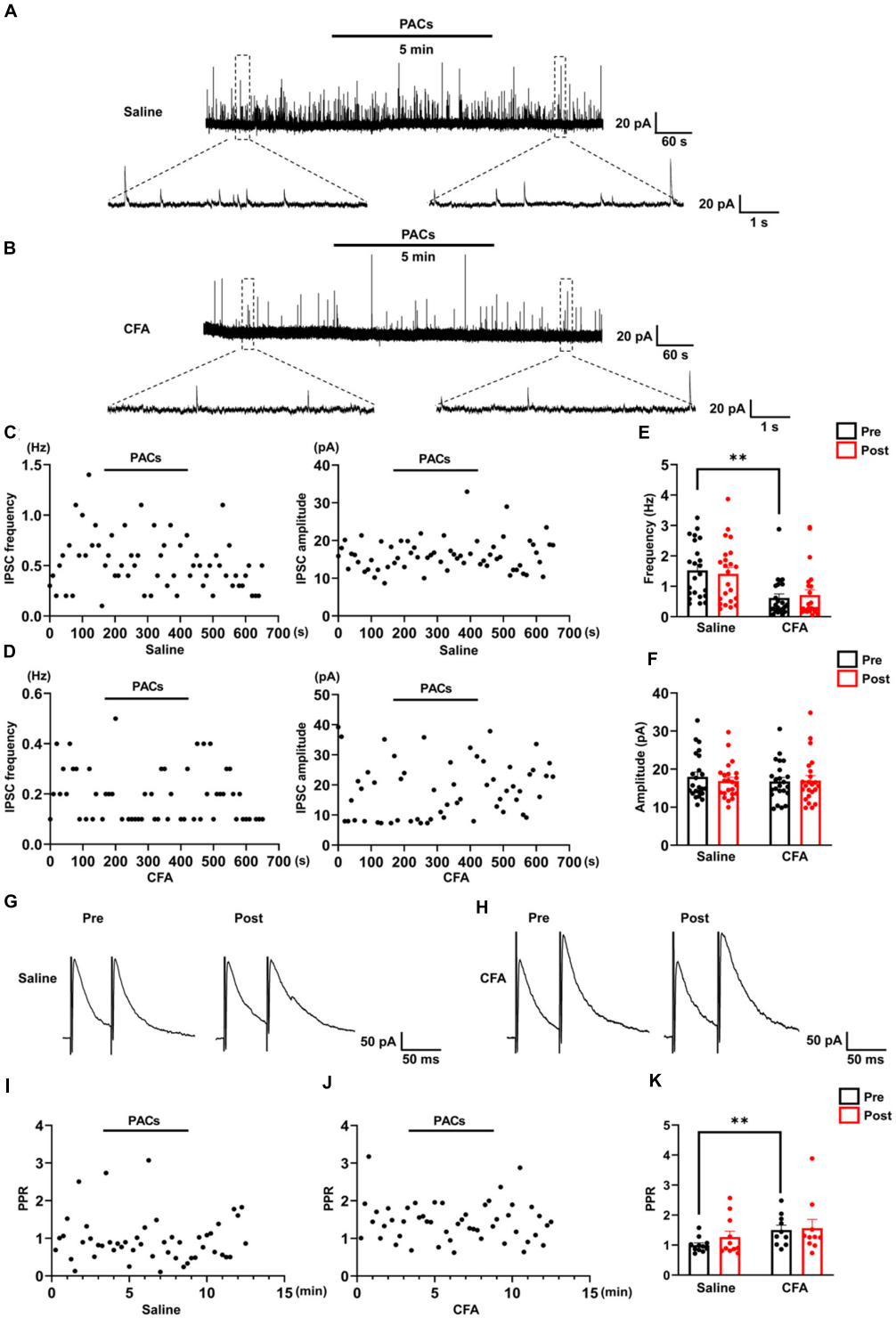

FIGURE 3 | The effect of proanthocyanidins on sIPSCs of PBN-projecting neurons in the spinal dorsal horn. Representative electrophysiological samples **(A)** and scatter plots **(C)** showing sIPSCs with bath application of proanthocyanidins (50 μM) in the saline group. Representative electrophysiological samples **(B)** and scatter plots **(D)** showing sIPSCs with bath application of proanthocyanidins in the CFA group. Application of proanthocyanidins had no effect on the frequency **(E)** and amplitude **(F)** of sIPSCs in the CFA or saline group. Representative electrophysiological samples **(G)** and scatter plots **(I)** showing the PPR with bath application of proanthocyanidins in the saline group. Representative electrophysiological samples **(H)** and scatter plots **(J)** showing the PPR with bath application of proanthocyanidins in the CFA group. **(K)** Application of proanthocyanidins had no effect on the PPR in the CFA or saline group. $^{**}P < 0.01$. CFA, Complete Freund's Adjuvant; PACs, proanthocyanidins; PPR, paired-pulse ratio.

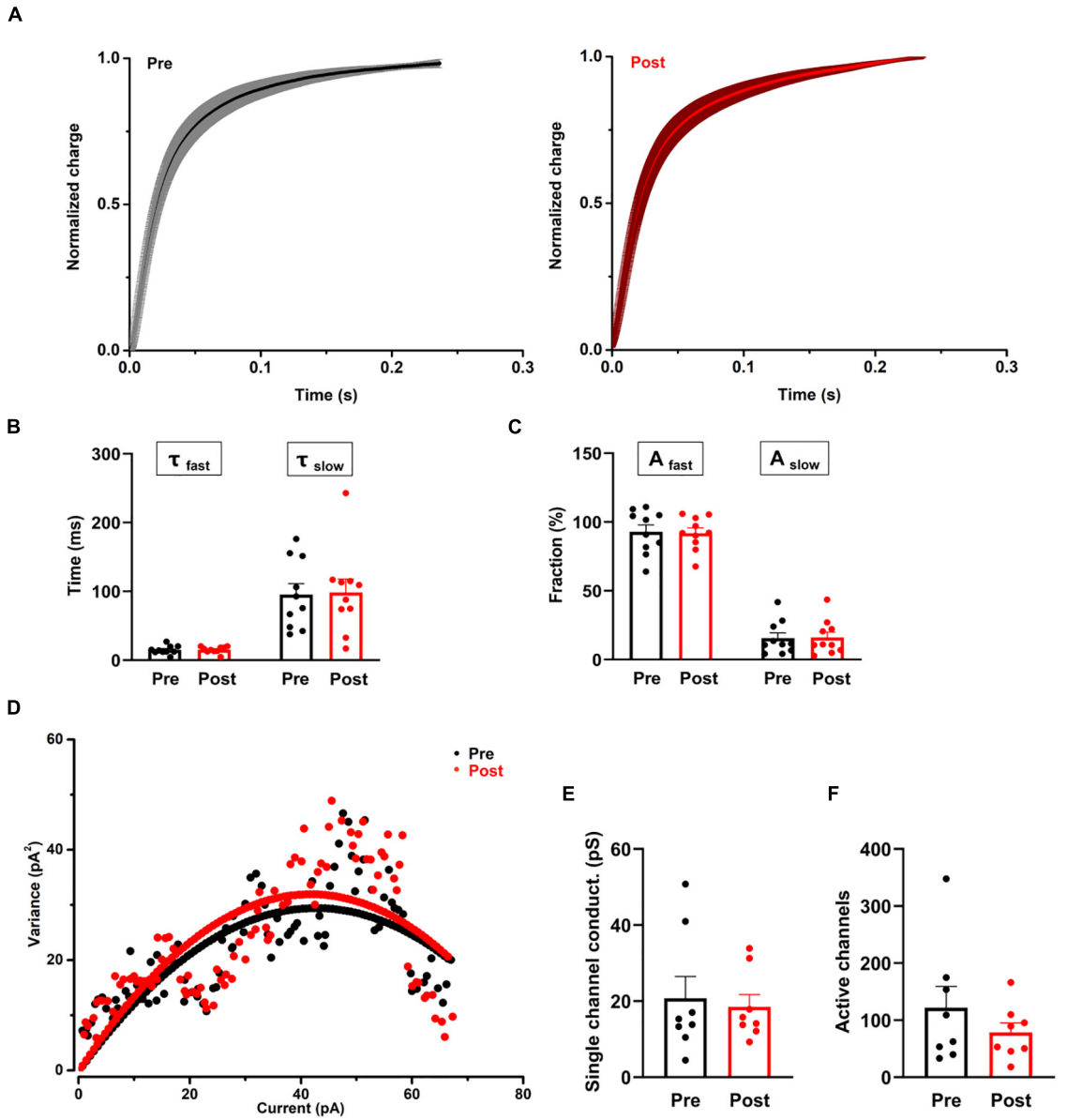

FIGURE 4 | The effect of proanthocyanidins on the kinetic properties of the synaptic transmission of PBN-projecting neurons in the spinal dorsal horn. **(A–C)** Application of proanthocyanidins did not change the fast (τ_{fast}) and slow (τ_{slow}) decay time constants and the fast (A_{fast}) and slow (A_{slow}) fraction constituent in the TMR-positive spinal cord neurons. **(D–F)** The non-stationary fluctuation analysis (NSFA) indicated that bath application of proanthocyanidins affected neither the single channel conductance nor the AMPAR channel number in the TMR-positive spinal cord neurons.

confirm that proanthocyanidins do not affect the amplitude of AMPA receptor-mediated EPSCs (**Figure 2**).

Bath Application of Procyanidins Does Not Affect the Intrinsic Properties of Parabrachial Nucleus-Projecting Neurons in the Spinal Cord

To investigate whether procyanidins alter the intrinsic properties of PBN-projecting spinal neurons, we studied the single action potential properties and firing patterns of TMR^+ spinal neurons before and after bath application of procyanidins. The parameters of a single action potential, such as the resting membrane potential (RMP) ($P = 0.0026$, $n = 12$ cells and 25 cells from 5 mice in the saline and CFA groups, respectively, unpaired t-test), rheobase ($P < 0.0001$, $n = 10$ cells and 25 cells from 5 mice in the saline and CFA groups, respectively, unpaired t-test) or membrane input resistance ($P = 0.0128$, $n = 11$ cells and 15 cells from 5 mice in the saline and CFA groups, respectively, unpaired t-test), but not the action potential amplitude ($P = 0.18$, $n = 11$ cells and 25 cells from 5 mice in the saline and CFA groups, respectively, unpaired t-test) was significantly different between

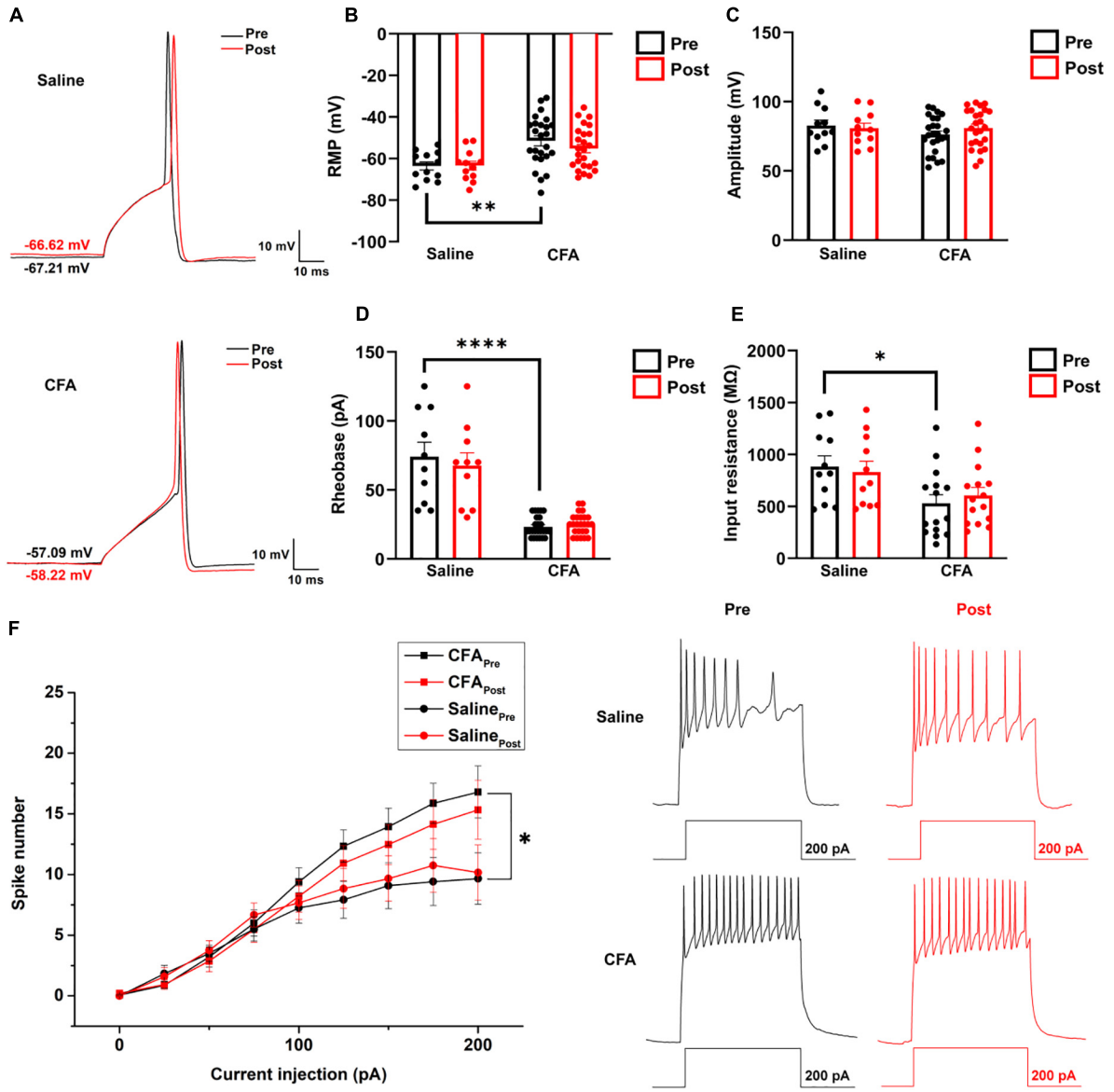

FIGURE 5 | The effect of proanthocyanidins on the intrinsic properties of PBN-projecting neurons in the spinal dorsal horn. **(A)** Representative samples showing a single action potential of one PBN-projecting neuron before and after the application of proanthocyanidins in saline and CFA group, respectively. Application of proanthocyanidins did not change the resting membrane potential (RMP) **(B)**, amplitude **(C)**, rheobase **(D)**, and membrane input resistance **(E)** in the CFA or saline group. **(F)** Application of proanthocyanidins did not change the neuronal spike number in the CFA or saline group. $^{*}P < 0.05$; $^{**}P < 0.01$; $^{****}P < 0.0001$. RMP, resting membrane potential; CFA, Complete Freund's Adjuvant.

mice with CFA or saline injection (**Figures 5A–E**). Application of procyanidins did not change the RMP, action potential amplitude, rheobase, and membrane input resistance in the CFA (RMP: $P = 0.17$; amplitude: $P = 0.20$; rheobase: $P = 0.41$; input resistance: $P = 0.47$, $n = 15$ or 25 cells from 5 mice, paired t-test) or saline group (RMP: $P = 0.86$; amplitude: $P = 0.45$; rheobase: $P = 0.23$; input resistance: $P = 0.56$, $n = 10$–12 cells from 5 mice, paired t-test) (**Figures 5A–E**). Meanwhile, the spike number induced by step depolarized current injection was increased in mice with CFA injection. However, bath application of procyanidins did not change the spike number (two-way ANOVA, $n = 15$ cells and 11 cells from 5 mice in the CFA and saline groups, respectively) (**Figure 5F**).

Proanthocyanidins Inhibit Phosphorylated Activation of the PI3K/Akt/mTOR Signaling Pathway in the Dorsal Root Ganglia Neurons

Since proanthocyanidins inhibit excitatory peripheral inputs to PBN-projecting fibers, we explored whether proanthocyanidins affected the expression of intracellular signaling molecules in

the DRG neurons. We first assessed the expression of PKA, PKC, and PI3K proteins in the DRG neurons after 30 min of incubation of the DRG with procyanidins-containing ACSF. We found that the protein expression of PKA (P = 0.009), phosphorylated PKC (p-PKC) (P = 0.039), and phosphorylated PI3K (p-PI3K) (P = 0.0086) was significantly increased in mice with CFA injection compared to those with saline injection (n = 8 mice in each group, unpaired t-test) (**Figures 6A–D**). In the case of incubation with proanthocyanidins, the increased p-PI3K expression (P = 0.003), but not the PKA (P = 0.44) and p-PKC (P = 0.97) expression, was reversed (proanthocyanidins vs. ACSF, n = 8 mice in each group, unpaired t-test). This suggests that proanthocyanidins primarily inhibit phosphorylated activation of the PI3K pathway in the DRG neurons in mice with CFA injection.

We then examined whether proanthocyanidins affected the expression of downstream molecules in the PI3K pathway. Compared to the saline group, expression of p-Akt (P = 0.014), p-mTOR (P = 0.007), and NF-κB (P = 0.023) proteins was increased in CFA-injected mice (n = 8 mice in each group, unpaired t-test) (**Figures 6E–H**). In the case of incubation with proanthocyanidins, the increased expression of p-Akt (P = 0.019), p-mTOR (P = 0.02), and NF-κB (P = 0.025) was reversed (n = 8 mice in each group, paired t-test).

DISCUSSION

Proanthocyanidins are a type of pigment in plants. They are common in the flowers, nuts, fruits, bark, and seeds of various plants. Berries and fruits are the best sources of proanthocyanidins for human intake. In the stomach environment, 3–6 U of proanthocyanidins will be hydrolyzed into free catechins and catechin dimers and then absorbed into the blood (Spencer et al., 2000). These results indicate the possible application of procyanidins as raw materials in medicine, health care products, food, cosmetics, and other fields.

In the area of human health, proanthocyanidins exert diverse protective effects on the human body. Oligomeric proanthocyanidin complexes have antioxidant, antibacterial, antiviral, anticancer, anti-inflammatory, antiallergic, and vasodilator effects (Fine, 2000; Bao et al., 2015). The protective effects have also been observed in neurodegenerative diseases. Previous research indicated that the neuroprotective effect of proanthocyanidins on Alzheimer's disease (AD) is mediated by inhibiting amyloid β aggregation, reducing amyloid β production, and preventing small amyloid β neurotoxicity in the mouse brain (Li et al., 2016). Proanthocyanidins' analgesic effect has also been reported. Gavage of plant extracts rich in proanthocyanidins significantly reduces acute inflammatory pain in a variety of mouse inflammatory pain models induced by carrageenan, capsaicin, cinnamaldehyde, or formalin (Fongang et al., 2017). Gavage of proanthocyanidins significantly alleviates the hyperalgesia caused by abnormal peripheral nerve function in type 2 diabetic rats (Ding et al., 2014) and sciatic nerve injury mice (Pan et al., 2018). In our present study, we also found that intrathecal application of proanthocyanidins (20 μg) induced a significant analgesic effect in mice with inflammatory pain. Our present results and previous works all suggest that proanthocyanidins are good candidates for clinical analgesic agent exploitation, especially considering that proanthocyanidins are easily absorbed by oral intake.

Studies of the potential mechanism of proanthocyanidins in the central nervous system and in spinal analgesia are very limited, and the involvement of ion channels in proanthocyanidins' effect may be considered. In our experiments, proanthocyanidins did not affect the decay kinetics of the eEPSC and the post-synaptic AMPA receptor ion conduction. We thus propose that proanthocyanidins should not affect the properties of pre- and post-synaptic ion channels in the spinal cord. However, it's shown that proanthocyanidins induce hyperpolarization of rat aorta endothelial cells *via* multiple activations of K^+ channels and play a protective role in Ca^{2+} influx into endothelial cells (Byun et al., 2012). Proanthocyanidins are also reported to help maintain the intracellular Ca^{2+}-homeostasis after NMDA receptor overactivation, protecting neurons from Ca^{2+}-induced adverse effects (Franchi et al., 2020). Besides that, restricting Ca^{2+} influx can reduce the activation of PI3K and Akt, and then produce a protective effect on glutamate-induced excitotoxicity. We thus think that the effect of proanthocyanidins in the properties of ion channels, especially Ca^{2+} channels, should be further investigated in the future.

In addition, studies reporting that the regulation of synaptic plasticity by proanthocyanidins cannot be ignored. Procyanidins promote basic synaptic transmission and long-term synaptic potentiation in hippocampal slices, and significantly improve the cognitive impairment caused by AD (Wang et al., 2012), through inhibiting oxidative stress and retaining AKT and ERK activity (Gao et al., 2020). In our results, procyanidins also inhibited the short-term plasticity of the synaptic transmission in the spinal cord, which may be mediated by affecting the pre-synaptic vesicle release, since procyanidins did not affect the number and ion conductance of post-synaptic AMPAR. However, whether and how procyanidins affect the long-term plasticity of the spinal cord is not known yet and is interesting for future investigation.

In previous works, it has been shown that the mechanisms of proanthocyanidin analgesia in peripheral nerves may primarily derive from strong antioxidants (Mao et al., 2015), anti-swelling (Cordeiro et al., 2016), and inhibition of Ca^{2+}-ATPase activities (Ding et al., 2014). Although one study reports that the gavage of proanthocyanidins inhibits the activity of spinal MMP-9 and MMP-2 (Pan et al., 2018), whether proanthocyanidins affect the synaptic transmission of nociceptive information in the central nervous system, which is the primary pathological change in central hypersensitization, remains obscure. Our study is the first to observe the presynaptic inhibitory effect of proanthocyanidins on spinal cord neurons projecting to supraspinal areas in mice with inflammatory pain, providing preliminary evidence for the central application of proanthocyanidins in the field of analgesia.

We also noticed that proanthocyanidins are beneficial to exercise management. This is in consistent with previous works that intraperitoneal injection of a moderate dose of proanthocyanidins increases the exercise capacity of rats

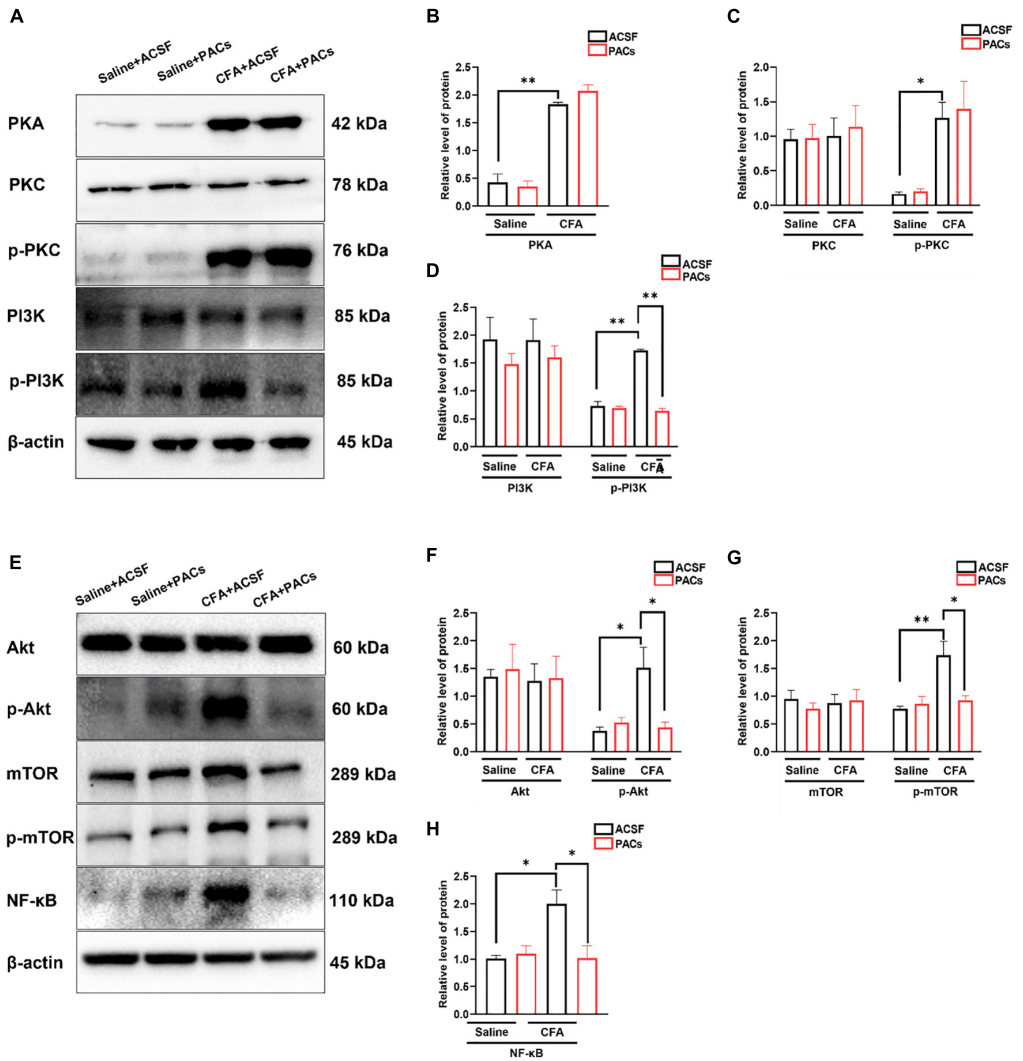

FIGURE 6 | The role of proanthocyanidins in the PI3K/Akt/mTOR signaling pathway. **(A)** Representative bands of PKA, PKC/p-PKC, and PI3K/p-PI3K. **(B–D)** Application of proanthocyanidins reversed the activation of p-PI3K but not PKA, PKC/p-PKC, or PI3K in the CFA group. **(E)** Representative bands of Akt/p-Akt, mTOR/p-mTOR, and NF-κB. **(F–H)** Application of proanthocyanidins reversed the activation of p-Akt, p-mTOR, and NF-κB but not Akt and mTOR in the CFA group. $^{*}P < 0.05$; $^{**}P < 0.01$. CFA, Complete Freund's Adjuvant; ACSF, artificial cerebrospinal fluid; PACs, proanthocyanidins.

(Moreira et al., 2010). We found that proanthocyanidins did not rescue the damaged exercise capacity in the rotary rod experiment but rescued the reduced movement distance in the open field test, in mice with CFA injection. Our point of view for these results is that proanthocyanidins have an analgesic effect but do not impact the animal's ability to move, instead of increasing the animal's desire for movement. Under the unique environment of the rotary rod, plantar swelling-caused damage of exercise ability should not be reduced by *i.t.* injection of proanthocyanidins. On the contrary, in the open field experiment, application of proanthocyanidins reduces the pain and negative emotion and increases animals' motivation for exploration.

In summary, we find that proanthocyanidins, as food-grade substances, have a potent relieving effect on inflammatory pain in animals with CFA injection, through inhibition of the nociceptive inputs to the PBN-projecting spinal neurons. However, although their application in the treatment of inflammatory pain is of potential interests, many questions need to be clarified, such as their possible effect on the long-term synaptic plasticity and ion channels, as well as the underlying molecular mechanisms in addition to inhibition of PI3K pathways and their effects on different groups of DRG neurons sending projections to spinal neurons.

DATA AVAILABILITY STATEMENT

The raw data supporting the conclusions of this article will be made available by the authors, without undue reservation.

ETHICS STATEMENT

The animal study was reviewed and approved by the Animal Care and Use Committee for Research and Education of the Fourth Military Medical University.

AUTHOR CONTRIBUTIONS

ZW, YL, and TC: concept and design. HF, ZW, DZ, JG, MX, MZ, and HD: data collection analysis and interpretation. HF, ZW, and TC: manuscript writing. HF, ZW, DZ, JG, MX, MZ, HD, and TC: final approval of the manuscript. All authors contributed to the article and approved the submitted version.

FUNDING

This manuscript processing charge was funded by the National Natural Science Foundation of China (32071000 and 32192410 to TC and 81901128 to ZW) and the Foundation for Distinguished Young Scholar of Shaanxi (2019JC-21 to TC).

REFERENCES

Bai, Y. M., Li, Y., Ma, J. B., Li, J. N., Teng, X. Y., Chen, Y. B., et al. (2020). Enkephalinergic circuit involved in nociceptive modulation in the spinal dorsal horn. *Neuroscience* 429, 78–91. doi: 10.1016/j.neuroscience.2019.12.020

Bao, L., Zhang, Z., Dai, X., Ding, Y., Jiang, Y., Li, Y., et al. (2015). Effects of grape seed proanthocyanidin extract on renal injury in type 2 diabetic rats. *Mol. Med. Rep.* 11, 645–652. doi: 10.3892/mmr.2014.2768

Byun, E. B., Korematsu, S., Ishikawa, T., Nishizuka, T., Ohshima, S., Kanda, T., et al. (2012). Apple procyanidins induce hyperpolarization of rat aorta endothelial cells via activation of K+ channels. *J. Nutr. Biochem.* 23, 278–286. doi: 10.1016/j.jnutbio.2010.12.005

Chacón, M. R., Ceperuelo-Mallafré, V., Maymó-Masip, E., Mateo-Sanz, J. M., Arola, L., Guitiérrez, C., et al. (2009). Grape-seed procyanidins modulate inflammation on human differentiated adipocytes in vitro. *Cytokine* 47, 137–142. doi: 10.1016/j.cyto.2009.06.001

Chen, Y. B., Huang, F. S., Fen, B., Yin, J. B., Wang, W., and Li, Y. Q. (2015). Inhibitory effects of endomorphin-2 on excitatory synaptic transmission and the neuronal excitability of sacral parasympathetic preganglionic neurons in young rats. *Front. Cell Neurosci.* 9:206. doi: 10.3389/fncel.2015.00206

Cordeiro, K. W., Felipe, J. L., Malange, K. F., do Prado, P. R., de Oliveira Figueiredo, P., Garcez, F. R., et al. (2016). Anti-inflammatory and antinociceptive activities of *Croton urucurana* Baillon bark. *J. Ethnopharmacol.* 183, 128–135. doi: 10.1016/j.jep.2016.02.051

Demir, I. E., Schäfer, K. H., Tieftrunk, E., Friess, H., and Ceyhan, G. O. (2013). Neural plasticity in the gastrointestinal tract: chronic inflammation, neurotrophic signals, and hypersensitivity. *Acta Neuropathol.* 125, 491–509. doi: 10.1007/s00401-013-1099-4

Ding, Y., Dai, X., Jiang, Y., Zhang, Z., and Li, Y. (2014). Functional and morphological effects of grape seed proanthocyanidins on peripheral neuropathy in rats with type 2 diabetes mellitus. *Phytother. Res.* 28, 1082–1087. doi: 10.1002/ptr.5104

Fine, A. M. (2000). Oligomeric proanthocyanidin complexes: history, structure, and phytopharmaceutical applications. *Altern. Med. Rev.* 5, 144–151.

Fongang, A., Laure Nguemfo, E., Djouatsa Nangue, Y., Bogning Zangueu, C., Fouokeng, Y., Azebaze, A. G. B., et al. (2017). Antinociceptive and anti-inflammatory effects of the methanolic stem bark extract of *Antrocaryon klaineanum* Pierre (Anacardiaceae) in mice and rat. *J. Ethnopharmacol.* 203, 11–19. doi: 10.1016/j.jep.2017.03.036

Franchi, A., Pedrazzi, M., Casazza, A. A., Millo, E., Damonte, G., Salis, A., et al. (2020). A bioactive olive pomace extract prevents the death of murine cortical neurons triggered by NMDAR over-activation. *Molecules* 25:4385. doi: 10.3390/molecules25194385

Gao, W. L., Li, X. H., Dun, X. P., Jing, X. K., Yang, K., and Li, Y. K. (2020). Grape seed proanthocyanidin extract ameliorates streptozotocin-induced cognitive and synaptic plasticity deficits by inhibiting oxidative stress and preserving AKT and ERK activities. *Curr. Med. Sci.* 40, 434–443. doi: 10.1007/s11596-020-2197-x

Hylden, J. L., and Wilcox, G. L. (1980). Intrathecal morphine in mice: a new technique. *Eur. J. Pharmacol.* 67, 313–316. doi: 10.1016/0014-2999(80)90515-4

Li, P., Wilding, T. J., Kim, S. J., Calejesan, A. A., Huettner, J. E., and Zhuo, M. (1999). Kainate-receptor-mediated sensory synaptic transmission in mammalian spinal cord. *Nature* 397, 161–164. doi: 10.1038/16469

Li, W., Jiang, Y., Sun, T., Yao, X., and Sun, X. (2016). Supplementation of procyanidins B2 attenuates photooxidation-induced apoptosis in ARPE-19 cells. *Int. J. Food Sci. Nutr.* 67, 650–659. doi: 10.1080/09637486.2016.1189886

Liu, H. J., Pan, X. X., Liu, B. Q., Gui, X., Hu, L., Jiang, C. Y., et al. (2017). Grape seed-derived procyanidins alleviate gout pain via NLRP3 inflammasome suppression. *J. Neuroinflammation* 14:74. doi: 10.1186/s12974-017-0849-y

Mao, X., Hao, S., Zhu, Z., Zhang, H., Wu, W., Xu, F., et al. (2015). Procyanidins protects against oxidative damage and cognitive deficits after traumatic brain injury. *Brain Inj.* 29, 86–92. doi: 10.3109/02699052.2014.968621

Martinez-Micaelo, N., González-Abuín, N., Ardèvol, A., Pinent, M., and Blay, M. T. (2012). Procyanidins and inflammation: molecular targets and health implications. *Biofactors* 38, 257–265. doi: 10.1002/biof.1019

Martinez-Micaelo, N., González-Abuín, N., Pinent, M., Ardévol, A., and Blay, M. (2015). Procyanidin B2 inhibits inflammasome-mediated IL-1β production in lipopolysaccharide-stimulated macrophages. *Mol. Nutr. Food Res.* 59, 262–269. doi: 10.1002/mnfr.201400370

Moreira, E. L., Rial, D., Duarte, F. S., de Carvalho, C. R., Horst, H., Pizzolatti, M. G., et al. (2010). Central nervous system activity of the proanthocyanidin-rich fraction obtained from *Croton celtidifolius* in rats. *J. Pharm. Pharmacol.* 62, 1061–1068. doi: 10.1111/j.2042-7158.2010.01124.x

Muley, M. M., Krustev, E., and McDougall, J. J. (2016). Preclinical assessment of inflammatory pain. *CNS Neurosci. Ther.* 22, 88–101. doi: 10.1111/cns.12486

Pan, C., Wang, C., Zhang, L., Song, L., Chen, Y., Liu, B., et al. (2018). *Procyanidins attenuate* neuropathic pain by suppressing matrix metalloproteinase-9/2. *J. Neuroinflammation* 15:187. doi: 10.1186/s12974-018-1182-9

Rashid, M. H., Furue, H., Yoshimura, M., and Ueda, H. (2006). Tonic inhibitory role of alpha4beta2 subtype of nicotinic acetylcholine receptors on nociceptive transmission in the spinal cord in mice. *Pain* 125, 125–135. doi: 10.1016/j.pain.2006.05.011

Sobrinho, A. P., Minho, A. S., Ferreira, L. L. C., Martins, G. R., Boylan, F., and Fernandes, P. D. (2017). Characterization of anti-inflammatory effect and possible mechanism of action of *Tibouchina granulosa*. *J. Pharm. Pharmacol.* 69, 706–713. doi: 10.1111/jphp.12712

Spencer, J. P., Chaudry, F., Pannala, A. S., Srai, S. K., Debnam, E., and Rice-Evans, C. (2000). Decomposition of cocoa procyanidins in the gastric milieu. *Biochem. Biophys. Res. Commun.* 272, 236–241. doi: 10.1006/bbrc.2000.2749

Sun, L., Han, R., Guo, F., Chen, H., Wang, W., Chen, Z., et al. (2020). Antagonistic effects of IL-17 and Astragaloside IV on cortical neurogenesis and cognitive behavior after stroke in adult mice through Akt/GSK-3β pathway. *Cell Death Discov.* 6:74. doi: 10.1038/s41420-020-00298-8

Todd, A. J. (2010). Neuronal circuitry for pain processing in the dorsal horn. *Nat. Rev. Neurosci.* 11, 823–836. doi: 10.1038/nrn2947

Wang, J., Ferruzzi, M. G., Ho, L., Blount, J., Janle, E. M., Gong, B., et al. (2012). Brain-targeted proanthocyanidin metabolites for Alzheimer's disease

treatment. *J. Neurosci.* 32, 5144–5150. doi: 10.1523/JNEUROSCI.6437-11.2012

Yin, J. B., Liang, S. H., Li, F., Zhao, W. J., Bai, Y., Sun, Y., et al. (2020). dmPFC-vlPAG projection neurons contribute to pain threshold maintenance and antianxiety behaviors. *J. Clin. Invest.* 130, 6555–6570. doi: 10.1172/JCI127607

Yu, J., Moutal, A., Dorame, A., Bellampalli, S. S., Chefdeville, A., Kanazawa, I., et al. (2019). Phosphorylated CRMP2 regulates spinal nociceptive neurotransmission. *Mol. Neurobiol.* 56, 5241–5255. doi: 10.1007/s12035-018-1445-6

Conflict of Interest: The authors declare that the research was conducted in the absence of any commercial or financial relationships that could be construed as a potential conflict of interest.

Publisher's Note: All claims expressed in this article are solely those of the authors and do not necessarily represent those of their affiliated organizations, or those of the publisher, the editors and the reviewers. Any product that may be evaluated in this article, or claim that may be made by its manufacturer, is not guaranteed or endorsed by the publisher.

frontiers | Frontiers in Pharmacology

ORIGINAL RESEARCH
published: 25 April 2022
doi: 10.3389/fphar.2022.757490

Transformation of Stilbene Glucosides From *Reynoutria multiflora* During Processing

Junqi Bai[1,2], *Wanting Chen*[1], *Juan Huang*[1,2], *He Su*[1], *Danchun Zhang*[1], *Wen Xu*[1,2], *Jing Zhang*[1], *Zhihai Huang*[1,2]* *and Xiaohui Qiu*[1,2,3]*

[1]*Guangdong Provincial Hospital of Traditional Chinese Medicine, The Second Clinical Medical College of Guangzhou University of Chinese Medicine, Guangzhou, China,* [2]*Guangzhou Key Laboratory of Chirality Research on Active Components of Traditional Chinese Medicine, Guangzhou, China,* [3]*Guangdong Provincial Key Laboratory of Clinical Research on Traditional Chinese Medicine Syndrome, Guangzhou, China*

The root of *Reynoutria multiflora* Thunb. Moldenke (RM, syn.: *Polygonum multiflorum* Thunb.) has been widely used in TCM clinical practice for centuries. The raw *R. multiflora* (RRM) should be processed before use, in order to reduce toxicity and increase efficiency. However, the content of trans-2, 3, 5, 4′-tetrahydroxystilbene-2-O-β-D-glucopyranoside (trans-THSG), which is considered to be the main medicinal ingredient, decreases in this process. In order to understand the changes of stilbene glycosides raw *R. multiflora* (RRM) and processed *R. multiflora* (PRM), a simple and effective method was developed by ultra high performance liquid chromatography tandem quadrupole/electrostatic field orbitrap high-resolution mass spectrometry (UHPLC-Q-Exactive plus orbitrap MS/MS). The content and quantity of stilbene glycosideshave undergone tremendous changes during the process. Seven parent nucleus of stilbene glycosides and 55 substituents, including 5-HMF and a series of derivatives, were identified in PM. 146 stilbene glycosides were detected in RRM, The number of detected compounds increased from 198 to 219 as the processing time increased from 4 to 32 h. Among the detected compounds, 102 stilbene glycosides may be potential new compounds. And the changing trend of the compounds can be summarized in 3 forms: gradually increased, gradually decreased, first increased and then decreased or decreased first. The content of trans-THSG was indeed decreased during processing, as it was converted into a series of derivatives through the esterification reaction with small molecular compounds. The clarification of secondary metabolite group can provide a basis for the follow-up study on the mechanism of pharmacodynamics and toxicity of PM, and for screening of relevant quality markers.

Keywords: *Reynoutria multiflora*, stilbene glycosides, processed, UHPLC-Q-Exactive plus orbitrap MS/MS, structural and content changes

OPEN ACCESS

Edited by:
Gokhan Zengin,
Selcuk University, Turkey

Reviewed by:
Xiaoxiao Huang,
Shenyang Pharmaceutical University, China
Sengul Uysal,
Erciyes University, Turkey
Ying-Yong Zhao,
Northwest University, China

***Correspondence:**
Zhihai Huang
zhhuang7308@163.com
Xiaohui Qiu
qiuxiaohui@gzucm.edu.cn

Specialty section:
This article was submitted to Ethnopharmacology, a section of the journal Frontiers in Pharmacology

Received: *12 August 2021*
Accepted: *11 March 2022*
Published: *25 April 2022*

Citation:
Bai J, Chen W, Huang J, Su H, Zhang D, Xu W, Zhang J, Huang Z and Qiu X (2022) Transformation of Stilbene Glucosides From Reynoutria multiflora During Processing. Front. Pharmacol. 13:757490. doi: 10.3389/fphar.2022.757490

Abbreviations: DDMP, 2, 3-dihydro-3, 5-dihydroxy-6-methyl-4H-pyranone; 5-HMF, 5-hydromethylfurfura; RM, *Reynoutria multiflora* Thunb; PRM, processed *Reynoutria multiflora*; RRM, raw *Reynoutria multiflora*; TCM, Traditional Chinese Medicine; Trans-THSG, tran-2, 3, 5, 4′-tetrahydroxystilbene-2-O-β-D-glucopyranoside; UHPLC-Q-Exactive plus orbitrap MS/MS, ultra high performance liquid chromatography tandem quadrupole/electrostatic field orbitrap high-resolution mass spectrometry.

1 INTRODUCTION

Traditional Chinese medicine processing is a unique pharmaceutical technology derived from the theory of traditional Chinese medicine. It has played a prominent role in the clinical practice of traditional Chinese medicine for thousands of years, ensuring the safety and effectiveness of treatment. After processing with different temperatures, durations, solvents or excipients, the components of traditional Chinese medicine have undergone different changes. Ingredients will be dissolved, decomposed or transformed into new components, resulting in increasing or decreasing of the compounds. All these changes are closely related to the property and efficacy of traditional Chinese medicine. Therefore, it is of great significance to study the changes of chemical components before and after processing of traditional Chinese medicine.

The root of *Reynoutria multiflora* Thunb. (*Polygonum multiflorum* Thunb.), well known as He-shou-wu in China, has been widely used in TCM clinical practice for centuries (Li et al., 2017). Lots of research have shown that RRM and its processed products have different pharmacological effects. RRM has the effect of detoxification, carbuncle elimination, relaxing bowel. And PRM shows the effect of tonifying liver and kidney, tonic medicines and hair-blacking (Cheung et al., 2014; Lin et al., 2015; Chinese Pharmacopoeias Commission, 2020). RRM is commonly processed by steaming with black bean or water, which has been officially documented in the Chinese pharmacopoeia. However, the processing time was not specified in the processing specification. Therefore, the processing time of PRM on the market varies greatly, ranging from 2 to 18 h (Lin et al., 2018). But in our previous studies, we have screened out that the best effect of PRM was processing for 24–32 h (Qiu et al., 2008). The quality of PRM is inhomogeneous in the market, the main reason for this phenomenon is that the processing mechanism of PRM is not clear. The increased reports of hepatotoxicity of RRM in recent years (Dong et al., 2014; Lei et al., 2015; Zhang et al., 2019) may also be related to incomplete processing.

Previous research indicated that the main chemical components of RM were secondary metabolites, including stilbene glycosides, anthraquinone and polyphenols were the most representative (Choi et al., 2007; Lin et al., 2015; Sun et al., 2015). The fragmentation pathways of typical constituents and chemical profiles of RM have been studied by an on-line UHPLC-ESI-linear ion trap-Orbitrap hybrid mass spectrometry method (Xu et al., 2012; Qiu et al., 2013). The secondary metabolites were quantitatively analyzed by HPLC/LC-MS/MS to study the chemical components before and after processing of *R. multiflora*, which showed that the content of some chemical substances was changed by processing. In our previous study, the contents of 5-HMF, THSG, emodin and physcion are changed during the processing (Chen et al., 2012). The content of THSG, a compound that possess anti-oxidative, anti-aging, anti-tumor, anti-inflammatory and liver protective activities (Lv et al., 2007; Shao et al., 2012; Lin et al., 2015; Yang et al., 2020), was decreased (Qiu et al., 2006; Fu, 2011). However, there is no research report on the secondary metabolite group produced by stilbene glycosides in the process, and the clarification of secondary metabolite group can provide a basis for the follow-up study on the mechanism of pharmacodynamics and toxicity of PM, and for screening of relevant quality markers.

In this study, a simple and rapid method for the determination of RRM and PRM by UHPLC-Q-Exactive plus orbitrap MS/MS was established, and the qualitative analysis of RRM and PRM were carried out *in vitro* to obtain a clear chemical map. The fragment ions at *m/z* 405.1087 and 243.0656 were selected as characteristic fragments, the secondary metabolites in RRM and processed PRM samples prepared with different durations were characterized and identified, then, the changes of stilbene glycosides during processing were further analyzed.

2 MATERIALS AND METHODS

2.1 Materials

RRM and PRMs that had been processed for 4, 8, 12, 18, 24 and 32 h were provided by Shanghai Dehua Traditional Chinese Medicine CO., Ltd., and the corresponding batch numbers were HSW2018051101-S, HSW2018051101-4H, HSW2018051101-8H, HSW2018051101-12H, HSW2018051101-18H, HSW2018051101-24H, and HSW2018051101-32H. The samples were authenticated by Professor Zhihai Huang, and voucher specimens were deposited in the Materials Medica Preparation Lab of the Second Affiliated Hospital of the Guangzhou University of Chinese Medicine.

Trans-2, 3, 5, 4′-tetrahydroxystilbene-2-O-β-D-glucopyranoside (THSG), cis-THSG and polydatin were purchased from yuanye Bio-Technology Co., Ltd. Acetonitrile (No. H08J11E115101, P27A11P107214, T15A10F85743, purity ≥98%, Shanghai, China). acetonitrile and methanol (HPLC grade), were supplied by E. Merck (Darmstadt, Germany), formic acid (HPLC grade) was purchased from fisher (United States), ultra-pure water was prepared by a Mili-Q water purification system (Millipore, MA, United States).

2.2 Sample Processing Method

All the samples were prepared using following method: 1 g sample powder was ultrasonicated for 30 min with 25 ml of 70% ethanol, followed by filtration and then evaporated the filtrate. 5 ml of ultrapure water were added to dissolve the residue and then extracted twice with 15 ml of ethyl acetate. The resulting mixture was combined with an ethyl acetate solution and evaporated over a water bath; after that, 1 ml of methanol was added to dissolve the residue and centrifugation (15,000 rpm, 4°C) for 10 min by a 1.5 ml centrifuge tube. Finally, the supernatant of the treatment samples was injected into the UPLC-Q-Exactive plus orbitrap MS/MS system.

2.3 UHPLC-Q-Exactive Plus Orbitrap MS/MS Analysis

2.3.1 Liquid Chromatography

All the samples were analysed using an Ultimate 3000 UPLC system (Dionex, United States) that was controlled with Thermo Xcalibur software (Thermo Fisher Scientific, United States). The samples were separated using a Kinetex UPLC C18 column

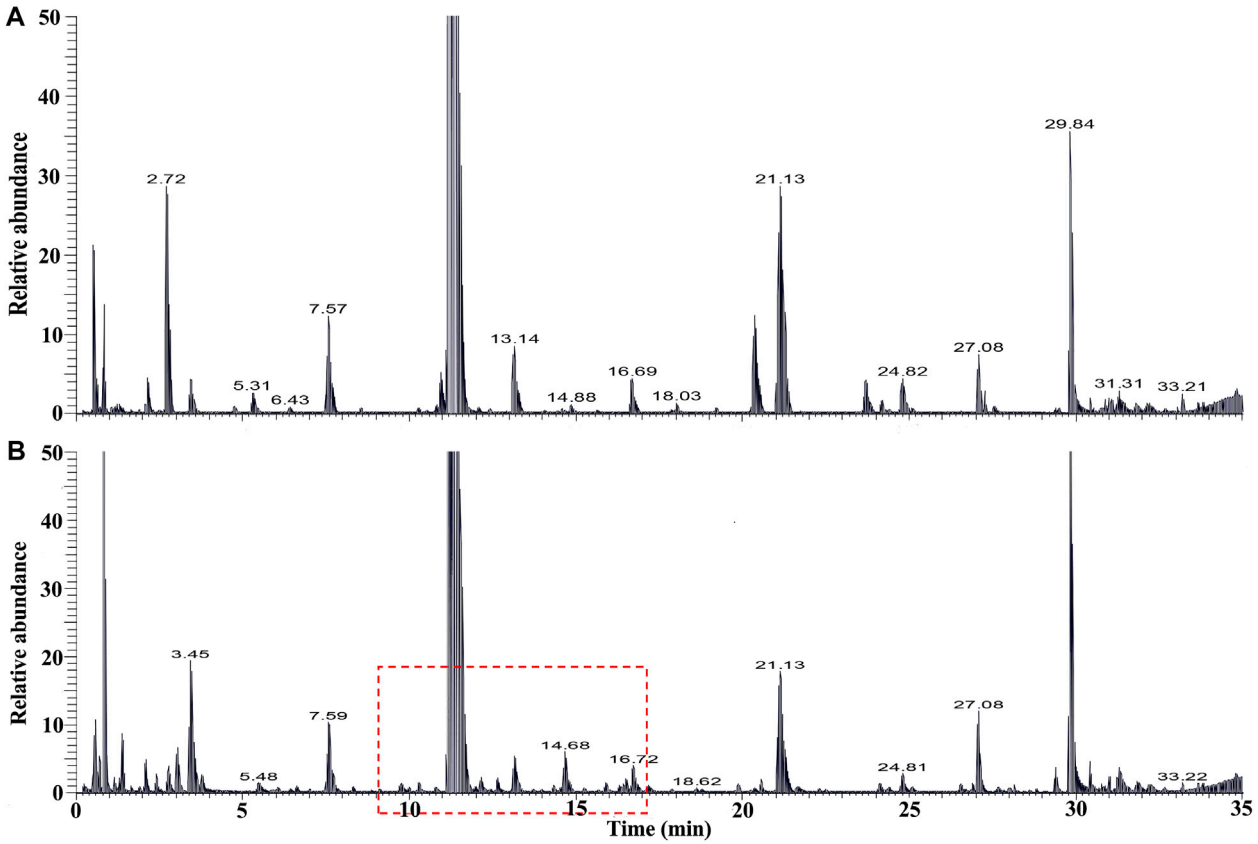

FIGURE 1 | The Base peak intensity chromatograms of samples of *raw Reynoutria multiflora* Thunb. [RRM, **(A)**] and processed *Reynoutria multiflora* Thunb. [PRM for 24h, **(B)**] derived from UHPLC-Q-Exactive plus orbitrap MS/MS.

(100*2.1 mm, 1.7 μm) (Phenomenex, United States). The mobile phase consisted of solvent A (0.1% formic acid) and solvent B (acetonitrile). A gradient elution was applied using the following optimized gradient program: 8-8% B at 0–3 min, 8–28% B at 3–25 min, 28–40% B at 25–26 min, 40–50% B at 26–28 min, 50–70% B at 28–30 min, 70–90% B at 30–32 min, and 90–90% B at 32–35 min. The flow rate was kept at 0.4 ml/min, the sample injection volume was 1 μL, and the column temperature was maintained at 25°C.

2.4 Mass Spectrometry

Mass spectrometry was performed on a Q-Exactive Plus™ quadrupole-Orbitrap mass spectrometer (Thermo Fisher Scientific, United States) in negative ion mode. The scan mass range was set at *m/z* 100–1,200. The parameter settings were as follows: a full scan and fragment spectral resolution of 70,000 FWHM and 17, 50 FWHM, respectively; capillary temperature was 350°C; auxiliary gas heater temperature was 350°C; spray voltage was −3.2 KV; sheath gas flow rate was 40 Arb; auxiliary gas flow rate was 15 Arb; and S-lens RF level was set at 50. The acquisition mode of stepped NCE (normalized collision energy) was using with settings of 30, 50, and 70 eV. The accumulated resultant fragment ions were injected into the Orbitrap mass analyzer for single-scan detection.

Considering the possible elemental composition of the RM components, the types and quantities of expected atoms were set as follows: carbon ≤50, hydrogen ≤200, oxygen ≤20, nitrogen ≤3. The accuracy error threshold was fixed at 5 ppm.

3 RESULTS AND DISCUSSION

3.1 Base Peak Chromatograms

The chemical profiles of RRM and processing PRMs were analyzed by UHPLC-Q-Exactive plus orbitrap MS/MS, the representative base peak chromatograms of RRM and processing PRM (24 h) are shown in **Figure 1**. Some differences were observed between the two base peak chromatograms. The stilbene glycosides and their derivatives were distributed from 7 to 22 min. The representative base peak chromatograms of processing of PRM (7–22 min) are shown in **Figure 2**.

3.2 Fragmentation Pathway of THSG and Derivatives

To identify the derivatives of THSG in the processing RM, the trans-THSG and cis-THSG standard were firstly analyzed by

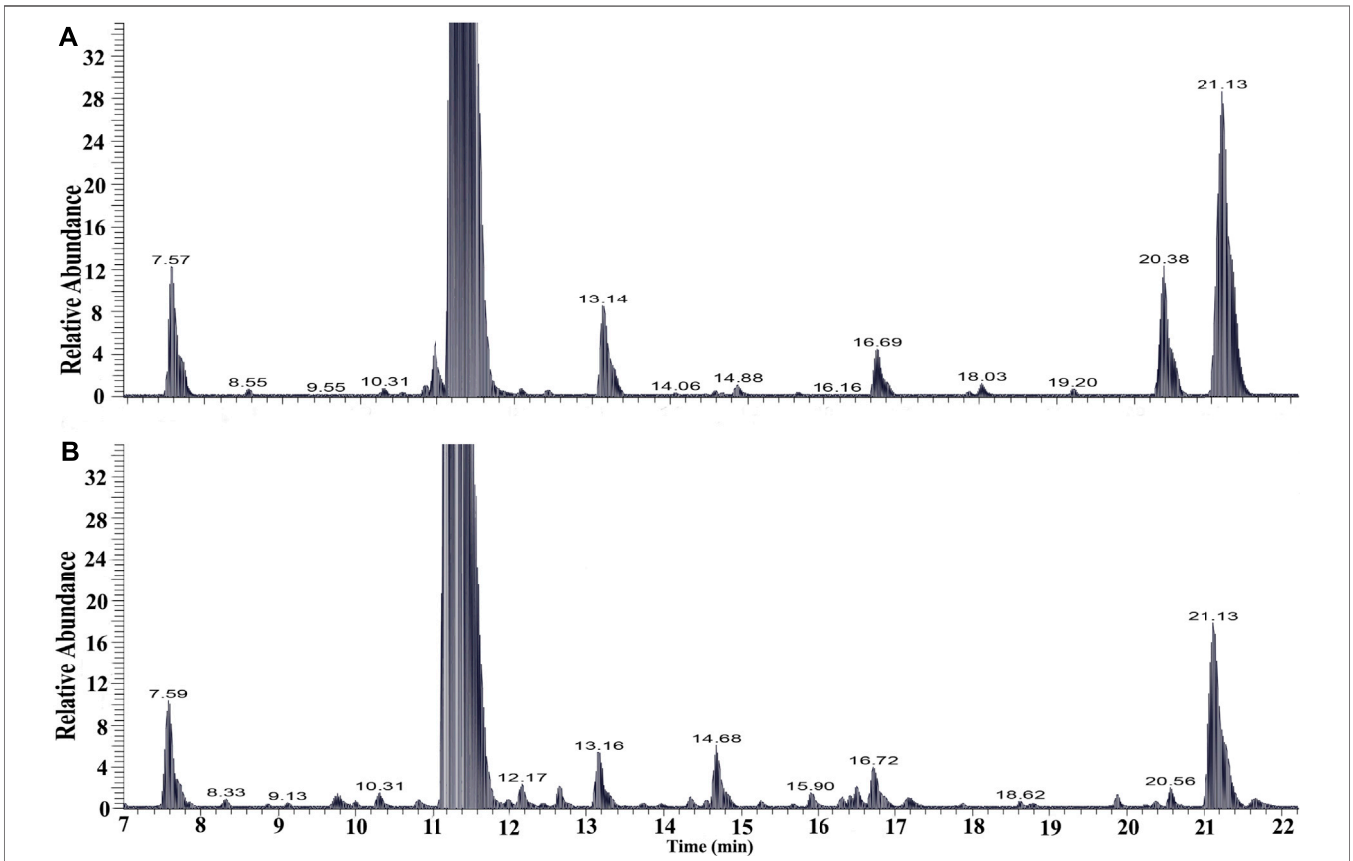

FIGURE 2 | The base peak intensity chromatograms of samples *raw Reynoutria multiflora* Thunb. (RRM, **A)** and processed *Reynoutria multiflora* Thunb. (PRM for 24 h, **B)** derived from UHPLC-Q-Exactive plus orbitrap MS/MS (7–22 min).

UPLC-Q-Exactive plus MS/MS under the above-mentioned conditions. Trans-THSG (**A3-5**, t_R = 11.18 min) and cis-THSG (**A3-2**, t_R = 7.58 min) had a $[M-H]^-$ ion at *m/z* 405.1187 with only a dominant ion at *m/z* 243.0654 ($C_{14}H_{11}O_4$) in MS^2 spectrum. These two ions could be used as a diagnostic ion for identify stilbene glycosides. Compound **A3-1, A3-3 and A3-4** (t_R = 6.67, 9.75 and 9.89 min) also had an $[M-H]^-$ ion at *m/z* 405.1187 ($C_{20}H_{21}O_9$), and showed a fragment ion at *m/z* 243.0654 in their MS^2 spectrum, indicating that they are isomers of THSG. **A3-5** was identified as trans-THSG and **A3-2** was cis-THSG, and **A3-1** should be isomer of cis-THSG, **A3-3 and A3-4** should be isomers of trans-THSG. (**Figure 3**).

3.3 Identification of Tetrahydroxystilbene-O-Hexoside Derivatives

During the processing, Maillard reaction occurred, producing a large number of compounds, including acetone alcohol, 2, 3-butanediol, succinic acid, 2, 3-dihydro-3, 5-dihydroxy-6-methyl-4H-pyranone (DDMP), 5-hydroxymethyl furfural (5-HMF) and its derivatives (Liu, 2018). Stilbene glycosides may react with products of Maillard reaction or small moleculars, such as gallic acid and catechuic acid, in high temperature and high humidity environment.

Most stilbene glycosides in RM showed common fragmentation pathways and two diagnostic fragment ions at *m/z* 405.1192($C_{20}H_{21}O_9$) and 243.0654 ($C_{14}H_{11}O_4$). These were used for rapidly extracting and analyzing unknown stilbene glycosides. According to the structural characteristics of THSG, the linking points of stilbene derivatives with other compounds contain glycosyl hydroxyl moiety and phenyl hydroxyl moiety. According to the cleaved fragments, it can be inferred as follows: 1. if there is a fragment from loss of $C_6H_{10}O_5$ by parent ion, the linking point should be phenyl hydroxyl moiety; 2. The cleavage fragment contains the ion at *m/z* 405.1187 of THSG and the ion at *m/z* (hexoside + substituent), and there is no fragment to loss of $C_6H_{10}O_5$, so the linking point should be glycosyl hydroxyl moiety; 3. if the fragment is only the ion at *m/z* 243.0654, most of the glycosyl hydroxyl moiety may be linked, but there is also a probability that the hexoside of THSG and the substituent on the phenyl hydroxyl moiety will split at the same time, so the linking point cannot be determined in this case. We use tetrahydroxystilbene-O-(substituent)-hexoside to name them.

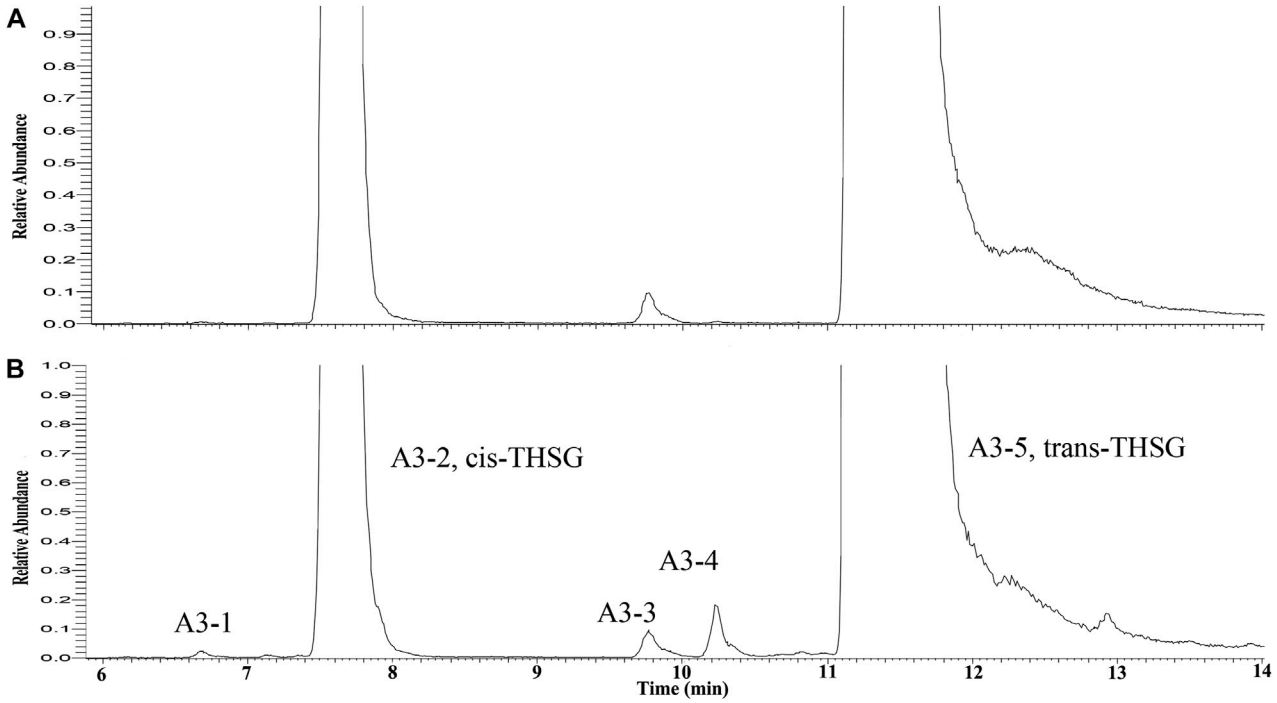

FIGURE 3 | The extracted ion chromatograms of ion at *m/z* = 405.1187 **(A***: raw Reynoutria multiflora* Thunb. RRM), **B:** processed *Reynoutria multiflora* Thunb. (PRM 24 h)).

Compounds **A1-1** and **A1-2** displayed a $[M-H]^-$ ion at *m/z* 375.1081 ($C_{19}H_{19}O_8$) and the product ion at *m/z* 243.0654 derived from the loss of a pentose (mostly arabinose). By comparing with literature, Compounds **A1-1** and **A1-2** were tentatively identified as tetrahydroxystilbene-O-pentose.

Compounds **A2-1, A2-2**, and **A2-3** gave a $[M-H]^-$ ion at *m/z* 389.1242 ($C_{20}H_{21}O_8$) and the product ion at *m/z* 243.0654 derived from the loss of a deoxyhexose (mostly rhamnose), indicated that it was a THSG derivative. Compounds **A2-1, A2-2**, and **A2-3** were tentatively characterized as tetrahydroxystilbene-O-deoxyhexoside.

Compounds **A4-1** and **A4-2** displayed a high resolution $[M-H]^-$ ion at *m/z* 423.1295 and gave element composition of $C_{20}H_{23}O_{10}$. The MS^2 spectra gave identical ions at *m/z* 261.0764 ($C_{14}H_{13}O_5$) and 243.0654 ($C_{14}H_{11}O_4$), respectively. The loss of $C_6H_{10}O_5$ (hexoside) and H_2O to produce the deprotonated moiety ion at *m/z* 243.0655, indicated can be identified as stilbene derivatives, but the specific structure is not yet determined.

Compounds **A5-1** ~ **A5-4** showed the same $[M-H]^-$ ion at *m/z* 433.1136 ($C_{21}H_{21}O_{10}$) and the MS^2 spectra gave ions at *m/z* 271.0608 ($C_{15}H_{11}O_5$) and 243.0654 ($C_{14}H_{11}O_4$). Without further information, compounds **A5-1** ~ **A5-4** were tentatively characterized as tetrahydroxystilbene-O-hexoside-O-formic acid acyl (phenolic hydroxyl moiety).

Compounds **A6-1** and **A6-2** showed the same $[M-H]^-$ ion at *m/z* 437.1450 ($C_{21}H_{25}O_{10}$) and the MS^2 spectra gave ions at *m/z* 275.0922 ($C_{15}H_{15}O_5$) and *m/z* 243.0655 ($C_{14}H_{11}O_4$), the loss of $C_6H_{10}O_5$ (hexoside) and CH_4O to produce the deprotonated moiety ion at *m/z* 243.0655, allowed us to infer that they were tetrahydroxystilbene derivative, but the specific structure is not yet determined.

Compounds **A7-1** ~ **A7-5** gave a $[M-H]^-$ ion at *m/z* 447.1300 ($C_{22}H_{23}O_{10}$) and loss 204 Da to produce ion at *m/z* 243.0656 in the MS^2 spectrum, which indicated that the presence of a hexose group and an acetyl. Thus, compounds **A7-1**~ **A7-5** were preliminarily characterized as tetrahydroxystilbene-O-(acetyl)-hexoside.

Compounds **A8-1** and **A8-2** showed the same $[M-H]^-$ ion at *m/z* 449.1086 ($C_{21}H_{21}O_{11}$) and the MS^2 spectra gave ions at *m/z* 287.0554 ($C_{15}H_{11}O_6$) and 243.0654 ($C_{14}H_{11}O_4$) form continuous loss of $C_6H_{10}O_5$ and CO_2. Thus, the carbonate acyl substituted THSG was detected and compounds **A8-1** and **A8-2** were identified as tetrahydroxystilbene-O-hexoside-O-carbonate acyl (phenolic hydroxyl moiety).

Compound **A9** displayed a high resolution $[M-H]^-$ ion at *m/z* 457.1116 and gave element composition of $C_{23}H_{21}O_{10}$, the product ion at *m/z* 243.0654 originated from the loss of $C_9H_{10}O_6$ (hexoside + hydroxycyclopropenon). By investigating literature, compound **A9** was preliminarily identified as tetrahydroxystilbene-O-(hydroxycyclopropenon)-hexoside. Similarly, compounds **A10** and **A11** were tentatively identified as tetrahydroxystilbene-O-(acrylic acid acyl)-hexoside and tetrahydroxystilbene-O-(propionyl)-hexoside, since the loss of $C_9H_{12}O_6$ (hexoside + acrylic acid) and $C_9H_{14}O_6$ (hexoside + propionic acid) were detected.

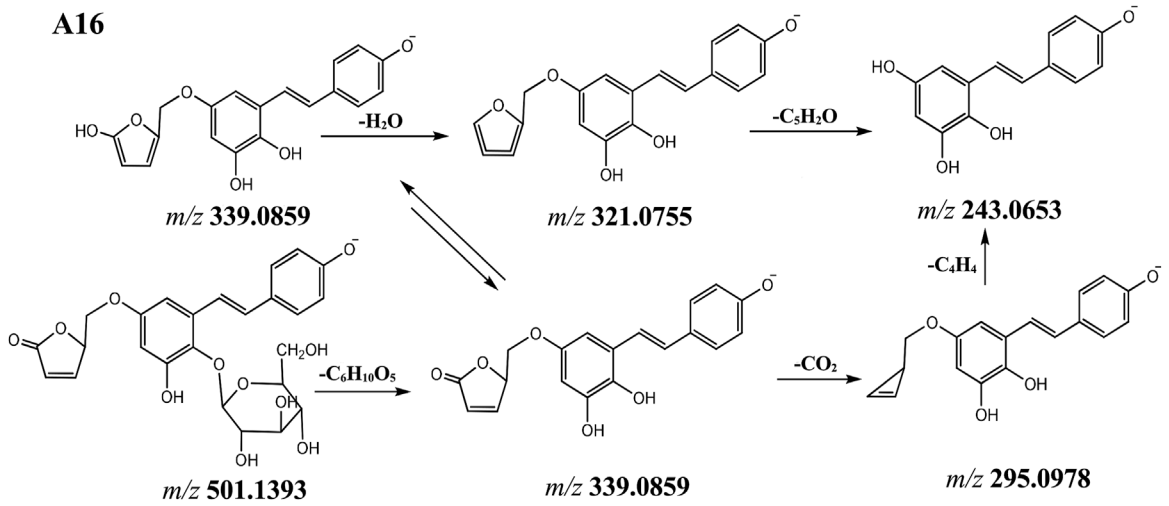

FIGURE 4 | The proposal fragmentation pathway of compound of A16.

Compounds **A12-1** and **A12-2** showed the same $[M-H]^-$ ion at *m/z* 463.1244 ($C_{22}H_{23}O_{11}$) and the MS^2 spectra gave ion at *m/z* 243.0654 ($C_{14}H_{11}O_4$) form loss of $C_8H_{12}O_7$ ($C_6H_{10}O_5$ and $C_2H_2O_2$). Thus, the glycolic acid substituted THSG was detected and compounds **A12-1** and **A12-2** were identified as tetrahydroxystilbene-O- (glycolic acid acyl)-hexoside.

Compounds **A13-1**, **A13-2**, and **A13-3** showed the same $[M-H]^-$ ion at *m/z* 477.1396 ($C_{23}H_{25}O_{11}$) and the MS^2 spectra gave ions at *m/z* 405.1184 ($C_{20}H_{21}0_9$), 315.0859 ($C_{17}H_{15}O_6$), 297.0763 ($C_{17}H_{13}O_5$) and 243.0655 ($C_{14}H_{11}O_4$). The ion at *m/z* 477.1396 loss of $C_3H_4O_2$ produce the ion at *m/z* 405.1184, By comparing literature, compounds **A13-1**, **A13-2**, and **A13-3** were tentatively identified as tetrahydroxystilbene-O-hexoside-O-lactic acid acyl (phenolic hydroxyl moiety).

Compounds **A14-1** ~ **A14-4** showed the same $[M-H]^-$ ion at *m/z* 489.1759 ($C_{25}H_{29}O_{10}$) and the MS^2 spectra gave identical ions at *m/z* 405.1176 ($C_{20}H_{21}0_9$), 327.1222 ($C_{19}H_{19}O_5$) and 243.0656 ($C_{14}H_{11}O_4$). The loss of C_5H_8O to produce the deprotonated THSG moiety ion at *m/z* 405.1176, Furthermore, the ion at *m/z* 327.1222 assigned as loss of $C_6H_{10}O_5$ form the *m/z* 489.1759. By investigating literatures, compounds **A14-1** ~ **A14-4** were identified as tetrahydroxystilbene-O-hexoside-O-valerate acyl (phenolic hydroxyl moiety).

Compound **A15** displayed a high resolution $[M-H]^-$ ion at *m/z* 499.1241 and gave element composition of $C_{25}H_{23}O_{11}$, the product ions at *m/z* 337.0704 ($C_{19}H_{13}O_6$), 293.0812 ($C_{18}H_{13}O_4$) and 243.0654 ($C_{14}H_{11}O_4$) originated from the consecutive loss of $C_6H_{10}O_5$ (hexoside), CO_2 and C_4H_2 (5-hydroxyfuran-2-carbaldehyde). By investigating literature, compound **A15** was preliminarily identified as tetrahydroxystilbene-O-hexoside-O-5-hydroxyfuran-2-carbaldehyde (phenolic hydroxyl moiety).

Compounds **A16-1** and **A16-2** showed the same $[M-H]^-$ ion at *m/z* 501.1393 ($C_{25}H_{25}O_{11}$) and the MS^2 spectra gave ions at *m/z* 339.0858, 321.0756 and 243.0654 form continuous loss of $C_6H_{10}O_5$ (hexoside), CO_2 and C_4H_4 (**Figure 4**). By investigating literature, compounds **A16-1** and **A16-2** were identified as tetrahydroxystilbene-O-hexoside-O-4-hydroxymethyl-5H-furan-2-one (phenolic hydroxyl moiety).

Compound **A17** gave a $[M-H]^-$ ion at *m/z* 503.1553 ($C_{25}H_{27}O_{11}$) and the product ions at *m/z* 341.1019 ($C_{19}H_{17}O_6$), 297.1125 ($C_{18}H_{17}O_4$) and 243.0656 ($C_{14}H_{11}O_4$). By comparing literature, compound **A17** was tentatively characterized as tetrahydroxystilbene-O-hexoside-O- 5-hydroxymethyl-4, 5-dihydrofuranone (phenolic hydroxyl moiety).

Compounds **A18-1** ~ **A18-5** showed the same $[M-H]^-$ ion at *m/z* 505.1346 ($C_{24}H_{25}O_{12}$) and in **A18-1** and **A18-2** MS^2 spectra, gave ions at *m/z* 405.1178 and *m/z* 243.0655, in **A18-3** ~ **A18-5** MS^2 spectra, gave ions at *m/z* 343.0799 and *m/z* 243.0655. By comparing literature, compounds **A18-1** and **A18-2** were preliminarily characterized as tetrahydroxystilbene-O-(succinic acid acyl)-hexoside, and compounds **A18-3** ~ **A18-5** were identified as tetrahydroxystilbene-O-hexoside-O-succinic acid acyl (phenolic hydroxyl moiety).

Compounds **A19-1** and **A19-2** were eluted at 11.85 and 12.00 min, and the molecular formula was $C_{24}H_{27}O_{12}$ (*m/z* 507.1500). The MS^2 spectra gave identical ions at *m/z* 345.0966 ($C_{18}H_{17}O_7$), *m/z* 313.0709 ($C_{17}H_{13}O_6$), *m/z* 285.0763 ($C_{16}H_{13}O_5$), *m/z* 255.0656 ($C_{15}H_{11}O_4$) and *m/z* 243.0654 ($C_{14}H_{11}O_4$). By comparing literature, compounds **A19-1** and **A19-2** were identified as tetrahydroxystilbene-O-hexoside-O-dihydroxybutyrate (phenolic hydroxyl moiety).

Compound **A20** gave a $[M-H]^-$ ion at *m/z* 511.1603 ($C_{27}H_{27}O_{10}$) and the product ions at *m/z* 349.1068 ($C_{21}H_{17}O_5$) and 243.0655 ($C_{14}H_{11}O_4$) form continuous loss of $C_6H_{10}O_5$ (hexoside) and C_7H_6O (salicyloyl). By comparing literature, compound **A20** was tentatively characterized as tetrahydroxystilbene-O-hexoside-O-salicyloyl (phenolic hydroxyl moiety).

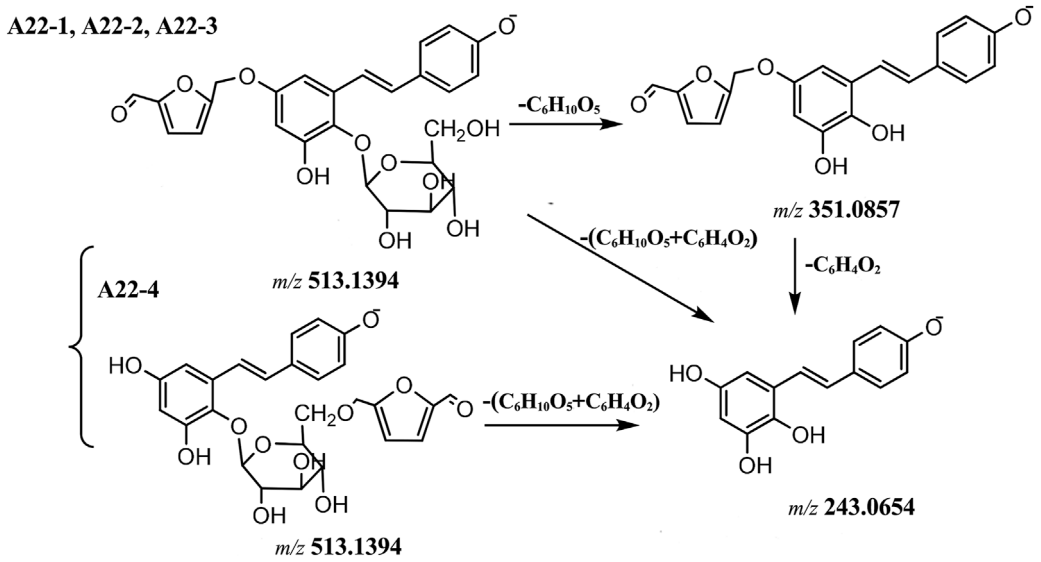

FIGURE 5 | The proposal fragmentation pathway of compounds of A22.

Compounds **A21-1** and **A21-2** showed the same $[M-H]^-$ ion at *m/z* 512.1555 ($C_{26}H_{26}O_{10}N$) and the MS^2 spectra gave ions at *m/z* 405.1175 ($C_{20}H_{21}O_9$) and 243.0655 ($C_{14}H_{11}O_4$). By comparing literature, compounds **A21-1** and **A21-2** were tentatively identified as tetrahydroxystilbene-O-(aminocatecholoyl)-hexosides. Similarly, compound **A25** was tentatively identified as tetrahydroxystilbene-O-(pyroglutamyl)-hexoside.

Compounds **A22-1** ~ **A22-4** showed the same $[M-H]^-$ ion at *m/z* 513.1497 ($C_{26}H_{25}O_{11}$), compounds **A22-1**, **A22-2** and **A22-3** loss 162 Da to produce ion at *m/z* 351.0862, and then loss 108 Da ($C_6H_4O_2$) to produce ion at *m/z* 243.0656 in the MS^2 spectrum. And in compound **A22-4** MS^2 spectra, there was a fragment ion at *m/z* 243.0655, the proposal fragmentation pathway shown in **Figure 5**. By investigating literatures, compounds **A22-1**, **A22-2**, and **A22-3** were identified as tetrahydroxystilbene-O-hexoside-O-5-HMF (phenolic hydroxyl moiety), **A22-4** was identified as tetrahydroxystilbene-O-(5-HMF)-hexoside.

Compounds **A23-1** and **A23-2** were eluted at 15.29 and 15.69 min, and the molecular formula was $C_{26}H_{27}O_{11}$ (*m/z* 515.1555). In addition, the product ions at *m/z* 353.1021 ($C_{20}H_{17}O_6$) and *m/z* 243.0654 ($C_{14}H_{11}O_4$) originated from the consecutive loss of hexoside ($C_6H_{10}O_5$) and $C_6H_6O_2$ (2, 5-bis-hydroxymethyl furan). By comparing literature, compounds **A23-1** and **A23-2** identified as tetrahydroxystilbene-O-hexoside-O-2, 5-bis-hydroxymethyl furan (phenolic hydroxyl moiety). And compound **A24** displayed a high resolution $[M-H]^-$ ion at *m/z* 515.1179 and gave element composition of $C_{25}H_{23}O_{12}$, the loss of $C_5H_2O_3$ and $C_6H_{10}O_5$ to produce the deprotonated moiety ion at *m/z* 243.0655. By investigating literatures, compound **A24** was tentatively characterized as tetrahydroxystilbene-O-(5-hydroxyfuran-2-carboxylic acid)-hexoside.

Compounds **A26-1** ~ **A26-4** showed the same $[M-H]^-$ ion at *m/z* 519.1495 ($C_{25}H_{27}O_{12}$). In **A26-1** MS^2 spectra, the fragment ion at *m/z* 243.0655, in **A26-2**, **A26-3** and **A26-4** MS^2 spectra, the fragment ions at *m/z* 405.1167 ($C_{20}H_{21}O_9$), 357.0967 ($C_{19}H_{17}O_7$), 339.0855 ($C_{19}H_{15}O_6$), 297.0760 ($C_{17}H_{13}O_5$) and 243.0655 ($C_{14}H_{11}O_4$), by investigating literatures, compound **A26-1** was identified as tetrahydroxystilbene-O-(glutaryl)-hexoside, **A26-2**, **A26-3** and **A26-4** were identified as tetrahydroxystilbene-O-hexoside-O-glutaryl (phenolic hydroxyl moiety).

Compounds **A27-1** (t_R = 12.84 min), **A27-2** (t_R = 13.07 min) and **A27-3** (t_R = 13.82 min) showed the same $[M-H]^-$ ion at *m/z* 521.1294 ($C_{24}H_{25}O_{13}$) and the MS^2 spectra gave identical ions at *m/z* 405.1177 ($C_{20}H_{21}O_9$), 359.1115 ($C_{19}H_{19}O_7$) and 243.0754 ($C_{14}H_{11}O_4$). The loss of $C_4H_4O_4$ to produce the deprotonated THSG moiety ion at *m/z* 405.1177, thus, compounds **A27-1**, **A27-2**, and **A27-3** identified as tetrahydroxystilbene-O-hexoside-O-malic acid acyl (phenolic hydroxyl moiety).

Compounds **A28-1** ~ **A28-5** showed the same $[M-H]^-$ ion at *m/z* 525.1398 ($C_{27}H_{25}O_{11}$), the MS^2 of **A28-1** ~ **A28-3** spectra gave ions at *m/z* 525.1398, 405.1179, 363.0883, 243.0858 and 137.0228. The product ions at *m/z* 363.0883 originated from the loss of hexoside ($C_8H_{10}O_5$). Thus, the salicylic acid acyl substituted THSG was detected and compounds **A28-1** ~ **A28-3** identified as tetrahydroxystilbene-O-hexoside-O-salicylic acid acyl (phenolic hydroxyl moiety). The MS^2 of **A28-4** and **A28-5** spectra gave ions 405.1179, 243.0858 and 137.0228, but there were no 363.0833 fragment ion. Thus, compounds **A28-4** and **A28-5** were identified as tetrahydroxystilbene-O- (salicylic acid acyl)-hexoside.

Compounds **A29-1**, **A29-2** and **A29-3** gave a $[M-H]^-$ ion at *m/z* 527.1190 ($C_{26}H_{23}O_{12}$) and the MS^2 spectra showed identical ions at *m/z* 365.0652 ($C_{20}H_{13}O_7$) and 243.0659 ($C_{14}H_{11}O_4$). The MS^2 spectrum showed losses of $C_6H_{10}O_5$ and $C_6H_2O_3$, respectively, to produce characteristic aglycone ion at *m/z* 243.0659. By comparing literature, compounds **A29-1**, **A29-2**, and **A29-3** were tentatively identified as tetrahydroxystilbene-O-

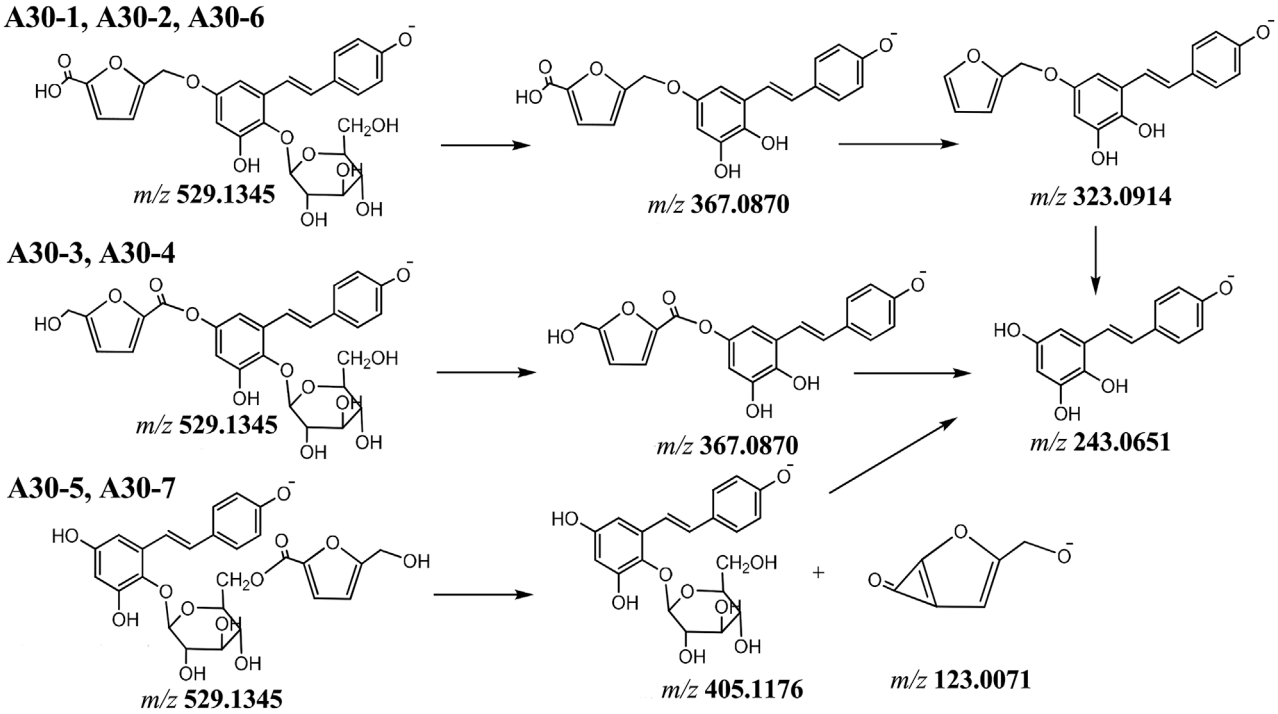

FIGURE 6 | The proposal fragmentation pathway of compounds of A30.

hexoside-O-5-formylfuran-2-carboxylyl (phenolic hydroxyl moiety).

Compounds **A30-1** ~ **A30** ~ **7** showed the same $[M-H]^-$ ion at *m/z* 529.1345 ($C_{26}H_{25}O_{12}$), the MS^2 spectra of **A30-1**, **A30-2** and **A30-6** gave ions at *m/z* 367.0870 ($C_{20}H_{15}O_7$), 323.0914 ($C_{19}H_{15}O_5$) and 243.0651 ($C_{14}H_{11}O_4$). The product ions originated from the consecutive loss of hexoside ($C_6H_{10}O_5$), CO_2 and C_5H_4O. In **A30-3** and **A30-4** spectra, gave ions at *m/z* 367.0807 ($C_{20}H_{15}O_7$), 243.0656 ($C_{14}H_{11}O_4$) and 123.0071 ($C_6H_3O_3$), and in **A30-5** and **A30-7** spectra, gave ions at *m/z* 405.1176 ($C_{20}H_{21}O_9$), 243.0656 ($C_{14}H_{11}O_4$) and 123.0071 ($C_6H_3O_3$). By investigating literatures, the substituent group of the compound was 5-hydroxymethyl-furfural. And according to the fragmentation fragments, it can be inferred that the binding sites are different (**Figure 6**). **A30-1, A30-2**, and **A30-6** were tentatively identified as tetrahydroxystilbene (phenolic hydroxyl moiety)-O-5-hydroxymethylfuran-2-carboxylyl-hexosides (hydroxyl moiety), **A30-3** and **A30-4** were identified as tetrahydroxystilbene (phenolic hydroxyl moiety)-O-5-hydroxymethylfuran- 2-carboxylyl-hexoside (carboxyl moiety), **A30-5** and **A30-7** were identified as tetrahydroxystilbene-O-(5-hydroxymethylfuran-2-carboxylyl)-hexoside.

Compounds **A31-1** ~ **A31-10** were eluted at 2.58, 2.75, 3.58, 4.66, 5.00 min 5.64, 12.14, 15.02, 15.36, 15.74 min, they both showed an accurate $[M-H]^-$ ion at *m/z* 531.1511 ($C_{26}H_{27}O_{12}$), which were 128 Da higher than that of THSG. In their MS^2 spectra, the $[M-H]^-$ ion showed fragment ions at *m/z* 405.1180 ($C_{20}H_{21}O_9$), 369.0966 ($C_{20}H_{17}O_7$), 351.0863 ($C_{20}H_{15}O_6$), 319.0796 ($C_{18}H_{13}O_5$), 295.0609 ($C_{17}H_{11}O_5$), and 243.0655 ($C_{14}H_{11}O_4$). All the MS^2 of the compounds have molecular fragment *m/z* 369.0966, indicated that the compounds are formed by dehydration of substituents and phenolic hydroxyl groups of stilbene glycosides. By investigating literature (Liu, 2018), compounds **A31-1** ~ **A31-10** were tentatively characterized as tetrahydroxystilbene-O-hexoside-DDMP (phenolic hydroxyl moiety).

Compounds **A32-1** ~ **A32-5** showed the same $[M-H]^-$ ion at *m/z* 533.1658 ($C_{26}H_{29}O_{12}$) and the MS^2 spectra gave identical ions at *m/z* 371.1124 ($C_{20}H_{18}O_7$), 327.0863 ($C_{18}H_{16}O_6$) and 243.0657 ($C_{14}H_{11}O_4$). The MS^2 showed losses of $C_6H_3O_3$ and $C_6H_{10}O_5$ due to substituent and hexose moiety, respectively, to produce characteristic aglycone ion at *m/z* 243.0657 ($C_{14}H_{11}O_4$). By comparing literature, compounds **A32-1** ~ **A32-5** were tentatively characterized as tetrahydroxystilbene-O-hexoside-adipic acid acyl (phenolic hydroxyl moiety).

Compound **A33-1** ad **A33-2** gave a $[M-H]^-$ ion at *m/z* 537.1609 ($C_{25}H_{29}O_{13}$) and the product ion at *m/z* 243.0655 ($C_{14}H_{11}O_4$) form loss of $C_{11}H_{18}O_9$ ($C_6H_{10}O_5$ and $C_5H_8O_4$). By comparing literature, compound **A33-1** and **A33-2** were tentatively characterized as tetrahydroxystilbene-O-(arabinoyl)-hexoside.

Compounds **A34-1** ~ **A34-4** showed a $[M-H]^-$ ion at *m/z* 541.1353 ($C_{27}H_{25}O_{12}$) and the MS^2 spectra of **A34-1** and **A34-2**, showed fragment ions at *m/z* 405.1175 ($C_{20}H_{21}O_9$), 297.0610 ($C_{13}H_{13}O_8$), 243.0657 ($C_{14}H_{11}O_4$), 153.0179 ($C_7H_5O_4$),

respectively, indicated that they were THSG derivatives. The loss of $C_7H_5O_4$ to produce the deprotonated THSG moiety ion at *m/z* 405.1175, allowed us to infer that they were protocatechuic acid substituted THSG products. And the ion at m/z 297.0610 assigned as protocatechuic acid acyl-hexoside moiety, produced protocatechuic acid ion at m/z 153.0179. **A34-3** and **A34-4** were eluted at 21.70 and 22.07 min, the $[M-H]^-$ ions showed fragment ions at *m/z* 379.0793 ($C_{21}H_{15}O_7$) and 243.0657 ($C_{14}H_{11}O_4$), respectively, originated from the consecutive loss of hexoside ($C_6H_{10}O_5$) and protocatechuic acid ($C_7H_5O_4$). There results indicate that protocatechuic acid substituted to the phenolic hydroxyl moiety in compounds **A34-3** and **A34-4**. Therefore, compounds **A34-1** and **A34-2** were identified as tetrahydroxystilbene-O-hexoside-O-protocatechuic acid acyl (glycosyl hydroxyl moiety), and **A34-3** and **A34-4** were identified as tetrahydroxystilbene-O-hexoside-O-protocatechuic acid acyl (phenolic hydroxyl moiety).

Compound **A35** gave a $[M-H]^-$ ion at *m/z* 543.1121 ($C_{26}H_{33}O_{13}$) and the product ions at *m/z* 405.1196 ($C_{20}H_{21}O_9$) and 243.0655 ($C_{14}H_{11}O_4$) form consecutive loss of $C_6H_{12}O_4$ and $C_6H_{10}O_5$. By comparing literatures, compound **A35** was tentatively identified as tetrahydroxystilbene-O- (furan-dicarboxylic acid acyl)-hexoside. And compound **A36** gave a $[M-H]^-$ ion at *m/z* 543.1501 ($C_{27}H_{27}O_{12}$) and the product ion at *m/z* 381.0963 ($C_{21}H_{17}O_7$), 337.1069 ($C_{20}H_{17}O_5$) and 243.0655 ($C_{14}H_{11}O_4$) form consecutive loss of $C_6H_{10}O_5$, CO_2 and C_6H_6O. By investigating literatures, **A36** was tentatively identified as tetrahydroxystilbene-O-hexoside-methoxymethyl-furancarboxylic acid acyl (phenolic hydroxyl moiety).

Compounds **A37-1** and **A37-2** showed the same $[M-H]^-$ ion at *m/z* 547.1453 ($C_{26}H_{27}O_{13}$) and the MS^2 spectra gave ions at *m/z* 385.0914 ($C_{20}H_{17}O_8$) and 243.0655 ($C_{14}H_{11}O_4$) from consecutive loss of $C_6H_{10}O_5$ and $C_6H_6O_4$. By comparing literature, compounds **A37-1** and **A37-2** were tentatively identified as tetrahydroxystilbene-O-hexoside-oxoadipic acid acyl (phenolic hydroxyl moiety). Similarly, compounds **A38-1**, **A38-2** and **A38-3** were tentatively identified as tetrahydroxystilbene-O-hexoside-hydroxyadipic acid acyl (phenolic hydroxyl moiety), since the ions at *m/z* 387.1066 ($C_{20}H_{19}O_8$) and 243.0655 ($C_{14}H_{11}O_4$) from consecutive loss of $C_6H_{10}O_5$ and $C_6H_8O_4$.

Compounds **A39-1** ~ **A39-5** displayed a high resolution $[M-H]^-$ ion at *m/z* 551.1556 and gave element composition of $C_{29}H_{27}O_{11}$. In **A39-2** ~ **A39-5** MS^2 spectra, the $[M-H]^-$ showed fragment ions at *m/z* 405.1180 ($C_{20}H_{21}O_9$), 243.0656 ($C_{14}H_{11}O_4$), 163.0397($C_9H_7O_3$) and 145.0280 ($C_9H_5O_2$). The product ions at *m/z* 405.1180 and 234.0656 originated from the consecutive loss of *p*-hydroxycinnamoyl ($C_9H_6O_2$) and hexoside ($C_6H_{10}O_5$), Thus, *p*-hydroxycinnamoyl substituted THSG was detected and compounds **A39-2** ~ **A39-5** were identified as tetrahydroxystilbene-O-(*p*-hydroxycinnamoyl)-hexoside. In **A39-1** MS^2 spectra, the $[M-H]^-$ showed fragment ions at 399.1018 ($C_{23}H_{17}O_6$, M-$C_6H_{10}O_5$), 243.0655, 163.0396 and 145.0279, indicated *p*-hydroxycinnamoyl was linked to phenolic hydroxyl moiety. Thus, compound **A39-1** was identified as tetrahydroxystilbene-O-hexoside-*p*-hydroxycinnamoyl (phenolic hydroxyl moiety).

Compounds **A40-1** ~ **A40-8** showed the same $[M-H]^-$ ion at *m/z* 557.1295 ($C_{27}H_{25}O_{13}$) and the MS^2 spectra gave identical ions at *m/z* 405.1179 ($C_{20}H_{21}O_9$), 313.0555 ($C_{13}H_{13}O_9$), 243.0654 ($C_{14}H_{11}O_4$) and 169.0127 ($C_7H_5O_5$). The loss of $C_6H_{10}O_5$ and $C_7H_4O_4$ to produce the deprotonated resveratrol moiety ion at *m/z* 243.0654, a galloyl group was present, the ion at 313 ([galloylglucose—H]) appeared as base peak in the MS^2 spectra. It could further fragment ion *m/z* 169 ([gallic acid – $H]^-$). Therefore, compounds **A40-1** ~ **A40-8** were identified as tetrahydroxystilbene-O-hexoside-O-galloyl (glycosyl hydroxyl moiety) (Qiu et al., 2013).

Compounds **41-1** and **41-2** showed the same $[M-H]^-$ ion at *m/z* 561.1609 ($C_{27}H_{29}O_{13}$) and the MS^2 spectra gave identical ions at *m/z* 405.1174 ($C_{20}H_{21}O_9$) and 243.0654 ($C_{14}H_{11}O_4$). By comparing literatures, compounds **41-1** and **41-2** were identified as tetrahydroxystilbene-O- (gabosine C)-hexoside.

Compounds **A 42-1 ~ A 42-13** gave precursor ion $[M-H]^-$ at *m/z* 567.1712 ($C_{26}H_{31}O_{14}$), in **A42-2 ~ A42-4** and **A42-7 ~ A42-13** MS^2 spectra, the $[M-H]^-$ ion showed fragment ion at *m/z* 243.0654 ($C_{14}H_{11}O_4$), indicated that the consecutive neutral loss of hexoside, they were disaccharide THSGs. By comparing literature, they were tentatively characterized as tetrahydroxystilbene-O-di-hexosides (**Figure 7**). But in **A42-1, A42-5**, and **A42-6** MS^2 spectra, the $[M-H]^-$ ion showed fragment ions at *m/z* 477.1401 ($C_{23}H_{25}O_{11}$), 447.1278 ($C_{22}H_{23}O_{10}$), 315.0857 ($C_{17}H_{15}O_6$), 285.0761 ($C_{16}H_{13}O_5$), and 243.0655 ($C_{14}H_{11}O_4$), respectively. The fragment ions 477.1401 [M-H-90 Da, $C_3H_6O_3]^-$, 447.1278 [M-H-120 Da, $C_4H_8O_4]^-$ are diagnostic the last two neutral loss fragments suggested that a C-glycoside was connected with the stilbene glycoside. Therefore, **A42-1, A42-5** and **A42-6** were determined as tetrahydroxystilbene-O-hexoside-C-glycoside.

A42-14 (t_R = 18.29 min)**, A42-15** (t_R = 19.50 min) and **A42-16** (t_R = 21.64 min) showed the molecular formula were $C_{29}H_{27}H_{12}$ (*m/z* = 567.1504), which was 162 Da heavier than that of THSG, and different from **A42-1 ~ A42-13**. In their MS^2 spectra, the $[M-H]^-$ ion showed fragment ions at *m/z* 405.1203 ($C_{20}H_{21}O_9$), 243.0654 ($C_{14}H_{11}O_4$), 161.0229 ($C_9H_5O_3$), respectively. Indicated that the consecutive loss of caffeoyl ($C_9H_6O_3$) and hexoside ($C_6H_{10}O_5$). Thus, the caffeoyl substituted THSG was detected and compound **A42-14**, **A42-15** and **A42-16** identified as tetrahydroxystilbene-O-(caffeoyl)-hexoside.

Compounds **A43-1** ~ **A43-6** showed the same $[M-H]^-$ ion at *m/z* 573.1251 ($C_{27}H_{25}O_{14}$) and the MS^2 spectra gave identical ions at *m/z* 243.0657 ($C_{14}H_{11}O_4$), 166.9971 ($C_7H_3O_5$) and 123.0071 ($C_6H_3O_3$). By comparing literature, Compounds **A43-1** ~ **A43-6** were tentatively identified as tetrahydroxystilbene-O- (tetrahydroxybenzoic acid acyl)-hexoside.

Compound **A44** gave a $[M-H]^-$ ion at *m/z* 575.1402 ($C_{27}H_{27}O_{14}$) and the product ions at *m/z* 337.0707 ($C_{19}H_{13}O_6$) and 244.0655 ($C_{14}H_{11}O_4$). By comparing

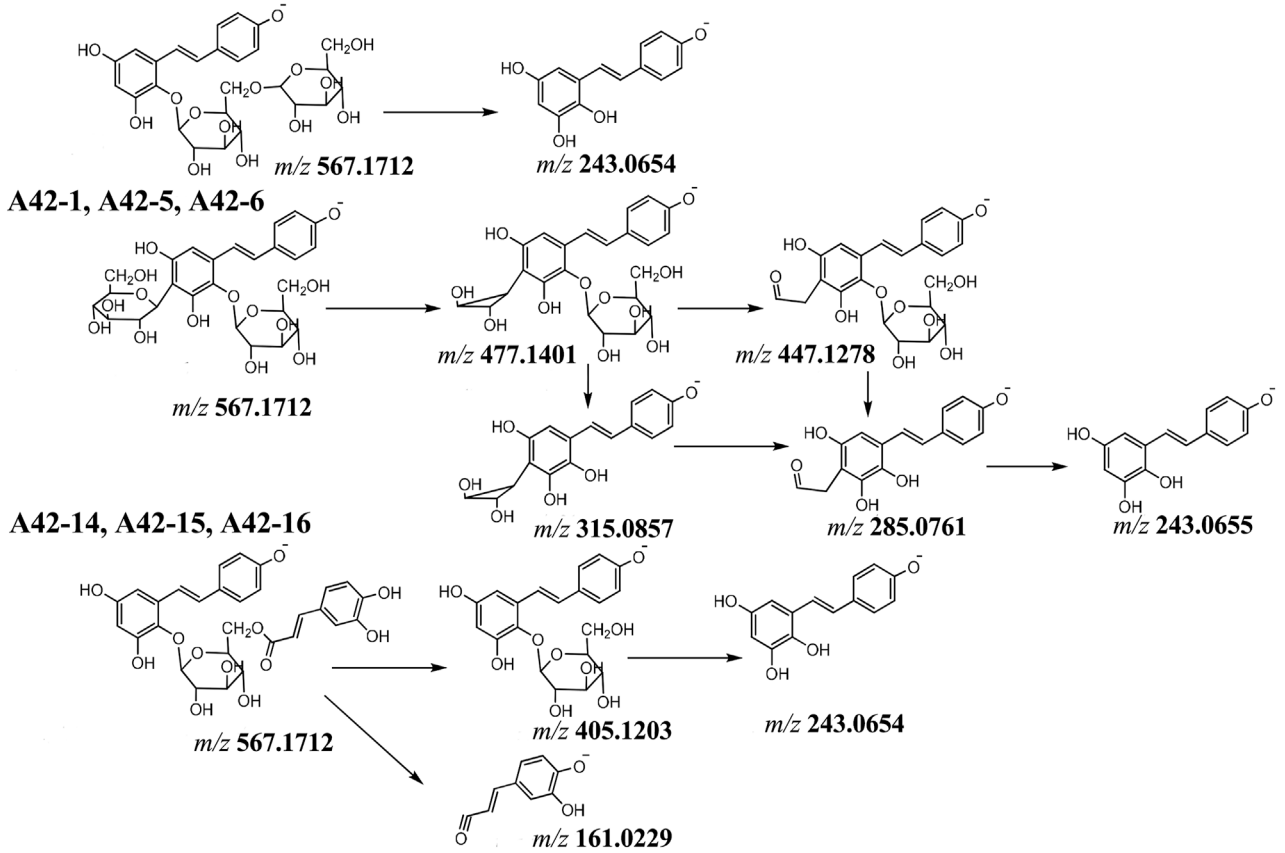

FIGURE 7 | The proposal fragmentation pathway of compounds of A42.

literatures, compound **A44** was tentatively identified as tetrahydroxystilbene-O- (dioxoheptane-dicarboxylic acid acyl)-hexoside.

Compounds **A45-1** ~ **A45-5** showed the same $[M-H]^-$ ion at *m/z* 581.1655 ($C_{30}H_{29}O_{12}$), the MS^2 spectra gave ions at *m/z* 405.1177 ($C_{20}H_{21}O_9$), 337.0921($C_{16}H_{17}O_8$), 243.0655($C_{14}H_{11}O_4$), 193.0493 ($C_{10}H_9O_4$) and 175.0387 ($C_{10}H_7O_3$). Its MS^2 spectrum gave characteristic ions at *m/z* 337.0921 ([feruoylglucose-H]$^-$), *m/z* 193.0493 ([ferulic acid-H]$^-$) and *m/z* 175.0387, therefore, compounds **A45-1** ~ **A45-5** were identified as tetrahydroxystilbene-O-hexoside-O-feruloyl (glycosyl hydroxyl moiety).

Compound **A46** gave a $[M-H]^-$ ion at *m/z* 591.2075 ($C_{29}H_{35}O_{13}$) and the product ions at *m/z* 405.1203 ($C_{20}H_{21}O_9$), 243.0655 ($C_{14}H_{11}O_4$) and 185.0806 ($C_9H_{13}O_4$). By comparing literature, compound **A46** was tentatively identified as tetrahydroxystilbene-O- (hydroxynonanedioic acid acyl)-hexoside.

Compound **A47** gave a $[M-H]^-$ ion at *m/z* 613.1769 ($C_{27}H_{33}O_{16}$) and the product ions at *m/z* 405.1203 ($C_{20}H_{21}O_9$) and 243.0655 ($C_{14}H_{11}O_4$). By comparing literatures, compound **A47** was tentatively identified as tetrahydroxystilbene-O-(Glucoheptanoyl)-hexoside.

Compounds **A48-1**, **A48-2** and **A48-3** showed the same $[M-H]^-$ ion at *m/z* 719.1825 ($C_{33}H_{35}O_{18}$) and the MS^2 spectra gave identical ions at *m/z* 557.1287 ($C_{27}H_{25}O_{13}$), 405.1174 ($C_{20}H_{21}O_9$), 313.0557 ($C_{13}H_{13}O_9$), 243.0655 ($C_{14}H_{11}O_4$) and 169.0126 ($C_7H_5O_5$), the loss of $C_6H_{10}O_5$ to produce compound **A39** ion at *m/z* 557.1287, and the fragmentation ions were the same. Therefore, **A48-1**, **A48-2** and **A48-3** were identified as tetrahydroxystilbene-O-dihexoside -galloyl (glycosyl hydroxyl moiety).

Compounds **A49-1** ~ **A49-6** displayed a high resolution $[M-H]^-$ ion at *m/z* 827.2399 and gave element composition of $C_{40}H_{43}O_{19}$. The MS^2 spectra gave ions at 405.1165 ($C_{20}H_{21}O_9$), 259.0607 ($C_{14}H_{11}O_5$) and 243.0656 ($C_{14}H_{11}O_4$), forming the ions 405.1165 and 243.0656 indicated that they should be THSG derivatives. By comparing literature, compounds **A49-1** ~ **A49-6** were tentatively identified as polygonumoside C/D.

Compounds **A50-1** ~ **A50-8** displayed a high resolution $[M-H]^-$ ion at *m/z* 837.2601 and gave element composition of

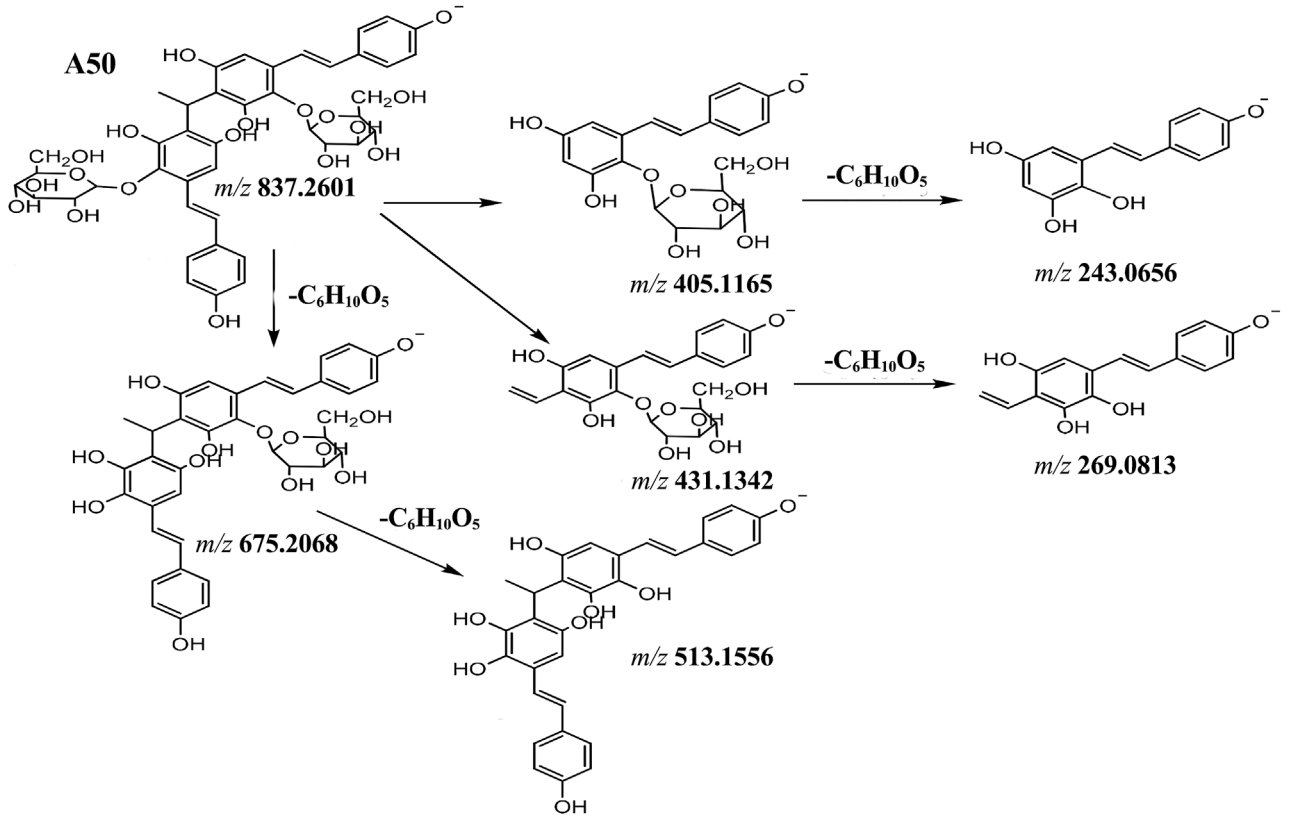

FIGURE 8 | The proposal fragmentation pathway of compound of A50.

$C_{42}H_{45}O_{18}$. The MS^2 spectra gave ions at *m/z* 675.2068 ($C_{36}H_{35}O_{13}$), 513.1556 ($C_{30}H_{25}O_8$), 431.1342 ($C_{22}H_{23}O_9$), 405.1165 ($C_{20}H_{21}O_9$), 269.0813 ($C_{16}H_{13}O_4$) and 243.0656 ($C_{14}H_{11}O_4$). The consecutive neutral loss of hexoside, forming ions at *m/z* 675.2068 and 513.1556, and forming the ions 405.1165, 243.0656 and 431.1342, 269.0813 indicated that was cleavage into two glycosides. By comparing literature, compounds **A50-1** ~ **A50-8** were identified as polygonumnolide D (**Figure 8**). Similarly, compound **A52** was tentatively characterized as hydroxylation polygonumnolide D, since the $[M-H]^-$ ion at *m/z* 853.2560 ($C_{42}H_{45}O_{19}$), which was 16 Da (O) higher than that of **A50**, and the MS^2 spectra gave ions at *m/z* 447.1300 ($C_{22}H_{23}O_{10}$), 405.1175 ($C_{20}H_{21}O_9$), 285.0765 ($C_{16}H_{13}O_5$) and 243.0656 ($C_{14}H_{11}O_4$).

Compounds **A51-1** ~ **A51-5** showed the same $[M-H]^-$ ion at *m/z* 841.2551 ($C_{41}H_{45}O_{19}$), which was 14 Da (CH_2) higher than that of **A49**. The MS^2 spectra gave ions at *m/z* 405.1182 ($C_{20}H_{21}O_9$), 273.0764($C_{15}H_{13}O_5$) and 243.0655($C_{14}H_{11}O_4$), and the ion *m/z* 273.0764 was 14 Da (CH_2) higher than that of **A49** ion *m/z* 259.0607. therefore, compounds **A51-1** ~ **A51-5** were identified as methylation polygonumoside C/D. Similarly, compounds **A53-1** ~ **A53-4** were identified as hydroxylation methylation polygonumoside C/D. since the $[M-H]^-$ ions at *m/z* 857.2502 ($C_{41}H_{45}O_{20}$), which was 14 Da (CH_2) higher than that of **A51**, and the MS^2 spectra gave ions at *m/z* 405.1172 ($C_{20}H_{21}O_9$), 289.0709 ($C_{15}H_{13}O_6$) and 243.0656 ($C_{14}H_{11}O_4$).

3.4 Identification of Trihydroxystilbene-O-Hexoside Derivatives

Compounds **B1-1**, **B1-2** and **B1-3** gave a $[M-H]^-$ ion at *m/z* 389.1240 ($C_{20}H_{21}O_8$) and the product ion at *m/z* 227.0702 ($C_{14}H_{11}O_3$). The loss of $C_6H_{10}O_5$ was confirmed by MS^2 spectra and indicated a hexose neutral loss. Compared with the control substance, **B1-2** was identified as polydatin, compounds **B1-1** and **B1-3** were identified as isomer polydatin.

Compounds **B2-1** ~ **B2-4** showed the same $[M-H]^-$ ion at *m/z* 541.1345 ($C_{27}H_{25}O_{12}$) and the MS^2 spectra gave ions at *m/z* 313.0559 ($C_{13}H_{13}O_9$), 227.0702 ($C_{14}H_{11}O_3$), 169.0128 ($C_7H_5O_5$). Similar with compounds A40, compounds **B2-1** ~ **B2-4** were identified as trihydroxystilbene-O-hexoside-O-*galloyl* (glycosyl hydroxyl moiety).

Compounds **B3-1** and **B3-2** showed the same $[M-H]^-$ ion at *m/z* 457.1136 ($C_{23}H_{21}O_{10}$) and the MS^2 spectra gave ions at *m/z* 295.0605 ($C_{17}H_{11}O_5$) and 227.0702 ($C_{14}H_{11}O_3$). By comparing literature, compounds **B3-1** and **B3-2** were identified as

trihydroxystilbene-O-hexoside-O-acid deltique acyl (phenolic hydroxyl moiety).

Compound **B4** gave a $[M-H]^-$ ion at *m/z* 535.1816 ($C_{26}H_{31}O_{12}$) and the product ion at *m/z* 227.0702 ($C_{14}H_{11}O_3$) derived from the loss of $C_6H_{10}O_5$ (hexoside) and $C_6H_{10}O_4$ (deoxyhexose, mostly rhamnose). By investigating literatures, compound **B4** was identified as trihydroxystilbene-(deoxyhexose)-O-hexoside.

Compound **B5** displayed a high resolution $[M-H]^-$ ion at *m/z* 359.1132 and gave element composition of $C_{19}H_{19}O_7$, the product ions at *m/z* 359.1129 ($C_{19}H_{19}O_7$) and 227.0701 ($C_{14}H_{11}O_3$). The product ion at *m/z* 227.0701 originated from the loss of pentose (mostly arabinose). Therefore, compound **B5** was identified as trihydroxystilbene-O-pentose.

3.5 Identification of Pentahydroxystilbene Glycoside Derivatives

Compounds **C1-1** ~ **C1-7** displayed a high resolution $[M-H]^-$ ion at *m/z* 421.1138, and gave element composition of $C_{20}H_{21}O_{10}$, which was 14 Da (CH_2) higher than that of THSG, the MS^2 spectra gave ion at 259.0609 ($C_{14}H_{11}O_5$). By comparing literature, compounds **C1-1** ~ **C1-7** were tentatively identified as pentahydroxystilbene glycosides.

Compound **C2** gave a $[M-H]^-$ ion at *m/z* 545.1291 ($C_{26}H_{25}O_{13}$) and the product ions at *m/z* 421.1128 ($C_{20}H_{21}O_{10}$), 259 ($C_{14}H_{11}O_5$) and 123.0070 ($C_6H_3O_3$) derived from the loss of $C_6H_5O_5$ (5-HMF) and $C_{16}H_{10}O_5$ (hexoside). By investigating literatures, compound **C2** was identified as pentahydroxystilbene-(5-HMF)-O-hexoside.

3.6 Identification of Tetrahydroxy-Phenanthrene-O-Hexoside Derivatives

Compounds **D1-1** and **D1-2** gave a $[M-H]^-$ ion at *m/z* 403.1030 ($C_{20}H_{19}O_9$) and prominent fragment ion at *m/z* 241.0497 ($C_{14}H_9O_4$) in MS^2 spectrum, which were showed 2 Da less than that of THSG. It can be inferred that they were dehydrogenated product of THSG. By comparing literatures (Qiu et al., 2013), compounds **D1-1** and **D1-2** were identified as tetrahydroxy-phenanthrene-O-hexoside.

Compounds **D2-1** ~ **D2-8** showed the same $[M-H]^-$ ion at *m/z* 549.1605 ($C_{26}H_{29}O_{13}$) and the MS^2 spectra gave ions at *m/z* 387.1072 ($C_{20}H_{19}O_8$), 297.0760 ($C_{17}H_{13}O_5$) and 241.0497 ($C_{14}H_9O_4$). Similarly compounds **A38**, compounds **D2-1** ~ **D2-8** were identified as tetrahydroxy-phenanthrene-O-hexoside-O-*p*-hydroxycinnamoyl (phenolic hydroxyl moiety).

3.7 Identification of Dihydrotetrahydroxystilbene-O-Hexoside Derivatives

Compound **E1** gave a $[M-H]^-$ ion at *m/z* 407.1343 ($C_{20}H_{23}O_9$) and prominent fragment ion at *m/z* 245.0811 ($C_{14}H_{13}O_4$) in MS^2 spectrum, which were showed 2 Da higher than that of THSG. It can be inferred that they were dihydrogenated product of THSG. By comparing literatures, compounds **E1** was identified as dihydrotetrahydroxystilbene-O-hexoside.

Compounds **E2-1** and **E2-2** showed the same $[M-H]^-$ ion at *m/z* 527.1552 ($C_{27}H_{27}O_{11}$) and the MS^2 spectra gave ions at *m/z* 365.1017 ($C_{21}H_{17}O_6$), 335.0918 ($C_{20}H_{15}O_5$) and 245.0814 ($C_{14}H_{13}O_4$). Similarly compounds **A27**, compounds **E2-1** and **E2-2** were identified as dihydrotetrahydroxystilbene-O-hexoside-salicylic acid acyl (phenolic hydroxyl moiety).

Compound **E3** displayed a high resolution $[M-H]^-$ ion at *m/z* 539.1766, and gave element composition of $C_{25}H_{31}O_{13}$. The MS^2 spectra gave ion at 245.0811 ($C_{14}H_{13}O_4$) derived from the loss of $C_6H_{10}O_5$ (hexoside) and $C_5H_8O_4$ (pentose, mostly arabinose). Compound **E3** was identified as dihydrotetrahydroxystilbene-O-(pentose)-hexoside.

3.8 Identification of Pentahydroxy-Phenanthrene-O-Hexoside

Compounds **F1-1** and **F1-2** showed the same $[M-H]^-$ ion at *m/z* 419.0980 ($C_{20}H_{19}O_{10}$) and the MS^2 spectra gave ion at *m/z* 257.0542 ($C_{14}H_9O_5$), which were showed 16 Da higher than that of compounds D1. Therefore, compounds **F1-1** and **F1-2** were identified as pentahydroxy-phenanthrene-O-hexosides.

3.9 Identification of Dihydroxystilbene-O-Hexoside Derivatives

Compound **G1** gave a $[M-H]^-$ ion at *m/z* 373.1286 ($C_{20}H_{21}O_7$) and prominent fragment ion at *m/z* 211.0751 ($C_{14}H_{13}O_2$) in MS^2 spectrum, which were showed 32 Da less than that of THSG. It can be inferred that they were dedihydroxylation product of THSG. Therefore, compounds **G1** was identified as dihydroxystilbene-O-hexoside.

Compounds **G2-1** and **G2-2** showed the same $[M-H]^-$ ion at *m/z* 525.1396 ($C_{27}H_{25}O_{11}$) and the fragment ions at *m/z* 525.1392, 313.0558 ($C_{13}H_{13}O_9$), 211.0751 ($C_{14}H_{13}O_2$), 169.0128 ($C_7H_5O_5$) and 151.0020 ($C_7H_3O_4$) in MS^2 spectra. Similar with compounds **A39** and compounds **B2**, compounds **G2-1** and **G2-2** were identified as dihydroxystilbene-O-hexoside-O-galloyl (glycosyl hydroxyl moiety).

3.10 Structural Changes of Stilbene Glycosides

3.10.1 Structural Changes of Parent Stilbene Glycosides

Stilbenes are regared to be derived from phenylalanine metabolism in plants (Isvett et al., 2009) (**Figure 9**). THSG is the highest and most reported compound in RM Studies have shown that resveratrol was the intermediate product of THSG, which was hydroxylated to form terahydroxystilbene, and then glycosylated to form THSG (compounds **A3**) (Zhao, 2017). Polydatin (compound **B1-2**) was glycosylated form resveratrol. Pentahydroxystilben-O-hexoside (compounds **C1**) was synthesized by rehydroxylation of tetrahydroxystilbene and

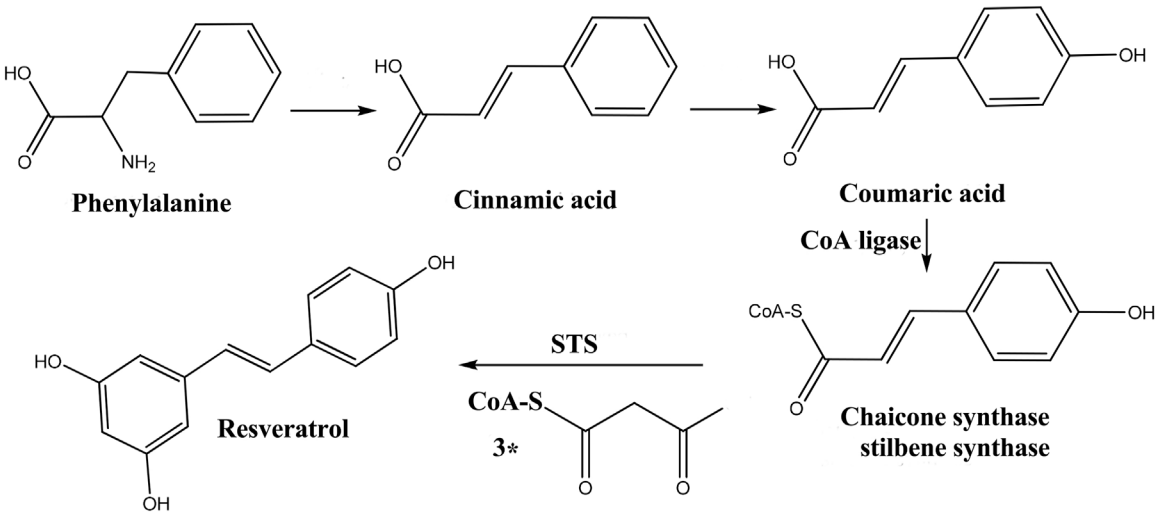

FIGURE 9 | The biosynthesis pathway of resveratrol.

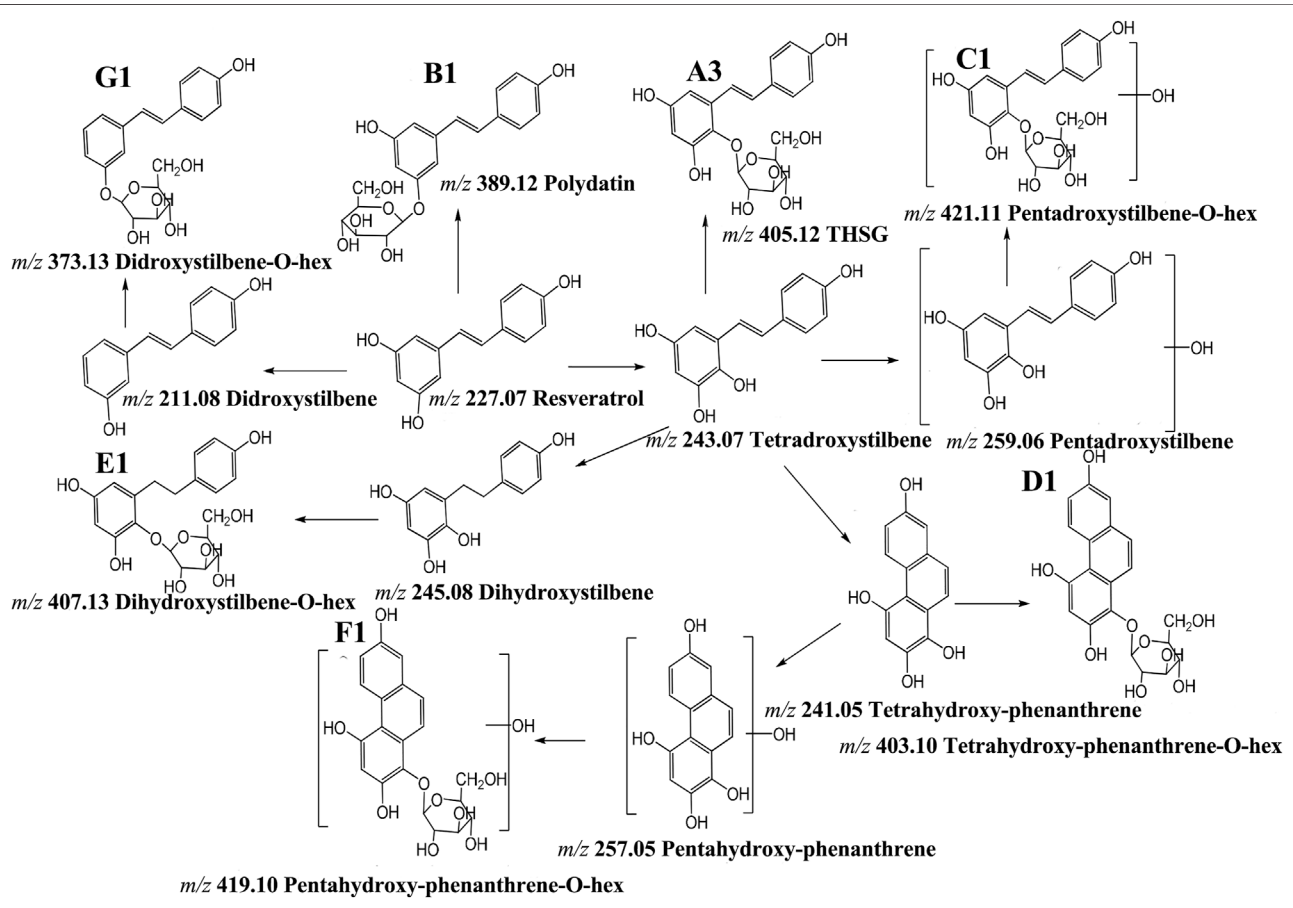

FIGURE 10 | The structural changes pathway of stilbene glycosides.

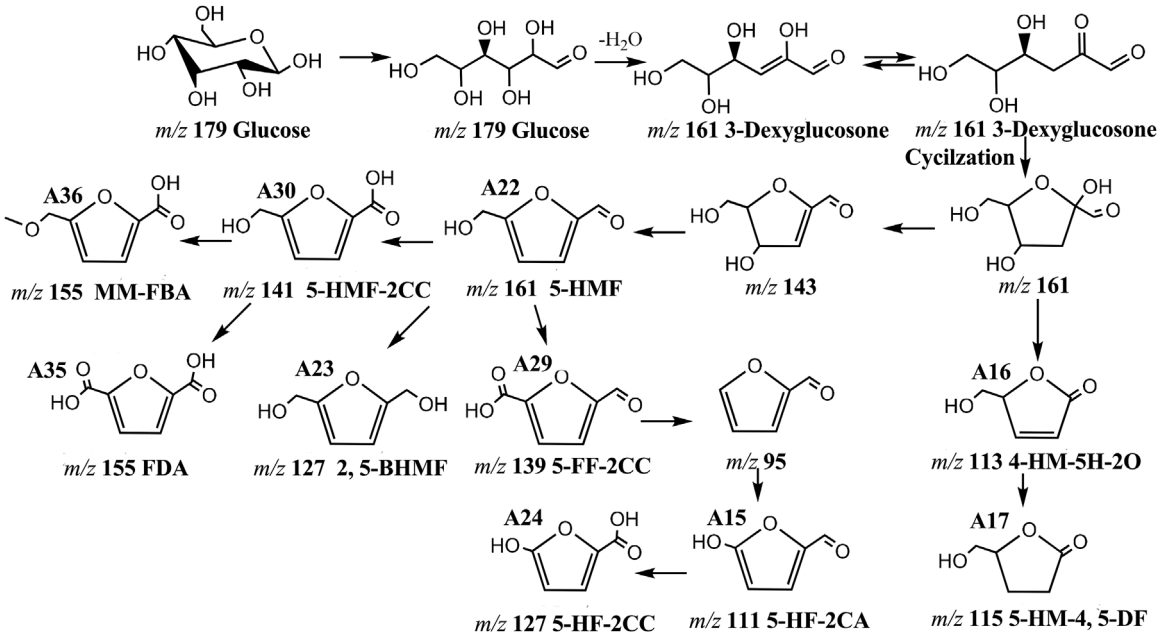

FIGURE 11 | The structural changes pathway of 5-HMF.

then glycosylation. The phenanthrene moiety was formed by cyclization of 6-H and 2′-H positions of tetrahydroxystilbene, which can stabilize the cyclization of aglycone, and then glycosylated to form tetrahydroxy-phenanthrene-O-hexoside (compounds **D1**). The tetrahydroxy-phenanthrene was hydroxylated to form pentahydroxy-phenanthrene, then glycosylated to form pentahydroxy-phenanthrene-O-hexoside (compounds **F1**). Dihydrotetrahydroxystilbene-O-hexoside (compounds **E1**) was synthesized from tetrahydroxystilbene by double bond opening and then glycosylated. The resveratrol lost a hydroxyl group in the plant, and dihydroxystilbene-O-hexoside (**G1**) was obtained by the glycosylation of dihydroxystilbene (**Figure 10**).

3.11 Structural Changes in Stilbene Glycosides Substituents

Compounds containing malonyl, acetyl, caffeoyl and other aromatic acyls are very common in various plants (Barnes et al., 1994; Klejdus et al., 2001; Ye et al., 2007). And galloyl, malonyl, acetyl, caffeoyl, coumaroyl, feruloyl substituent have been reported in raw PM in our previous research (Qiu et al., 2013). In total, fifty-five substituents were found in this study. Except for the above-mentioned substituents, there was also some organic acids existed, such as formic acid, acetic acid, carbonic acid, propionic acid, glycolic acid, lactic acid, valeric acid, succinic acid, dihydroxy butyric acid, salicylic acid, glutaric acid, malic acid, catechuic acid and *p*-hydroxybenzoic acid. Maillard reaction products, mainly includes 2, 3-dihydro-3, 5-dihydroxy-6-methyl-4H-pyranone (DDMP, **A31**) and 5-hydromethylfurfura (5-HMF, **A22**) and its derivatives from glucose or glycine were also observed as stilbene glycosides substituents (Perez Locas and Yaylayan, 2008; Harishchandra et al., 2011; Liu, 2018). The aldehyde end of 5-HMF is oxidized to carboxylic acid, 5-hydroxymethylfuran-2-carboxyl acid (5-HMF-2-CC, **A30**) was produced, then methylation and oxidation produced methoxymethyl-furancarboxylic acid (MM-FBA, **A36**) and furan-dicarboxylic acid (FDA, **A35**). 2, 5-bis-(hydroxymethyl) furan (2, 5-BHMF, **A23**) was synthesized by the reduction of 5-HMF. 5-formylfuran-2-carboxyl acid (5-FF-2CC, **A29**) was synthesized by the oxidation of the hydroxyl end of 5-HMF. Then decarboxylation and reoxidation were carried out to form 5-hydroxyfuran-2-carbaldehyde (5HF-2CA, **A15**), then, 5-hydroxyfuran-2-carboxylic acid (5-HF-2CC, **A24**) was formed by oxidation of aldehyde end. 4-hydroxymethyl-5h-furan-2-one (4-HM-5H-2O, **A16**) was synthesized from 2, 4-dihydroxy-5-(hydroxymethyl) oxolane-2-carbaldehyde by dehydration and CH_2O removal, then hydrogenation reaction was reacted to produce 5-hydroxymethyl-4,5-dihydrofuranone (5-HM-4, 5-DF, **A17**), and the change path of 5-HMF is shown in **Figure 11**) all substituents information is shown in **Supplementary Table S1**.

3.12 Content Change Trend of Stilbene Derivatives

The peak areas of all compounds were based on the extracted ion chromatographic peaks. The mean and SD values were calculated and the column diagram of each compound was drawn (**Supplementary Table S1**). A total of 219 compounds were identified in this study, 73 compounds were not found in RRM, 21 compounds were not found in 4 h PRM, 9 compounds were not found in 8 h PRM and 1 compound

was not found in 12 h PRM. During the process of PM, THSG dehydrated with other small molecules to form new compounds.

The change trend of the highest content compound trans-THSG and its cis-THSG slightly increased before 8 h, then decreased gradually, and was lower than that of RRM at 24 h. This is a model of content change, but the peak time may be 4, 8, 12 or 18 h. The second model, such as compound **A3-4** (isomer trans-THSG), gradually increase during the processing time. The third model, such as compound **A45-1** (tetrahydroxystilbene-O-hexoside-feruloyl (glycosyl hydroxyl moiety), gradually decreased with processing time.

The results showed that the content and quantity of stilbene glycoside compounds have undergone tremendous changes during the processing process. Although the content of THSG in PRM is indeed lower than that in RRM, a large number of stilbene glycoside derivatives are produced in the processing process, so the total content of stilbene glycoside compounds in the PRM will not be reduced. Conventional understanding, RRM after processing can enhance efficiency and reduce toxicity, and the content of THSG also decreases with the processing time, is THSG toxic? After this experimental study, it can be proved that THSG should not be a toxic component, because its derivatives will metabolize into compounds similar to THSG *in vivo*, enhancing the efficacy of THSG.

4 CONCLUSION

In the present study, a simple and effective method was developed for characterization of stilbene compounds in the roots of RRM and PRMs by UHPLC-Q-Exactive plus orbitrap MS/MS. Stilbene glycosides were distinguished by diagnostic fragment ions at *m/z* 405.1087 and 243.0656, accurate mass measurements and fragmentation pathways. Based on the proposed strategy, the metabolic process of 7 stilbene glycosides in plants was identified, and 55 substituent and Maillard reaction process were identified. Finally, 219 stilbene glycosides derivatives were identified, of which 102 compounds may be potential new compounds. The 55 substituents include monosaccharide, disaccharide, organic acid and Maillard reaction products (DDMP, 5-HMF and its derivatives) and so on. The quality and quantity of stilbene glycosides changed during the processing of RM. 73 compounds were not found in RRM, 21 compounds were not found in 4 h PRM, 9 compounds were not found in 8 h PRM and 1 compound was not found in 12 h PRM, and the change trend of the compounds can be summarized into 3 models: gradually increased, gradually decreased, first increased and then decreased. 181 trans-THSG derivative products were obtained through the hydrolysis and dehydration reaction between trans-THSG and small molecules compounds, after this experimental study, it can be proved that THSG should not be a toxic component, because its derivatives will metabolize into compounds similar to THSG *in vivo*, enhancing the efficacy of THSG.

DATA AVAILABILITY STATEMENT

The raw data supporting the conclusion of this article will be made available by the authors, without undue reservation.

AUTHOR CONTRIBUTIONS

XQ and ZH conceived and designed the experiments; JB, WC, and HS preformed the experiments and analyzed the data; JH, WX, and JZ contributed reagents/materials/analysis tools; JB wrote the paper.

FUNDING

National Natural Science Foundations of China 81373967 XQ Guangdong Provincial Hospital of Chinese Medicine Special Fund YN2019QJ14 JH GuangDong Basic and Applied Basic Research Foundation 2020A1515110383 JH Science and Technology Planning Project of Guangdong Province 2017B030314166 XQ the special foundation of Guangzhou Key Laboratory XQ, ZH.

SUPPLEMENTARY MATERIAL

The Supplementary Material for this article can be found online at: https://www.frontiersin.org/articles/10.3389/fphar.2022.757490/full#supplementary-material

REFERENCES

Barnes, S., Kirk, M., and Coward, L. (1994). Isoflavones and Their Conjugates in Soy Foods: Extraction Conditions and Analysis by HPLC-Mass Spectrometry. *J. Agric. Food Chem.* 42, 2466–2474. doi:10.1021/jf00047a019

Chen, Q. T., Zhuo, L. H., Xu, W., Huang, Z. H., and Qiu, X. H. (2012). Content Changes of 5 Components in *Polygonum Multiflorum* during Processing. *Chin. J. Exp. Tradit. Med. Form.* 18, 66–71. doi:10.13422/j.cnki.syfjx.2012.05.028

Cheung, F. W., Leung, A. W., Liu, W. K., and Che, C. T. (2014). Tyrosinase Inhibitory Activity of a Glucosylated Hydroxystilbene in Mouse Melan-A Melanocytes. *J. Nat. Prod.* 77, 1270–1274. doi:10.1021/np4008798

Chinese Pharmacopoeia Commission (2020). *Pharmacopoeia of the People's Republic of China*, 184. Beijing: China Medical Science and Technology Publishing House.

Choi, S. G., Kim, J., Sung, N. D., Son, K. H., Cheon, H. G., Kim, K. R., et al. (2007). Anthraquinones, Cdc25B Phosphatase Inhibitors, Isolated from the Roots of *Polygonum Multiflorum* Thunb. *Nat. Prod. Res.* 21, 487–493. doi:10.1080/14786410601012265

Dong, H., Slain, D., Cheng, J. C., Alma, W. H., and Liang, W. F. (2014). Eighteen Cases of Liver Injury Following Ingestion of *Polygonum Multiflorum*. *Complement. Ther. Med.* 22, 70–74. doi:10.1016/j.ctim.2013.12.008

Fu, W. H. (2011). HPLC Determination of the Main Chemical Ingredients Content in *Polygonum Multiflorum* during the Processing. *Asia-pacific Tradit. Medic.* 9, 50–51. doi:10.3969/j.issn.1673-2197.2013.07.021

Harishchandra, J., Christian, M. P., Theis, S., and Mikael, B. (2011). 3-Deoxy-Glucosone Is an Intermediate in the Formation of Furfurals from D-Glucose. *Chem. Sus. Chem.* 4, 1049–1051. doi:10.1002/cssc.201100249

Isvett, J., Flores, S., and Robert, V. (2009). Plant Polyketide Synthases: A Fascinating Group of Enzymes. *Plant Physiol. Biochem* 47, 167–174. doi:10.1016/j.plaphy.2008.11.005

Klejdus, B., Vitamvásová-Štěrbová, D., and Kubáň, V. (2001). Identification of Isoflavone Conjugates in Red clover (Trifolium Pratense) by Liquid Chromatography-Mass Spectrometry after Two-Dimensional Solid-phase Extraction. *Analytica Chim. Acta* 450, 81–97. doi:10.1016/S0003-2670(01)01370-8

Lei, X., Chen, J., Ren, J., Li, Y., Zhai, J., Mu, W., et al. (2015). Liver Damage Associated with *Polygonum Multiflorum* Thunb.: a Systematic Review of Case Reports and Case Series. *Evid. Based Complement. Alternat. Med.* 2015, 459749. doi:10.1155/2015/459749

Li, C., Niu, M., Bai, Z., Zhang, C., Zhao, Y., Li, R., et al. (2017). Screening for Main Components Associated with the Idiosyncratic Hepatotoxicity of a Tonic Herb, *Polygonum Multiflorum*. *Front. Med.* 11, 253–265. doi:10.1007/s11684-017-0508-9

Lin, L., Ni, B., Lin, H., Zhang, M., Li, X., Yin, X., et al. (2015). Traditional Usages, Botany, Phytochemistry, Pharmacology and Toxicology of Polygonum Multiflorum Thunb.: a Review. *J. Ethnopharmacol.* 159, 158–183. doi:10.1016/j.jep.2014.11.009

Lin, X. N., Chen, P. Y., Zhang, Q. F., Zhao, W. H., Cai, Y. K., and Mo, J. L. (2018). The Analyses on the Preparation Process and GMP of *Polygonum Multiflorum*. *Guangdong Chem. Industry* 15, 93–95. doi:10.3969/j.issn.1007-1865.2018.15.041

Liu, Z. L. (2018). *Changes in Chemical Components of Root of* Polygonum Multiflorum *Thunb. And How Maillard Reaction Involves during the Heating Process*. Beijing: China Academy of Chinese Medical Sciences.

Lv, L., Gu, X., Tang, J., and Ho, C. (2007). Antioxidant Activity of Stilbene Glycoside from *Polygonum Multiflorum* Thunb *In Vivo*. *Food Chem.* 104, 1678–1681. doi:10.1016/j.foodchem.2007.03.022

Perez Locas, C., and Yaylayan, V. A. (2008). Isotope Labeling Studies on the Formation of 5-(hydroxymethyl)-2-Furaldehyde (HMF) from Sucrose by Pyrolysis-GC/MS. *J. Agric. Food Chem.* 56, 6717–6723. doi:10.1021/jf8010245

Qiu, X. H., Li, J. H., and Huang, Z. H. (2006). Content Comparative Analysis of Water Soluble Saccharides in *Radix Polygoni Multiflora* before and after its Processing. *J. China. Pharm.* 17, 954–956. CNKI.SUN.ZGYA.0.2006-12-039.

Qiu, X. H., Song, Y. G., Sun, J. B., and Min, J. (2008). Effect of Radix Polygoni Multifori Praeparata by Different Processing on Model of Blood Deficiency Rats. *Zhong Yao Cai* 31, 14–17. doi:10.13863/j.issn1001-4454.2008.01.009

Qiu, X., Zhang, J., Huang, Z., Zhu, D., and Xu, W. (2013). Profiling of Phenolic Constituents in *Polygonum Multiflorum* Thunb. By Combination of Ultra-high-pressure Liquid Chromatography with Linear Ion Trap-Orbitrap Mass Spectrometry. *J. Chromatogr. A.* 1292, 121–131. doi:10.1016/j.chroma.2012.11.051

Shao, L., Zhao, S. J., Cui, T. B., Liu, Z. Y., and Zhao, W. (2012). 2,3,5,4'-Tetrahydroxystilbene-2-O-β-D-Glycoside Biosynthesis by Suspension Cells Cultures of *Polygonum Multiflorum* Thunb and Production Enhancement by Methyl Jasmonate and Salicylic Acid. *Molecules* 17, 2240–2247. doi:10.3390/molecules17022240

Sun, Y. N., Li, W., Kim, J. H., Yan, X. T., Kim, J. E., Yang, S. Y., et al. (2015). Chemical Constituents from the Root of *Polygonum Multiflorum* and Their Soluble Epoxide Hydrolase Inhibitory Activity. *Arch. Pharm. Res.* 38, 998–1004. doi:10.1007/s12272-014-0520-4

Xu, W., Zhang, J., Huang, Z., and Qiu, X. (2012). Identification of New Dianthrone Glycosides from *Polygonum Multiflorum* Thunb. Using High-Performance Liquid Chromatography Coupled with LTQ-Orbitrap Mass Spectrometry Detection: A Strategy for the Rapid Detection of New Low Abundant Metabolites from Traditional Chinese Medicines. *Anal. Methods* 4, 1806–1812. doi:10.1039/c2ay00009a

Yang, J. B., Ye, F., Tian, J. Y., Song, Y. F., Gao, H. Y., Liu, Y., et al. (2020). Multiflorumisides HK, Stilbene Glucosides Isolated from Polygonum Multiflorum and Their *In Vitro* PTP1B Inhibitory Activities. *Fitoterapia* 146, 104703. doi:10.1016/j.fitote.2020.104703

Ye, M., Han, J., Chen, H., Zheng, J., and Guo, D. (2007). Analysis of Phenolic Compounds in Rhubarbs Using Liquid Chromatography Coupled with Electrospray Ionization Mass Spectrometry. *J. Am. Soc. Mass. Spectrom.* 18, 82–91. doi:10.1016/j.jasms.2006.08.009

Zhang, G. P., Zhang, H. J., Chen, T. F., Hou, H. P., Su, P., Gao, Y. H., et al. (2019). Screening and Identifying Hepatotoxic Components in *Polygoni Multiflori* Radix and *Polygoni Multiflori* Radix Praeparata. *World J. Tradit. Chin. Med.* 3, 164–170. doi:10.4103/wjtcm.wjtcm_29_19

Zhao, S. J. (2017). *Study on the 2, 3, 5, 4′-Tetrahydroxystilbene-2-O-β-D-Glucopyranoside (THSG) Biosynthetic Pathway in* Fallopia Nultiflora. Guangzhou: South China University of Technology.

Conflict of Interest: The authors declare that the research was conducted in the absence of any commercial or financial relationships that could be construed as a potential conflict of interest.

Publisher's Note: All claims expressed in this article are solely those of the authors and do not necessarily represent those of their affiliated organizations, or those of the publisher, the editors and the reviewers. Any product that may be evaluated in this article, or claim that may be made by its manufacturer, is not guaranteed or endorsed by the publisher.

frontiers | Frontiers in Neuroscience

REVIEW
published: 16 May 2022
doi: 10.3389/fnins.2022.884345

Natural Therapeutics in Aid of Treating Alzheimer's Disease: A Green Gateway Toward Ending Quest for Treating Neurological Disorders

Basharat Ahmad Bhat[1†], Abdullah Almilaibary[2†], Rakeeb Ahmad Mir[3], Badr M. Aljarallah[4], Wajahat R. Mir[1], Fuzail Ahmad[5] and Manzoor Ahmad Mir[1]*

[1] Department of Bioresources, School of Biological Sciences, University of Kashmir, Srinagar, India, [2] Department of Family and Community Medicine, Faculty of Medicine, Albaha University Alaqiq, Alaqiq, Saudi Arabia, [3] Department of Biotechnology, Baba Ghulam Shah Badshah University, Rajouri, India, [4] Department of Gastroenterology and Hepatology, Qassim University, Buraydah, Saudi Arabia, [5] College of Applied Medical Science, Majmaah University, Al Majma'ah, Saudi Arabia

OPEN ACCESS

Edited by:
Gokhan Zengin, Selçuk University, Turkey

Reviewed by:
Sengul Uysal, Erciyes University, Turkey
Muthuswamy Anusuyadevi, Bharathidasan University, India

***Correspondence:**
Manzoor Ahmad Mir
drmanzoor@kashmiruniversity.ac.in

[†] These authors have contributed equally to this work

Specialty section:
This article was submitted to Neuropharmacology, a section of the journal Frontiers in Neuroscience

Received: *26 February 2022*
Accepted: *18 March 2022*
Published: *16 May 2022*

Citation:
Bhat BA, Almilaibary A, Mir RA, Aljarallah BM, Mir WR, Ahmad F and Mir MA (2022) Natural Therapeutics in Aid of Treating Alzheimer's Disease: A Green Gateway Toward Ending Quest for Treating Neurological Disorders. Front. Neurosci. 16:884345. doi: 10.3389/fnins.2022.884345

The current scientific community is facing a daunting challenge to unravel reliable natural compounds with realistic potential to treat neurological disorders such as Alzheimer's disease (AD). The reported compounds/drugs mostly synthetic deemed the reliability and therapeutic potential largely due to their complexity and off-target issues. The natural products from nutraceutical compounds emerge as viable preventive therapeutics to fill the huge gap in treating neurological disorders. Considering that Alzheimer's disease is a multifactorial disease, natural compounds offer the advantage of a multitarget approach, tagging different molecular sites in the human brain, as compared with the single-target activity of most of the drugs so far used to treat Alzheimer's disease. A wide range of plant extracts and phytochemicals reported to possess the therapeutic potential to Alzheimer's disease includes curcumin, resveratrol, epigallocatechin-3-gallate, morin, delphinidins, quercetin, luteolin, oleocanthal, and other phytochemicals such as huperzine A, limonoids, and azaphilones. Reported targets of these natural compounds include inhibition of acetylcholinesterase, amyloid senile plaques, oxidation products, inflammatory pathways, specific brain receptors, etc. We tenaciously aimed to review the in-depth potential of natural products and their therapeutic applications against Alzheimer's disease, with a special focus on a diversity of medicinal plants and phytocompounds and their mechanism of action against Alzheimer's disease pathologies. We strongly believe that the medicinal plants and phytoconstituents alone or in combination with other compounds would be effective treatments against Alzheimer's disease with lesser side effects as compared to currently available treatments.

Keywords: Alzheimer's disease, phytoconstituents, inflammation, neurological disorders, effective treatments

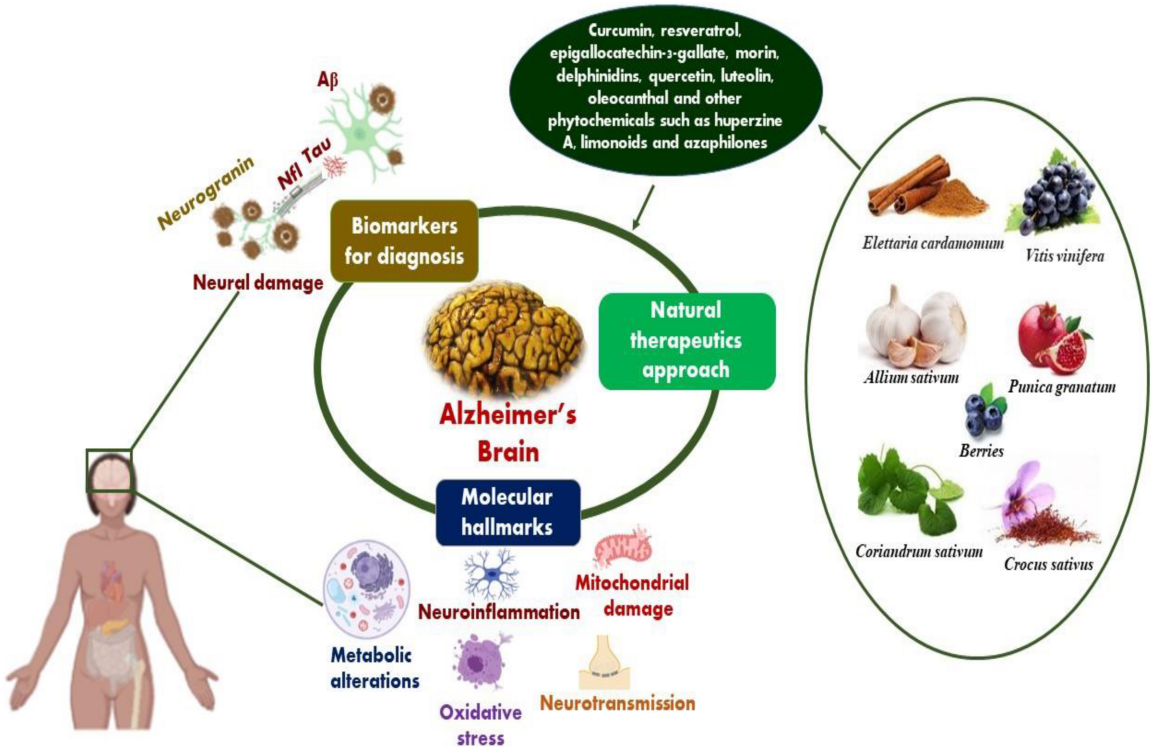

GRAPHICAL ABSTRACT | The graphical abstract displays therapeutic potential of plant extracts and their derived metabolites such as curcumin, resveratrol, epigallocatechin-3-gallate, huperzine A, limonoids, and azaphilones etc., to reduce the clinical features associated with Alzheimer's disease and possible end to quest for global prevalence of AD in humans.

INTRODUCTION

Alzheimer's disease (AD) is attributed to the inception of amyloid plaques and tangled fibers which consequently results in neurodegeneration featured by impairment of cognitive function and amnesia (memory loss) (Anand et al., 2014; Sahebkar et al., 2021). AD manifests the highest prevalence in the elderly and is adjudged as predominant neurodegenerative disorders, ostensive with limited and inefficacious treatment regimes. Discerning the pathophysiology expounds the significant hallmarks of AD and assists in diagnosis wherein a patient is screened for one or more of the following characteristics: amnesia (memory loss), aphasia (expressive aphasia is an inability to find right words while receptive aphasia demonstrates an inability to understand), apraxia (loss of motor function) and agnosia (loss of functioning of 5 senses) (Sahebkar et al., 2021). The FDA (Food and Drug Association) approved drugs for the treatment of AD includes the administration of AChEIs (acetylcholinesterases inhibitors), NMDA (N-methyl-D-aspartate receptor antagonists) (Auld et al., 2002; Anand et al., 2014), Selegiline (used in the treatment of Parkinson's Disorder) (Anand et al., 2014; Abeysinghe et al., 2020), estrogen therapy (Auld et al., 2002), NSAIDs (Non-Steroids Anti-Inflammatory Drugs) (Abeysinghe et al., 2020). A comprehensive overview of these drugs is listed in **Table 1**. Addressing Alzheimer's is not limited to timely diagnosis and implementation of constructive treatment plans. The preponderance of AD in the elderly is often misleading as the symptoms are misread for aging. The classification of different stages of the disease progression of AD is depicted in **Figure 1**. Proper intervention in accordance with diseases progression ameliorates disease management. The irreversible damage to the brain cells and involuted pathophysiological, events associated with AD have always emphasized the need for the development of novel drugs and therapeutics, which render better outcomes with fewer or no side effects.

The plethora of bioactive phytocompounds, useful vitamins and chemicals has maximized the need to derive their therapeutic potentials (Garriga et al., 2015). Their feasibility to be taken as a dietary supplement, unparallel chemical diversity, remarkable efficacy, and their dexterity to interact with biological targets to positively revamp biological functions is superlative (Mir and Albaradie, 2014; Yuan et al., 2016). The presence of alkaloids, flavonoids, carotenoids, and other phytonutrients in natural products is the underpinning for nutraceuticals, which believes that diet has an undeniable effect on epigenetics (Mir and Agrewala, 2008; Mir, 2015). Moreover, the consumption of functional foods which enhances brain functioning (often termed as brain foods) will aid in overall management of AD (Mir and Albaradie, 2015; Bhat et al., 2022). Though the current research is oriented toward food-based novel drugs, it is fundamental to develop pharmacological preparations to address AD. The principle of nutraceuticals emphasizes developing interventions

TABLE 1 | FDA approved drugs in the treatment of Alzheimer's diseases.

Generic name	Target	Type	Treated for	Function	Possible side effects
Aducanumab Aduhelm	Beta-amyloid	anti-amyloid antibody intravenous (iv) infusion	Alzheimer's disease	Enhances Memory, orientation language	Abnormal brain changes Headache Swelling in the brain
Cholinesterase inhibitors					
Donepezil Aricept	Acetylcholine esterase	Oral drug	All stages of Alzheimer's disease	Cholinergic transmission Increases synaptic availability of acetylcholine	Nausea Vomiting loss of appetite increased frequency of bowel movements. Stomach pain Weight loss
Rivastigmine Axelon	Acetylcholine esterase	Oral or transdermal patch	Mild-moderate Alzheimer's disease	Treats dementia	Nausea Vomiting loss of appetite o Stomach pain Weight loss
Galantamine Razadyne	Acetylcholine esterase	Oral drug	Mild-moderate Alzheimer's disease	Improves the function of nerve cells in the brain	Nausea Vomiting Diarrhea Heartburn Headache Pale skin
Memantine Namenda	NMDA receptor antagonist	Oral drug	Moderate- severe Alzheimer's disease	Increases normal brain functioning, memory, cognition	Headache Constipation Sleepiness Dizziness Aggression
Memantine + donepezil Namzaric	NMDA receptors	Oral drug	Moderate- severe Alzheimer's disease	Restores neurotransmitters	Cramps Nausea Convulsions Difficulty in urinating
Suvorexant (Belsomra)	Orexin receptor antagonist	Oral drug	Mild-moderate Alzheimer's disease	Improves behavior and psychological symptoms	Drowsiness Dizziness Headache Cough Diarrhea

that are beyond the diet and healthy eating and shouldn't be misapprehended for devising a diet plan rich with supplements as this can only compensate the nutritional requirements and is ineffective to combat a malady. Significant pharmacological properties like neuroprotective, anti-oxidant, anti-inflammatory, anti-apoptotic, etc., demonstrated by phytonutrients like tannins, alkaloids, phenols, carotenoids can be inspected to devise potential drugs (Mir et al., 2019; Lautie et al., 2020; Qadri et al., 2021). In this review, we will constructively look into important hallmarks of AD, neuroprotective and anti-Alzheimer's properties exhibited by phytonutrients and explore their food sources.

PATHOPHYSIOLOGY ASSOCIATED WITH ALZHEIMER'S DISEASES

The prominent hallmarks of AD are hypothesized to be the production of Aβ plaques and the neurofibrillary tangles (NFTs) in different regions of patients. Further, AD is grossly progressed by aberrant phosphorylation and agglomeration of neurofibrillary tau proteins (Majeed et al., 2021), causing instability of microtubules and concomitantly includes functional abnormalities in the axon transportation (Atlante et al., 2020).

Subsequently the cognitive impairment and neurodegeneration is currently thought to be a primary driver for NFTs (Dey et al., 2017). These occurrences suggest a link between aberrant tau proteins and memory deficits in Alzheimer's patients associated with various AD associated hallmarks and recognized potential therapeutic targets (**Figure 2**). Originally, it was presumed that Aβ peptide accumulation caused abnormal modifications of tau functioning, these processes work in tandem, amplifying each other's detrimental consequences and causing the intellectual loss associated with AD (Mir et al., 2018; Mir). The evolved Aβ are further deposited in hippocampus and basal segment to form amyloid plaques and recruits the Aβ insoluble aggregates and hence damage to mitochondria resulting in severe decline in production of ATPs (Mir et al., 2021). Subsequently the astrocytes and microglia induce oxidation and inflammatory related reactions after activation leading to dysfunctioning of neurons and their apoptosis to lead clinical features of Alzheimer's disease. Additionally, Aβ activate

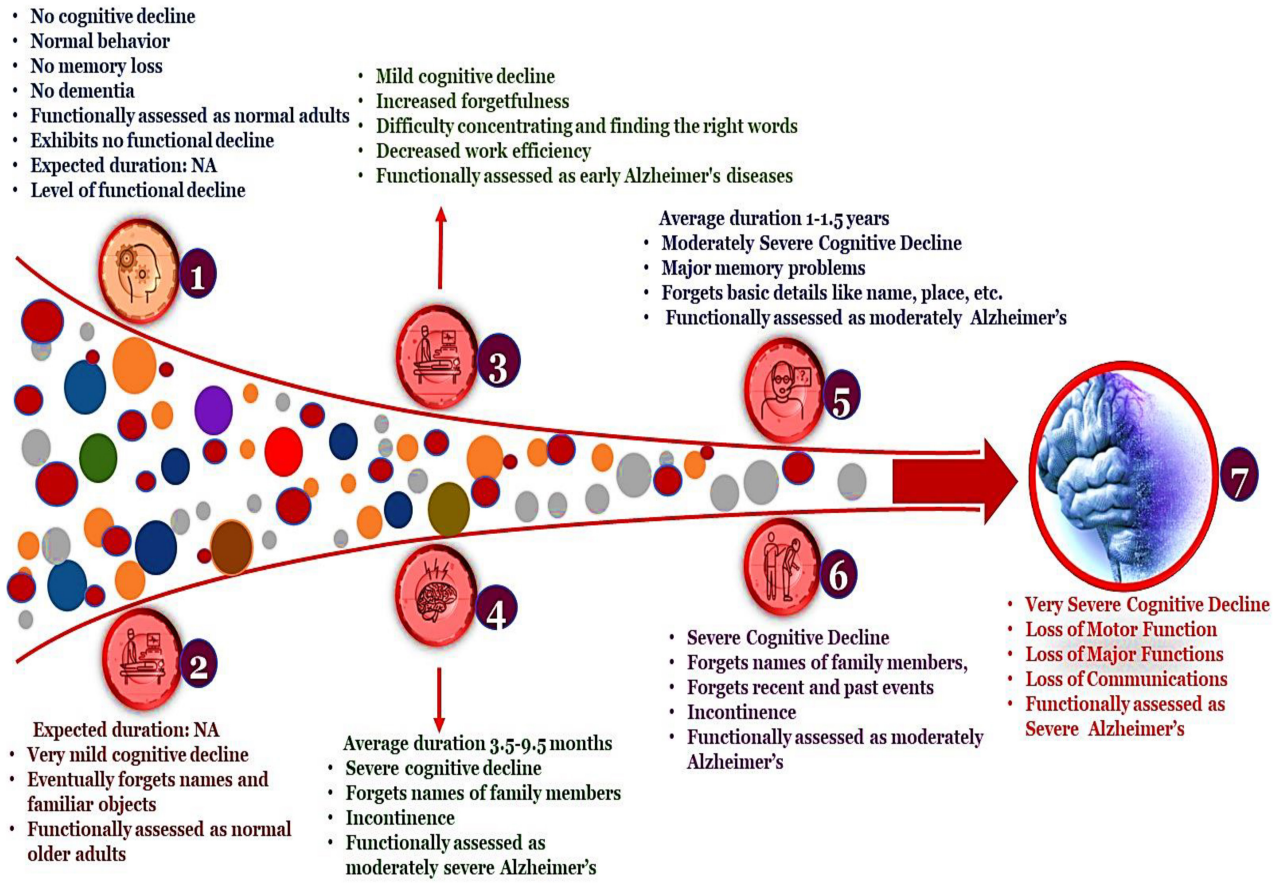

FIGURE 1 | Different stages of Alzheimer's disease. The above classification is based on the Global Deterioration Scale/Reisberg Scale for rating dementia. This classification of AD mainly relies on the Functional Assessment Staging Test (FAST) wherein the individual is examined for their cognitive decline depending on their aptness to engage in daily activities.

tau protein kinase which in turn phosphorylates the tau proteins (Shao and Xiao, 2013).

Following an extensive investigation into the processes of Aβ peptide-related damage, the underlying mechanisms that induce toxicity remain unknown. Researchers have indicated that Aβ aggregate receptor interaction influences several critical neuronal processes, but they haven't disclosed the whole profile of these receptors or the associated signal transduction pathways linked with them, implying that further investigation is necessary (Yadav, 2021). The complexity of neurodegeneration is not fully decoded and therefore we have various hypothesis that attempts to decipher the pathophysiology of AD. The pathogenesis of Alzheimer's disease is shown in **Figure 3**.

THE CHOLINERGIC HYPOTHESIS

Cholinergic synapses are omnipresent in the brain, nerve cells, and spinal cord. This synaptic conduction is essential for cognition, concentration, memory, attention, and other superior cognitive mental abilities. Multiple studies imply that cholinergic synaptic transmission plays a key role in enhancing cognitive performance, brain functioning, and plasticity. As a result, subsequent research is oriented toward investigating the normal cognitive abilities and age-associated cognitive impairments caused due to the brain's cholinergic system (Kaur et al., 2021; Pluta et al., 2021). The cholinergic theory transformed Alzheimer's investigational studies from an observational and explanatory neuropathological study to the present paradigm of synaptic neurotransmission. The identification of rapidly depleting pre-synaptic cholinergic markers in the cerebral cortex (Scheltens et al., 2016), validation of Nucleus Basalis of Meynert (NBM) as the provenance of cortical innervation and the affirmation of its neurodegeneration specific to AD (Fu et al., 2017). Further, corroborating the cognitive decline caused due to cholinergic antagonists are the breakthrough discoveries supporting this hypothesis (Kaur et al., 2021). According to researchers, cholinergic synaptic transmission (CST) is important to cultivate memory as well as establishing learning abilities and any dysfunction in this system results in cognitive decline. In AD, neurodegeneration in the basal forebrain and the hippocampus region is substantial (Bennett et al., 2017). The acetylcholine (ACh) produced during CST is hydrolyzed by acetylcholinesterase AChE and butyrylcholinesterase (BuChE) to

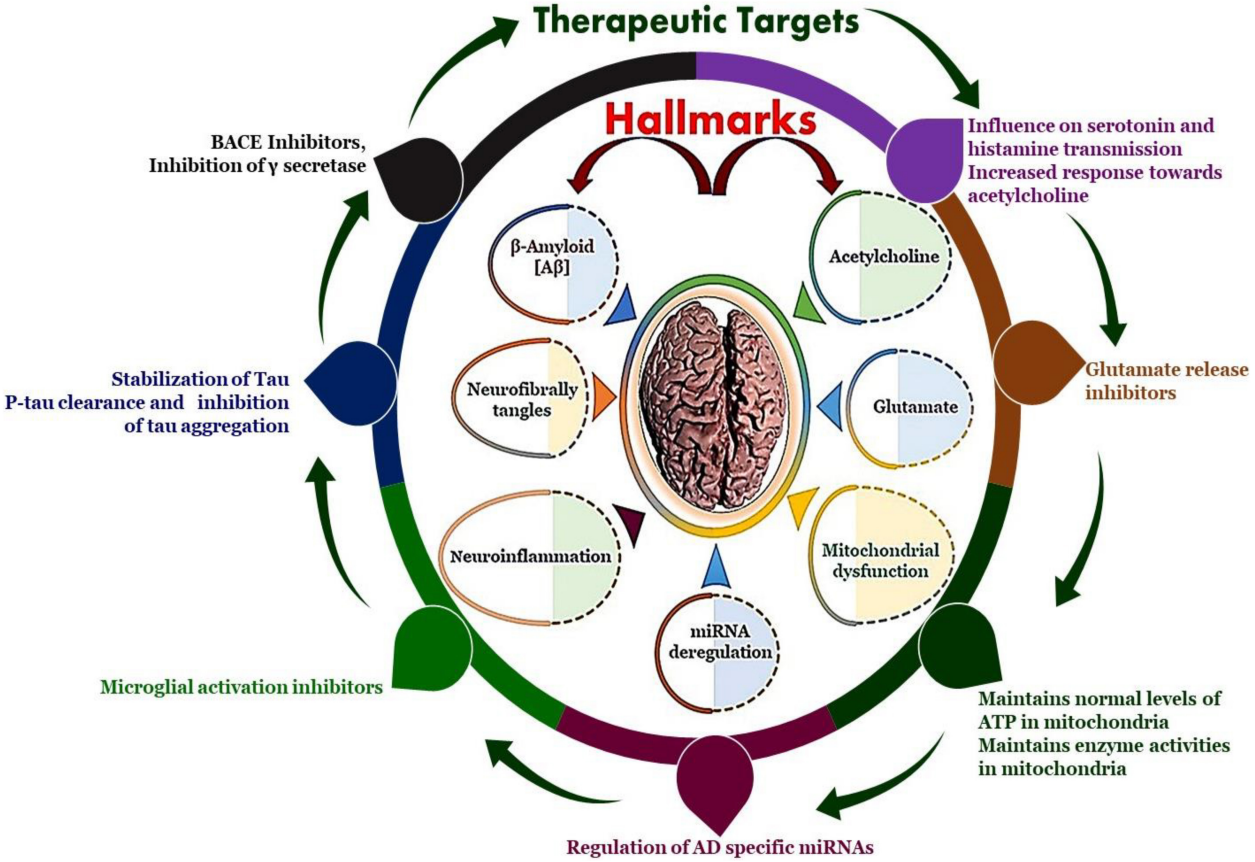

FIGURE 2 | The neuropathological hallmarks of Alzheimer's disease: formation of amyloid-beta plaques, formation of neurofibrillary tangles, miRNA deregulation, mitochondrial dysfunction, neuroinflammation and therapeutic targets such as BACE inhibitors and Inhibition of γ secretase, stabilization of Tau protein, influence on serotonin and histamine transmission, maintains normal levels of ATP in mitochondria and maintains enzyme activities in mitochondria, microglial activation inhibitors and regulation of specific miRNAs.

terminate the signal conduction. The BuChE levels are either elevated or unaltered in AD patients. AChE agglomeration promotes the AD neurotoxic A fibrils, as AChE is fundamental for the production of neurotoxin A fibrils (Bloom, 2014).

TAU HYPOTHESIS

The pathophysiology of tau is initiated in the human brain even before the development of Aβ plaques, specifically aspiring the glutamate projection neurons. The aberrant phosphorylation of the tau among susceptible nerves in elderly rhesus macaques is linked to calcium imbalance (Hunt and Castillo, 2012; Vergara et al., 2019). The endosome that incorporates APP (Amyloid Precursor Protein) are confined by the improperly phosphorylated tau (pTau) on the microtubules, which eventually enhance Aβ synthesis. The aberrant tau phosphorylation caused by Aβ oligomers contributed to the pathogenesis of AD (Ferreira et al., 2015). Tau is a phosphoprotein composed of a microtubule-binding domain (MBD) and a projection domain in the brain, it entails 38 phosphorylation sites and has 6 isoforms composed of 352–441 amino acids. Additionally, the projection domain is separated into the proline-rich residual region and amino-terminal region. The tubulin-binding and carboxy-terminal regions encompass the MBD. Tau protein that has phosphorylated interfaces with tubulins to reinforce the assemblage of microtubules at the axon and is implicated in intracellular trafficking (Hampel et al., 2019). Normal tau is modified to paired helical filament tau (PHF-tau) and neurofibrillary tangles as a consequence of aberrant tau phosphorylation (NFTs). Hyperphosphorylated tau drastically alters microtubules and causes their deformation, ultimately culminating in the death of nerve cells. The proportion of hyperphosphorylated tau in an AD patient's brain was 3–4 times greater than in a healthy brain (Hampel et al., 2018).

AMYLOID HYPOTHESIS

The identification of amyloid-β as the principal constituent of senile plaques and tau protein was proved to be a cardinal element of the NFTs was a major milestone in AD research as it provides significant insights about the pathophysiology of AD. This was followed by the discovery of genetic variations

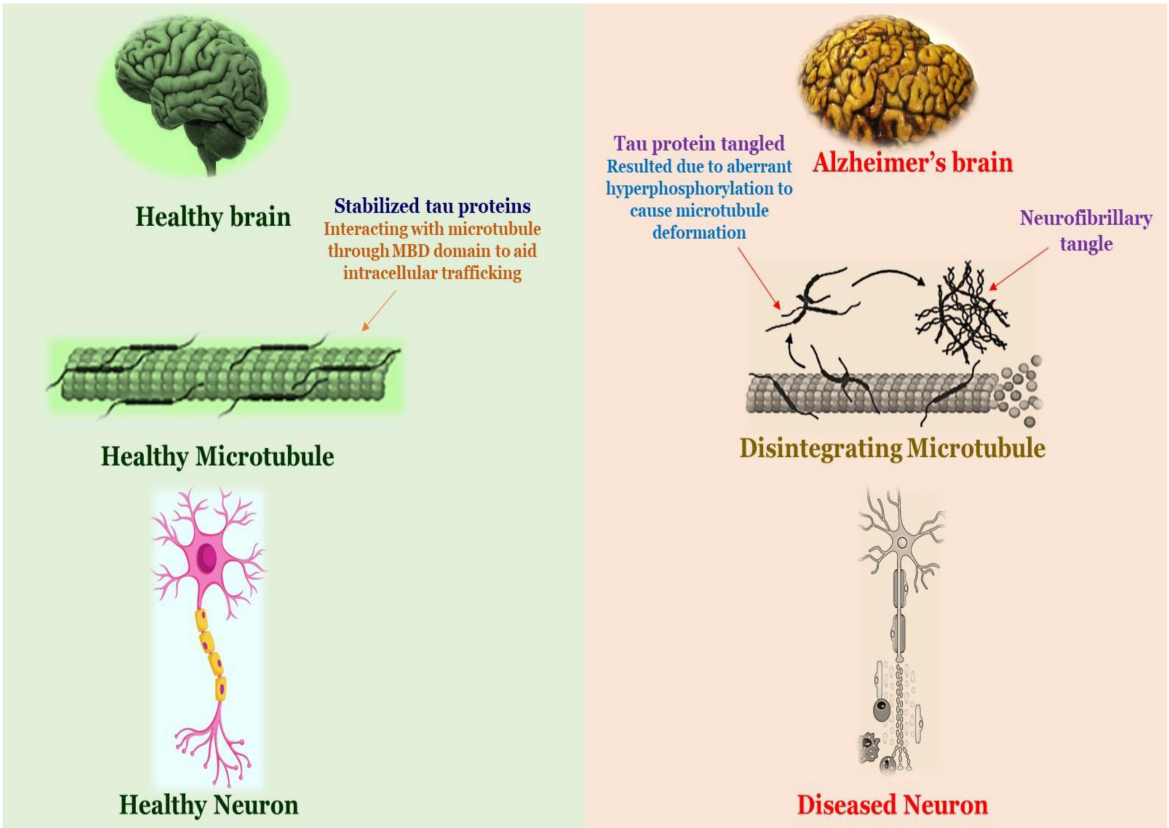

FIGURE 3 | Schematic diagram of the pathology of Alzheimer's disease.

in the APP which directed the research toward autosomal dominant familial Alzheimer's disease. These findings, coupled with other research findings, observations, and assumptions have fostered the amyloid hypothesis, which posits that amyloid-beta is the principal component that facilitates the pathogenesis of Alzheimer's disease (Bowen et al., 1976; Whitehouse et al., 1981). The discrepancy in the rate of Aβ42 and related Aβ proteins synthesis and elimination is the driving factor to initiate AD. APP695, APP751, and APP770 are the three isoforms of APP that are indispensable for neurogenesis, synaptic plasticity regulation, cell attachment, and intracellular stabilization of calcium ion levels. APP (soluble) exerts neurotrophic and neuroprotective effects (Kilimann et al., 2014). The primary amyloidogenic pathway generates soluble βA protein and C-terminal α residues by separating the Lys16 residue from APP utilizing the enzyme α-secretase. The non-amyloidogenic peptide p3 is then produced by the degradation of the C-terminal component α by the enzyme γ-secretase. When β-secretase degrades APP, it creates soluble βA peptides and the C-terminal β residues.

The latter is fragmented at numerous locations by the catalysis of γ-secretase, yielding in βA monomers, which contain 38–43 amino acid residues. Self-assemblage of the βA monomers into neurotoxic oligomers, proceeded by the development of fibrillary clusters, induces neural impairment, which eventually leads to dementia. The clustered oligomers also stimulate the production of amyloid plaques, which are a hallmark of AD. In AD patients, concentrations of the βA42 peptides are seen to be higher. The primary form of APP in the brain is a 695 amino acid membrane protein that is systematically broken by 2 specific enzymes amyloidogenic pathway, i.e., the β-site APP cleavage enzyme (BACE) and γ-secretase. It can be concluded that the underlying mechanism implicated in AD pathogenesis is the generation of insoluble βA peptides via disintegration of APP (Jiang et al., 2017). Further, current aim of therapeutic strategies is to overcome the global AD prevalence is to decrease the formation and subsequent aggregation of Aβ and their clearance from AD patients (Jakob-Roetne and Jacobsen, 2009; Morris et al., 2018; Barthélemy et al., 2019; Arnsten et al., 2021).

NEUROINFLAMMATION

Anti-amyloid approaches were employed in the past to treat AD, but the outcomes were unsatisfactory. As demonstrated by autopsy and imaging experiments, the amyloid cascade hypothesis isn't adequate to describe neural destruction in AD. Neuroinflammation has a key part in Alzheimer's disease, however, the exact influence of neuroinflammation, presumably beneficial or detrimental, is still being questioned

(Savelieff et al., 2018). The advent of neuroinflammation has been corroborated by investigations that reveal tissues of CNS has a sophisticated and naturally adaptable capacity to modify its fundamental paracrine systems through independently created and modulated inflammatory chemicals (Gallardo and Holtzman, 2019).

Neuroinflammation has distinct traits based on fundamental reasons, such as its persistence, intensity and severity of occurrence, and duration time. Age-associated deterioration of anti-inflammatory pathways generates inflammation and develops mild clinical signs, such as neural inflammatory responses followed by severe brain damage, which can persevere for few years before its clinical presentation as AD (Hampel et al., 2018). Overexpression of microglial cells and astrocytes promotes prolonged and recurrent neuroinflammation by releasing proinflammatory cytokines such as interleukins, TNF-α, and γ-interferon, which influence the central nervous system are detected in AD patients. The γ-secretase activity cleaves APP to generate βA peptides, which are stimulated by reactive oxygen species (ROS). The anti-inflammatory methodologies are implemented to produce new compounds to address AD (Barage and Sonawane, 2015).

OXIDATIVE STRESS

The brain is highly susceptible to oxidative damage in comparison to other organs, as the constituents of nerve cells are oxidized in Alzheimer's due to alterations in the functioning of mitochondria, which subsequently elevates the level of metal ions, inflammatory molecules, and β-amyloid (Aβ) proteins (Villaflores et al., 2012). Oxidative stress exerts a critical role in the development of AD. An accelerating accumulation of tau hyperphosphorylation, and consequent decrease of synaptic connections and neuronal cell, oxidative damage accelerates the pathogenesis of AD. Various experiments have validated the irreversible and severe damage of nerve cells caused due to oxidative stress (Lin et al., 2011). AD is a condition of aberrant aging and exhibits oxidative injury at concentrations that far exceed those of senior individuals (controls), implying the presence of other unknown factors that could have positively contributed to the pathogenesis of the disorder (Lin et al., 2011; Villaflores et al., 2012). The degradation of synaptic plasticity in the afflicted areas of the brain is thought to be the initial factor that prefaces neurodegeneration in AD, and it is linked to cognitive dysfunction. Oxidative stress advances the process of aging and the development of a plethora of neurological illnesses, notably Alzheimer's disease. Excessive generation of reactive oxygen species (ROS) is linked to age/disorder-related mitochondrial dysfunction, disrupted mental equilibrium, and diminished antioxidant defense, which influences synaptic plasticity and neurotransmission, which directs toward cognitive impairment (Selkoe, 1991).

Reactive oxygen species also modulates DNA, triglycerides, peptides, amino acids, calcium levels, functioning efficacy and kinetics of mitochondrial, cellular morphology, receptors traffic, and energy balance, among other molecular targets (Hardy and Higgins, 1992).

NATURAL PRODUCT-BASED THERAPEUTICS FOR ALZHEIMER'S DISEASE

The reported preventative properties of natural products are resultant of anti-oxidative or anti-neuroinflammatory effects, which action by blocking the agglomeration of Aβ and tau peptides and boosting cholinergic signaling. Natural compounds that tackle several pathogenic pathways may be capable of reducing/delaying or even preventing the occurrence and advancement of Alzheimer's disease (Graham et al., 2017). Owing to the unavailability of efficacious pharmacological interventions for AD, alternative initiatives centered on diet modifications, intake of food supplements, consumption of functional food ingredients and organic products to avoid the disease conditions (Karran et al., 2011). Novel medications are critical for enhancing the quality of care and alleviating the symptoms of affected individuals. Multiple pharmacological options to diagnose and control Alzheimer's disease are presented in recent times, but none have yielded optimistic results in clinical studies.

Recent studies have revealed that some dietary factors lower the incidence of AD, which has motivated scientists to investigate the benefits of phytoconstituents and extracted bioactive elements (Hensley, 2010; Calsolaro and Edison, 2016).

Natural remedies, have potential drug-like qualities, that enable them to pass the biological membranes, and allow them to interfere in protein-protein associations (Chen and Zhong, 2014; Wang X. et al., 2014; Calsolaro and Edison, 2016). Chemicals derived from different plant parts, including the roots, bulbs, tubers, rhizome, foliage, pods, seeds, and buds inhibit harmful amyloid plaque development and increase cholinergic signaling (Tönnies and Trushina, 2017). Antioxidant-rich foods have been shown to lower oxidative damage in the CNS. As a result, natural compounds have a wide spectrum of pharmacological effects, drawing the interest of scientists who want to use them in the production of therapeutic molecules to cure a variety of ailments (Kennedy and Wightman, 2011; Grant, 2016; Bhat et al., 2021; Chen X. et al., 2021).

The use of food and other natural sources as supplements to address several conditions is a traditional knowledge used in Ayurveda, Siddha, Unani, Chinese Herbal Medicines, and others in conventional traditional practices. Over the decades, the approach of utilizing these bioactive phytocompounds is changing constantly. Previously, the research was mainly centered on demonstrating various pharmacological properties of a different plant parts or of the whole extract itself (Vassallo, 2008; NewmanDj, 2016; Mir et al., 2021a). Presently, with the emergence of nutraceuticals, the applications of bioactive phytocompounds are not just limited to the consumption of natural products as dietary supplements, but to explore their specific therapeutic properties to develop potential drugs. With the vast diversity of bioresources, we have various plants, herbs, fruits, vegetables, seafood, meat, dairy products, nuts, berries,

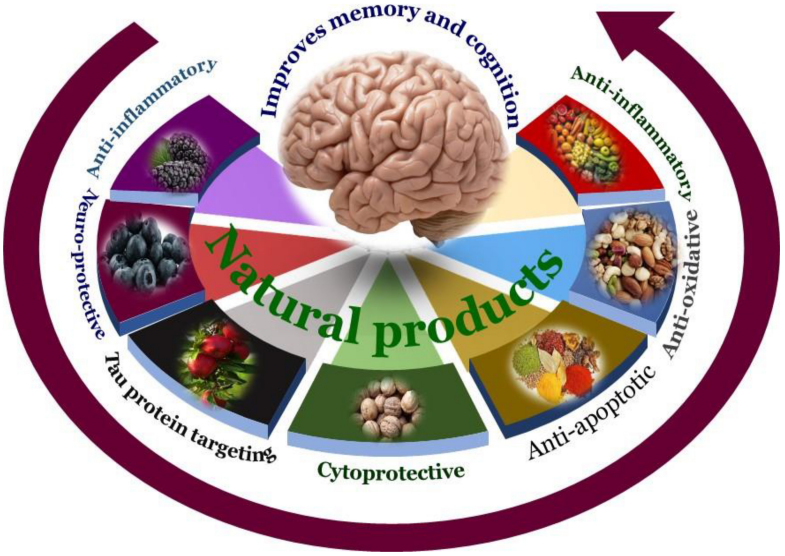

FIGURE 4 | Overview of the natural products' targets in AD. Many natural products show neuroprotective effects in the various experimental models of AD through multiple mechanisms of action. These include direct effect on neurotoxic agents such as Aβ plaque formation or tau hyperphosphorylation events.

etc., are all rich with various phytocompounds which have neuroprotective properties are shown in **Figure 4**.

ANTI-AMYLOID EFFECTS

The key domain of investigation in AD pathophysiology is treatment techniques targeting Aβ oligomers. Various treatment techniques are employed, including blocking Aβ production (Silva et al., 2014) to reduce Aβ oligomers, lowering soluble levels of Aβ, and eliminating Aβ from the brain (Yang et al., 2016). AD causes neuroinflammatory reactions, mitochondrial malfunction, oxidative stress, loss of synaptic plasticity, transportation, and tau hyperphosphorylation, in addition to other associated cellular abnormalities. Aβ is produced as a predictable consequence of these physiological modifications (Tariq et al., 2021). Numerous botanical herbs demonstrated anti-amyloidogenic properties, indicating its influences on the accumulation and instability of pre-existing Aβ fibrillary aggregates in the CNS (Maccioni et al., 2010; Mir et al., 2021b; Nomoto et al., 2021; Wainwright et al., 2022). Aside from the medicinal herbs listed, studies have investigated the anti-amyloidogenic properties of ellagic acids, garlic acid, dry ginger extract, isolates of mulberry leaf, and caper buds, which are all consumable dietary elements (Fujiwara et al., 2006, 2009; Papandreou et al., 2006).

INHIBITORS OF β AND γ-SECRETASE

Targeting BACE-1 or γ-secretase enzymes is identified as the most effective treatment method for AD because Aβ build-up leads to aberrant enzymatic cleavage of APP by β- and γ-secretase enzymes, resulting in the production of Aβ oligomers (Durairajan et al., 2008; Fujiwara et al., 2009). Several herbal extractions that combine with β-secretases impact Aβ synthesis. Ellagic acid and punicalagin were reported to suppress β-secretase in, *Punica granatum L. (Lythraceae)*. Lipophilic alkylated flavonoids from *S. flavescens* Aiton *(Fabaceae)* have a strong non-competitive BACE-1 inhibition effect. Polyphenols derived from green and black tea, as well as *Smilax china L. (Smilacaceae)*, are effective BACE-1 inhibitors, which aids in slowing the advancement of Alzheimer's disease.

TAU HYPOPHOSPHORYLATION

Tau peptides action to stabilize microtubules, but their aberrant hyperphosphorylation causes tau agglomeration. AD is caused by these aggregates and constraining the development of tau clusters, controlling tau with kinases, limiting tau disintegration with chaperones, and stabilizing tau microtubules are successful methods to address post-symptomatic AD. Anti-tau effects have been demonstrated in herbal medications and extracts. Curcumin, a diarylheptanoid identified in turmeric (*Curcuma longa*) extracts, stimulates the generation of the anti-inflammatory IL-4 cytokine and lowers Aβ and tau concentrations in mice with Aβ overexpression (Kang et al., 2011).

The cinnamon (*Cinnamomum zeylanicum*) extraction inhibited tau assembly and additionally exhibited the inhibitory effect that is attributed to both cinnamaldehyde and procyanidin. The bioactive constituent paclitaxel, derived from *Taxus brevifolia,* exhibited therapeutic properties by combatting the functional loss in the tau pathology (Kang et al., 2011).

Severe oxidative damage in AD pathogenesis stimulates the production of reactive oxygen species (ROS) by activating microglial cells with Aβ oligomers (Syad and Devi, 2014). For instance, the validated efficacy of Ginko biloba contained

metabolites such as, tocopherol, bioflavonoid pycnogenol, ascorbyl palmitate and other antioxidants ineffectively suppressing the apoptotic cells in the hippocampus of ApoE-deficient mice. Similarly, *Salvia officinalis* is notable for its antioxidant properties, anti-inflammatory characteristics, and mild suppression of AChEs (Fujiwara et al., 2009). The active element in sage, rosmarinic acid, inhibits the development of ROS, peroxidation of lipids, activation of caspase-3, fragmentation of nucleic acids, and Aβ oligomeric hyperphosphorylation of tau protein (Fujiwara et al., 2009). *Panchagavya Ghrita*, an Ayurveda composition, reduces seizures, cognitive decline, and oxidative damage (Joshi et al., 2015). As discussed in this review there are ample number of natural products that are neuroprotective in nature. The neuroprotective properties of some common fruits, vegetables, herb, berries, nuts species, and condiments are discussed in the proceeding section.

Vaccinium angustifolium

The blueberry is high in anthocyanins, which are cytoprotective polyphenols having anti-oxidant properties. Blueberries aids in recovering cognitive and memory deficits in the CNS. For instance, Blueberry nutrition has been linked to improved cognition and motor function in elderly animals in preclinical investigations (Veerendra Kumar and Gupta, 2003; Calcul et al., 2012; Mathew and Subramanian, 2014). During a 12-week administration of natural blueberry juice, older persons with initial memory impairment reported significant amelioration in memory and cognitive function (Iuvone et al., 2006). This study discovered increased pair associated memorization and word identification recall. For instance, irradiated mice exhibited functioning benefits with blueberry supplementation in latency assessments, which entails retrograde training. The striatum is affected by polyphenols present in blueberry; it is important to note that this striatum is critical in retrograde learning (Youdim et al., 2000; Kumar et al., 2011). With the supplementation of blueberries increased accumulation of anthocyanin in the hippocampal and neocortex was noticed (Casadesus et al., 2004).

Morus alba

Mulberries are enriched with hydroxyl stilbene, an antioxidant that is comparable to resveratrol but lacks an additional OH group that acts as a proton donor (Krikorian et al., 2010). In Aβ-induced neurotoxic conditions in cortical neurons, hydroxyl stilbene was found to exhibit neuroprotective properties. Hydroxyl stilbene reduces intracellular calcium ion levels, ROS production, and neurotransmitter glutamate production in Aβ-induced neurotoxicity (Shukitt-Hale et al., 2007). More research is required to determine the therapeutic potential of hydroxyl stilbene found in mulberry in AD models (Andres-Lacueva et al., 2005).

Malus domestica

Apple Juice Concentrate (AJC) increased cognition, oxidative stress, and synaptic signaling in laboratory experiments (Spangler et al., 2003; Essa et al., 2012). In cultured cells research, Aβ and presenilin-1 concentrations were reduced, but synaptic transmission and ACh levels were boosted. The neuroprotective benefits of AJC are due to phytonutrients to antioxidant activity. PS-1 amplification is caused by faulty DNA methylation caused by a lack of SAM (S-adenosylmethionine). According to investigations, AJC offers adequate SAM to reduce the production of presenilin-1. Furthermore, mice administered with AJC had higher amounts of ACh in brain homogenates. As a result, drinking AJC is a healthy way to impede AD symptoms (Andres-Lacueva et al., 2005; Chen C. et al., 2021).

Juglans regia

Walnut contains healthy triglycerides, α tocopherol, vitamins, and polyphenolic compounds, particularly ellagic acid. Research suggests that adapting to walnut-rich nutrition is linked to a decreased risk of neurological illnesses (Freyssin et al., 2020). Thioflavin T experiments were used to examine the possible suppressive properties of walnut extraction on Aβ fibril production (Remington et al., 2010). The amyloidogenic action of walnuts is due to phenolic acids. The findings imply that walnut extracts protect cells from death induced by Aβ. This beneficial effect is achieved by reducing the production of ROS and reducing cell membrane damage and DNA fragmentation. This beneficial impact could be due to the antioxidant polyphenols found in walnuts (Freyssin et al., 2020). As a result, walnut-rich nutrition is viable to prevent and delay the development of Alzheimer's disease (Tripathi and Mazumder, 2020).

Piper nigrum and *Piper longum*

Piperine is a nitrogen-containing alkaloid found in the fruit black pepper and long pepper. It is utilized in herbal treatment for therapeutic applications to manage a variety of diseases (Chan and Shea, 2006; Ichwan et al., 2021). Multimodal health advantages such as anti-depressive impact, better cognitive functioning, neuroprotective effect, and antioxidant properties activity has been documented based on pharmaceutical data (Chauhan et al., 2004; Muthaiyah et al., 2011; Hussain et al., 2021). It also has anti-inflammatory, anti-convulsant, analgesic, and anti-ulcerous properties. In AD patients, ethyl choline aziridinium can cause a cholinergic action. More research on the molecular and cellular mechanisms of neurogenesis is required. Piperine demonstrated significant enhancement in cognition and neurodegeneration in the hippocampus (Bano et al., 1987; Wattanathorn et al., 2008; Luca et al., 2021).

Cinnamomum verum

Cinnamon is traditionally utilized as a condiment and medicinal supplement to treat various illnesses (Selvendiran et al., 2003). The alkaloids, flavonoids, ad cinnamic acid derivatives like cinnamaldehyde, eugenol, cinnamyl acetate, and cinnamyl alcohol, have versatile therapeutic applications like anti-inflammatory, antibacterial and antioxidant properties (Khan et al., 2021). The isolates prevent oligomers and amyloid filament production in fly and mouse models of AD. Cinnamon has a number of phytoconstituents that can penetrate the blood-brain barrier. Additional exploration of the impact of cinnamon extracts on various processes associated with AD is required (Hua et al., 2019).

Allium sativum

Allium sativum is utilized in cuisine and healing all over the globe (D'Hooge et al., 1996). Tg2576 mice were used to examine the impact of aged garlic extraction. The use of aged garlic extract improved hippocampal-based cognitive dysfunction significantly. Supplemental research is needed to better understand the neuroprotective pathways (Bai and Xu, 2000).

Zingiber officinale

Zingiber officinale is a common spice with ethnomedicinal characteristics similar to garlic. It's regularly utilized as an infusion in ginger tea, or as nutritional supplements. The predominant bioactive constituents in ginger are gingerols, shagols, bisabolene, zingiberene, and monoterpenes (Singh et al., 2021). White and red ginger were tested for their ability to inactivate AChE and were measured using colorimetric analysis (Momtaz et al., 2018). Ginger extract has an inhibitory potential on AChE, particularly white ginger which displays a strong impact. Ginger's suppressive properties work both collaboratively and independently (Frydman-Marom et al., 2011). Ginger's ability to decrease oxidative damage is also useful in the prevention of AD (Tesfaye, 2021).

Curcuma longa

Traditional therapies have widely used curcumin to treat various ailments. Though they have been mainly postulated to treat inflammation and dermal conditions, their neuroprotective protective properties have guided the researchers to explore the benefits of their derivatives in brain disorders (Chauhan and Sandoval, 2007). The anti-amyloidogenic ability, suppression of APP, and the inhibition of amyloid-β peptide of the curcumin derivatives is due to the presence of phenyl methoxy groups (Joshi et al., 2021). Curcumin exhibits anti-inflammatory, antioxidant, and anti-Alzheimer's effects. Curcumin potentially inhibits AD-related enzymes like AChE, BChE, BACE-1, and aggregation of Aβ -tau proteins. Curcumins are beneficial in reducing oxidative stress (Joshi et al., 2021). Curcumin interacts with amyloid-beta and suppresses Aβ-tau agglomeration, and disintegrates the fibrils via meta binding which reduces the rate of nerve cell damage (Zhang M. et al., 2021). The generation of ROS is a critical factor in the pathogenesis of Alzheimer's disease, which can be reduced by the antioxidant and free radical scavenging properties of curcumin (Talebi et al., 2021a). It lowers amyloid formation and oxidative stress-induced neuronal damage by inhibiting lipid peroxidation. Curcumin reduces protein oxidation and isopropyl propionate in the body (Talebi et al., 2021a).

Cocos nucifera

The hypoglucose metabolism that occurs in the brain is a major indicator of Alzheimer's. The lack of glucose supplementation to the brain has to compensate by an external source to which coconut oil can be a potential candidate as it is rich with medium-chain fatty acids which can directly reach the hepatic system (Oboh et al., 2012). The lack of cholesterol level in AD brain is an indicator of the disease. Therefore, while devising a treatment and management plan, it is important to include sufficient levels of saturated fats to maintain the levels of high-density lipoproteins. The saturated fats in the coconut oil supplement the brain with medium-chain triglycerides which are further converted into ketone bodies during periods of starvation or fasting (Bhat et al., 2019). The glutamate levels in the hippocampal and prefrontal cortex cells were significantly reduced in the rats administered with virgin coconut oil (Chainoglou and Hadjipavlou-Litina, 2020). The virgin coconut oil exhibits anti-oxidant, anti-inflammatory, and neuroprotective properties (Zhang L. et al., 2021).

Bacopa monnieri

Bacopa monnieri is a nootropic herb that is rich in polyphenolic compounds like bacosides which prevents the brain from oxidative injury and age-related cognitive decline. The neuroprotective properties of the bacosides include destabilizing fibrils, suppression of Aβ-tau agglomeration, and protection from Aβ induced toxicity. The bacosides can easily cross the blood-brain barrier and they associate with the neurotransmitters to enhance memory, learning, and other cognitive functions. The administration of *B. monnieri* suppresses lipid peroxidation (Talebi et al., 2021b). The extract of *B. monnieri* reduced amyloid peptide-induced cell death by reducing the activity of AChE (Kappally et al., 2015). *B. monnieri* supplementation colchicine-induced dementia (Chatterjee et al., 2020).

Elettaria cardamomum

Elettaria cardamomum has anti-bacterial, anti-microbial, anti-inflammatory, antioxidant properties which makes it a potential therapeutic compound (Alghamdi, 2018; Mirzaei et al., 2018). The cardamom oil has AChE inhibitory activity, anti-anxiety, and anti-depressant properties. A research study has revealed that a terpenoid isolated from *E. cardamomum* called alpha-terpinyl acetate which can be used as a suitable lead to develop a molecule that might have multi-targeted directed ligand (MTDL) potential and disease amelioration effects in AD (Abdul Manap et al., 2019). One more research study concluded that terpenoid-rich *E. cardamomum* extract prevents Alzheimer-like alterations induced in diabetic rats via inhibition of GSK3β activity, oxidative stress and pro-inflammatory cytokines (Uabundit et al., 2010).

Salvia rosmarinus

Rosemary is an important herb in the Mediterranean diet and it has various culinary and therapeutic benefits. The herb is rich in antioxidants; especially phenolic diterpenes. This herb has anti-diabetic, anti-tumor, anti-inflammatory, antioxidant, neuroprotective properties, etc. Rosemary essential oil is rich in bioactive phytocompounds like terpineol, 1,8-cineole, pinene, camphene, and borneol. It also has an abundance of secondary metabolites, flavonoids, and phenolic acid derivatives like homoplantaginin, rosmarinic acid, gallocatechin, luteolin, etc. The diterpenes prevent the cells from oxidative damage and inhibit lipid peroxidation (Saini et al., 2019). The carnosic acid present in rosemary protects nerve cells from ischemic injury by generating the quinone derivatives which are accompanied

by the loss of hydrogen radicals from their phenolic groups (Kumar and Kumari, 2021). The derivative of rosemary plays an important role in Aβ mechanism as they modulate amyloidogenic and non-amyloidogenic pathways; the major pathways associated with AD pathogenesis (Sengottuvelu, 2011). Carnosic acid reduces the generation of amyloid-β 1-42, Aβ-tau agglomeration and protects the cells from beta-amyloid-induced toxicity (Kumar and Kumari, 2021). Rosemary leaf extract enhances memory and learning ability and is directly proportional to the activity of enzymes like AChE, BuChE, etc., (Sengottuvelu, 2011).

Crocus sativus

The extensively used spice saffron is rich in volatile compounds wherein safranal is the most abundant non-volatile compound of saffron. Non-volatile compounds like crocins, crocetin, quercetin and kaempferol, isophorones, carotenoids, zeaxanthin, lycopene, etc., are present in saffron (Gomaa et al., 2019; Chowdhury and Kumar, 2020). Saffron and its bioactive phytocompounds are speculated to have an effect on AChE activity, dopamine pathways signaling, Aβ peptides and tau aggregate formation, ROS, activation of glial cells, notch pathway, Keap1/Nrf2 signaling pathway, mitogen-activated protein kinases signaling pathway, etc. Saffron has been reported to prevent abnormal indicators such as cognitive performance, cognitive function, motor dysfunction, tremors, spasm and convulsions. Therefore, saffron has been postulated to treat various brain-related disorders; including Alzheimer's (Gomaa et al., 2019; Chowdhury and Kumar, 2020).

Camellia sinensis

Green tea's catechin polyphenols help to slow down age-related cognitive deficits, motor nerves, and other associated neurological dysfunction in neurodegenerative disorders. Animal experiments with green tea extract showed a positive influence on brain and cognitive abilities. The catechin components can reverse neuropathological changes, stimulate nerve cell regeneration, and neuroplasticity. Catechin polyphenols play a role in the stimulation of antioxidative defense enzymes and in the prevention of monoamine oxidase and nitric oxide synthase (Wijeratne and Cuppett, 2007). Catechins regulate the activity of iron regulatory proteins, APP, AChE, and BuChE activity, fibrils disintegration, etc., (Wijeratne and Cuppett, 2007; Yoshida et al., 2014). The amyloid-induced dysfunction of mitochondria can be addressed with epigallocatechin-3-gallate and luteolin which can effectively restore the functions of the mitochondrial cells (Ozarowski et al., 2013). The treatment with epigallocatechin-3-gallate was effective in restoring mitochondrial function, generation of reactive oxygen species, and production of ATP in the hippocampus, cortex, and striatum mitochondria for up to 85% (Ozarowski et al., 2013).

Moringa oleifera

The leaves of *Moringa oleifera* have anti-inflammatory, anti-oxidant and neuroprotective properties. *M. oleifera* was investigated on hyperhomocysteinemia-induced Alzheimer's pathophysiology in mice. The study followed a 14-day homocysteine administration to establish AD-like pathology. *M. oleifera* shields cells against oxidative damage and cognitive deficits caused by Hcy administration. *M. oleifera* reduced dementia by restoring depleted synapse peptides like PSD93, PSD95, Synapsin 1, and Synaptophysin. It inhibited Hyc-induced tau hyperphosphorylation at multiple locations, including S-199, T-231, S-396, and S-404, while also lowering Aβ synthesis via BACE1 suppression (Shafiee et al., 2018). The leaf extraction of *M. oleifera* induces the differentiation of neurites and neuronal cell development, formation of spatial cognition and protects the cells from neurotoxicity (Finley and Gao, 2017).

Punica granatum

In PC12 cells, *Punica granatum* extract was evaluated for its ability to protect cells from oxidative cytotoxicity. The findings of this investigation revealed that the ethyl alcohol extract of *P. granatum* reduced hydrogen peroxide instigated oxidative damage in PC12 cells (Mandel and Bh Youdim, 2012). *P. granatum* contains potent anti-dementia molecules like ellagic acid and punicalagin, which are BACE1 inhibitors. α -secretase, chymotrypsin, trypsin, and elastase were barely inhibited by ellagic acid and punicalagin, suggesting their specificity as inhibitors of BACE1 (Ide et al., 2018). The age-induced or scopolamine-induced retention impairments in mice dramatically improved after chronic administration of *P. granatum* extract and ascorbic acid for 3 weeks (Dragicevic et al., 2011). The age-induced or scopolamine-induced retention impairments in mice were dramatically improved after chronic administration of *P. granatum* extract and ascorbic acid for 3 weeks (Dragicevic et al., 2011).

Rosmarinus officinalis

A polyphenol herbal ingredient called rosmarinic acid isolated from *Rosmarinus officinalis* is used to investigate the novel mechanism. It prevents the build-up of amyloid β (Aβ) in mice. Using DNA microarray analysis, the brain of mice (Alzheimer's disease model) was examined to see if the dopamine signaling pathway was increased in the control group vs. those administered rosmarinic acid. Monoamines such as 3,4 dihydroxyphenyl acetic acid, levodopa, dopamine, and norepinephrine were increased in the cerebral cortex following rosmarinic acid administration. As a result, the ventral tegmental region and substantia nigra showed decreased expression of DA-degrading enzymes such as monoamine oxidase B. Monoamines have been shown to suppress amyloid aggregation by *in vitro* studies. *In vivo* studies showed that rosmarinic acid consumption increased monoamine concentrations via a decrease in monoamines B gene expression. According to this investigation, the increase in monoamines in the brain caused by rosmarinic acid may have a favorable effect on Alzheimer's disease (Mahaman et al., 2018).

Clitoria ternatea

Shankhpushpi is the popular name for it. A research study investigated the ethanolic root extract of *C. ternatea* against stress-induced amnesia in rats using the oral mode of administration at dosages of 150 and 300 mg/kg. Significant

inhibitions of nitric oxide and DPPH production were detected in this experiment, as well as the protective effects of *C. ternatea* 77. Another research study examined the memory and central cholinergic activity of an alcoholic extract of *C. ternatea* roots and aerial portion in rats given 300 and 500 mg/kg. This extract boosted the activity of the enzyme acetylcholinesterase and the amount of acetylcholine in rat brains as well as memory function. *C. ternatea* root extract was shown to be more effective than aerial components (Kou et al., 2018).

Melissa officinalis

The memory-enhancing action of *M. officinalis* extract was investigated via the cholinergic system. *M. officinalis* leaves were extracted using the maceration process with an ethanol concentration of 80 percent. *M. officinalis* extract (alone) was given intraperitoneally with scopolamine at various levels (50–400 mg/kg) before to training in a Morris Water Maze. After training was completed, the acetylcholinesterase enzyme level was determined in the hippocampus. *M. officinalis* extract at a dosage of 200 mg/kg significantly improved naive rats' memory and learning and may potentially mitigate the scopolamine-induced learning impairment. However, the extract had no dose-dependent impact, and dosages greater than 200 mg/kg had no effect on memory enhancement or reversal in naive rats. Both scopolamine-induced memory impairment and naïve rats demonstrated a decrease in AChE activity. The findings indicated that *M. officinalis* extract may enhance the extract's cholinergic and memory functions. This trial demonstrated that *M. officinalis* possesses high therapeutic effectiveness in Alzheimer's disease-related memory impairment (Choi et al., 2011).

Emblica officinalis

It is commonly known as Amla. It has been revealed that the effects of a hydroalcoholic extract of the fruit of *E. officinalis* on cholinergic function and oxidative stress were investigated in scopolamine-induced amnesic rats administered via the intraperitoneal route at dosages of 150, 300, 450, and 600 mg/kg. Amnesic mice had considerable reversal of GSH, MDA, and AchE activity (Kwak et al., 2005). In another research study, the tannoid principle of *E. officinalis* restored cognitive impairments and increased amyloid pathogenesis in rats exposed to aluminum chloride. Parle et al. evaluated the memory-enhancing effect of *E. officinalis* at three different dosages of 50, 100, and 200 mg/kg orally against diazepam and scopolamine-induced amnesia for 15 days (Kumar et al., 2009). Total cholesterol levels decreased considerably, whereas AchE activity reversed as well. All trials demonstrated that *E. officinalis* may be a very useful medicinal herb for treating Alzheimer's disease (Hase et al., 2019).

Glycyrrhiza glabra

Glycyrrhiza glabra, also known as liquorice, is an ornamental plant. The aqueous extract of *G. glabra* was tested for learning and memory in rats utilizing the oral route of administration at four different doses: 75, 150, 225, and 300 mg/kg versus the diazepam-induced amnesic model in rats by using the oral route of administration for 6 weeks. All *G. glabra* aqueous extracts improved memory and learning capacities according to the findings 58. Another research study employed the oral mode of administration to assess the memory and learning activity of Glabridin rich extract (5 and 10 mg/kg) and aqueous extract of liquorice (400 mg/kg) against diazepam and scopolamine-induced amnesia in mice, with results showing improvements in memory and learning activities (Taranalli and Cheeramkuzhy, 2000).

Myristica fragrans

In this study, the n-butanol fraction of *M. fragrans* was studied against a scopolamine-induced model of Alzheimer's disease at doses of 100 and 200 mg/kg. The mice's AchE activity, retention transfer latency, and thiobarbituric acid reactive substances (TBARS) level all went down because the lipid peroxidation process was stopped by the drug. It also showed that the levels of glutathione peroxidase, SOD, and catalase had risen (Ozarowski et al., 2016). Another research study by Cuong et al. (2014) examined the methanolic extract of seeds from *M. fragrans* for its ability to block cholinergic transmission. AchE activity was slowed down by this extract: As a possible treatment for AD (Golechha et al., 2012). There was another study done by Parle et al. (2004) that found that the n-hexane extract of seeds from *M. fragrans* was tested for memory improvement at the doses of 5, 10, and 20 mg/kg orally against the diazepam and scopolamine model (Kumar et al., 2009). They didn't know how the extract of *M. fragrans* made the memory better, but they observed that the extract of *M. fragrans* enhanced the memory (Kumar et al., 2009). All of the tests showed that *M. fragrans* can help treat AD.

Evolvulus alsinoides

The leaves of *E. alsinoides* were tested for Alzheimer's disease, antioxidants, as well as diabetes using several extracts (n-hexane, ethyl acetate, aqueous, methanol, petroleum ether, and chloroform). The effectiveness of FRAP reduction, AchE blockade, -glucosidase, and -amylase was investigated in this experiment. The aqueous extract performed better than the other extracts, according to the findings (Parle et al., 2004). In another research study, the oral administration of an ethanolic extract of *E. alsinoides* was reported to protect the brains of scopolamine-induced amnesic mice at two different doses of 250 and 500 mg/kg. The results revealed that AchE inhibition was effective.

Celastrus paniculatus

The anti-Alzheimer's diseases and antioxidant effects of a methanolic extract of seeds and its other organic soluble component of *C. paniculatus* were studied. Total reactive oxygen species formation, authentic peroxynitrite (ONOO) activity, and AchE and butyrylcholinesterase (BchE) inhibition were all significantly inhibited by this extract. The results revealed that EtOAc extract has the most potential compared to others *C. paniculatus* extract (Justin Thenmozhi et al., 2016). The effects of *C. paniculatus* seed oil on an aluminum chloride-induced neurodegenerative model were examined. All animal's

TABLE 2 | Anti- Alzheimer's activity of medicinal plants.

Plant	Part used	Bioactive phytocompounds	Activities	References
Salvia officinalis	Leaf extract	Diterpenes, rosmarinic acid, carnosic acid, quercetin	AchE, BchE inhibitor	Mook-Jung et al., 2001
Rosmarinus officinalis	Whole plant	Rosmarinic acid	Inhibition of Aβ accumulation	Mahaman et al., 2018
Melissa officinalis	Leaf extract	Flavonoids	Anticholinesterase activity	Choi et al., 2011
Ginkgo ginseng	Powder extract	Alkaloids, flavonoids	Memory enhancement	Xiao et al., 2010
Ficus racemosa	Bark extract	Tannins, saponins	Anticholinesterase activity	Song et al., 2014
Ficus carica	Fruit extract	Flavonoids, phenolic compounds, vitamins	Antioxidant and immunostimulant activity	Zhao et al., 2012
Tinospora cordifolia	Leaf extract	Flavonoids	Memory enhancement	Gomes et al., 2018
Lepidium meyenii	Root extract	Proteins	Anticholinesterase and antioxidant activity	Singh, 2019
Panax ginseng	Whole plant extract	Ginsenosides	Memory enhancement	Ma et al., 2020
Celastrus paniculatus	Seed extract	Alkaloids, sesquiterpenes	AchE, BchE inhibitory activity and anti-oxidant	Desai et al., 2012
Coriandrum sativum	Seed and leaf extracts	Carbohydrates, proteins, vitamins, volatile oils	Neuroprotective activity	Dajas, 2012
Cissampelos pareira	Root and leaf extracts	Alkaloids	Inhibition of Aβ accumulation	Joshi and Parle, 2006
Moringa oleifera	Leaf extract	Proteins, fatty acid	Inhibition of Aβ accumulation	Smach et al., 2015
Nardostachys jatamansi	Root and leaf extracts	Sesquiterpenes	Inhibition of Aβ accumulation and anti-oxidant properties	Cuong et al., 2014
Evolvulus alsinoides	Leaf extract	Alkaloids and flavonoids	Anticholinesterase and antidiabetic activity	Wesnes et al., 2000
Bacopa monnieri	Flower and leaf extract	Alkaloids, bacoside-A, terpenoids	Anticholine esterase, antidementia, inhibition of Aβ accumulation	Kappally et al., 2015
Glycyrrhiza glabra	Root and leaf extract and glabridin	Glabridin, volatile oils	Antiamnesic	Taranalli and Cheeramkuzhy, 2000
Myristica fragrans	Seeds, fruits and leaf extract	Terpenes, flavonoids	Antioxidant, memory enhancement, ache inhibitor	Kumar et al., 2009
Magnolia officinalis	Fruits, leaf extract	Flavonoids, phenolics and anthocyanins	Antioxidant, anticholinesterase, neuroprotective	Ahmed et al., 2011
Punica granatum	Peel, seeds, and leaf extract	Flavonoids, phenolics and anthocyanins	Antioxidant, neuroprotective	Sumanth and Mamatha, 2014
Rhodiola rosea	Leaf and root extract	Phenols, flavonoids, alkaloids	Neuroprotective, antiapoptotic	Ahmed, 2021
Withania somnifera	Fruits, leaf extract	Alkaloids, saponins, steroidal lactone, withanamides A and B	Anticholinesterase, inhibition of Aβ	Lee et al., 2008
Sargassum sagamianum	Whole part	Plastoquinones, sargaquinoic acid and sargam chromenol	AchE and BchE inhibitor	Mani and Parle, 2009
Ecklonia cava	Whole part	Eckol, 6-6'-bieckol, 8.8-bieckol, dieckol, phlorofucofuroeckol-a	Aβ accumulation, bche, ache inhibitory activity	Nomoto et al., 2021

latency was increased. All biochemical parameters were analyzed, and it was discovered that AchE was considerably inhibited, malondialdehyde (MDA) levels significantly rose, and superoxide dismutase (SOD) levels significantly decreased. These findings concluded that *C. paniculatus* possesses powerful anti-disease Alzheimer's activity (Desai et al., 2012).

Lepidium meyenii

It is commonly referred to as black maca. The memory impairment generated by ovariectomized mice was examined using an aqueous extract of *L. meyenii* administered orally at two different doses of 0.5 and 2.0 g/kg. Chemicals such as monoamine oxidase (MAO), acetylcholinesterase (AchE), and malondialdehyde (MDA) were measured at various levels. In this experiment, the levels of MAO and AchE were both inhibited but there were no variations found in MDA levels. According to these findings, *L. meyenii* has the potential to impair memory (Singh, 2019).

Nardostachys jatamansi

In young and old mice, the ethanolic extract of *N. jatamansi* was tested for memory and learning via the oral route at 50, 100, and 200 mg/kg against scopolamine and diazepam induced amnesia. In both old and young mice, a dose of 200 mg/kg improved learning and memory and restored amnesia caused by diazepam and scopolamine. This investigation demonstrated that *N. jatamansi* might be effective in the treatment of Alzheimer's disease (Cuong et al., 2014).

Another research study, mice were given 200 and 400 mg/kg of methanolic extract of *N. jatamansi* for memory and cognition deficits in a sleep deprivation scenario. In behavioral tests, this trial indicated a significant

TABLE 3 | Plant-derived phytochemicals that affect Alzheimer's diseases.

Phytochemicals	Plant source	Plant family	Pharmacological effects/Mechanism	References
Berberine	*Coptis chinensis*	Ranunculaceae	Activates the AKT/GSK-3/Nrf2 signaling pathways -mediated regulation, cholinergic activity-mediated neurite outgrowth, increases the release of NGF and BDNF, and suppresses the levels of Cox2, TNF-, NF-B, IL-1, and iNOS.	Sutalangka et al., 2013
Curcumin	*Curcuma longa*	Zingiberaceae	Activates PKC/ERK-dependent CREB regulation and AKT/GSK-3-dependent BDNF release, while inhibiting Cas3, TNF-, and NF-B levels.	Lee et al., 2012; Yadav et al., 2019
Huperzine-A	*Huperzia serrata*	Lycopodiaceae	Increase GST, SOD, and BDNF secretion Caspase-3, TNF-, NF-kB, and AChE inhibition	Fatima et al., 2017; Tang et al., 2017
Tetrandrine	*Stephania tetrandra*	Menispermaceae	Inhibits NF-KB and TNF- activity	Jayaprakasam et al., 2010
Galantamine	*Galanthus*	Amaryllidaceae	Inhibition of acetylcholinesterase, production of interleukin-IB, and microglial agglomeration	Choi et al., 2007
Glaucocalyxin B	*Rabdosia japonica*	Lamiaceae	Reduces the expression of nitric oxide, iNOS, and TNF- in LPS-activated microglial cells. Additionally, the stimulation of p38, NF-Kb, MAPK, and the formation of ROS were suppressed.	Jia et al., 2012
Oridonin	*Rabdosia rubescens*	Lamiaceae	In AD mice, activation of the BDNF and Nrf2 signaling pathways	Ambegaokar et al., 2003
Quercetin	*Morus alba*	Moraceae	Accumulation of hydroxyl radicals (OH) and superoxide anions (O2) Inhibitory action against LOX and COX enzymes	Wang et al., 2011
Curcumin	*Curcumin longa*	Zingiberaceae	Inhibition of the NF-KB pathway (PPARY) receptor activation	Wang et al., 2011
Naringenin	*Citrus paradise*	Rutaceae	Increases resistance to oxidative stress, cytokines, and NO, while decreasing NF-kB expression. In SH SY5Y cells, Nrf2 signaling is upregulated.	Shakibaei et al., 2007
Resveratrol	*Veratrum grandiflorum*	Liliaceae	Suppresses the expression of pro-inflammatory mediators such as NF-kB, TNF-, and IL-10 The decline in A42 and β-secretase 1 levels	Chen et al., 2006; Peng et al., 2006; Lei et al., 2015
Oxyresveratrol	*M. alba*	Moraceae	Reduce the release of NO from LPS-stimulated macrophages by decreasing the expression of the iNOS protein. TNF-, IL-1B, and IL-6 gene expression suppression	Chen et al., 1997; Woodruff-Pak et al., 2001
Rosmarinic acid	*Melissa officinalis*	Lamiaceae	By phosphorylating the ERK1/2 signaling pathway, increases cholinergic activity during cell differentiation. Interferes with fibrillization and β sheets	Gan et al., 2015; Wang et al., 2016
Quinic acid	*Pimpinella brachycarpa*	Apiaceae	Inhibits the production of a variety of inflammatory mediators in activated BV-2 microglial cell lines in response to LPS Protects SH-SY5Y cells against H2O2-induced harm through the activation of a variety of antioxidant enzymes	Raza et al., 2013; Sawda et al., 2017
Apigenin	*Passiflora edulis*	Passifloraceae	Apart from in PC 12 cells, inhibiting the synthesis of NO and PGE2. Reduced cytokine and NO oxide production	Chen et al., 2019
α -Mangostin	*Garcinia mangostana*	Clusiaceae	Prevent Aβ plaques from aggregating. Suppresses the β -secretase and – γ secretase enzymes, hence decreasing the synthesis of A.	Niidome et al., 2007
6-Shogaol	*Zingiber officinale*	Zingiberaceae	Increases NGF and pre- and postsynaptic proteins levels in the hippocampus COX-2, MAPK, and NF-KB repression	Wang C.P. et al., 2014; Moon et al., 2014
Epigallocatechin-3-Gallate (EGCG)	*Citrus sinensis*	Rutaceae	Blocking MAPK and NF-kB activation. Inhibit LPS-induced microglial activation	Bayat et al., 2012
Ginkgolide B	*Ginko biloba*	Ginkgoaceae	Inhibits pro-apoptotic protein expression and promotes NO production. Protective effect against neurotoxicity caused by reactive oxygen species	Yoo and Park, 2012
Ginsenoside Rg3	*Panax pseudoginseng*	Araliaceae	Reduced Aβ levels in the brains of mice with Alzheimer's disease Suppressing the activation of the neurofibrillary tyrosine kinase (NF-kB)	Lee et al., 2013; Cornejo et al., 2017
Prosapogenin III	*Liriope platyphylla*	Asparagaceae	MAPK/NF-κB signaling inhibition. Phosphorylation of p38 is inhibited in response to H2O2-induced stress.	Soh et al., 2003
Diosgenin	*Dioscorea villosa*	Dioscoreaceae	Rectification of axonal degeneration. Enhancing memory deficits in the 5XFAD mouse model of Alzheimer's disease COX-2, TNF-, and NF-κBp65 inhibition	Nikbakht et al., 2019

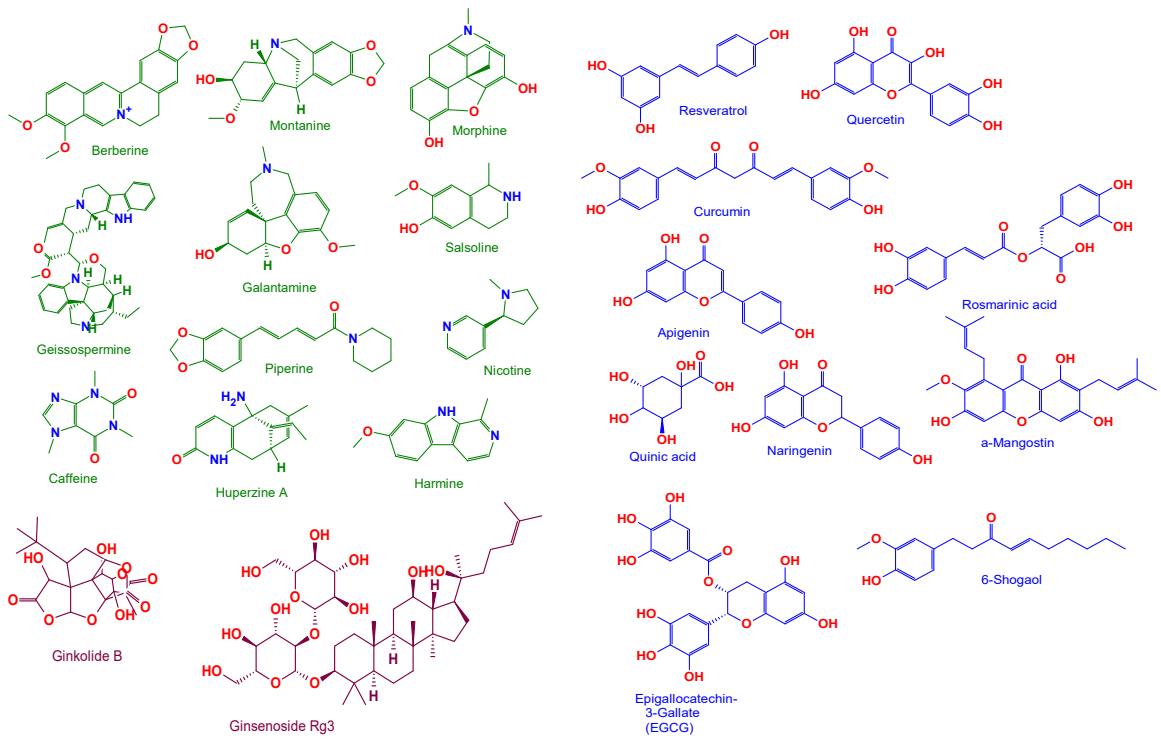

FIGURE 5 | Anti-AD chemical compounds from medicinal plants. Berberine, Curcumin, Huperzine-A, Tetrandrine, Galantamine, Glaucocalyxin B, Oridonin, Quercetin, Curcumin, Naringenin, Resveratrol, Oxyresveratrol, Rosmarinic acid, Quinic acid, Apigenin, α-Mangostin, 6-Shogaol, Epigallocatechin-3-Gallate (EGCG), Ginkgolide B, Ginsenoside Rg3, Prosapogenin III and Diosgenin. Structures are obtained from the free chemical structure database (www.chemspider.com). For more details about their chemical properties see PubChem (http://pubchem.ncbi.nlm.nih.gov/).

improvement in cognition and memory. In this study, it was found that the methanolic extract of *N. jatamansi* has a neuroprotective effect (Sundaramoorthy and Packiam, 2020). A Drosophila AD model was used to test the ethanolic extract of *N. jatamansi* against amyloid toxicity *in vitro* and *in vivo* study. In SH-SY5Y cells, the extract of this plant decreased amyloid-induced cell death, reduced glial cell populations, reduced ROS levels, and suppressed A42-induced cell death. According to these findings, *N. jatamansi* could be an important plant in the treatment of Alzheimer's disease (Alama and Haque, 2011).

Coriandrum sativum

The Apiaceae family includes *Coriandrum sativum* L., which is popularly known as dhanya (Raut et al., 2015). Flavonoids like quercetin 3-glucoronide and polyphenolics such as protocatechuic acid, glycitin, and caffeic acid are among the most abundant phytochemicals present in *C. sativum*. The flavonoid content in seeds was reported to be 12.6 quercetin equivalents/kg, and the polyphenolic content to be 12.2 gallic acid equivalents/kg (Raut et al., 2015). The *C. sativum* extract increased total protein concentration and CAT, SOD, and GSH enzyme levels in the experimental rat, as well as reducing the amount of brain infarct, calcium levels, and lipid peroxidation (LPO). *C. sativum* leaves were also found to reduce scopolamine and diazepam-induced memory impairments (Rubio et al., 2011). Also, the leaves have antioxidant properties. They can scavenge free radicals like DPPH, and they can stop lipoxygenase and phospholipid peroxidation, which helps to improve memory.

Cissampelos pareira

In mice, the hydroalcoholic extract of C. *pareira* was tested for learning and memory boosting activities against aging and scopolamine-induced amnesia at three distinct doses of 100, 200, and 400 mg/kg administered orally. The activity of acetylcholinesterase was reduced by these extracts. Due to its antioxidant and anti-inflammatory effect, a dose of 400 mg/kg (p.o.) demonstrated a more significant improvement in learning and memory-enhancing activity. Therefore, *C. pareira* may have an important role in Alzheimer's disease management, according to the findings (Joshi and Parle, 2006). **Table 2** summarizes the medicinal plants having anti-Alzheimer's disease properties.

NEUROPROTECTIVE BIOMOLECULES: POSSIBLE ROLE AGAINST ALZHEIMER'S DISEASES

As discussed earlier a number of plant-derived or natural bioactive phytocompounds like phenols, alkaloids, strolls,

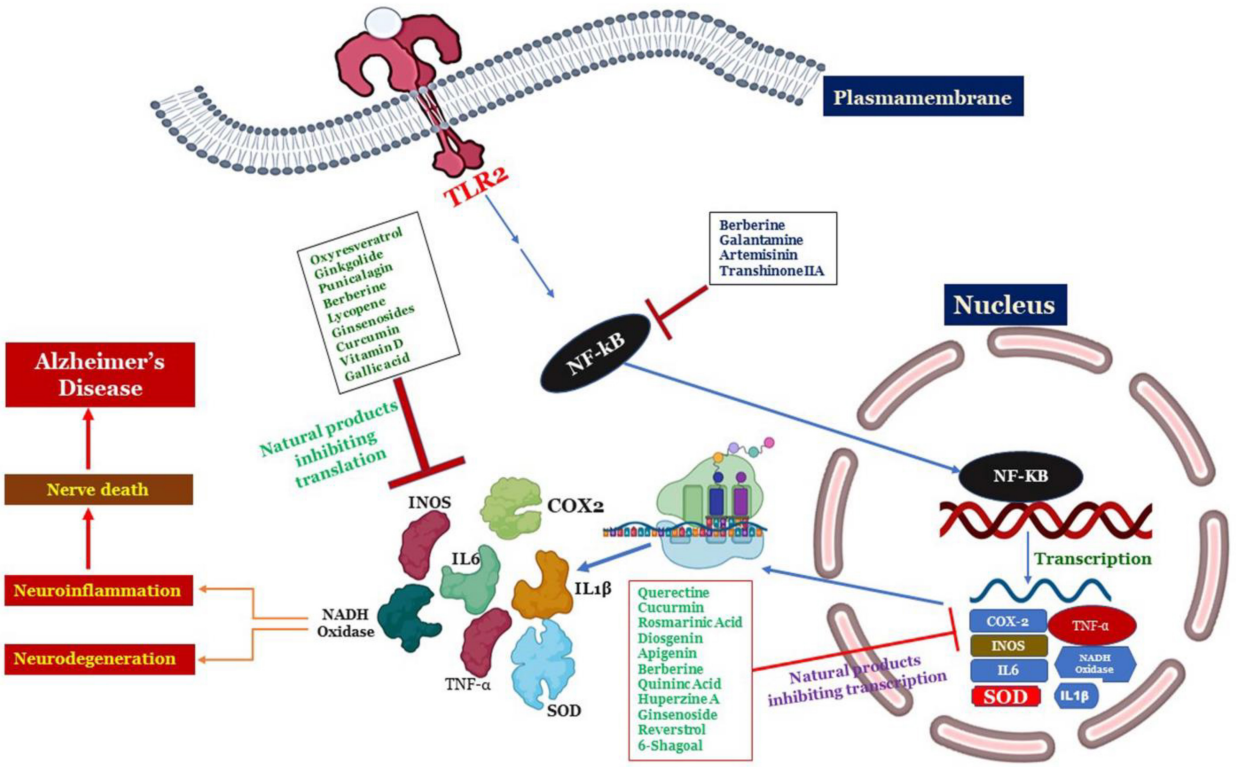

FIGURE 6 | Schematics showing the activation of signaling pathways responsible for clinical features of AD through TLR signaling cascades largely governed by NK-KB resulting in the neuroinflammation and nerve degeneration. On the other hand the novel intervention of natural products such as Diosgenin, Prosapogenin III, Quercetin, Apigenin, Ginsenoside Rg3, Rosmarinic acid, Ginkgolide B, Limonoid, Quinic acid, Curcumin, Resveratrol, Berberine, 6- Shagoal, Ligraminol E4-O-β-d-xyloside, Huperzine A, Sophocarpidine, Naringenin, Epigallocatechin-3-galate (EGCG), Oxyresveratrol, α-Mangostin, Galantamine are shown to inhibit this signaling cascade at the junction of NK-KB, and then inhibition of transcription as well as translation of proteins responsible for neuroinflammation.

carotenoids, flavonoids, etc., have cytoprotective, neuroprotective properties due to their antioxidant, anti-inflammatory, anti-apoptotic, properties. Origins and chemical structures of discussed phytochemicals were shown in **Table 3** and **Figure 5** and the mechanism of phytochemicals against AD is depicted in **Figure 6**.

ALKALOIDS

Besides intervening as muscarinic receptor agonists, anti-oxidants, anti-amyloid inhibitors, AChE and BuChE inhibitors, α-synuclein agglomeration inhibitors, dopaminergic and nicotine agonists, alkaloids help to alleviate the pathophysiology of AD (Rahman and Muralidharan, 2010).

Alkaloids have a broad spectrum of therapeutic potency in biomedicine, including analgesics (e.g., morphine), anti-diabetic (e.g., piperine), anti-tumor (e.g., berberine), and anti-microbial effects (e.g., berberine) (e.g., ciprofloxacin). Certain alkaloids have both stimulating and neuropsychiatric effects on the central nervous system (e.g., cocaine, caffeine, and nicotine) (e.g., psilocin). Despite the fact that alkaloids have a strong tradition and a wide range of properties, few are presented as functional and efficient medicines. They have a wide range of protective effects in conditions like seizures, psychiatric problems, cerebral ischemia, Alzheimer and memory lapses, anxiety, stress, and many more. Alkaloids suppress the establishment of neurodegenerative disorders by multiple mechanisms, including blocking the AChE, boosting GABA levels, and acting as NMDA antagonists (Rahman and Muralidharan, 2010; Liu et al., 2018).

TERPENOIDS

Multiple research and clinical trials have validated that essential oils have positive benefits in AD patients. Plant essential oils and specific terpenes have been demonstrated to have antioxidant and AChEIs properties (Asgarpanah and Kazemivash, 2012). Effective anti-AD compounds include terpenoids such as ginsenosides, ginkgolides, and cannabinoids. Ginsenoside Rg3 (minimizes Aβ production by 84 percent in CHO-2B7 cells and by 31 percent in Tg2576) transgenic mice (Kulkarni et al., 2011; Avneet et al., 2018). Ginsenoside Rg3 lowers Aβ concentration by boosting Aβ breakdown and by increasing the production of neprilysin, a rate-limiting enzyme in Aβ degradation. PC12 cells are protected from Aβ-induced neurotoxic effects by ginsenoside Re. Moreover, ginsenoside Rb1 reduces neuroinflammatory

biomarkers in the hippocampal cells, by reversing Aβ-induced cognitive impairment in mice. By boosting synapse plasticity in the brain, ginsenoside Rb1 has a positive influence on spatial working memory (Ng et al., 2015; Lima and Hamerski, 2019). Ginkgolides is a labdane-form of cyclic diterpenes that are often extracted from *Ginkgo biloba*. Ginkgolide A and B therapy preserves nerve cells from synaptic injury as measured by synaptophysin loss, a presynaptic synaptic indicator, and enhances nerve cell survival despite A-induced toxicity. Ginkgolide B protects hippocampus nerve cells against Aβ-directed cell death by boosting the synthesis of brain-derived neurotrophic factors and by reducing nerve cell apoptosis in hemorrhaging rat brain cells (Yoo and Park, 2012).

PHENOLS

Resveratrol is proven to suppress the expression of pro-inflammatory molecules such as NF-kB and TNF-α in glial cells, while also increasing the amount of the anti-inflammatory cytokine IL-10, which is linked to Alzheimer's diseases. Resveratrol improves spatial cognitive performance in Alzheimer's disease rats via increasing anti-oxidant function. Resveratrol aids in the expression of SIRT1, which increases the preservation of nerve cells against ROS, free radicals, and Aβ -generated inflammation of the nerve cells (Chen et al., 2006; Awasthi et al., 2018). Oxyresveratrol, a compound derived from the *Morus alba* tree, reduces the production of the iNOS molecule in LPS- mediated macrophages, hence inhibiting the NO generation. Moreover, Oxyresveratrol has neuroprotective properties against Aβ protein-mediated neurotoxic effects in the cortical nerve cells, and anti-inflammatory and anti-apoptotic properties by lowering TNF-α, IL-1β, and IL-6 secretion and inhibiting caspase-1 and NF-kB expression (Chen et al., 2006). For its antioxidant capacity, ROS (OH, superoxide anions) scavenging effects, transversal BBB quercetin has been shown to have neuroprotective properties. Quercetin's neuroprotective properties are mostly demonstrated through the dysregulation of cytokines via (MAPK) signaling pathways and p13K/Akt networks. Quercetin is also documented for inhibiting the LOX and COX proteases, which are related to the process of eicosanoids and the induction of NF-kB (Wang et al., 2011).

CONCLUSION AND FUTURE PERSPECTIVES

Alzheimer's is a complex, slow-progressing neurological illness. Even though AD associated pathologies are not greatly explored, current findings approved several factors responsible for its clinical manifestations. Multiple treatment strategies are explored at different stages as potential medication therapeutic interventions to successfully combat and control AD. FDA anti-AD medications deliver symptomatic treatment but have their drawbacks and side effects like nausea, vomiting, dizziness, headache, loss of appetite, loss of weight, diarrhea, etc. As a result, innovative alternate treatment techniques utilizing herbal medications to address AD is needed. Proper intervention in accordance with diseases progression ameliorates disease management. The irreversible damage to the brain cells and involuted pathophysiological, events associated with AD have always emphasized the need for the development of novel drugs and therapeutics, which render better outcomes with fewer or no side effects. Natural compounds and their bioactive phytochemicals have been shown to have significant neuroprotective potential in the treatment and management of AD, with limited negative side effects. Significant pharmacological properties like neuroprotective, anti-oxidant, anti-inflammatory, anti-apoptotic, etc., demonstrated by phytonutrients like tannins, alkaloids, phenols, carotenoids can be inspected to devise potential drugs. The degenerative pathway connected with Alzheimer's disease is thought to be complex, despite the fact that it is not entirely comprehended. For the diagnosis and intervention of AD, neuroprotective treatments encompassing several molecular pathways are crucial. In the development of anti-AD drugs, organic product combinations or preparations containing several active pharmacological ingredients having the potential to execute diverse neuroprotective pathways and restorative mechanisms are sought. Green therapy could play a significant role in precluding AD and in devising therapeutics for symptom and disease management with the establishment of QA (Quality Assurance) and QC (Quality Control) guidelines to ensure the development of a safe and effective novel neuroprotective drugs. Our review strongly backs up use of medicinal plants and phytoconstituents alone or in combination with other compounds for effective treatments against Alzheimer's disease with lesser side effects as compared to currently available treatments.

AUTHOR CONTRIBUTIONS

MM designed and supervised the study, and made a substantial contribution to the concept of study, and revision of the manuscript thoroughly. BB and AA equally contributed to this work in the analysis and writing of the manuscript. MM, BB, RM, WM, FA, and BA performed interpretation, drew the figures and tables, and critical review and drafting of the manuscript. All authors listed have made a substantial, direct, and intellectual contribution to the work, and read and approved the final manuscript.

FUNDING

This work was funded by the JK Science Technology and Innovation Council DST India with Grant No. JKST&IC/SRE/885-87 to MM.

SUPPLEMENTARY MATERIAL

The Supplementary Material for this article can be found online at: https://www.frontiersin.org/articles/10.3389/fnins.2022.884345/full#supplementary-material

REFERENCES

Abdul Manap, A. S., Vijayabalan, S., Madhavan, P., Chia, Y. Y., Arya, A., Wong, E. H., et al. (2019). "Bacopa monnieri, a neuroprotective lead in Alzheimer disease: a review on its properties, mechanisms of action, and preclinical and clinical studies". *Drug Target Insights* 13:1177392819866412. doi: 10.1177/1177392819866412

Abeysinghe, A., Deshapriya, R., and Udawatte, C. (2020). "Alzheimer's disease; a review of the pathophysiological basis and therapeutic interventions". *Life Sci.* 256:117996.

Ahmed, F., Chandra, J. N. N. S., and Manjunath, S. (2011). Acetylcholine and memory-enhancing activity of Ficus racemosa bark. *Pharmacogn. Res.* 3, 246–249. doi: 10.4103/0974-8490.89744

Ahmed, O. M. (2021). "Tinospora cordifolia" in *Naturally Occurring Chemicals Against Alzheimer's Disease*, eds T. Belwal, S. M. Nabavi, S. F. Nabavi, A. R. Dehpour, and S. Shirooie Amsterdam. Elsevier, 351–358. doi: 10.1016/B978-0-12-819212-2.00029-3

Alama, B., and Haque, E. (2011). Anti-alzheimer and antioxidant activity of Celastrus paniculatus seed. *Iran J. Pharmace. Sci.* 7, 49–56. doi: 10.1515/jcim-2021-0251

Alghamdi, B. S. A. (2018). Possible prophylactic anti-excitotoxic and anti-oxidant effects of virgin coconut oil on aluminium chloride-induced Alzheimer's in rat models. *J. Integrat. Neurosci.* 17, 593–607. doi: 10.3233/JIN-180089

Ambegaokar, S. S., Wu, L., Alamshahi, K., Lau, J., Jazayeri, L., Chan, S., et al. (2003). Curcumin inhibits dose-dependently and time-dependently neuroglial cell proliferation and growth,". *Neuroendocrinol. Lett.* 24, 469–469.

Anand, R., Gill, K. D., and Mahdi, A. A. (2014). "Therapeutics of Alzheimer's disease: past, present and future. *Neuropharmacology* 76, 27–50. doi: 10.1016/j.neuropharm.2013.07.004

Andres-Lacueva, C., Shukitt-Hale, B., Galli, R. L., Jauregui, O., Lamuela-Raventos, R. M., and Joseph, J. A. (2005). Anthocyanins in aged blueberry-fed rats are found centrally and may enhance memory. *Nutr. Neurosci.* 8, 111–120. doi: 10.1080/10284150500078117

Arnsten, A. F. T., Datta, D., Del Tredici, K., and Braak, H. (2021). Hypothesis: Tau pathology is an initiating factor in sporadic Alzheimer's disease. *Alzheimer's Dement.* 17, 115–124. doi: 10.1002/alz.12192

Asgarpanah, J., and Kazemivash, N. (2012). Phytochemistry, pharmacology and medicinal properties of Coriandrum sativum L. *Africa. J. Pharm. Pharmacol.* 6, 2340–2345.

Atlante, A., Amadoro, G., Bobba, A., and Latina, V. (2020). Functional foods: an approach to modulate molecular mechanisms of Alzheimer's disease. *Cells* 9:2347. doi: 10.3390/cells9112347

Auld, D. S., Kornecook, T. J., Bastianetto, S., and Quirion, R. (2002). Alzheimer's disease and the basal forebrain cholinergic system: relations to β-amyloid peptides, cognition, and treatment strategies. *Prog. Neurobiol.* 68, 209–245. doi: 10.1016/s0301-0082(02)00079-5

Avneet, G., Pal, S. M., and Siddhraj, S. S. (2018). A review on herbal Ayurvedic medicinal plants and its association with memory functions,". *J. Phytopharmacol.* 7, 162–166. doi: 10.2174/187221411794351833

Awasthi, M., Upadhyay, A. K., Singh, S., Pandey, V. P., and Dwivedi, U. N. (2018). Terpenoids as promising therapeutic molecules against Alzheimer's disease: amyloid beta-and acetylcholinesterase-directed pharmacokinetic and molecular docking analyses. *Mol. Simulat.* 44, 1–11. doi: 10.1080/08927022.2017.1334880

Bai, Y.-F., and Xu, H. (2000). Protective action of piperine against experimental gastric ulcer. *Acta Pharmacol. Sin.* 21, 357–359.

Bano, G., Amla, V., Raina, R. K., Zutshi, U., and Chopra, C. L. (1987). The effect of piperine on pharmacokinetics of phenytoin in healthy volunteers. *Plant. Med.* 53, 568–569. doi: 10.1055/s-2006-962814

Barage, S. H., and Sonawane, K. D. (2015). Amyloid cascade hypothesis: Pathogenesis and therapeutic strategies in Alzheimer's disease. *Neuropeptides* 52, 1–18. doi: 10.1016/j.npep.2015.06.008

Barthélemy, N. R., Mallipeddi, N., Moiseyev, P., Sato, C., and Bateman, R. J. (2019). Tau phosphorylation rates measured by mass spectrometry differ in the intracellular brain vs. extracellular cerebrospinal fluid compartments and are differentially affected by Alzheimer's disease. *Front. Aging Neurosci.* 11:121. doi: 10.3389/fnagi.2019.00121

Bayat, M., Azami Tameh, A., Hossein Ghahremani, M., Akbari, M., Mehr, S. E., Khanavi, M., et al. (2012). Neuroprotective properties of Melissa officinalis after hypoxic-ischemic injury both in vitro and in vivo,". *DARU J. Pharmace. Sci.* 20:42. doi: 10.1186/2008-2231-20-42

Bennett, R. E., DeVos, S. L., Dujardin, S., Corjuc, B., Gor, R., Gonzalez, J., et al. (2017). Enhanced tau aggregation in the presence of amyloid β,". *Am. J. Pathol.* 187, 1601–1612. doi: 10.1016/j.ajpath.2017.03.011

Bhat, A., Mahalakshmi, A. M., Ray, B., Tuladhar, S., Hediyal, T. A., Manthiannem, E., et al. (2019). "Benefits of curcumin in brain disorders,". *BioFactors* 45, 666–689. doi: 10.1002/biof.1533

Bhat, B. A., Mir, W. R., Sheikh, B. A., Rather, M. A., Dar, T. U. H., and Mir, M. A. (2022). In vitro and in silico evaluation of antimicrobial properties of Delphinium cashmerianum L., a medicinal herb growing in Kashmir, India. *J. Ethnopharmacol.* 291:115046. doi: 10.1016/j.jep.2022.115046

Bhat, B. A., Nisar, S., Sheikh, B. A., Mir, W. R., and Mir, M. A. (2021). *Antioxidants (Natural and Synthetic) Screening Assays: An Overview," Bentham Briefs in Biomedicine and Pharmacotherapy Oxidative Stress and Natural Antioxidants*. Sharjah: Bentham Science Publishers, 105–126.

Bloom, G. S. (2014). Amyloid-β and tau: the trigger and bullet in Alzheimer disease pathogenesis. *JAMA Neurol.* 71, 505–508. doi: 10.1001/jamaneurol.2013.5847

Bowen, D. M., Smith, C. B., White, P., and Davison, A. N. (1976). Neurotransmitter-related enzymes and indices of hypoxia in senile dementia and other abiotrophies. *Brain* 99, 459–496. doi: 10.1093/brain/99.3.459

Calcul, L., Zhang, B., Jinwal, U. K., Dickey, C. A., and Baker, B. J. (2012). Natural products as a rich source of tau-targeting drugs for Alzheimer's disease. *Fut. Med. Chem.* 4, 1751–1761. doi: 10.4155/fmc.12.124

Calsolaro, V., and Edison, P. (2016). , "Neuroinflammation in Alzheimer's disease: current evidence and future directions. *Alzheimers Dement* 12, 719–732. doi: 10.1016/j.jalz.2016.02.010

Casadesus, G., Shukitt-Hale, B., Stellwagen, H. M., Zhu, X., Lee, H.-G., Smith, M. A., et al. (2004). "Modulation of hippocampal plasticity and cognitive behavior by short-term blueberry supplementation in aged rats,". *Nutr. Neurosci.* 7, 309–316. doi: 10.1080/10284150400020482

Chainoglou, E., and Hadjipavlou-Litina, D. (2020). Curcumin in health and diseases: Alzheimer's disease and curcumin analogues, derivatives, and hybrids. *Int. J. Mol. Sci.* 21:1975. doi: 10.3390/ijms21061975

Chan, A., and Shea, T. B. (2006). Supplementation with apple juice attenuates presenilin-1 overexpression during dietary and genetically-induced oxidative stress. *J. Alzheimer's Dis.* 10, 353–358. doi: 10.3233/jad-2006-10401

Chatterjee, P., Fernando, M., Fernando, B., Dias, C. B., Shah, T., Silva, R., et al. (2020). Potential of coconut oil and medium chain triglycerides in the prevention and treatment of Alzheimer's disease. *Mechan. Ageing Dev.* 186:111209. doi: 10.1016/j.mad.2020.111209

Chauhan, N. B., and Sandoval, J. (2007). Amelioration of early cognitive deficits by aged garlic extract in Alzheimer's transgenic mice. *Phytother. Res.* 21, 629–640. doi: 10.1002/ptr.2122

Chauhan, N., Wang, K. C., Wegiel, J., and Malik, M. N. (2004). Walnut extract inhibits the fibrillization of amyloid beta-protein, and also defibrillizes its preformed fibrils. *Curr. Alzheimer Res.* 1, 183–188. doi: 10.2174/1567205043332144

Chen, C., Mohamad Razali, U. H., Saikim, F. H., Mahyudin, A., and Mohd Noor, N. Q. I. (2021). Morus alba L. Plant: Bioactive Compounds and Potential as a Functional Food Ingredient. *Foods* 10:689. doi: 10.3390/foods10030689

Chen, F., Eckman, E. A., and Eckman, C. B. (2006). Reductions in levels of the Alzheimer's amyloid beta peptide after oral administration of ginsenosides. *FASEB J.* 20, 1269–1271. doi: 10.1096/fj.05-5530fje

Chen, F., Sun, S., Kuhn, D. C., Lu, Y., Gaydos, L. J., Shi, X., et al. (1997). "Tetrandrine inhibits signal-induced NF-κB activation in rat alveolar macrophages,". *Biochem. Biophys. Res. Commun.* 231, 99–102. doi: 10.1006/bbrc.1997.6057

Chen, X., Drew, J., Berney, W., and Lei, W. (2021). Neuroprotective Natural Products for Alzheimer's Disease. *Cells* 10:1309. doi: 10.3390/cells10061309

Chen, Y., Shi, G. W., Liang, Z. M., Sheng, S. Y., Shi, Y. S., Peng, L., et al. (2019). Resveratrol improves cognition and decreases amyloid plaque formation in Tg6799 mice. *Mol. Med. Rep.* 19, 3783–3790. doi: 10.3892/mmr.2019.10010

Chen, Z., and Zhong, C. (2014). Oxidative stress in Alzheimer's disease. *Neurosci. Bull.* 30, 271–281.

Choi, B. W., Ryu, G., Park, S. H., Kim, E. S., Shin, J., Roh, S. S., et al. (2007). Anticholinesterase activity of plastoquinones from Sargassum sagamianum: lead compounds for Alzheimer's disease therapy. *Phytother. Res.* 21, 423–426. doi: 10.1002/ptr.2090

Choi, S. J., Lee, J.-H., Heo, H. J., Cho, H. Y., Kim, H. K., Kim, C.-J., et al. (2011). Punica granatum protects against oxidative stress in PC12 cells and oxidative stress-induced Alzheimer's symptoms in mice. *J. Med. Food* 14, 695–701. doi: 10.1089/jmf.2010.1452

Chowdhury, S., and Kumar, S. (2020). Alpha-terpinyl acetate: A natural monoterpenoid from Elettaria cardamomum as multi-target directed ligand in Alzheimer's disease. *J. Fun. Foods* 68:103892. doi: 10.1016/j.jff.2020.103892

Cornejo, A., Aguilar Sandoval, F., Caballero, L., Machuca, L., Muñoz, P., Caballero, J., et al. (2017). Rosmarinic acid prevents fibrillization and diminishes vibrational modes associated to β sheet in tau protein linked to Alzheimer's disease. *J. Enzyme Inhibit. Med. Chem.* 32, 945–953. doi: 10.1080/14756366.2017.1347783

Cuong, T. D., Hung, T. M., Han, H. Y., Sik Roh, H., Seok, J.-H., Lee, J. K., et al. (2014). Potent acetylcholinesterase inhibitory compounds from Myristica fragrans. *Nat. Prod. Commun.* 9, 499–502.

Dajas, F. (2012). Life or death: neuroprotective and anticancer effects of quercetin. *J. Ethnopharmacol.* 143, 383–396. doi: 10.1016/j.jep.2012.07.005

Desai, S. K., Pandey, C. H., and Mulgaonkar, S. S. (2012). Memory-strengthening activity of aqueous liquorice extractand glabridin extract inbehavioral models. *Int. J. Pharm. Sci. Rev. Res.* 16, 120–124.

Dey, A., Bhattacharya, R., Mukherjee, A., and Pandey, D. K. (2017). Natural products against Alzheimer's disease: Pharmaco-therapeutics and biotechnological interventions. *Biotechnol. Adv.* 35, 178–216. doi: 10.1016/j.biotechadv.2016.12.005

D'Hooge, R., Pei, Y. Q., Raes, A., Lebrun, P., Van Bogaert, P. P., and De Deyn, P. P. (1996). Anticonvulsant activity of piperine on seizures induced by excitatory amino acid receptor agonists. *Arzneimittel-Forschung* 46, 557–560.

Dragicevic, N., Smith, A., Lin, X., Yuan, F., Copes, N., Delic, V., et al. (2011). Green tea epigallocatechin-3-gallate (EGCG) and other flavonoids reduce Alzheimer's amyloid-induced mitochondrial dysfunction. *J. Alzheimer's Dis.* 26, 507–521. doi: 10.3233/JAD-2011-101629

Durairajan, S. S. K., Yuan, Q., Xie, L., Chan, W.-S., Kum, W.-F., Koo, I., et al. (2008). Salvianolic acid B inhibits Aβ fibril formation and disaggregates preformed fibrils and protects against Aβ-induced cytotoxicty,". *Neurochem. Int.* 52, 741–750. doi: 10.1016/j.neuint.2007.09.006

Essa, M. M., Vijayan, R. K., Castellano-Gonzalez, G., Memon, M. A., Braidy, N., and Guillemin, G. J. (2012). Neuroprotective effect of natural products against Alzheimer's disease. *Neurochem. Res.* 37, 1829–1842. doi: 10.1007/s11064-012-0799-9

Fatima, F., Rizvi, D. A., Abidi, A., Ahmad, A., Shukla, P., Qadeer, F., et al. (2017). A study of the neuroprotective role of Punica granatum and rosuvastatin in scopolamine induced cognitive deficit in rats. *Int. J. Basic Clin. Pharmacol.* 6, 2319–2003.

Ferreira, S. T., Lourenco, M. V., Oliveira, M. M., and De Felice, F. G. (2015). Soluble amyloid-b oligomers as synaptotoxins leading to cognitive impairment in Alzheimer's disease. *Front. Cell. Neurosci.* 9:191. doi: 10.3389/fncel.2015.00191

Finley, J. W., and Gao, S. (2017). A perspective on Crocus sativus L.(Saffron) constituent crocin: a potent water-soluble antioxidant and potential therapy for Alzheimer's disease. *J. Agric. Food Chem.* 65, 1005–1020. doi: 10.1021/acs.jafc.6b04398

Freyssin, A., Page, G., Fauconneau, B., and Bilan, A. R. (2020). Natural stilbenes effects in animal models of Alzheimer's disease. *Neural Regen. Res.* 15, 843–849. doi: 10.4103/1673-5374.268970

Frydman-Marom, A., Levin, A., Farfara, D., Benromano, T., Scherzer-Attali, R., Peled, S., et al. (2011). Orally administrated cinnamon extract reduces β-amyloid oligomerization and corrects cognitive impairment in Alzheimer's disease animal models. *PLoS One* 6:e16564. doi: 10.1371/journal.pone.0016564

Fu, H., Rodriguez, G. A., Herman, M., Emrani, S., Nahmani, E., Barrett, G., et al. (2017). Tau pathology induces excitatory neuron loss, grid cell dysfunction, and spatial memory deficits reminiscent of early Alzheimer's disease. *Neuron* 93, 533–541. doi: 10.1016/j.neuron.2016.12.023

Fujiwara, H., Iwasaki, K., Furukawa, K., Seki, T., He, M., Maruyama, M., et al. (2006). Uncaria rhynchophylla, a Chinese medicinal herb, has potent antiaggregation effects on Alzheimer's β-amyloid proteins. *J. Neurosci. Res.* 84, 427–433. doi: 10.1002/jnr.20891

Fujiwara, H., Tabuchi, M., Yamaguchi, T., Iwasaki, K., Furukawa, K., Sekiguchi, K., et al. (2009). "A traditional medicinal herb Paeonia suffruticosa and its active constituent 1, 2, 3, 4, 6-penta-O-galloyl-β-d-glucopyranose have potent anti-aggregation effects on Alzheimer's amyloid β proteins in vitro and in vivo. *J. Neurochem.* 109, 1648–1657. doi: 10.1111/j.1471-4159.2009.06069.x

Gallardo, G., and Holtzman, D. M. (2019). Amyloid-β and Tau at the Crossroads of Alzheimer's Disease. *Adv. Exp. Med. Biol.* 1184, 187–203. doi: 10.1007/978-981-32-9358-8_16

Gan, P., Zhang, L., Chen, Y., Zhang, Y., Zhang, F., Zhou, X., et al. (2015). Anti-inflammatory effects of glaucocalyxin B in microglia cells. *J. Pharmacol. Sci.* 128, 35–46. doi: 10.1016/j.jphs.2015.04.005

Garriga, M., Milà, M., Mir, M., Al-Baradie, R., Huertas, S., and Castejon, C., et al. (2015). "123I-FP-CIT SPECT imaging in early diagnosis of dementia in patients with and without a vascular component. *Front. Syst. Neurosci.* 9:99. doi: 10.3389/fnsys.2015.00099

Golechha, M., Bhatia, J., and Singh Arya, D. (2012). Studies on effects of Emblica officinalis (Amla) on oxidative stress and cholinergic function in scopolamine induced amnesia in mice. *J. Environ. Biol.* 33, 95–100.

Gomaa, A. A., Makboul, R. M., El-Mokhtar, M. A., Abdel-Rahman, E. A., Ahmed, I. A., and Nicola, M. A. (2019). Terpenoid-rich Elettaria cardamomum extract prevents Alzheimer-like alterations induced in diabetic rats via inhibition of GSK3β activity, oxidative stress and pro-inflammatory cytokines. *Cytokine* 113, 405–416. doi: 10.1016/j.cyto.2018.10.017

Gomes, B. A. Q., Silva, J. P. B., Romeiro, C. F. R., Dos, Santos SM, Rodrigues, C. A., Gonçalves, P. R., et al. (2018). Neuroprotective mechanisms of resveratrol in Alzheimer's disease: role of SIRT1. *Oxid. Med. Cell. Long.* 2018:8152373. doi: 10.1155/2018/8152373

Graham, W. V., Bonito-Oliva, A., and Sakmar, T. P. (2017). Update on Alzheimer's disease therapy and prevention strategies. *Ann. Rev. Med.* 68, 413–430. doi: 10.1146/annurev-med-042915-103753

Grant, W. B. (2016). Using multicountry ecological and observational studies to determine dietary risk factors for Alzheimer's disease. *J. Am. College Nut.* 35, 476–489. doi: 10.1080/07315724.2016.1161566

Hampel, H., Mesulam, M. M., Cuello, A. C., Farlow, M. R., Giacobini, E., Grossberg, G. T., et al. (2018). The cholinergic system in the pathophysiology and treatment of Alzheimer's disease. *Brain* 141, 1917–1933. doi: 10.1093/brain/awy132

Hampel, H., Mesulam, M. M., Cuello, A. C., Khachaturian, A. S., Vergallo, A., Farlow, M. R., et al. (2019). Revisiting the cholinergic hypothesis in Alzheimer's disease: emerging evidence from translational and clinical research. *J. Prevent. Alzheimer's Dis.* 6, 2–15.

Hardy, J. A., and Higgins, G. A. (1992). Disease: Alzheimer's cascade hypothesis amyloid. *Sci. New Ser.* 256, 184–185.

Hase, T., Shishido, S., Yamamoto, S., Yamashita, R., Nukima, H., Taira, S., et al. (2019). "Rosmarinic acid suppresses Alzheimer's disease development by reducing amyloid β aggregation by increasing monoamine secretion. *Sci. Rep.* 9:8711. doi: 10.1038/s41598-019-45168-1

Hensley, K. (2010). Neuroinflammation in Alzheimer's disease: mechanisms, pathologic consequences, and potential for therapeutic manipulation. *J. Alzheimer's Dis.* 21, 1–14. doi: 10.3233/JAD-2010-1414

Hua, S., Wang, B., Chen, R., Zhang, Y., Zhang, Y., Li, T., et al. (2019). Neuroprotective effect of dichloromethane extraction from piper nigrum L. and piper longum L. on permanent focal cerebral ischemia injury in rats. *J. Stroke Cerebrovasc. Dis.* 28, 751–760. doi: 10.1016/j.jstrokecerebrovasdis.2018.11.018

Hunt, D. L., and Castillo, P. E. (2012). Synaptic plasticity of NMDA receptors: mechanisms and functional implications. *Curr. Opin. Neurobiol.* 22, 496–508. doi: 10.1016/j.conb.2012.01.007

Hussain, S. Z., Naseer, B., Qadri, T., Fatima, T., and Bhat, T. A. (2021). "Walnut (Juglans Regia)-Morphology, Taxonomy, Composition and Health Benefits," in *Fruits Grown in Highland Regions of the Himalayas*, eds S. Z. Hussain, B. Naseer, T. Qadri, and T. Fatima (Cham: Springer), 269–281. doi: 10.1007/978-3-030-75502-7_21

Ichwan, M., Walker, T. L., Nicola, Z., Ludwig-Müller, J., Böttcher, C., Overall, R. W., et al. (2021). "Apple peel and flesh contain pro-neurogenic compounds. *Stem Cell Rep.* 16, 548–565. doi: 10.1016/j.stemcr.2021.01.005

Ide, K., Matsuoka, N., Yamada, H., Furushima, D., and Kawakami, K. (2018). Effects of tea catechins on Alzheimer's disease: Recent updates and perspectives. *Molecules* 23:2357. doi: 10.3390/molecules23092357

Iuvone, T., De Filippis, D., Esposito, G., D'Amico, A., and Izzo, A. A. (2006). The spice sage and its active ingredient rosmarinic acid protect PC12 cells from amyloid-β peptide-induced neurotoxicity. *J. Pharmacol. Exp. Ther.* 317, 1143–1149. doi: 10.1124/jpet.105.099317

Jakob-Roetne, R., and Jacobsen, H. (2009). , "Alzheimer's disease: from pathology to therapeutic approaches. *Angewandte Chemie Int. Ed.* 48, 3030–3059. doi: 10.1002/anie.200802808

Jayaprakasam, B., Padmanabhan, K., and Nair, M. G. (2010). Withanamides in Withania somnifera fruit protect PC-12 cells from β-amyloid responsible for Alzheimer's disease. *Phytother. Res.* 24, 859–863. doi: 10.1002/ptr.3033

Jia, L., Liu, J., Song, Z., Pan, X., Chen, L., Cui, X., et al. (2012). Berberine suppresses amyloid-beta-induced inflammatory response in microglia by inhibiting nuclear factor-kappaB and mitogen-activated protein kinase signalling pathways. *J. Pharm. Pharmacol.* 64, 1510–1521. doi: 10.1111/j.2042-7158.2012.01529.x

Jiang, Y., Gao, H., and Turdu, G. (2017). Traditional Chinese medicinal herbs as potential AChE inhibitors for anti-Alzheimer's disease: a review. *Bioorgan. Chem.* 75, 50–61. doi: 10.1016/j.bioorg.2017.09.004

Joshi, H., and Parle, M. (2006). Nardostachys jatamansi improves learning and memory in mice. *J. Med. Food* 9, 113–118. doi: 10.1089/jmf.2006.9.113

Joshi, R., Reeta, K. H., Sharma, S. K., Tripathi, M., and Gupta, Y. K. (2015). Panchagavya Ghrita, an Ayurvedic formulation attenuates seizures, cognitive impairment and oxidative stress in pentylenetetrazole induced seizures in rats. *Indian J. Exp. Biol.* 53, 446–451.

Joshi, T., Singh, L., Jantwal, A., Durgapal, S., Upadhyay, J., Kumar, A., et al. (2021). "Zingiber officinale," in *Naturally Occurring Chemicals Against Alzheimer's Disease*, eds T. Belwal, S. Nabavi, S. Nabavi, A. Dehpour, and S. Shirooie Amsterdam. Elsevier, 481–494.

Justin Thenmozhi, A., Dhivyabharathi, M., William Raja, T. R., Manivasagam, T., and Essa, M. M. (2016). Tannoid principles of Emblica officinalis renovate cognitive deficits and attenuate amyloid pathologies against aluminum chloride induced rat model of Alzheimer's disease. *Nut. Neurosci.* 19, 269–278. doi: 10.1179/1476830515Y.0000000016

Kang, I.-J., Jeon, Y. E., Yin, X. F., Nam, J.-S., You, S. G., Hong, M. S., et al. (2011). Butanol extract of Ecklonia cava prevents production and aggregation of beta-amyloid, and reduces beta-amyloid mediated neuronal death. *Food Chem. Toxicol.* 49, 2252–2259. doi: 10.1016/j.fct.2011.06.023

Kappally, S., Shirwaikar, A., and Shirwaikar, A. (2015). Coconut oil–a review of potential applications. *Hygeia JD Med.* 7, 34–41.

Karran, E., Mercken, M., and De Strooper, B. (2011). The amyloid cascade hypothesis for Alzheimer's disease: an appraisal for the development of therapeutics. *Nat. Rev. Drug Dis.* 10, 698–712. doi: 10.1038/nrd3505

Kaur, P., Mehta, R. G., Thind, T. S., and Arora, S. (2021). *Bentham Briefs in Biomedicine and Pharmacotherapy Oxidative Stress and Natural Antioxidants*. Sharjah: Bentham Science Publishers.

Kennedy, D. O., and Wightman, E. L. (2011). "Herbal extracts and phytochemicals: plant secondary metabolites and the enhancement of human brain function. *Adv. Nutr.* 2, 32–50. doi: 10.3945/an.110.000117

Khan, A. U., Talucder, M. S. A., Das, M., Noreen, S., and Pane, Y. S. (2021). Prospect of The Black Pepper (Piper nigrum L.) as Natural Product Used to an Herbal Medicine. *Open Access Macedonian J. Med. Sci.* 9, 563–573. doi: 10.3889/oamjms.2021.7113

Kilimann, I., Grothe, M., Heinsen, H., Alho, E. J. L., Grinberg, L., Amaro, E. Jr., et al. (2014). "Subregional basal forebrain atrophy in Alzheimer's disease: a multicenter study. *J. Alzheimer's Dis.* 40, 687–700. doi: 10.3233/jad-132345

Kou, X., Li, B., Olayanju, J. B., Drake, J. M., and Chen, N. (2018). Nutraceutical or pharmacological potential of Moringa oleifera Lam. *Nutrients* 10:343. doi: 10.3390/nu10030343

Krikorian, R., Shidler, M. D., Nash, T. A., Kalt, W., Vinqvist-Tymchuk, M. R., Shukitt-Hale, B., et al. (2010). Blueberry supplementation improves memory in older adults. *J. Agric. Food Chem.* 58, 3996–4000. doi: 10.1021/jf9029332

Kulkarni, P. D., Ghaisas, M. M., Chivate, N. D., and Sankpal, P. S. (2011). Memory enhancing activity of Cissampelos pariera in mice. *Int. J. Pharm. Pharmaceut. Sci.* 3, 206–211.

Kumar, A., Prakash, A., and Dogra, S. (2011). *Centella asiatica* attenuates D-galactose-induced cognitive impairment, oxidative and mitochondrial dysfunction in mice. *Int. J. Alzheimer's Dis.* 2011:347569. doi: 10.4061/2011/347569

Kumar, S., and Kumari, R. (2021). Traditional, Phytochemical and Biological activities of Elettaria cardamomum (L.) Maton–A review. *Int. J. Pharmaceut. Sci. Res.* 12, 2320–5148.

Kumar, S., Maheshwari, K., and Singh, V. (2009). Protective effects of Punica granatum seeds extract against aging and scopolamine induced cognitive impairments in mice. *Africa. J. Trad. Complement. Alternat. Med.* 6, 49–56.

Kwak, H.-M., Jeon, S.-Y., Sohng, B.-H., Kim, J.-G., Lee, J.-M., Lee, K.-B., et al. (2005). "β-Secretase (BACE1) inhibitors from pomegranate (Punica granatum) husk,". *Arch. Pharmacal. Res.* 28, 1328–1332. doi: 10.1007/BF02977896

Lautie, E., Russo, O., Ducrot, P., and Boutin, J. A. (2020). Unraveling plant natural chemical diversity for drug discovery purposes. *Front. Pharmacol.* 11:397. doi: 10.3389/fphar.2020.00397

Lee, S. Y., Moon, E., Kim, S. Y., and Lee, K. R. (2013). Quinic acid derivatives from Pimpinella brachycarpa exert anti-neuroinflammatory activity in lipopolysaccharide-induced microglia. *Bioorgan. Med. Chem. Lett.* 23, 2140–2144. doi: 10.1016/j.bmcl.2013.01.115

Lee, S.-T., Chu, K., Sim, J.-Y., Heo, J.-H., and Kim, M. (2008). Panax ginseng enhances cognitive performance in Alzheimer disease. *Alzheimer Dis. Assoc. Dis.* 22, 222–226. doi: 10.1097/WAD.0b013e31816c92e6

Lee, Y. J., Choi, D. Y., Han, S. B., Kim, Y. H., Kim, K. H., Hwang, B. Y., et al. (2012). Inhibitory effect of ethanol extract of Magnolia officinalis on memory impairment and Amyloidogenesis in a transgenic mouse model of Alzheimer's disease via regulating β-secretase activity. *Phytother. Res.* 26, 1884–1892. doi: 10.1002/ptr.4643

Lei, Y., Yang, L., Ye, C. Y., Qin, M. Y., Yang, H. Y., Jiang, H. L., et al. (2015). Involvement of intracellular and mitochondrial Aβ in the ameliorative effects of huperzine A against oligomeric Aβ42-induced injury in primary rat neurons. *PLoS One* 10:e0128366. doi: 10.1371/journal.pone.0128366

Lima, J. A., and Hamerski, L. (2019). "Alkaloids as potential multi-target drugs to treat Alzheimer's disease. *Stud. Nat. Products Chem.* 61, 301–334. doi: 10.1016/b978-0-444-64183-0.00008-7

Lin, A. J., Koike, M. A., Green, K. N., Kim, J. G., Mazhar, A., Rice, T. B., et al. (2011). Spatial frequency domain imaging of intrinsic optical property contrast in a mouse model of Alzheimer's disease. *Ann. Biomed. Eng.* 39, 1349–1357. doi: 10.1007/s10439-011-0269-6

Liu, Q. F., Jeon, Y., Sung, Y.-W., Lee, J. H., Jeong, H., Kim, Y.-M., et al. (2018). Nardostachys jatamansi ethanol extract ameliorates Aβ42 cytotoxicity. *Biol. Pharmace. Bull.* 41, 470–477. doi: 10.1248/bpb.b17-00750

Luca, S. V., Gaweł-Bęben, K., Strzępek-Gomółka, M., Czech, K., Trifan, A., Zengin, G., et al. (2021). Insights into the phytochemical and multifunctional biological profile of spices from the genus Piper. *Antioxidants* 10:1642. doi: 10.3390/antiox10101642

Ma, X., Sun, Z., Han, X., Li, S., Jiang, X., Chen, S., et al. (2020). Neuroprotective effect of resveratrol via activation of Sirt1 signaling in a rat model of combined diabetes and Alzheimer's disease. *Front. Neurosci.* 13:1400. doi: 10.3389/fnins.2019.01400

Maccioni, R. B., Farías, G., Morales, I., and Navarrete, L. (2010). , "The revitalized tau hypothesis on Alzheimer's disease. *Arch. Med. Res.* 41, 226–231. doi: 10.1016/j.arcmed.2010.03.007

Mahaman, Y. A. R., Huang, F., Wu, M., Wang, Y., Wei, Z., Bao, J., et al. (2018). Moringa oleifera alleviates homocysteine-induced Alzheimer's disease-like pathology and cognitive impairments. *J. Alzheimer's Dis.* 63, 1141–1159. doi: 10.3233/JAD-180091

Majeed, M., Pirzadah, T. B., Mir, M. A., Hakeem, K. R., Alharby, H. F., Alsamadany, H., et al. (2021). "Comparative Study on Phytochemical Profile and Antioxidant Activity of an Epiphyte, Viscum album L.(White Berry Mistletoe), Derived from Different Host Trees,". *Plants* 10:1191. doi: 10.3390/plants10061191

Mandel, S. A., and Bh Youdim, M. (2012). In the rush for green gold: can green tea delay age-progressive brain neurodegeneration? *Recent Patents CNS Drug Discov.* 7, 205–217. doi: 10.2174/157488912803252005

Mani, V., and Parle, M. (2009). Memory-enhancing activity of Coriandrum sativum in rats. *Pharmacologyonline* 2, 827–839.

Mathew, M., and Subramanian, S. (2014). In vitro evaluation of anti-Alzheimer effects of dry ginger (Zingiber officinale Roscoe) extract. *Indian J. Exp. Biol.* 52, 606–612.

Mir, M. (2015). "Introduction to costimulation and costimulatory molecules". In *Developing Costimulatory Molecules for Immunotherapy of Diseases*. Cambridge, US: Academic Press. Vol. 1.

Mir, M. A. (2015). Natural herbs, human brain and neuroprotection. *Role Nat. Herbs Stroke Prevent. Treat.* 107.

Mir, M. A., and Agrewala, J. N. (2008). Dietary polyphenols in modulation of the immune system," Polyphenols and health: new and recent advances. *Nova Sci. Publish.* 23, 245–272. doi: 10.1016/j.jnutbio.2018.04.004

Mir, M. A., and Albaradie, R. S. (2014). Inflammatory mechanisms as potential therapeutic targets in stroke. *Adv. Neuroimmun. Biol.* 5, 199–216. doi: 10.3233/nib-140082

Mir, M. A., and Albaradie, R. S. (2015). Immunomodulation of inflammatory markers in activated macrophages by leaf extracts of Gingko biloba. *Adv. Neuroimmun. Biol.* 6, 9–17. doi: 10.3233/nib-150103

Mir, M. A., Bhat, B. A., Sheikh, B. A., Rather, G. A., Mehraj, S., and Mir, W. R. (2021a). "Nanomedicine in Human Health Therapeutics and Drug Delivery: Nanobiotechnology and Nanobiomedicine" in *Applications of Nanomaterials in Agriculture, Food Science, and Medicine*, eds M. Bhat, I. Wani, and S. Ashraf Pennsylvania, US: IGI Global, 229–251. doi: 10.4018/978-1-7998-5563-7.ch013

Mir, M. A., Hamdani, S. S., Sheikh, B. A., and Mehraj, U. (2019). Recent advances in metabolites from medicinal plants in cancer prevention and treatment. *Curr. Immunol. Rev.* 15, 185–201. doi: 10.2174/1573395515666191102094330

Mir, M. A., Mehraj, U., and Sheikh, B. A. (2021b). Recent advances in chemotherapeutic implications of deguelin: a plant-derived retinoid. *Nat. Products J.* 11, 169–181. doi: 10.2174/2210315510666200128125950

Mir, M. A., Shabir, N., Mehraj, U., Rather, Y. M., and Farhat, S. (2018). Study on the quality control analysis of antiepileptic drugs using high-performance liquid chromatography. *Int. J. Pharmaceut. Investigat.* 8, 115–121. doi: 10.4103/jphi.jphi_45_18

Mir, R. H., Shah, A. J., Mohi-Ud-Din, R., Pottoo, F. H., Dar, M. A., Jachak, S. M., et al. (2021). Natural Anti-inflammatory compounds as Drug candidates in Alzheimer's disease. *Curr. Med. Chem.* 28, 4799–4825. doi: 10.2174/0929867327666200730213215

Mirzaei, F., Khazaei, M., Komaki, A., Amiri, I., and Jalili, C. (2018). Virgin coconut oil (VCO) by normalizing NLRP3 inflammasome showed potential neuroprotective effects in Amyloid-β induced toxicity and high-fat diet fed rat. *Food Chem. Toxicol.* 118, 68–83. doi: 10.1016/j.fct.2018.04.064

Momtaz, S., Hassani, S., Khan, F., Ziaee, M., and Abdollahi, M. (2018). Cinnamon, a promising prospect towards Alzheimer's disease. *Pharmacol. Res.* 130, 241–258. doi: 10.1016/j.phrs.2017.12.011

Mook-Jung, I., Hong, H. S., Boo, J. H., Lee, K. H., Yun, S. H., Cheong, M. Y., et al. (2001). "Ginsenoside Rb1 and Rg1 improve spatial learning and increase hippocampal synaptophysin level in mice". *J. Neurosci. Res.* 63, 509–515. doi: 10.1002/jnr.1045

Moon, M., Kim, H. G., Choi, J. G., Oh, H., Lee, P. K. J., Ha, S. K., et al. (2014). 6-Shogaol, an active constituent of ginger, attenuates neuroinflammation and cognitive deficits in animal models of dementia. *Biochem. Biophys. Res. Commun.* 449, 8–13. doi: 10.1016/j.bbrc.2014.04.121

Morris, G. P., Clark, I. A., and Vissel, B. (2018). "Questions concerning the role of amyloid-β in the definition, aetiology and diagnosis of Alzheimer's disease". *Acta Neuropathol.* 136, 663–689. doi: 10.1007/s00401-018-1918-8

Muthaiyah, B., Essa, M. M., Chauhan, V., and Chauhan, A. (2011). Protective effects of walnut extract against amyloid beta peptide-induced cell death and oxidative stress in PC12 cells. *Neurochem. Res.* 36, 2096–2103. doi: 10.1007/s11064-011-0533-z

NewmanDj, C. M. (2016). Naturalproductsassources ofnewdrugsfrom1981to2014. *JNatProd* 79, 629–661.

Ng, Y. P., Or, T. C. T., and Ip, N. Y. (2015). Plant alkaloids as drug leads for Alzheimer's disease. *Neurochem. Int.* 89, 260–270. doi: 10.1016/j.neuint.2015.07.018

Niidome, T., Takahashi, K., Goto, Y., Goh, S., Tanaka, N., Kamei, K., et al. (2007). Mulberry leaf extract prevents amyloid beta-peptide fibril formation and neurotoxicity. *Neuroreport* 18, 813–816. doi: 10.1097/WNR.0b013e3280dce5af

Nikbakht, F., Khadem, Y., Haghani, S., Hoseininia, H., Sadat, A. M., Heshemi, P., et al. (2019). "Protective role of apigenin against Aβ 25–35 toxicity via inhibition of mitochondrial cytochrome c release". *Basic Clin. Neurosci.* 10, 557–566.

Nomoto, D., Tsunoda, T., and Shigemori, H. (2021). Effects of clovamide and its related compounds on the aggregations of amyloid polypeptides. *J. Nat. Med.* 75, 299–307. doi: 10.1007/s11418-020-01467-w

Oboh, G., Ademiluyi, A. O., and Akinyemi, A. J. (2012). Inhibition of acetylcholinesterase activities and some pro-oxidant induced lipid peroxidation in rat brain by two varieties of ginger (Zingiber officinale). *Exp. Toxicol. Pathol.* 64, 315–319. doi: 10.1016/j.etp.2010.09.004

Ozarowski, M., Mikolajczak, P. L., Bogacz, A., Gryszczynska, A., Kujawska, M., Jodynis-Liebert, J., et al. (2013). Rosmarinus officinalis L. leaf extract improves memory impairment and affects acetylcholinesterase and butyrylcholinesterase activities in rat brain. *Fitoterapia* 91, 261–271. doi: 10.1016/j.fitote.2013.09.012

Ozarowski, M., Mikolajczak, P. L., Piasecka, A., Kachlicki, P., Kujawski, R., Bogacz, A., et al. (2016). Influence of the Melissa officinalis leaf extract on long-term memory in scopolamine animal model with assessment of mechanism of action. *Evid. Based Complement. Alt. Med.* 2016:9729818. doi: 10.1155/2016/9729818

Papandreou, M. A., Kanakis, C. D., Polissiou, M. G., Efthimiopoulos, S., Cordopatis, P., Margarity, M., et al. (2006). "Inhibitory activity on amyloid-β aggregation and antioxidant properties of Crocus sativus stigmas extract and its crocin constituents". *J. Agric. Food Chem.* 54, 8762–8768. doi: 10.1021/jf061932a

Parle, M., Dhingra, D., and Kulkarni, S. K. (2004). Improvement of mouse memory by Myristica fragrans seeds. *J. Med. Food* 7, 157–161. doi: 10.1089/1096620041224193

Peng, Y., Jiang, L., Lee, D. Y. W., Schachter, S. C., Ma, Z., and Lemere, C. A. (2006). Effects of huperzine A on amyloid precursor protein processing and β-amyloid generation in human embryonic kidney 293 APP Swedish mutant cells. *J. Neurosci. Res.* 84, 903–911. doi: 10.1002/jnr.20987

Pluta, R., Czuczwar, S. J., Januszewski, S., and Jabłoński, M. (2021). The many faces of post-ischemic tau protein in brain neurodegeneration of the Alzheimer's disease type. *Cells* 10:2213. doi: 10.3390/cells10092213

Qadri, H., Shah, A. H., and Mir, M. (2021). Novel strategies to combat the emerging drug resistance in human pathogenic microbes. *Curr. Drug Targets* 22, 1424–1436. doi: 10.2174/1389450121666201228123212

Rahman, H., and Muralidharan, P. (2010). Nardostacys Jatamansi DC Protects from the loss of memory and cognition deficits in sleep deprived Alzheimer's disease (Ad) mice model. *Int. J. Pharm. Sci. Rev. Res.* 5, 160–167.

Raut, S. B., Parekar, R. R., Jadhav, K. S., Marathe, P. A., and Rege, N. N. (2015). Effect of Jyotişmatī seed oil on spatial and fear memory using scopolamine induced amnesia in mice. *Ancient Sci. Life* 34, 130–133. doi: 10.4103/0257-7941.157149

Raza, S. S., Khan, M. M., Ahmad, A., Ashafaq, M., Islam, F., Wagner, A. P., et al. (2013). "Neuroprotective effect of naringenin is mediated through suppression of NF-κB signaling pathway in experimental stroke". *Neuroscience* 230, 157–171. doi: 10.1016/j.neuroscience.2012.10.041

Remington, R., Chan, A., Lepore, A., Kotlya, E., and Shea, T. B. (2010). Apple juice improved behavioral but not cognitive symptoms in moderate-to-late stage Alzheimer's disease in an open-label pilot study. *Am. J. Alzheimer's Dis. Other Dementias§.* 25, 367–371. doi: 10.1177/1533317510363470

Rubio, J., Qiong, W., Liu, X., Jiang, Z., Dang, H., Chen, S.-L., et al. (2011). Aqueous extract of black maca (Lepidium meyenii) on memory impairment induced by ovariectomy in mice. *Evid. Based Complement. Alt. Med.* 2011:253958. doi: 10.1093/ecam/nen063

Sahebkar, A., Mohajertehran, F., and Goloobi, A. (2021). "Alzheimer's disease as a neurodegenerative disorder and the apolipoprotein E gene as its genetic biomarker. *Cent. Asian J. Med. Pharm. Sci. Innov.* 1, 205–217.

Saini, N., Singh, D., and Sandhir, R. (2019). Bacopa monnieri prevents colchicine-induced dementia by anti-inflammatory action. *Metabolic. Brain Dis.* 34, 505–518. doi: 10.1007/s11011-018-0332-1

Savelieff, M. G., Nam, G., Kang, J., Lee, H. J., Lee, M., and Lim, M. H. (2018). Development of multifunctional molecules as potential therapeutic candidates for Alzheimer's disease, Parkinson's disease, and amyotrophic lateral sclerosis in the last decade. *Chem. Rev.* 119, 1221–1322. doi: 10.1021/acs.chemrev.8b00138

Sawda, C., Moussa, C., and Turner, R. S. (2017). Resveratrol for Alzheimer's disease. *Ann. N. York Acad. Sci.* 1403, 142–149.

Scheltens, P., Blennow, K., Breteler, M. M., de Strooper, B., Frisoni, G. B., Salloway, S., et al. (2016). Alzheimer's disease. *Lancet* 388, 505–517.

Selkoe, D. J. (1991). The molecular pathology of Alzheimer's disease. *Neuron* 6, 487–498.

Selvendiran, K., Singh, J. P. V., Krishnan, K. B., and Sakthisekaran, D. (2003). Cytoprotective effect of piperine against benzo [a] pyrene induced lung cancer with reference to lipid peroxidation and antioxidant system in Swiss albino mice. *Fitoterapia* 74, 109–115. doi: 10.1016/s0367-326x(02)00304-0

Sengottuvelu, S. (2011). "Cardamom (Elettaria cardamomum Linn. Maton) seeds in health," in *Nuts and Seeds in Health and Disease Prevention*, eds V. R. Preedy, R. R. Watson, and V. B. Patel (Amsterdam. Elsevier), 285–291. doi: 10.1016/b978-0-12-375688-6.10034-9

Shafiee, M., Arekhi, S., Omranzadeh, A., and Sahebkar, A. (2018). Saffron in the treatment of depression, anxiety and other mental disorders: Current evidence and potential mechanisms of action. *J. Affect. Disord.* 227, 330–337. doi: 10.1016/j.jad.2017.11.020

Shakibaei, M., John, T., Schulze-Tanzil, G., Lehmann, I., and Mobasheri, A. (2007). , "Suppression of NF-κB activation by curcumin leads to inhibition of expression of cyclo-oxygenase-2 and matrix metalloproteinase-9 in human articular chondrocytes: implications for the treatment of osteoarthritis". *Biochem. Pharmacol.* 73, 1434–1445. doi: 10.1016/j.bcp.2007.01.005

Shao, R., and Xiao, J. (2013). Natural products for treatment of Alzheimer's disease and related diseases: understanding their mechanism of action. *Curr. Neuropharmacol.* 11:337. doi: 10.2174/1570159x11311040001

Shukitt-Hale, B., Carey, A. N., Jenkins, D., Rabin, B. M., and Joseph, J. A. (2007). Beneficial effects of fruit extracts on neuronal function and behavior in a rodent model of accelerated aging. *Neurobiol. Aging* 28, 1187–1194. doi: 10.1016/j.neurobiolaging.2006.05.031

Silva, T., Reis, J., Teixeira, J., and Borges, F. (2014). Alzheimer's disease, enzyme targets and drug discovery struggles: from natural products to drug prototypes. *Ageing Res. Rev.* 15, 116–145. doi: 10.1016/j.arr.2014.03.008

Singh, D. (2019). N-butanol fraction of myristica fragrans attenuates scopolamine-induced memory impairment in the experimental model of alzheimer's disease in mice. *J. Neurol. Sci.* 405, 72–73. doi: 10.1016/j.jns.2019.10.1698

Singh, N., Rao, A. S., Nandal, A., Kumar, S., Yadav, S. S., Ganaie, S. A., et al. (2021). "Phytochemical and pharmacological review of Cinnamomum verum J. Presl-a versatile spice used in food and nutrition". *Food Chem.* 338:127773. doi: 10.1016/j.foodchem.2020.127773

Smach, M. A., Hafsa, J., Charfeddine, B., Dridi, H., and Limem, K. (2015). Effects of sage extract on memory performance in mice and acetylcholinesterase activity. *Ann. Pharm. Fr.* 73, 281–288. doi: 10.1016/j.pharma.2015.03.005

Soh, Y., Kim, J.-A., Sohn, N. W., Lee, K. R., and Kim, S. Y. (2003). Protective effects of quinic acid derivatives on tetrahydropapaveroline-induced cell death in C6 glioma cells. *Biol. Pharmaceut. Bull.* 26, 803–807. doi: 10.1248/bpb.26.803

Song, J., Cheon, S. Y., Jung, W., Lee, W. T., and Lee, J. E. (2014). Resveratrol promotes the expression of interleukin-10 and brain-derived neurotrophic factor in microglia under hypoxia. *Int. J. Mol. Sci.* 15, 15512–15529. doi: 10.3390/ijms150915512

Spangler, E. L., Duffy, K., Devan, B., Guo, Z., Bowker, J., Shukitt-Hale, B., et al. (2003). *Rats Fed a Blueberry-Enriched Diet Exhibit Greater Protection against a Kainate-induced Learning Impairment*. Washington, DC: Society for Neuroscience.

Sumanth, M., and Mamatha, K. (2014). Learning and Memory enhancing activity of Ficus carica (Fig): An experimental study in rats. *Drug Dev. Ther.* 5, 2394–2002.

Sundaramoorthy, P. M. K., and Packiam, K. K. (2020). In vitro enzyme inhibitory and cytotoxic studies with Evolvulus alsinoides (Linn.) Linn. Leaf extract: a plant from Ayurveda recognized as Dasapushpam for the management of Alzheimer's disease and diabetes mellitus. *BMC Complement. Med. Ther.* 20:129. doi: 10.1186/s12906-020-02922-7

Sutalangka, C., Wattanathorn, J., Muchimapura, S., and Thukham-mee, W. (2013). Moringa oleifera mitigates memory impairment and neurodegeneration in animal model of age-related dementia. *Oxid. Med. Cell. Long.* 2013:695936. doi: 10.1155/2013/695936

Syad, A. N., and Devi, K. P. (2014). Botanics: a potential source of new therapies for Alzheimer's disease? *Botanics* 4, 11–26. doi: 10.2147/btat.s33554

Talebi, M., Ilgün, S., Ebrahimi, V., Talebi, M., Farkhondeh, T., Ebrahimi, H., et al. (2021a). "Zingiber officinale ameliorates Alzheimer's disease and cognitive impairments: lessons from preclinical studies". *Biomed. Pharmacother.* 133:111088. doi: 10.1016/j.biopha.2020.111088

Talebi, M., Kakouri, E., Talebi, M., Tarantilis, P. A., Farkhondeh, T., Ýlgün, S., et al. (2021b). "Nutraceuticals-based therapeutic approach: Recent advances to combat pathogenesis of Alzheimer's disease". *Expert Rev. Neurother.* 21, 625–642. doi: 10.1080/14737175.2021.1923479

Tang, H., Wang, J., Zhao, L., and Zhao, X.-M. (2017). Rhodiola rosea L extract shows protective activity against Alzheimer's disease in 3xTg-AD mice. *Tropic. J. Pharmaceut. Res.* 16, 509–514. doi: 10.4314/tjpr.v16i3.3

Taranalli, A. D., and Cheeramkuzhy, T. C. (2000). Influence of Clitoria ternatea extracts on memory and central cholinergic activity in rats. *Pharmaceut. Biol.* 38, 51–56. doi: 10.1076/1388-0209(200001)3811-BFT051

Tariq, L., Bhat, B. A., Hamdani, S. S., and Mir, R. A. (2021). "Phytochemistry, Pharmacology and Toxicity of Medicinal Plants," in *Medicinal and Aromatic Plants*, eds T. Aftab and K. R. Hakeem (Cham: Springer), 217–240. doi: 10.1007/978-3-030-58975-2_8

Tesfaye, A. (2021). Revealing the Therapeutic Uses of Garlic (Allium sativum) and Its Potential for Drug Discovery. *Sci. World J.* 2021:8817288. doi: 10.1155/2021/8817288

Tönnies, E., and Trushina, E. (2017). Oxidative stress, synaptic dysfunction, and Alzheimer's disease. *J. Alzheimer's Dis.* 57, 1105–1121. doi: 10.3233/jad-161088

Tripathi, S., and Mazumder, P. M. (2020). Apple cider vinegar (ACV) and their pharmacological approach towards Alzheimer's disease (AD): A review. *Indian J. Pharm. Educ. Res.* 54, s67–s74.

Uabundit, N., Wattanathorn, J., Mucimapura, S., and Ingkaninan, K. (2010). Cognitive enhancement and neuroprotective effects of Bacopa monnieri in Alzheimer's disease model. *J. Ethnopharmacol.* 127, 26–31. doi: 10.1016/j.jep.2009.09.056

Vassallo, N. (2008). *Polyphenols and Health: New and Recent Advances*. Hauppauge: Nova Publishers.

Veerendra Kumar, M. H., and Gupta, Y. K. (2003). Effect of *Centella asiatica* on cognition and oxidative stress in an intracerebroventricular streptozotocin model of Alzheimer's disease in rats. *Clin. Exp. Pharmacol. Physiol.* 30, 336–342. doi: 10.1046/j.1440-1681.2003.03842.x

Vergara, C., Houben, S., Suain, V., Yilmaz, Z., De Decker, R., Vanden Dries, V., et al. (2019). Amyloid-β pathology enhances pathological fibrillary tau seeding induced by Alzheimer PHF in vivo. *Acta Neuropathol.* 137, 397–412. doi: 10.1007/s00401-018-1953-5

Villaflores, O. B., Chen, Y.-J., Chen, C.-P., Yeh, J.-M., and Wu, T.-Y. (2012). Curcuminoids and resveratrol as anti-Alzheimer agents. *Taiwanese J. Obstet. Gynecol.* 51, 515–525. doi: 10.1016/j.tjog.2012.09.005

Wainwright, C. L., Teixeira, M. M., Adelson, D. L., Buenz, E. J., David, B., Glaser, K. B., et al. (2022). Future Directions for the Discovery of Natural Product-Derived Immunomodulating Drugs. *Pharmacol. Res.* 177:106076. doi: 10.1016/j.phrs.2022.106076

Wang, C. P., Zhang, L. Z., Li, G. C., Shi, Y. W., Li, J. L., Zhang, X. C., et al. (2014). Mulberroside a protects against ischemic impairment in primary culture of rat cortical neurons after oxygen–glucose deprivation followed by reperfusion. *J. Neurosci. Res.* 92, 944–954. doi: 10.1002/jnr.23374

Wang, S., Yu, L., Yang, H., Li, C., Hui, Z., Xu, Y., et al. (2016). Oridonin attenuates synaptic loss and cognitive deficits in an Aβ1–42-induced mouse model of Alzheimer's disease. *PLoS One* 11:e0151397. doi: 10.1371/journal.pone.0151397

Wang, X., Wang, W., Li, L., Perry, G., Lee, H.-G., and Zhu, X. (2014). Oxidative stress and mitochondrial dysfunction in Alzheimer's disease. *Biochim. et Biophys. Acta Mol. Basis Dis.* 1842, 1240–1247.

Wang, Y., Liu, J., Zhang, Z., Bi, P., Qi, Z., and Zhang, C. (2011). Anti-neuroinflammation effect of ginsenoside Rbl in a rat model of Alzheimer disease. *Neurosci. Lett.* 487, 70–72. doi: 10.1016/j.neulet.2010.09.076

Wattanathorn, J., Chonpathompikunlert, P., Muchimapura, S., Priprem, A., and Tankamnerdthai, O. (2008). Piperine, the potential functional food for mood and cognitive disorders. *Food Chem. Toxicol.* 46, 3106–3110. doi: 10.1016/j.fct.2008.06.014

Wesnes, K. A., Ward, T., McGinty, A., and Petrini, O. (2000). The memory enhancing effects of a Ginkgo biloba/Panax ginseng combination in healthy middle-aged volunteers. *Psychopharmacology* 152, 353–361. doi: 10.1007/s002130000533

Whitehouse, P. J., Price, D. L., Clark, A. W., Coyle, J. T., and DeLong, M. R. (1981). Alzheimer disease: evidence for selective loss of cholinergic neurons in the nucleus basalis. *Ann. Neurol.* 10, 122–126. doi: 10.1002/ana.410100203

Wijeratne, S. S. K., and Cuppett, S. L. (2007). Potential of rosemary (Rosemarinus officinalis L.) diterpenes in preventing lipid hydroperoxide-mediated oxidative stress in Caco-2 cells. *J. Agric. Food Chem.* 55, 1193–1199. doi: 10.1021/jf063089m

Woodruff-Pak, D. S., Vogel, R. W., and Wenk, G. L. (2001). Galantamine: effect on nicotinic receptor binding, acetylcholinesterase inhibition, and learning. *Proc. Natl. Acad. Sci.* 98, 2089–2094. doi: 10.1073/pnas.98.4.2089

Xiao, Q., Wang, C., Li, J., Hou, Q., Li, J., Ma, J., et al. (2010). Ginkgolide B protects hippocampal neurons from apoptosis induced by beta-amyloid 25–35 partly via up-regulation of brain-derived neurotrophic factor. *Eur. J. Pharmacol.* 647, 48–54. doi: 10.1016/j.ejphar.2010.08.002

Yadav, D. K. (2021). Potential Therapeutic Strategies of Phytochemicals in Neurodegenerative Disorders. *Curr. Topics Med. Chem.* 21, 2814–2838. doi: 10.2174/1568026621666211201150217

Yadav, M. K., Singh, S. K., Singh, M., Mishra, S. S., Singh, A. K., Tripathi, J. S., et al. (2019). "Neuroprotective activity of Evolvulus alsinoides & *Centella asiatica* Ethanolic extracts in scopolamine-induced amnesia in Swiss albino mice". *Open Access Macedonian J. Med. Sci.* 7, 1059–1066. doi: 10.3889/oamjms.2019.247

Yang, H. D., Lee, S. B., and Young, L. D. (2016). History of Alzheimer's Disease. *Dement. Neurocogn. Disord.* 15, 115–121.

Yoo, K.-Y., and Park, S.-Y. (2012). Terpenoids as potential anti-Alzheimer's disease therapeutics. *Molecules* 17, 3524–3538. doi: 10.3390/molecules17033524

Yoshida, H., Meng, P., Matsumiya, T., Tanji, K., Hayakari, R., Xing, F., et al. (2014). Carnosic acid suppresses the production of amyloid-β 1-42 and 1-43 by inducing an α-secretase TACE/ADAM17 in U373MG human astrocytoma cells. *Neurosci. Res.* 79, 83–93. doi: 10.1016/j.neures.2013.11.004

Youdim, K. A., Shukitt-Hale, B., Martin, A., Wang, H., Denisova, N., Bickford, P. C., et al. (2000). "Short-term dietary supplementation of blueberry polyphenolics: beneficial effects on aging brain performance and peripheral tissue function". *Nut. Neurosci.* 3, 383–397. doi: 10.1080/1028415x.2000.11747338

Yuan, H., Ma, Q., Ye, L., and Piao, G. (2016). "The Traditional Medicine and Modern Medicine from Natural Products. *Molecules* 21:559. doi: 10.3390/molecules21050559

Zhang, L., Sun, H., Zhao, J., Lee, J., Low, L. E., Gong, L., et al. (2021). Dynamic nanoassemblies for imaging and therapy of neurological disorders. *Adv. Drug Delivery Rev.* 175:113832. doi: 10.1016/j.addr.2021.113832

Zhang, M., Zhao, R., Wang, D., Wang, L., Zhang, Q., Wei, S., et al. (2021). Ginger (Zingiber officinale Rosc.) and its bioactive components are potential resources for health beneficial agents. *Phytother. Res.* 35, 711–742. doi: 10.1002/ptr.6858

Zhao, H., Niu, Q., Li, X., Liu, T., Xu, Y., Han, H., et al. (2012). Long-term resveratrol consumption protects ovariectomized rats chronically treated with D-galactose from developing memory decline without effects on the uterus. *Brain Res.* 1467, 67–80. doi: 10.1016/j.brainres.2012.05.040

Conflict of Interest: The authors declare that the research was conducted in the absence of any commercial or financial relationships that could be construed as a potential conflict of interest.

Publisher's Note: All claims expressed in this article are solely those of the authors and do not necessarily represent those of their affiliated organizations, or those of the publisher, the editors and the reviewers. Any product that may be evaluated in this article, or claim that may be made by its manufacturer, is not guaranteed or endorsed by the publisher.

frontiers | Frontiers in Pharmacology

BRIEF RESEARCH REPORT
published: 30 May 2022
doi: 10.3389/fphar.2022.910219

Myrtenol Reduces Orofacial Nociception and Inflammation in Mice Through p38-MAPK and Cytokine Inhibition

Janaíne P. Oliveira[1,2], *Fabíula F. Abreu*[1], *José Marcos M. Bispo*[1], *Anderson R. A. Cerqueira*[2], *José Ronaldo dos Santos*[1,3], *Cristiane B. Correa*[1,4], *Soraia K. P. Costa*[2] *and Enilton A. Camargo*[1,5]*

[1]Graduate Program in Physiological Sciences, Federal University of Sergipe, São Cristóvão, Brazil, [2]Department of Pharmacology, Institute of Biomedical Sciences, University of São Paulo, São Paulo, Brazil, [3]Department of Biosciences, Federal University of Sergipe, Itabaiana, Brazil, [4]Department of Morphology, Federal University of Sergipe, São Cristóvão, Brazil, [5]Department of Physiology, Federal University of Sergipe, São Cristóvão, Brazil

OPEN ACCESS

Edited by:
Gokhan Zengin,
Selcuk University, Turkey

Reviewed by:
Paul Durham,
Missouri State University, United States
Myrna Deciga Campos,
Instituto Politécnico Nacional (IPN), Mexico

***Correspondence:**
Enilton A. Camargo
enilton.camargo@pq.cnpq.br

Specialty section:
This article was submitted to Neuropharmacology, a section of the journal Frontiers in Pharmacology

Received: 01 April 2022
Accepted: 03 May 2022
Published: 30 May 2022

Citation:
Oliveira JP, Abreu FF, Bispo JMM, Cerqueira ARA, Santos JRd, Correa CB, Costa SKP and Camargo EA (2022) Myrtenol Reduces Orofacial Nociception and Inflammation in Mice Through p38-MAPK and Cytokine Inhibition. Front. Pharmacol. 13:910219. doi: 10.3389/fphar.2022.910219

Orofacial pain is one of the commonest and most complex complaints in dentistry, greatly impairing life quality. Preclinical studies using monoterpenes have shown pharmacological potential to treat painful conditions, but the reports of the effects of myrtenol on orofacial pain and inflammation are scarce. The aim of this study was to evaluate the effect of myrtenol in experimental models of orofacial pain and inflammation. Orofacial nociceptive behavior and the immunoreactivity of the phosphorylated p38 (P-p38)-MAPK in trigeminal ganglia (TG) and spinal trigeminal subnucleus caudalis (STSC) were determined after the injection of formalin in the upper lip of male Swiss mice pretreated with myrtenol (12.5 and 25 mg/kg, i.p.) or vehicle. Orofacial inflammation was induced by the injection of carrageenan (CGN) in the masseter muscle of mice pretreated with myrtenol (25 and 50 mg/kg, i.p.) or its vehicle (0.02% Tween 80 in saline). Myeloperoxidase (MPO) activity and histopathological changes in the masseter muscle and interleukin (IL)-1β levels in the TG and STSC were measured. The increase in face-rubbing behavior time induced by formalin and P-p38-MAPK immunostaining in trigeminal ganglia were significantly reduced by myrtenol treatment (12.5 and 25 mg/kg). Likewise, increased MPO activity and inflammatory histological scores in masseter muscle, as well as augmented levels of IL-1β in the TG AND STSC, observed after CGN injection, were significantly decreased by myrtenol (25 and 50 mg/kg). Myrtenol has potential to treat orofacial inflammation and pain, which is partially related to IL-1β levels in the trigeminal pathway and p38-MAPK modulation in trigeminal ganglia.

Keywords: orofacial pain, temporomandibular disorder, cytokine, mitogen-activated protein kinase, terpene, myrtenol

INTRODUCTION

Orofacial pain affects the head and neck regions and can be associated with inflammation. Temporomandibular disorders are mainly conditions of non-odontogenic origin related to orofacial pain (Hargreaves, 2011; Dym and Israel, 2012). They are complex pathologies in which myofascial pain has high prevalence (Fernandes et al., 2018).

The clinical management of orofacial pain is still a challenge. Besides the administration of drugs like non-steroidal anti-inflammatories, corticosteroids, anticonvulsants, and tricyclic antidepressants, behavioral (self-education), physiological and physical therapies (e.g., physiotherapy and acupuncture) also are potentially useful for the management of this condition (Shephard et al., 2014; Aggarwal et al., 2019). However, in many patients these treatments still lack efficacy or cause a wide range of undesired side effects.

It is clearly necessary to find new alternative approaches to reduce symptomatology and improve life quality of patients with orofacial pain (Aggarwal et al., 2019). In this respect, natural products possess therapeutic potential for the treatment of many diseases and conditions, including inflammation and pain (Dewick, 2009; Guimarães et al., 2013). Myrtenol is one these natural products, belonging to the class of terpenes. It has anti-inflammatory and antinociceptive properties (Silva et al., 2014; Gomes et al., 2017), but there is no information about its possible effects on painful orofacial disorders.

Evidence shows that other terpenes can reduce nociception in orofacial pain (Oliveira et al., 2020). Furthermore, myrtenol has been found to have antinociceptive action in models of acetic acid-induced abdominal contortions and formalin-, glutamate- and capsaicin-induced nociception in mouse paws (Silva et al., 2014). Thus, we evaluated the effect of myrtenol in experimental orofacial models of pain and inflammation and investigated possible mechanisms of action involved, to expand the possibilities of using this terpenoid substance to treat pain in the orofacial region.

MATERIALS AND METHODS

Animals

Male Swiss mice (25–35 g, 2–3 months of age) were obtained from the animal center of Federal University of Sergipe. The animals were kept at 21–23°C with free access to food and water under a 12-h light/dark cycle. All animals had the same environmental conditions and basal characteristics. They were maintained conscious or anesthetized with intraperitoneal (i.p.) ketamine (80 mg/kg) and xylazine (8 mg/kg) depending on the experimental protocol. All experiments were conducted in agreement with the guidelines of the Brazilian College of Animal Experimentation and the National Institutes of Health Guidelines and were approved by the Ethics Committee on Animal Use of our institution (CEPA 19/18). Allocation and group separation were performed randomly by using the setting available at *random.org*. At the end of the experiments, the animals were euthanized by overdose of anesthesia.

Orofacial Formalin Test

Orofacial nociception was assessed by the formalin test. For this, formalin was injected (20 μL; 2%) in the right upper lip with a 27 G needle (Quintans-Júnior et al., 2010). Thirty minutes before orofacial nociception induction, animals (n = 6 per group) were treated with myrtenol (12.5 or 25 mg/kg, i.p.), vehicle (0.9% saline with 0.02% Tween 80, i.p.) or morphine (an opioid analgesic used as positive control, 5 mg/kg). The quantification of nociception was measured by the time (in seconds) of face rubbing in the first (from 0 to 5 min) and the second phases (from 15 to 40 min) after formalin injection. For this, animals were maintained in mirror boxes and their orofacial movements were recorded by a camcorder (Samsung DV Mod. SC-D382) for 40 min. These records were analyzed by an investigator blinded to the group identity.

We performed immunohistochemistry analyses to investigate the participation of the p38-MAPK pathway in the action mechanism of myrtenol. Immediately after the formalin test, animals were deeply anesthetized by ketamine and xylazine injection (i.p.) and perfused with PBS (pH 7.4), followed by paraformaldehyde (4.0%) in phosphate buffer (0.1 M, pH 7.4). The brain and trigeminal ganglia ipsilateral to the formalin injection site were removed from the skull, postfixed in the same fixative solution for 24 h, and transferred to a solution containing sucrose (30% in 0.1 M PBS). Each sample was serially cut in the coronal plane into 30 μm thick sections with a cryostat microtome (Leica, Germany). The sections were placed in sheets. Primary antibodies for phosphorylated p38 (P-p38)-MAPK (1: 1,000, Cell Signaling Technology) were incubated overnight (for 18 h) at 4°C. Afterwards, the sections were incubated with the biotinylated goat anti-rabbit secondary antibodies (1:1,000; Sigma Chemical Company) for 2 h at room temperature, washed, and incubated with avidin–biotin-peroxidase solution (ABC Elite kit, Vector Labs, Burlingame, United States) for 90 min. The reaction was developed by the addition of diaminobenzidine tetrahydrochloride (DAB; Sigma, United States) and H_2O_2 (0.01%). Sections were examined under brightfield illumination (Olympus Microscope, BX-41), images were captured using a CCD camera (Nikon Eclipse Ci-S), and the spinal trigeminal subnucleus caudalis and trigeminal ganglia locations were determined using the atlas of Paxinos and Franklin (2001). The P-p38-MAPK positive cell count was performed for the whole extension of the evaluated regions within each section, using ImageJ (Version 1.46i, NIH). In each section, four fields evenly distributed throughout the areas of interest were analyzed by an investigator unaware of the experimental groups. Finally, all values were normalized considering the control group.

Orofacial Inflammation Induced by Carrageenan in Masseter Muscle

Orofacial inflammation was induced by injecting carrageenan (3%, 20 μL, n = 6–8 per group, Bagüés et al., 2017) into the

right masseter muscle of anesthetized mice (3% isoflurane). The control group received saline solution (0.9%, 20 μL). The injection site was determined by masseter muscle palpation between the mandible and zygomatic bone (Bagüés et al., 2017). Thirty minutes before induction, animals were intraperitoneally treated with myrtenol (25 or 50 mg/kg, Sigma-Aldrich, St. Louis, MO, United States), indomethacin (a non-steroidal anti-inflammatory, 10 mg/kg) or vehicle (0.9% saline with 0.02% Tween 80). After 6 hours, animals were euthanized by isoflurane overdose followed by cervical dislocation. Then the ipsilateral masseter muscle, trigeminal ganglia and spinal trigeminal subnucleus caudalis were collected, washed in PBS and immediately frozen for posterior analyses. All the treatments were performed by a researcher blinded to the group identification.

Myeloperoxidase (MPO) activity was determined in masseter muscle homogenates as previously described (Souza et al., 2018). Results were expressed as units of MPO per site per mg of tissue. A unit of MPO was considered to be the amount of enzyme that degraded 1 mmol of hydrogen peroxide/min (Bradley et al., 1982).

For histological analysis, masseter muscle samples were processed according to routine histological techniques. Transversal sections with 5 μm thickness were stained with hematoxylin and eosin and analyzed by light microscopy to determine the intensity of tissue alterations and leukocyte infiltration in muscle tissue. Scores were classified from 0 to 4 by a researcher blinded to group identity, where: 0 = absence of alterations; 1 = rare alterations; 2 = moderate alterations; 3 = intense alterations; 4 = severe alterations. These scores were used to evaluate edema, necrosis, and inflammatory infiltrate. The results were expressed as the sum of individual scores.

The levels of IL-1β were measured in ipsilateral trigeminal ganglia and spinal trigeminal subnucleus caudalis. Briefly, these tissues, obtained from 8 animals, were randomly pooled with 2 animals for each sample (resulting in n = 4 measurements) and homogenized in a solution of phosphate-buffered saline (pH 7.2) with Tween 20 (0.05%), phenylmethylsulfonyl fluoride (0.1 mM), benzethonium chloride (0.1 mM), EDTA (10 mM) and aprotinin A (2 ng/ml). Homogenates were centrifuged at 8,000*xg* for 10 min at 4°C and supernatants were collected. IL-1β levels were evaluated by a commercial ELISA kit according to the manufacturer's instructions (R&D Systems). Results were expressed in pg of cytokine/mg of protein. The protein quantity of each sample was measured by the Bradford method.

Statistical Analysis

The results are expressed as means ± SEM. For the statistical evaluation, data were analyzed by the Shapiro-Wilk normality test and no impediment to the use of parametric analysis was found. Thus, we performed one-way analysis of variance (ANOVA) followed by the Tukey test. *p*-values lower than 0.05 were considered significant.

RESULTS

Effect of Myrtenol on Formalin-Induced Orofacial Nociception and p38-MAPK Pathway

Pretreatment with myrtenol at 12.5 and 25 mg/kg reduced face-rubbing time in the second phase, but not in the first phase, of the formalin test in comparison with the vehicle group ($p < 0.05$ and $p < 0.01$, respectively; **Figure 1**). Pretreatment with morphine reduced face-rubbing time in both phases ($p < 0.01$ and $p < 0.001$ for the first and the second phase, respectively) in comparison with the vehicle group (**Figure 1**).

By using immunohistochemistry analysis, we detected a lower number of positively stained cells for P-p38 MAPK in the trigeminal ganglia ($p < 0.05$ and $p < 0.001$, respectively) of animals pretreated with myrtenol at the doses of 12.5 and 25 mg/kg in comparison with the vehicle group (**Figure 2**). We did not find alteration in positive cell counts for P-p38-MAPK in the spinal trigeminal subnucleus caudalis after nociception induction in all the groups evaluated (data not shown).

Effect of Myrtenol on Carrageenan-Induced Orofacial Inflammation in Masseter Muscle and Cytokine Production in Trigeminal Ganglia and Spinal Trigeminal Subnucleus Caudalis

To investigate the effects of myrtenol in the carrageenan-induced orofacial inflammation model, we used doses of 25 mg/kg (the same as in the formalin model) and 50 mg/kg of this monoterpene. In groups pretreated with myrtenol at these doses, we found lower MPO activity ($p < 0.001$ each dose) in comparison to the vehicle group. The same was noted for pretreatment with indomethacin ($p < 0.0001$ vs. vehicle group; **Figure 3A**).

We quantified the pro-inflammatory cytokine IL-1β levels in trigeminal ganglia and spinal trigeminal subnucleus caudalis of animals. Six hours after carrageenan injection, pretreatment with myrtenol reduced IL-1β levels both in trigeminal ganglia ($p < 0.01$–25 mg/kg and $p < 0.05$–50 mg/kg, **Figure 3B**) and in the spinal trigeminal subnucleus caudalis ($p < 0.05$ for each dose, **Figure 3C**) in comparison with the vehicle-treated group.

Histological analysis of masseter muscle sections was also performed to further investigate the anti-inflammatory effect. In the representative image of the saline group, we observed rare or moderate presence of edema, leukocyte infiltrate and necrosis of muscle fibers (**Figure 4B**). In sections of the carrageenan group, we detected intense or severe presence of these parameters (**Figure 4B**). In the group pretreated with myrtenol (50 mg/kg; **Figure 4C**), we observed moderate or intense presence of edema, inflammatory infiltrate, and necrosis. Similar alterations were observed in animals pretreated with indomethacin (**Figure 4D**). An increased total score was verified in the carrageenan group in comparison with

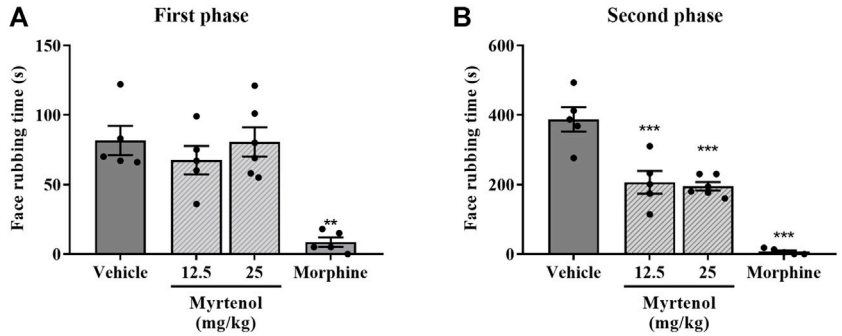

FIGURE 1 | Effect of myrtenol pretreatment on formalin-induced orofacial nociception. Nociceptive behavior was measured as the face rubbing time in seconds (n = 5–6). **(A)**: first phase of formalin test, **(B)**: second phase of formalin test. ANOVA [$F(3,17) = 13.18$, $p = 0.001$ and $F(3,17) = 40.93$, $p < 0.001$, respectively] followed by Tukey's post-test, $^{**}p < 0.01$ or $^{***}p < 0.001$ vs. vehicle.

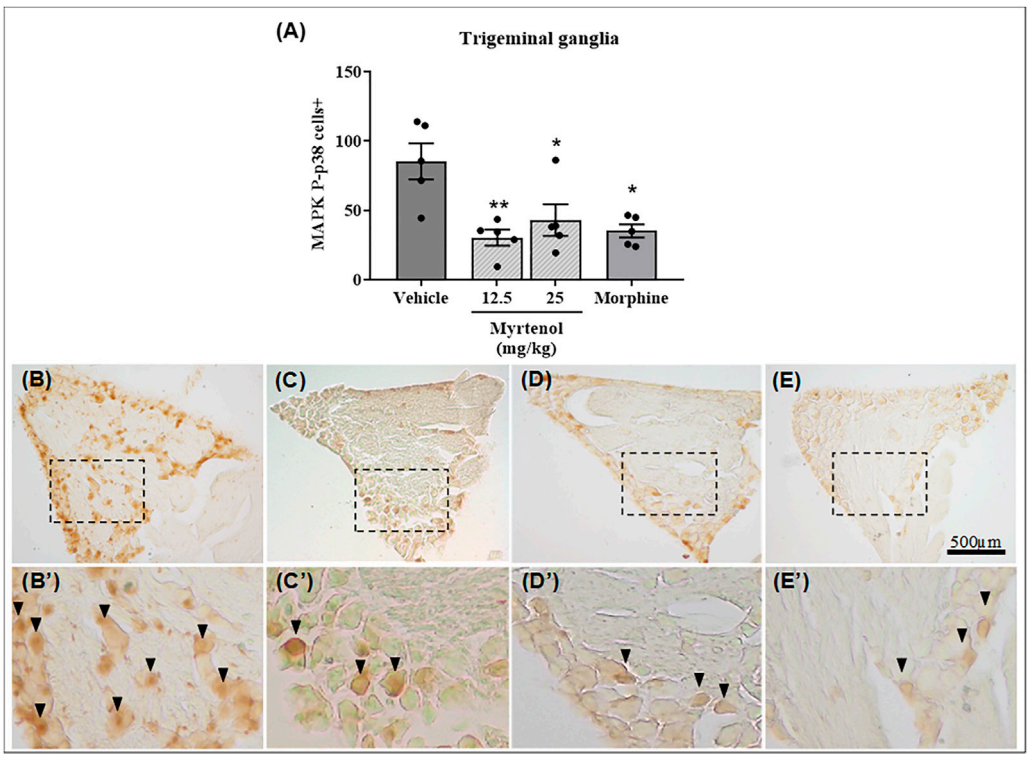

FIGURE 2 | Myrtenol reduces phosphorylated p38-MAPK staining in trigeminal ganglia of mice submitted to orofacial formalin test. **(A)**: Each bar represents the mean ± SEM of the number of the positive cells by phosphorylated p38-MAPK staining (n = 5). ANOVA [$F(3,16) = 7.19$, $p = 0.0028$] followed by Tukey's test, $^{*}p < 0.05$ or $^{**}p < 0.01$ vs. vehicle group. **(B–E)**: representative images (40 x) of vehicle + formalin **(B)**, myrtenol (12.5 mg/kg) + formalin **(C)**, myrtenol (25 mg/kg) + formalin **(D)** and morphine (5 mg/kg) + formalin **(E)** groups. Panels B′-E': higher magnification (100x) of dotted areas from **(B–E)**, respectively.

the saline group ($p < 0.01$, **Figure 4E**). In contrast, in the group pretreated with myrtenol, we observed a partial reduction of the total score in comparison with the carrageenan group ($p < 0.05$), like the alterations found in the group pretreated with indomethacin ($p < 0.01$, **Figure 4E**).

DISCUSSION

In this study, we present for the first-time data about the protective effect of myrtenol on nociception and inflammation in the orofacial region with modulation of the trigeminal pathway.

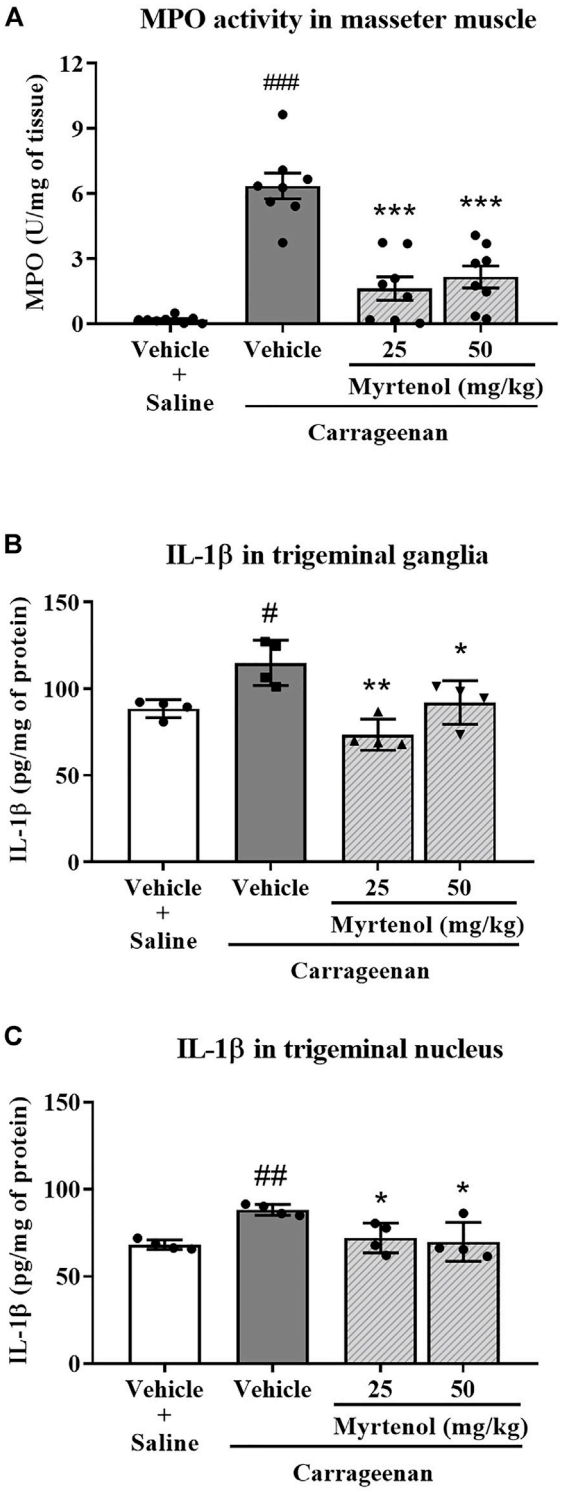

FIGURE 3 | Myrtenol decreases myeloperoxidase (MPO) activity in masseter muscle and IL-1β levels in trigeminal ganglia and spinal trigeminal subnucleus caudalis in carrageenan-induced orofacial inflammation in mice. **(A)**: MPO activity (n = 8) in masseter muscle. **(B,C)** (n = 4 each): IL-1β levels in trigeminal ganglia and spinal trigeminal subnucleus caudalis respectively. ANOVA [F (3,28) = 24.51, $p < 0.001$; F (3,12) = 10.81, $p = 0.001$ and F (3,12) = 6.79, $p = 0.0081$, respectively] followed by Tukey test, $^{\#}p <$ 0.05, $^{\#\#}p < 0.01$ or $^{\#\#\#}p < 0.001$ vs. saline + vehicle; $^{*}p < 0.05$, $^{**}p < 0.01$ or $^{***}p < 0.001$ vs. carrageenan + vehicle.

We first observed that myrtenol reduced face rubbing behavior after formalin challenge. In the first phase of this test, activation occurs of nociceptive terminals, which convey sensorial information to the trigeminal nociceptive system. In the second phase, inflammatory mediators are generated that enhance nerve fiber stimulation (Raboisson and Dallel, 2004). The fact that myrtenol affected the nociception in the second phase but not on the first phase of the formalin test suggests this response is related to the anti-inflammatory action of this compound. Silva and coworkers (2014) observed a similar effect in formalin-induced nociception in mouse paws by using 75 mg/kg of myrtenol, which is a much higher dose than ours (25 mg/kg), but they also found that myrtenol pretreatment reduced the nociceptive behavior only in the second phase. Furthermore, treatment with myrtenol did not

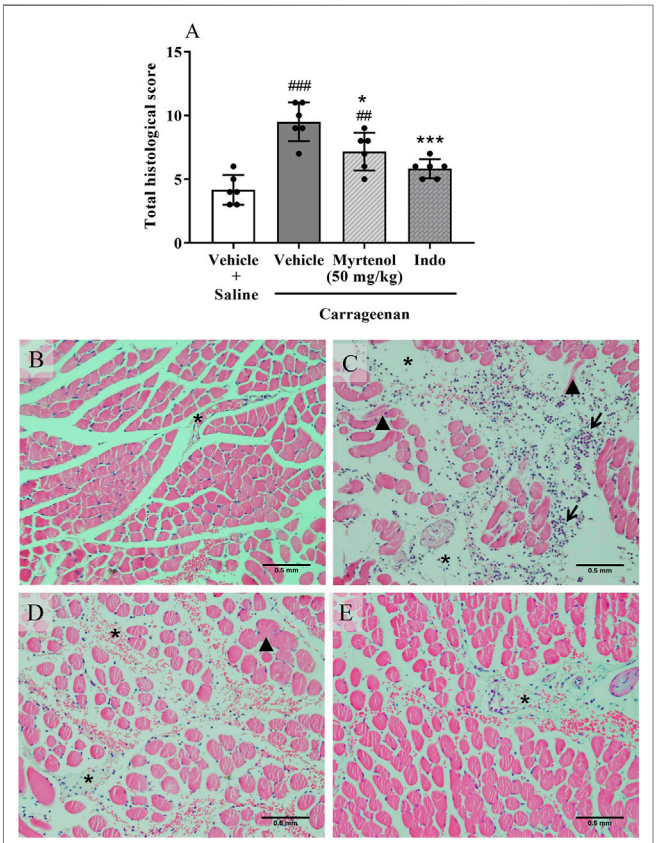

FIGURE 4 | Myrtenol ameliorates carrageenan-induced histopathological changes in mouse masseter muscle. **(A–D)**: representative images (40 x) of vehicle + saline **(A)**, vehicle + carrageenan **(B)**, myrtenol (50 mg/kg) + carrageenan **(C)** and indomethacin + carrageenan **(D)** groups, respectively. Asterisk: edema; arrow: inflammatory infiltrate; arrowhead: necrosis. **(E)**: sum of scores (n = 6). ANOVA [F (3,20) = 19.03, $p < 0.001$] followed by Tukey test, $^{\#\#}p < 0.01$ and $^{\#\#\#}p < 0.001$ vs. saline + vehicle, $^{*}p < 0.05$, $^{***}p < 0.01$ vs. carrageenan + vehicle.

affect nociception in the hot plate test (Silva et al., 2014), a method traditionally used to evaluate the central component of nociception (Gunn et al., 2011). A recent study showed that treatment with myrtenol complexed with β-cyclodextrin (25, 50, 100 mg/kg) reduced paw mechanical hyperalgesia induced by acid saline injection in the gastrocnemius muscle, a model of chronic widespread pain that is considered to mimic aspects of fibromyalgia in humans (Heimfarth et al., 2020). Together these studies, our data support the antinociceptive effect of myrtenol.

Of importance, other authors have reported that treatment with myrtenol at doses up to 75 mg/kg neither altered motor performance in the rota-rod test (Silva et al., 2014) nor modified spontaneous motor activity in open field testing (Gomes et al., 2017), which minimize the possibility that the inhibition of the nociceptive behavior of mice caused by myrtenol was biased by effects like muscular relaxation or central depression.

Many signaling pathways can contribute to the antinociception observed. We measured the phosphorylated p38-MAPK in trigeminal ganglia and spinal trigeminal subnucleus caudalis after orofacial formalin testing and found that the activation of this kinase was reduced by treatment with myrtenol only in trigeminal ganglia. This finding is important because the MAPK pathway is a crucial component of the peripheral and central nociceptive sensitization in neuropathic, chronic, and inflammatory pain (Ji et al., 2013; Edelmayer et al., 2014). The activation of this pathway occurs in many nociceptive animal models, including the formalin test in rodent paws and lips (Bastos et al., 2007; Li et al., 2010; Tan et al., 2012). It can also occur early in nociception pathways, more particularly in primary sensory neurons or satellite cells of dorsal root ganglia or trigeminal ganglia, as well as in second-order neurons located in the dorsal horn of the spinal medulla and trigeminal spinal trigeminal subnucleus caudalis to supraspinal neurons of cortico-thalamic regions (Edelmayer et al., 2014; Kiyomoto et al., 2015).

Considering the results of the second phase of formalin test, we tested the hypothesis that myrtenol could also affect acute orofacial inflammation induced by carrageenan. Interestingly, pretreatment with myrtenol reduced MPO activity in masseter muscle, an indication of reduction of neutrophils in this tissue. This hypothesis was supported by the decrease of edema, necrosis, and leukocyte infiltrate observed by histological analysis in the masseter muscle of animals treated with myrtenol. In agreement with these results, Silva and coworkers (2014) reported that treatment with myrtenol (75 mg/kg) reduced MPO activity in paws injected with carrageenan. Viana et al. (2016) also reported that myrtenol (50 mg/kg) reduced MPO activity in gastric lesions induced by ethanol in mice. Furthermore, Gomes and coworkers (2017) observed that incubation with myrtenol reduced cellular migration of human neutrophils stimulated with n-formylmethionine-leucyl-phenylalanine.

Carrageenan injection in the masseter muscle increased IL-1β levels in trigeminal ganglia and spinal trigeminal subnucleus caudalis, suggesting that neuroinflammation is triggered in this model of orofacial inflammation and might contribute to sensitization of the sensory fibers involved. Similar to our findings, other authors have reported that peripheral injection with pro-inflammatory agents is capable of triggering neuroinflammation. For example, carrageenan injection in mouse paws increased IL-1β levels in the spinal cord (Lu et al., 2013; Choi et al., 2015). In the orofacial region, masseter muscle inflammation induced by CFA increased IL-1β expression in the trigeminal spinal subnucleus caudalis (Guo et al., 2007).

Our data showed that treatment with myrtenol reduced levels of IL-1β in trigeminal ganglia and spinal subnucleus caudalis. These findings suggest that this compound can directly or indirectly modulate central nociceptive pathways due to inhibition of pro-inflammatory cytokine production. Previous studies have shown that myrtenol inhibits pro-inflammatory cytokines, but only peripherally. Silva and coworkers (2014) reported that pretreatment with myrtenol reduced IL-1β levels in peritoneal lavage of mice submitted to carrageenan-induced peritonitis. In the same way, daily treatment with myrtenol for a week reduced IL-1β, TNF-α and interferon-γ in bronchoalveolar lavage of rats challenged with ovalbumin (Bejeshk et al., 2019). In the model of gastric ulcer induced by acetic acid, myrtenol treatment for 7 days also reduced mRNA levels of IL-1β and TNF-α in rats (Viana et al., 2019).

We found reduction of IL-1β in trigeminal ganglia in the model of carrageenan-induced masseter inflammation, as well as decreased p38-MAPK activation in this neural structure in the model of formalin-induced nociception. Of interest, IL-1 β leads to nociceptor activation and contributes to pain hypersensitivity, which is a phenomenon described as depending on p38-MAPK activation in isolated dorsal root ganglion neurons (Binshtok et al., 2008). Therefore, despite the difference in models, our findings seem to corroborate, at least in part, the inhibitory effect of myrtenol in the p38-MAPK modulation in trigeminal ganglia after peripheral challenge with flogistic agents.

A limitation of our study is that we used only male mice, so we did not consider the gender variability, which is potentially important when analyzing the effect of drug candidates in models of nociception (Melchior et al., 2016).

CONCLUSION

Our study demonstrated that treatment with myrtenol causes antinociceptive action due to inhibition of p38-MAPK activation in trigeminal ganglia and anti-inflammatory effect related to the reduction of IL-1β levels in trigeminal ganglia.

DATA AVAILABILITY STATEMENT

The raw data supporting the conclusion of this article will be made available by the authors, without undue reservation.

ETHICS STATEMENT

The animal study was reviewed and approved by the Ethics Committee on Animal Use from Federal University of Sergipe.

AUTHOR CONTRIBUTIONS

JO, SC and EC participated in the conception and design; JO, FA, JB, and AC participated in the acquisition of data; JO, JS, CC, SC, and EC participated in the analysis and interpretation of data; JO and EC drafted the manuscript; JS, CC, SC, and EC revised the manuscript for important intellectual content. All authors approved the manuscript.

FUNDING

EC and SC are recipients of scientific productivity fellowships from the Brazilian National Council for Scientific and Technological Development (CNPq: 311671/2018-7 and 312514/2019-0). JO was supported by a research grant from Office to Coordinate Improvement of Higher Education Personnel (CAPES).

ACKNOWLEDGMENTS

The authors are grateful to governmental agencies of research. We are thankful for grants from CAPES, CNPq and the Sergipe State Foundation to Support Research and Technological Innovation (FAPITEC/SE; no. 2021/2017).

REFERENCES

Aggarwal, V. R., Fu, Y., Main, C. J., and Wu, J. (2019). The Effectiveness of Self-Management Interventions in Adults with Chronic Orofacial Pain: A Systematic Review, Meta-Analysis and Meta-Regression. *Eur. J. Pain* 23 (5), 849–865. doi:10.1002/ejp.1358

Bagüés, A., Martín-Fontelles, M. I., Esteban-Hernández, J., and Sánchez-Robles, E. M. (2017). Characterization of the Nociceptive Effect of Carrageenan: Masseter versus Gastrocnemius. *Muscle Nerve* 56 (4), 804–813. doi:10.1002/mus.25538

Bastos, L. F., Merlo, L. A., Rocha, L. T., and Coelho, M. M. (2007). Characterization of the Antinociceptive and Anti-inflammatory Activities of Doxycycline and Minocycline in Different Experimental Models. *Eur. J. Pharmacol.* 576 (1-3), 171–179. doi:10.1016/j.ejphar.2007.07.049

Bejeshk, M. A., Samareh Fekri, M., Najafipour, H., Rostamzadeh, F., Jafari, E., Rajizadeh, M. A., et al. (2019). Anti-inflammatory and Anti-remodeling Effects of Myrtenol in the Lungs of Asthmatic Rats: Histopathological and Biochemical Findings. *Allergol. Immunopathol. Madr.* 47 (2), 185–193. doi:10.1016/j.aller.2018.09.003

Binshtok, A. M., Wang, H., Zimmermann, K., Amaya, F., Vardeh, D., Shi, L., et al. (2008). Nociceptors Are Interleukin-1beta Sensors. *J. Neurosci.* 28 (52), 14062–14073. doi:10.1523/JNEUROSCI.3795-08.2008

Bradley, P. P., Priebat, D. A., Christensen, R. D., and Rothstein, G. (1982). Measurement of Cutaneous Inflammation: Estimation of Neutrophil Content with an Enzyme Marker. *J. Invest. Dermatol.* 78 (3), 206–209. doi:10.1111/1523-1747.ep12506462

Choi, H. S., Roh, D. H., Yoon, S. Y., Moon, J. Y., Choi, S. R., Kwon, S. G., et al. (2015). Microglial Interleukin-1β in the Ipsilateral Dorsal Horn Inhibits the Development of Mirror-Image Contralateral Mechanical Allodynia through Astrocyte Activation in a Rat Model of Inflammatory Pain. *Pain* 156 (6), 1046–1059. doi:10.1097/j.pain.0000000000000148

Dewick, P. M. (2009). *Medicinal Natural Products: A Biosynthetic Approach*. England: John Wiley & Sons. 9780470741689.

Dym, H., and Israel, H. (2012). Diagnosis and Treatment of Temporomandibular Disorders. *Dent. Clin. North. Am.* 56 (1), 149. doi:10.1016/j.cden.2011.08.002

Edelmayer, R. M., Brederson, J. D., Jarvis, M. F., and Bitner, R. S. (2014). Biochemical and Pharmacological Assessment of MAP-Kinase Signaling along Pain Pathways in Experimental Rodent Models: a Potential Tool for the Discovery of Novel Antinociceptive Therapeutics. *Biochem. Pharmacol.* 87 (3), 390–398. doi:10.1016/j.bcp.2013.11.019

Fernandes, G., Gonçalves, D. A. G., and Conti, P. (2018). Musculoskeletal Disorders. *Dent. Clin. North Am.* 62 (4), 553–564. doi:10.1016/j.cden.2018.05.004

Gomes, B. S., Neto, B. P. S., Lopes, E. M., Cunha, F. V. M., Araújo, A. R., WanderleyOliveira, C. W. S. F. A., et al. (2017). Anti-inflammatory Effect of the Monoterpene Myrtenol Is Dependent on the Direct Modulation of Neutrophil Migration and Oxidative Stress. *Chem. Biol. Interact.* 273, 73–81. doi:10.1016/j.cbi.2017.05.019

Guimarães, A. G., Quintans, J. S. S., and Quintans-Júnior, L. J., Jr (2013). Monoterpenes with Analgesic Activity-A Systematic Review. *Phytother. Res.* 27 (1), 1–15. doi:10.1002/ptr.4686

Gunn, A., Bobeck, E. N., Weber, C., and Morgan, M. M. (2011). The Influence of Non-nociceptive Factors on Hot-Plate Latency in Rats. *J. Pain* 12 (2), 222–227. doi:10.1016/j.jpain.2010.06.011

Guo, W., Wang, H., Watanabe, M., Shimizu, K., Zou, S., LaGraize, S. C., et al. (2007). Glial-cytokine-neuronal Interactions Underlying the Mechanisms of Persistent Pain. *J. Neurosci.* 27 (22), 6006–6018. doi:10.1523/JNEUROSCI.0176-07.2007

Hargreaves, K. M. (2011). Orofacial Pain. *Pain* 152 (3 Suppl. l), S25–S32. doi:10.1016/j.pain.2010.12.024

Heimfarth, L., Dos Anjos, K. S., de Carvalho, Y. M. B. G., Dos Santos, B. L., Serafini, M. R., de Carvalho Neto, A. G., et al. (2020). Characterization of β-cyclodextrin/myrtenol Complex and its Protective Effect against Nociceptive Behavior and Cognitive Impairment in a Chronic Musculoskeletal Pain Model. *Carbohydr. Polym.* 244, 116448. doi:10.1016/j.carbpol.2020.116448

Ji, R. R., Berta, T., and Nedergaard, M. (2013). Glia and Pain: Is Chronic Pain a Gliopathy? *Pain* 154 (Suppl. 10 1), S10–S28. doi:10.1016/j.pain.2013.06.022

Kiyomoto, M., Shinoda, M., Honda, K., Nakaya, Y., Dezawa, K., Katagiri, A., et al. (2015). p38 Phosphorylation in Medullary Microglia Mediates Ectopic Orofacial Inflammatory Pain in Rats. *Mol. Pain* 11, 48. doi:10.1186/s12990-015-0053-y

Li, K., Lin, T., Cao, Y., Light, A. R., and Fu, K. Y. (2010). Peripheral Formalin Injury Induces 2 Stages of Microglial Activation in the Spinal Cord. *J. Pain* 11 (11), 1056–1065. doi:10.1016/j.jpain.2010.01.268

Lu, Y., Zhao, L. X., Cao, D. L., and Gao, Y. J. (2013). Spinal Injection of Docosahexaenoic Acid Attenuates Carrageenan-Induced Inflammatory Pain through Inhibition of Microglia-Mediated Neuroinflammation in the Spinal Cord. *Neuroscience* 241, 22–31. doi:10.1016/j.neuroscience.2013.03.003

Melchior, M., Poisbeau, P., Gaumond, I., and Marchand, S. (2016). Insights into the Mechanisms and the Emergence of Sex-Differences in Pain. *Neuroscience* 338 (338), 63–80. doi:10.1016/j.neuroscience.2016.05.007

Oliveira, J. P., Souza, M. T. S., Cercato, L. M., Souza, A. W., Nampo, F. K., and Camargo, E. A. (2020). Natural Products for Orofacial Nociception in Pre-clinical Studies: A Systematic Review. *Arch. Oral Biol.* 117, 104748. doi:10.1016/j.archoralbio.2020.104748

Paxinos, G., and Franklin, K. B. (2001). *The Mouse Brain in Stereotaxic Coordinates*. San Diego: Elsevier Academic Press.

Quintans-Júnior, L. J., Melo, M. S., De Sousa, D. P., Araujo, A. A., Onofre, A. C., Gelain, D. P., et al. (2010). Antinociceptive Effects of Citronellal in Formalin-, Capsaicin-, and Glutamate-Induced Orofacial Nociception in Rodents and its Action on Nerve Excitability. *J. Orofac. Pain* 24 (3), 305–312.

Raboisson, P., and Dallel, R. (2004). The Orofacial Formalin Test. *Neurosci. Biobehav. Rev.* 28 (2), 219–226. doi:10.1016/j.neubiorev.2003.12.003

Shephard, M. K., Macgregor, E. A., and Zakrzewska, J. M. (2014). Orofacial Pain: a Guide for the Headache Physician. *Headache* 54 (1), 22–39. doi:10.1111/head.12272

Silva, R. O., Salvadori, M. S., Sousa, F. B. M., Santos, M. S., Carvalho, N. S., Sousa, D. P., et al. (2014). Evaluation of the Anti-inflammatory and Antinociceptive Effects of Myrtenol, a Plant-Derived Monoterpene Alcohol, in Mice. *Flavour Fragr. J.* 29 (3), 184–192. doi:10.1002/ffj.3195

Souza, A. C. A., Abreu, F. F., Diniz, L. R. L., Grespan, R., DeSantana, J. M., Quintans-Júnior, L. J., et al. (2018). The Inclusion Complex of Carvacrol and β-cyclodextrin Reduces Acute Skeletal Muscle Inflammation and Nociception in Rats. *Pharmacol. Rep.* 70 (6), 1139–1145. doi:10.1016/j.pharep.2018.07.002

Tan, Y. H., Li, K., Chen, X. Y., Cao, Y., Light, A. R., and Fu, K. Y. (2012). Activation of Src Family Kinases in Spinal Microglia Contributes to Formalin-Induced Persistent Pain State through P38 Pathway. *J. Pain* 13 (10), 1008–1015. doi:10.1016/j.jpain.2012.07.010

Viana, A. F., da Silva, F. V., Fernandes, Hde. B., Oliveira, I. S., Braga, M. A., Nunes, P. I., et al. (2016). Gastroprotective Effect of (-)-myrtenol against Ethanol-Induced Acute Gastric Lesions: Possible Mechanisms. *J. Pharm. Pharmacol.* 68 (8), 1085–1092. doi:10.1111/jphp.12583

Viana, A. F. S. C., Lopes, M. T. P., Oliveira, F. T. B., Nunes, P. I. G., Santos, V. G., Braga, A. D., et al. (2019). (-)-Myrtenol Accelerates Healing of Acetic Acid-Induced Gastric Ulcers in Rats and in Human Gastric Adenocarcinoma Cells. *Eur. J. Pharmacol.* 854, 139–148. doi:10.1016/j.ejphar.2019.04.025

Conflict of Interest: The authors declare that the research was conducted in the absence of any commercial or financial relationships that could be construed as a potential conflict of interest.

Publisher's Note: All claims expressed in this article are solely those of the authors and do not necessarily represent those of their affiliated organizations, or those of the publisher, the editors and the reviewers. Any product that may be evaluated in this article, or claim that may be made by its manufacturer, is not guaranteed or endorsed by the publisher.

frontiers | Frontiers in Pharmacology

ORIGINAL RESEARCH
published: 08 July 2022
doi: 10.3389/fphar.2022.912609

Gingerol-Enriched Ginger Supplementation Mitigates Neuropathic Pain *via* Mitigating Intestinal Permeability and Neuroinflammation: Gut-Brain Connection

Chwan-Li Shen[1,2,3]*, *Rui Wang*[1], *Vadim Yakhnitsa*[4], *Julianna Maria Santos*[1], *Carina Watson*[5], *Takaki Kiritoshi*[4], *Guangchen Ji*[4], *Abdul Naji Hamood*[6] and *Volker Neugebauer*[2,3,4,7]

[1]Department of Pathology, Lubbock, TX, United States, [2]Center of Excellence for Integrative Health, Lubbock, TX, United States, [3]Center of Excellence for Translational Neuroscience and Therapeutics, Lubbock, TX, United States, [4]Department of Pharmacology and Neuroscience, Lubbock, TX, United States, [5]Department of Medical Education, Lubbock, TX, United States, [6]Department of Microbiology and Infectious Disease, Lubbock, TX, United States, [7]Garrison Institute on Aging, Texas Tech University Health Sciences Center, Lubbock, TX, United States

OPEN ACCESS

Edited by:
Rajeev K. Singla,
Sichuan University, China

Reviewed by:
Laura López-Gómez,
Rey Juan Carlos University, Spain
Chung-Ming Chen,
Taipei Medical University, Taiwan

***Correspondence:**
Chwan-Li Shen
leslie.shen@ttuhsc.edu

Specialty section:
This article was submitted to Neuropharmacology, a section of the journal Frontiers in Pharmacology

Received: 04 April 2022
Accepted: 13 June 2022
Published: 08 July 2022

Citation:
Shen C-L, Wang R, Yakhnitsa V, Santos JM, Watson C, Kiritoshi T, Ji G, Hamood AN and Neugebauer V (2022) Gingerol-Enriched Ginger Supplementation Mitigates Neuropathic Pain via Mitigating Intestinal Permeability and Neuroinflammation: Gut-Brain Connection. Front. Pharmacol. 13:912609. doi: 10.3389/fphar.2022.912609

Objectives: Emerging evidence suggests an important role of the gut-brain axis in the development of neuropathic pain (NP). We investigated the effects of gingerol-enriched ginger (GEG) on pain behaviors, as well as mRNA expressions of inflammation *via* tight junction proteins in GI tissues (colon) and brain tissues (amygdala, both left and right) in animals with NP.

Methods: Seventeen male rats were randomly divided into three groups: Sham, spinal nerve ligation (SNL, pain model), and SNL+0.375% GEG (wt/wt in diet) for 4 weeks. Mechanosensitivity was assessed by von Frey filament tests and hindpaw compression tests. Emotional responsiveness was measured from evoked audible and ultrasonic vocalizations. Ongoing spontaneous pain was measured in rodent grimace tests. Intestinal permeability was assessed by the lactulose/D-mannitol ratio in urine. The mRNA expression levels of neuroinflammation (NF-κB, TNF-α) in the colon and amygdala (right and left) were determined by qRT-PCR. Data was analyzed statistically.

Results: Compared to the sham group, the SNL group had significantly greater mechanosensitivity (von Frey and compression tests), emotional responsiveness (audible and ultrasonic vocalizations to innocuous and noxious mechanical stimuli), and spontaneous pain (rodent grimace tests). GEG supplementation significantly reduced mechanosensitivity, emotional responses, and spontaneous pain measures in SNL rats. GEG supplementation also tended to decrease SNL-induced intestinal permeability markers. The SNL group had increased mRNA expression of NF-κB and TNF-α in the right amygdala and colon; GEG supplementation mitigated these changes in SNL-treated rats.

Conclusion: This study suggests GEG supplementation palliated a variety of pain spectrum behaviors in a preclinical NP animal model. GEG also decreased SNL-induced intestinal permeability and neuroinflammation, which may explain the behavioral effects of GEG.

Keywords: functional food, central nervous system, pain assessment, leaky gut, animals

INTRODUCTION

Neuropathic pain (NP) resulting from a lesion or disease of the somatosensory nervous system is a common chronic pain (Cavalli et al., 2019). NP in the general population is estimated to have a prevalence between 3% and 17% (Cavalli et al., 2019). NP is characterized by abnormal hypersensitivity to stimuli (hyperalgesia) and nociceptive responses to non-noxious stimuli (allodynia) (Colloca et al., 2017). Currently, available treatment options for NP are limited (Cavalli et al., 2019) and opioid analgesics have severe side effects and can result in opioid use disorder (Finnerup et al., 2015; Cooper et al., 2017).

Ample evidence shows NP is linked to excessive reactive oxygen species and inadequate endogenous antioxidants after nerve injury, resulting in neuroinflammation (Dai et al., 2020; Teixeira-Santos et al., 2020). Mitigating the neuroinflammation offers potential therapeutic targets in NP management. Dietary bioactive compounds have gained attention for NP and NP-related neuroinflammation due to their anti-inflammatory and anti-oxidant properties (Shen et al., 2022a). Therefore, the development and assessment of bioactive compounds for NP management could provide a new, safe, and effective analgesic alternative that is much needed.

A "leaky gut" refers to a damaged gut lining, which can no longer optimally function as a barrier, leading to an increase in the permeability of the intestinal mucosa along with low-grade inflammation (Yang et al., 2019; Lin et al., 2020). The link between leaky gut and neuroinflammation in NP and NP-associated behaviors has received increased attention, as shown by increased research into the permeability of the intestines (leaky gut) and the blood-brain barrier, followed by enhanced entrance of microbiota-produced substances into the peripheral and central nervous system (CNS) (Camilleri, 2019; Yang et al., 2019; Lin et al., 2020). Since the "leaky gut" may be linked to neuroinflammation, neuronal sensitization, and hyperexcitability in the development of NP, targeting the leaky gut using bioactive compounds *via* functional food or bioactive compounds may represent a new therapeutic strategy to manage NP.

Ginger (*Zingiber officinale* Roscoe) consists of a complex combination of biologically active constituents (6-, 8-, and 10-gingerol and 6-, 8-, and 10-shogaol) that contribute to ginger's anti-inflammatory properties (Tjendraputra et al., 2001). Ginger and its bioactive components have been shown to penetrate the blood-brain barrier via passive diffusion, providing the basis for positive effects of ginger in the CNS (Simon et al., 2020). Ginger's anti-nociceptive capabilities in a number of NP animal studies have been reviewed recently (Shen et al., 2022a). In brief, ginger consumption, in the forms of ginger extract, ginger essential oil, gingerols, and shogaols, has beneficial effects on NP-related parameters including mechanical allodynia and hyperalgesia, thermal and cold hyperalgesia, and anxiety-associated behaviors. Our team proposed that ginger's underlying mechanisms include the suppression of glial cell and neutrophil activation, inhibition of expression/production of pro-inflammatory cytokines/chemokines, and reduction of circulating cell-free mitochondrial DNA levels (Shen et al., 2022a). However, no study has investigated how GEG would impact leaky gut and neuroinflammation via the gut-brain connection in NP status. For that we focused on a particular brain area, the amygdala, because of its link to NP mechanisms (Neugebauer, 2020) in brain signaling (Cowan et al., 2018).

We previously reported that GEG supplementation into the diet decreased mechanical hypersensitivity assessed in the von Frey test and favored microbiome composition and fecal metabolites (Shen et al., 2022b). Such beneficial effects of GEG may be due to its anti-inflammatory property as shown in the suppression of circulating cell-free mitochondrial DNA (Shen et al., 2022b). The current study advances this concept by investigating 1) if GEG supplementation would affect different NP-related behaviors, including sensory (mechanical withdrawal thresholds), emotional-affective (audible and ultrasonic vocalization), and spontaneous components, 2) if GEG supplementation would improve leaky gut, and 3) if GEG supplementation would suppress neuroinflammation in the colon (gut) and amygdala (brain). We hypothesized that GEG supplementation into the diet would mitigate pain behaviors through alleviating leaky gut (decreasing intestinal instability) and suppressing neuroinflammation in the colon and amygdala of neuropathic rats (spinal nerve ligation model, SNL). We selected the gut (colon) and the brain (right amygdala and left amygdala) in order to explore the effects of ginger bioactive compounds on the gut-brain connection that is relevant to NP and provide the knowledge basis for the development of precision nutrition for NP management.

MATERIALS AND METHODS

Animals and Treatments

Seventeen male Sprague-Dawley rats (4-5-week-old, 140–170 g, Envigo, Cumberland, VA, United States) were housed individually under a 12-h light-dark cycle with food and water *ad libitum*. All procedures were approved by the Institutional Animal Care and Use Committee at Texas Tech University Health Sciences Center.

We used the spinal nerve ligation (SNL) model to study neuropathic pain, which is widely used for the preclinical

study of NP mechanisms and the development of new analgesic drugs/compounds. Lumbar spinal nerve (L5) ligation in this model results in acute hypersensitivity within 1 week that persists for multiple weeks (Chung et al., 2004). The SNL model is well-established in our laboratories (Ji et al., 2017; Ji et al., 2018; Ji and Neugebauer, 2019; Navratilova et al., 2019; Presto et al., 2021; Shen et al., 2022b). In brief, rats were anesthetized with isoflurane (2%–3%; precision vaporizer, Harvard Apparatus) and the left L5 spinal nerve was surgically exposed and tightly ligated using 6–0 sterile silk. In the sham-operated control group, the nerve was exposed but not ligated.

There were 3 treatment groups in this study: a Sham group, an SNL group, and an SNL + GEG at 0.375% in diet w/w (SNL + GEG) group. After 5 days of acclimatization, we randomly assigned rats to the Sham group (N = 6), SNL group (N = 6) and SNL + GEG group (N = 5). The Sham and SNL groups were given AIN-93G diet (catalog number #D10012G, Research Diet, Inc., New Brunswick, NJ, United States) for 4 weeks. The SNL + GEG group, after SNL induction, was given GEG at 0.375% (wt/wt diet) into AIN-93G diet for 4 weeks. At doses in the range of 100 mg/kg to 400 mg/kg GEG has been shown to reduce inflammation in rats in various inflammation models (Li et al., 2012; Mansour et al., 2019). Based on these studies, we selected a dose of 0.375% (weight/weight in diet) for our study in SNL-treated rats, which corresponds to ~150 mg/kg for rats. Based on the results of gas chromatography-mass spectrometry, GEG consists of 18.7% 6-gingerol, 1.81% 8-gingerol, 2.86% 10-gingerol, 3.09% 6-shogoal, 0.39% 8-shogaol, and 0.41% 10-shogaol. GEG was obtained from Sabinsa, Inc., Piscataway, NJ. Body weight, food intake, and water consumption was recorded weekly.

Assessment of Mechanosensitivity

Mechanical withdrawal thresholds of spinal nocifensive reflexes were measured on the left paw using Electronic von Frey Aesthesiometer (IITC Life Science, Woodland Hills, CA, United States) with a plastic tip in an exclusive testing area (catalog number 76-0488, Harvard Apparatus, Holliston, MA, United States) 1 day before-SNL and 1, 2, 3, and 4 weeks after respective treatments, as described in our previous studies (Ji et al., 2018; Shen et al., 2022b). The average of six measurements per subject, taken at least 30 s apart, was calculated.

Assessment of Emotional Responses

The pain-related emotional responses were assessed as vocalizations at 1 day pre-surgery and 4 weeks after feeding intervention. Vocalizations in the audible (20 Hz-16 kHz) and ultrasonic (25 ± 4 kHz) ranges were measured as in our previous studies (Han et al., 2005; Kiritoshi et al., 2016; Mazzitelli and Neugebauer, 2019; Presto et al., 2021). Animals were briefly anesthetized with isoflurane and placed in a custom designed recording chamber (U.S. Patent 7,213,538). After habituation to the chamber for 10 min, vocalizations were evoked by brief (15 s) innocuous (500 g/30 mm2) and noxious (1,500 g/30 mm2) stimuli applied to the left hind paw, using a calibrated forcep with a force transducer displaying output in grams. A microphone connected to a preamplifier and a bat detector were used to measure audible and ultrasonic vocalizations, respectively. Signals were digitized with UltraVox interface (Noldus Information Technology, Leesburg, VA, United States). Vocalizations were recorded for 1 min starting with the onset of mechanical stimulation and analyzed using Ultravox 2.0 software (Noldus Information Technology). Vocalizations were measured twice in the same animal with a 10 min interval, and then averaged.

Assessment of Spontaneous Pain

Grimace test scoring was performed before surgery (baseline) and after 4 weeks of feeding treatment intervention based on the published work (Sperry et al., 2018). The rats were placed in individual plexiglass chambers with home cage bedding in a quiet environment. Two video cameras (Sony Handycam HDR-CX455 9.2 megapixels with lenses Zeiss Vario-Tessar, Sony Corporation of America, New York, NY, United States) were placed on the outside perpendicular to the front and back of the chambers. Rats were video-recorded for a 10-min duration. For image extraction, still images were selected and retrieved every 2 s (1/2fps) out of a recorded video using customized Python scripts. Ten representative images (at least 30 s apart) of the rat's face/body were then selected for scoring from all the images generated and were assigned a random number code. Grimace scoring was performed by 5 treatment-blinded experienced evaluators as described before (Sotocinal et al., 2011; Sperry et al., 2018). Each image was scored based on four action units (parameters): orbital tightening, nose bulge, ear position, and whisker change. A score from 0–2 (0 = not present, 1 = moderate, 2 = severe) was assigned to each facial unit. A mean of each action unit for all 10 images scored by 5 evaluators was obtained. We analyzed the scores for each parameter individually averaging across the evaluators and also average score for all parameters.

Assessment of Intestinal Permeability

Intestinal permeability was evaluated by analyzing urinary lactulose and mannitol levels (Nguyen et al., 2019). After 4 weeks of intervention, a 2-ml fresh solution containing 60 mg/ml lactulose and 40 mg/ml D-mannitol were given to each rat by oral gavage. Rats were placed individually in metabolic cages and the rats had free access to food and water. Urine was collected over 24 h. Thymol (10% dissolved in isopropanol) was added to the collecting tubes to prevent degradation of urinary sugars due to bacterial growth. Collected urine samples were stored at −80C before assay. Concentrations of the lactulose and mannitol were measured using the EnzyChromTM Intestinal Permeability Assay Kit (EIPM-100, BioAssay System, Hayward, CA, United States) following manufacture's instruction. Lactulose and D-Mannitol concentrations were calculated by subtracting the optical density (O.D) from each sample from its own blank (O.D.), dividing by the slope of the standard curve of each compound and multiplying by the dilution factor of samples. Data is presented by ratio lactulose/D-Mannitol.

Sample Collection

At the end of study, the animals were anesthetized, euthanized, and their blood was drawn for plasma and serum collection. In

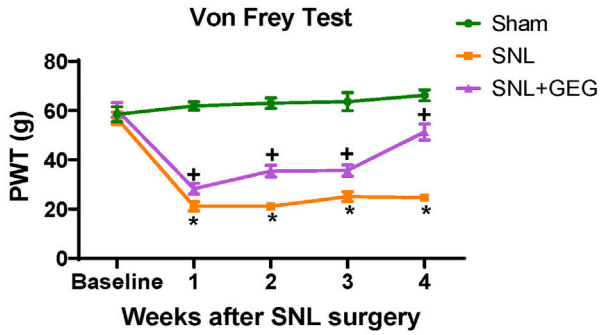

FIGURE 1 | GEG increased the mechanical thresholds of SNL rats as assessed by an electronic von Frey anesthesiometer. Data is expressed as mean ± SEM. n = 5–6 per group. Data was analyzed by mixed ANOVA followed by a *post hoc* Tukey's test. $^{*}p < 0.05$ vs. Sham. $^{+}p < 0.05$ vs. SNL.

addition, the colon and both right and left amygdala were collected, reserved in RNAlater, and stored at −80°C for later mRNA expression analyses.

RNA Isolation and qRT-PCR

Total RNA was isolated from amygdala (right and left) and colon using the RNAzol RT (RN190, Molecular Research Center Inc., Cincinnati, Ohio, United States), BAN ratio 1:200 (BN191, Molecular Research Center, Cincinnati, Ohio, United States). Total RNA was quantified using nanodrop at 260 nm (Nanodrop one, Thermo Scientific) then reverse transcribed into cDNA using Maxima first strand cDNA synthesis kit synthesis with dsDNase (Thermo Scientific, K1672, Waltham, MA, United States) using the thermal cycler Bio-rad S1000 (Bio-Rad Laboratories, Inc., Hercules, CA, United States). qRT-PCR was performed on Quant Studio 12 K Flex real time PCR system (Life Technologies, 4470689, Carlsbad, CA, United States) using samples cDNA for amplification of target genes with β-actin as the control with Universal SYBR green supermix (Bio-rad Laboratories, Inc., 17251-24, Hercules, CA, United States).

The following genes were tested: inflammation markers (NFkβ, TNFα). The primer sequences used are: β-actin, forward: 5′-ACA ACC TTC TTG CAG CTC CTC C-3′; Reverse: 5′-TGA CCC ATA CCC ACC ATC ACA-3′. TNFα, forwards: 5′- GAA CTC CAG GCG GTG TCT GT-3′; reverse: 5′ - CTG AGT GTG AGG GTC TGG GC-3′. NF-kB, forward: 5′- CCT CCA CCC CGA CGT ATT GC-3′; reverse: 5′- GCC AAG GCC TGG TTT GAG AT-3′. All genes expressions were normalized to our control β-actin. Gene expression was calculated by the following formula: 2-(ΔCT*1,000) (Rao et al., 2013).

Statistical Analysis

Results are presented as mean ± standard error of mean (SEM). For data of von Frey tests, mixed ANOVA followed by post-hoc Tukey test at each collection time was conducted to examine overall group difference (i.e., group effect), change over time (i.e., time effect), and group difference in this change (i.e., group-by-time interaction). For other data, one-way ANOVA was performed with post-hoc Tukey test. All analyses were conducted using SAS/STAT 9.4 (SAS Institute Inc.) and statistical significance was determined a 0.05 alpha level. Additionally, for some comparisons with $0.05 < p < 0.1$, the symbol # is used to show a tendency.

RESULTS

Gingerol-Enriched Ginger Supplementation Mitigated NP Hypersensitivity

Mechanical hypersensitivity was assessed in the von Frey test (**Figure 1**). The interaction effect was significant [$F(3, 42) = 18.51$, $p < .0001$], confirming that mechanosensitivity changed uniquely for different groups as shown in **Figure 1**. The post-hoc pairwise group comparisons were all significant at each time point (all adjusted $p < .05$)—the only exceptions were the difference between SNL and SNL + GEG at week 1 and week 3. Compared with the sham group, the SNL group had significantly greater mechanosensitivity starting at 1-week post-operation and persisting throughout the observation period (4 weeks after SNL induction). GEG supplementation significantly decreased hypersensitivity in the treatment group (SNL + GEG) relative to the SNL group as early as 1-week post-operation, and the effect persisted for 4 weeks, as shown by increased mechanical thresholds. At the end of the study (4 weeks after supplements started), the order of pain sensitivity was SNL group > SNL + GEG group > sham group.

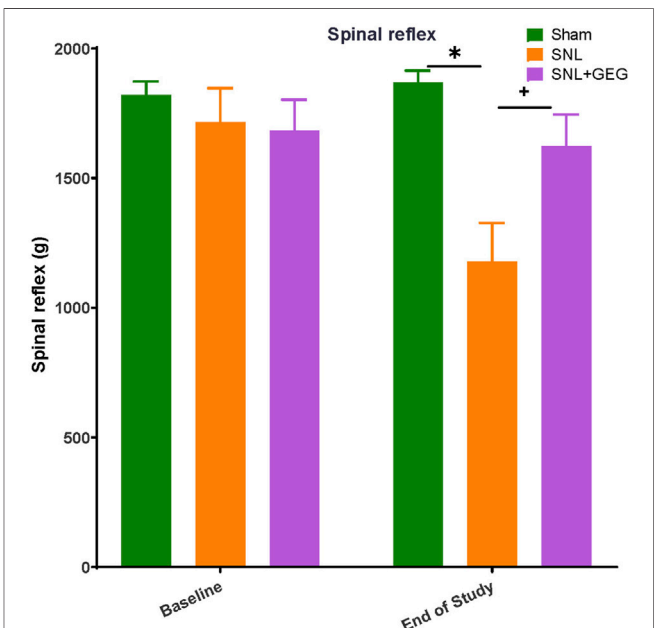

FIGURE 2 | GEG increased the mechanical thresholds of SNL rats as assessed by compression of the hind paw with calibrated forceps. Data is expressed as mean ± SEM. n = 5–6 per group. Data was analyzed by one-way ANOVA followed by a *post hoc* Tukey's test at each collection time. $^{*}p < 0.05$ vs Sham. $^{+}p < 0.05$ vs SNL.

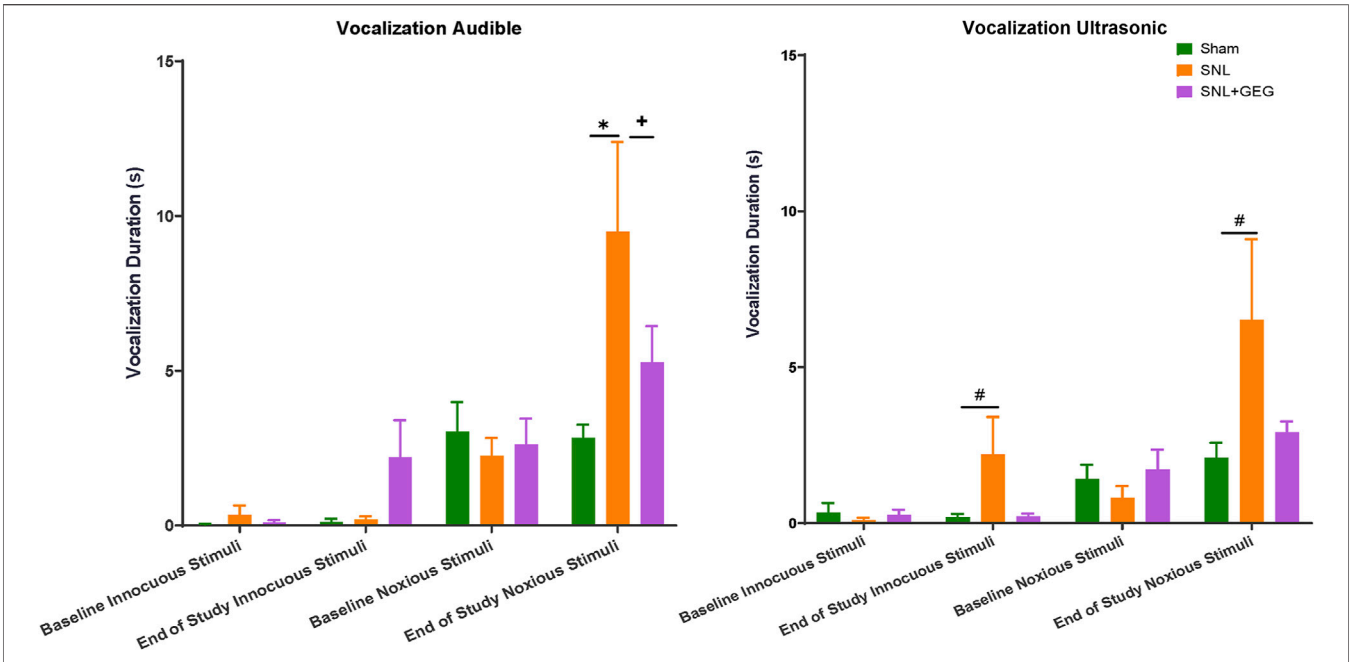

FIGURE 3 | Effect of GEG supplementation on audible, pain-induced vocalizations in response to innocuous stimuli (left) and noxious stimuli (right). Data is expressed as mean ± SEM. $n = 5–6$ per group. Data was analyzed by one-way ANOVA followed by a *post hoc* Tukey's test at each time point. $^{*}p < 0.05$. vs Sham. $^{\#}0.05 < p < 0.1$ vs Sham. $^{+}p < 0.05$ vs SNL.

Mechanical hypersensitivity was assessed in the left hind paw by a compression test (**Figure 2**). In the hind paw compression test, there were no significant differences in mechanical withdrawal thresholds (spinal reflex, g) among all groups at the baseline (**Figure 2**). 4 weeks postinduction of the spinal ligation procedure, the SNL group had significantly lower thresholds compared to the sham group. Supplementation of GEG into the diet increased mechanical thresholds in the SNL group significantly.

Gingerol-Enriched Ginger Supplementation Decreased NP-Induced Emotional Responses

GEG supplementation tended to reduce audible and ultrasonic vocalizations in response to innocuous and noxious stimuli. Effects of GEG supplementation on pain-related emotional responses were measured as audible and ultrasonic vocalizations in response to innocuous and noxious mechanical stimuli (**Figure 3**). At baseline, there were no differences in the duration of audible and ultrasonic vocalizations evoked by innocuous and noxious stimuli among all treatment groups. At the end of the study (4 weeks post-induction of SNL), the SNL group showed increased audible and ultrasonic vocalizations to innocuous and noxious mechanical stimuli compared to the sham group. Supplementation of GEG to the diet reduced the duration of audible vocalizations in SNL rats significantly, while the other outcome measures showed a trend of inhibition by GEG.

Gingerol-Enriched Ginger Supplementation Decreased NP-Induced Spontaneous Pain Behaviors

GEG supplementation reduced SNL-induced spontaneous pain in nose bulge, ears position, whisker change, and total score of rats. Non-evoked ongoing/spontaneous pain was assessed in the rodent grimace test for nose bulge (**Figure 4A**), orbital tightening (**Figure 4B**), ear position (**Figure 4C**), whisker change (**Figure 4D**), and total score (**Figure 4E**). At baseline, there were no significant differences between the 3 experimental groups in any parameters of spontaneous pain measured (nose bulge, orbital tightening, ear position, whisker change, and total score; $p > 0.05$). Some scores were rated "0" by coders at the baseline. 4 weeks after SNL induction, spontaneous pain was detected in nose bulge, ear position, whisker change, and total score, while there was no significant change in orbital tightening ($p > 0.05$). GEG supplementation for 4 weeks significantly mitigated SNL-induced spontaneous pain evidenced in significantly nose bulge, ear position, whiskers change, and total score of SNL-operated rats.

Gingerol-Enriched Ginger Supplementation Tended to Improve Intestinal Integrity in NP

Four weeks after SNL induction, there was an increase in intestinal permeability as shown in increased ratio of lactulose/D-mannitol concentrations in the urine of animals (**Figure 5**). GEG supplementation significantly decreased the lactulose/D-mannitol ratio, suggesting decreased intestinal permeability.

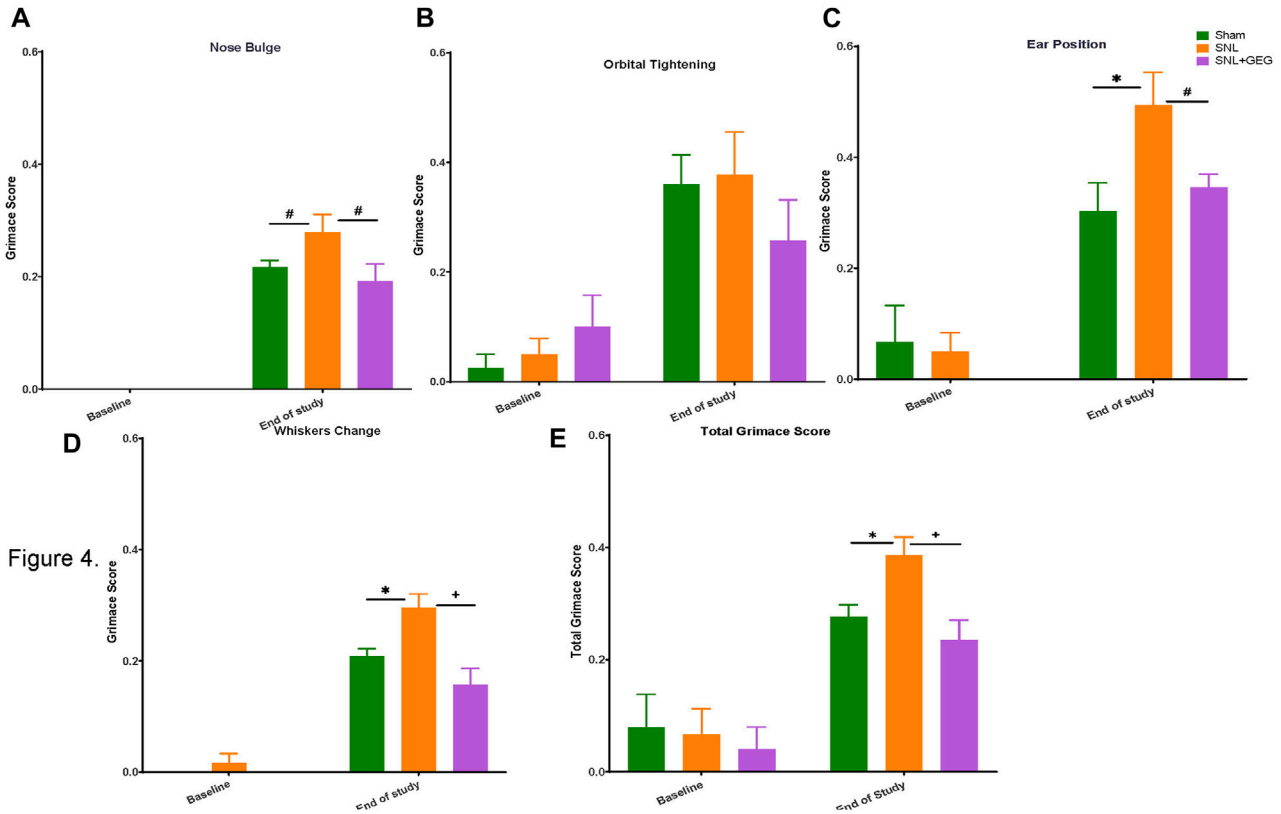

Figure 4.

FIGURE 4 | Effect of GEG supplementation on spontaneous pain in SNL rats as assessed by the rodent grimace test, showing scores for nose bulge **(A)**, orbital tightening **(B)**, ear position **(C)**, and whisker change **(D)**; total **(E)**. Data is expressed as mean ± SEM. $n = 5–6$ per group. Data was analyzed by one-way ANOVA followed by a *post hoc* Tukey's test at each collection time. $^{*}p < 0.05$ vs Sham. $^{\#}0.05 < p < 0.1$ vs Sham or vs SNL. $^{+}p < 0.05$ vs SNL.

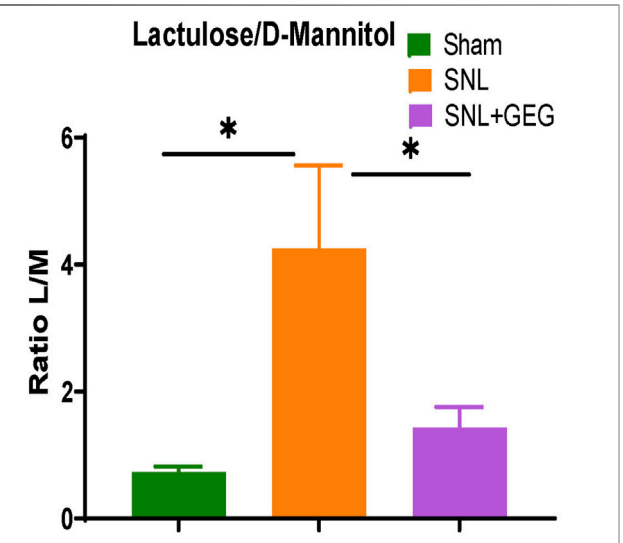

FIGURE 5 | Effect of GEG supplementation on intestinal permeability in SNL rats. The ratio of lactulose to D-mannitol (L/M) increased in the NP state. Data is expressed as mean ± SEM. $n = 4$ per group. Data was analyzed by one-way ANOVA followed by a *post hoc* Tukey's test. $^{*}p < 0.05$.

Gingerol-Enriched Ginger Supplementation Decreased mRNA Expression in Amygdala and Colon in NP

Effects of GEG supplementation on the mRNA expression of neuroinflammation markers NF-κB (**Figure 6A**) and TNF-α (**Figure 6B**) were assessed in the colon as well as right and left amygdala in the NP condition. Compared to the Sham group, the SNL group showed significantly increased mRNA expression of NF-κB in the right amygdala and colon. Supplementation of GEG into diet significantly decreased the NF-κB mRNA expression levels in the right amygdala and colon of SNL rats. Similar to the effects on NF-κB mRNA, TNF-α mRNA expression found in the colon of SNL rats also significantly increased, while GEG supplementation significantly decreased the SNL-induced TNF-α mRNA expression changes in colon.

Disscusion

This study shows for the first time that dietary GEG supplementation mitigated NP-induced sensory and affective pain-related behaviors in animals with NP, and these effects may involve GEG's impacts on intestinal permeability and neuroinflammation in the colon (gut) and amygdala (brain).

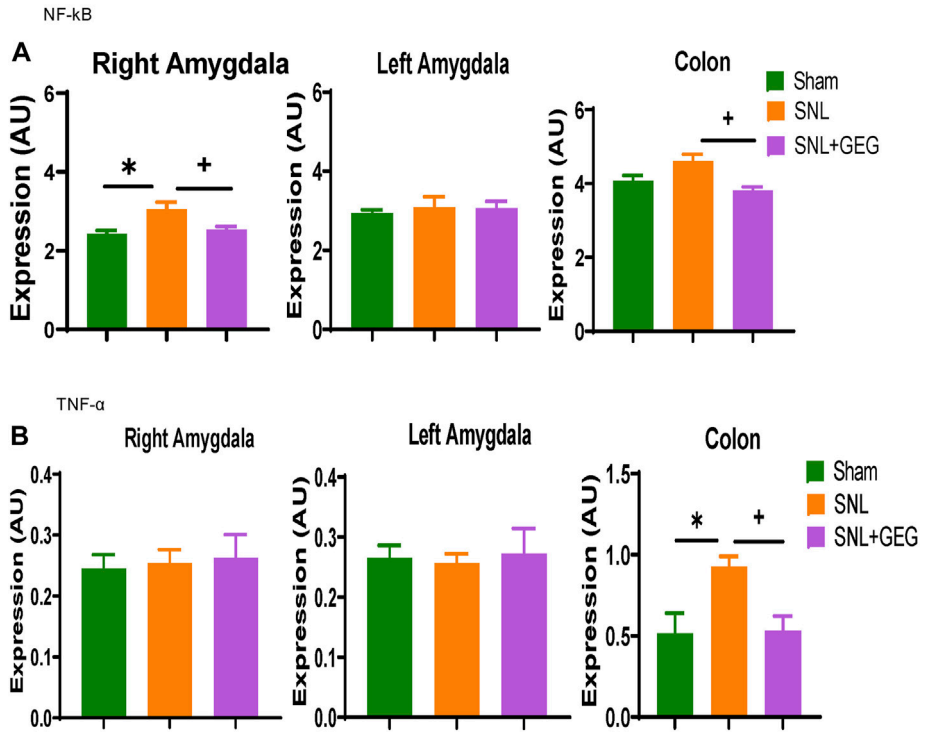

FIGURE 6 | Effect of GEG supplementation on mRNA expression of NF-κB **(A)** and TNF-α **(B)** in the right amygdala, left amygdala, and colon of SNL rats. Data is expressed as mean ± SEM. n = 5-6 per group. Data was analyzed by one-way ANOVA followed by a *post hoc* Tukey's test. $^{*}p < 0.05$ vs Sham. $^{+}p < 0.05$ vs SNL.

The results provide evidence for beneficial behavioral effects of GEG through the modulation of the brain-gut axis.

Natural or extracted ginger bioactive compounds (i.e., *Z. officinale* Roscoe rhizome extract, zerumbone, red ginger oil, shogaol-enriched ginger root extract, and 6-GEG), have been shown to mitigate mechanical allodynia and thermal hyperalgesia in animals with diabetic NP or surgical NP (Shen et al., 2022b). To the best of our knowledge, the present study is the first study to assess dietary GEG on a variety of pain-related behaviors using different pain assessment methods. The results for the sensory, emotional and spontaneous aspects of NP not only corroborate our previous study on sensory pain using the von Frey test (Shen et al., 2022b), but also expand our understanding of the breadth of the pain behavioral effects of GEG on NP.

Pain behavioral studies are a fundamental tool for the validation of pain mechanisms and for the assessment of potential nutraceutical approaches in NP management. In addition to sensory pain, we also examined emotional aspects of pain measuring vocalizations. The analysis of audible and ultrasonic vocalizations in response to noxious stimuli is a well-established approach to assess supraspinally organized pain behaviors (Portfors, 2007). Vocalizations in the audible range represent a nocifensive response, whereas ultrasonic vocalizations in the 25 kHz range reflect negative emotional-affective behavior (Han et al., 2005; Neugebauer et al., 2007; Presto et al., 2021). Therefore, vocalizations provide additional important information about higher integrated pain behaviors. The computerized analysis of audible and ultrasonic vocalization is a valid, quantitative, reliable, and convenient method, having been successfully employed in various pain models, including NP (Ji et al., 2017; Ji et al., 2018; Presto et al., 2021; Mazzitelli et al., 2022). In the present study, we also found increased audible and ultrasonic vocalization of SNL rats to innocuous and noxious stimuli compared to sham rats, which may reflect allodynic and hyperalgesic components of NP. Importantly, this study demonstrates that GEG supplementation decreased vocalizations. Though these effects did not reach the level of statistical significance, they further support an anti-allodynic effect of GEG in NP. The large variability (reflected in the standard error of mean) and small sample size could explain the lack of statistically significant differences between the SNL group and the SNL + GEG group. Further studies including more animals for vocalization assessment are needed to confirm the effects of GEG.

Another important aspect of pain is non-evoked spontaneous or ongoing pain. Evoked pain occurs in response to peripheral stimuli and can be categorized as hyperalgesia, in which sensitivity to noxious stimuli is increased, or allodynia, in which innocuous stimuli become noxious. Spontaneous NP occurs independently of external stimuli and is described by patients as an intermittent, burning or stabbing sensation commonly rated as severe (Schneider et al., 2017). In this study, we evaluated not only evoked pain (mechanical hypersensitivity and emotional responses) but also spontaneous pain using the rodent grimace scale test. In addition to mitigating evoked pain (see above), GEG also decreased various grimace metrics, suggesting beneficial/mitigating effects of GEG on clinically relevant spontaneous NP.

Neurobiological mechanisms include emotional network plasticity in the corticolimbic system (Meier et al., 2017; Elman

and Borsook, 2018; Nees and Becker, 2018). Specifically, the amygdala, a limbic structure, has emerged as a key player in the emotional-affective dimensions of pain and pain modulation (Veinante et al., 2013; Thompson and Neugebauer, 2019; Neugebauer, 2020). It is commonly believed that the interaction in the gut-brain axis is bi-directional (Lin et al., 2020). Our observations that SNL increased intestinal permeability and neuroinflammatory markers in the colon (gut) and amygdala (brain) support the critical role of the amygdala in brain-gut signaling as a neurobiological mechanism of NP.

There is evidence for right-hemispheric lateralization of amygdala function in pain, with the right amygdala being pain facilitatory and the left amygdala serving "anti-nociceptive" functions (Allen et al., 2021). Our study is the first study to demonstrate the beneficial effects of GEG in NP development *via* the gut-brain connection through actions in the amygdala and the improvement of leaky gut syndrome.

Neuroinflammation comprises activation of glial cells and mitochondrial dysfunction in the peripheral and central nervous system, leading to the release of proinflammatory cytokines and chemokines that have been implicated in pain mechanisms (Donnelly et al., 2020; Tan et al., 2021). Thus, the suppression of neuroinflammation by targeting proinflammatory cytokine and chemokine signaling would be a promising strategy to alleviate or prevent NP states. In the development of NP, NF-κB has been shown to trigger a self-perpetuating process resulting in progressive NP (Liu et al., 2017). Enhanced production of the cytokine TNF-α in the brain (locus coeruleus and hippocampus) also occurs during NP development (Sud et al., 2008). Intriguingly, the inhibition of SNL-induced increase in NF-κB and TNF-α mRNA expression in the right amygdala and colon by GEG supplementation found in this study, may, therefore, represent a mechanism of GEG's beneficial effect for the treatment of NP, again through the gut-brain axis.

There are study limitations in the present study. In order to confirm the connection between leaky gut (intestinal permeability), blood-brain barrier integrity, and tight junction proteins expression, sufficiently powered studies are warranted to assess not only mRNA but also protein expression of tight junction proteins in brain and GI tissues. This study focused on how GEG affects the changes in mRNA expression levels that are related to neuroinflammation in the amygdala and colon. We did not perform any histopathological assessment in the colon or amygdala to evaluate possible changes in glial cells with GEG. To the best of our knowledge, the effect of GEG on the number or morphology of glial cells in either colon or amygdala has not yet been evaluated. This important knowledge gaps remains to be addressed in future studies.

CONCLUSION

GEG supplementation into the diet decreased NP-related pain behaviors, namely mechanosensitivity, emotional pain responses, and spontaneous pain. GEG supplementation also decreased intestinal permeability as well as the mRNA expression of neuroinflammatory factors in both amygdala and colon, suggesting GEG has a beneficial impact on NP development via the gut-brain axis.

DATA AVAILABILITY STATEMENT

The original contributions presented in the study are included in the article/supplementary material, further inquiries can be directed to the corresponding author.

ETHICS STATEMENT

The animal study was reviewed and approved by the Institutional Animal Care and Use Committee at Texas Tech University Health Sciences Center.

AUTHOR CONTRIBUTIONS

C-LS, AH, and VN contributed to the conceptualization of the study, data interpretation, and manuscript preparation. RW contributed to behavioral data collection/analysis. VY contributed to NP surgery and behavioral data collection/analysis. CW performed mRNA expression analysis in amygdala and colon. JS contributed to behavioral data analysis and mRNA expression. VY, TK, and GI collected brain sections and interpreted pain-associated behavioral outcomes. All authors have read and agreed to the published version of the manuscript. The authors declare that there is no conflict of interest.

FUNDING

This work is supported by The Agricultural and Food Research Initiative (AFRI) grant No. 2021-67017-34026 from the USDA National Institute of Food and Agriculture and NIH R01 NS038261.

ACKNOWLEDGMENTS

Real-time PCR data were generated in the Molecular Biology Core Facility supported in part by TTUHSC. Authors thank Viren Bhakta, Jessica Contreras, Zarek Driver, Jacob Lovett, and Emily Stephens for scoring facial images. Authors also thank Jacob Lovett for colon collection and editorial work. Any opinions, findings, conclusion, or recommendations expressed in this publication are those of the authors and do not necessarily reflect the view of the U.S. Department of Agriculture.

REFERENCES

Allen, H. N., Bobnar, H. J., and Kolber, B. J. (2021). Left and Right Hemispheric Lateralization of the Amygdala in Pain. *Prog. Neurobiol.* 196, 101891. doi:10.1016/j.pneurobio.2020.101891

Camilleri, M. (2019). Leaky Gut: Mechanisms, Measurement and Clinical Implications in Humans. *Gut* 68 (8), 1516–1526. doi:10.1136/gutjnl-2019-318427

Cavalli, E., Mammana, S., Nicoletti, F., Bramanti, P., and Mazzon, E. (2019). The Neuropathic Pain: An Overview of the Current Treatment and Future Therapeutic Approaches. *Int. J. Immunopathol. Pharmacol.* 33, 2058738419838383. doi:10.1177/2058738419838383

Chung, J. M., Kim, H. K., and Chung, K. (2004). Segmental Spinal Nerve Ligation Model of Neuropathic Pain. *Methods Mol. Med.* 99, 35–45. doi:10.1385/1-59259-770-X:035

Colloca, L., Ludman, T., Bouhassira, D., Baron, R., Dickenson, A. H., Yarnitsky, D., et al. (2017). Neuropathic Pain. *Nat. Rev. Dis. Prim.* 3, 17002. doi:10.1038/nrdp.2017.2

Cooper, T. E., Chen, J., Wiffen, P. J., Derry, S., Carr, D. B., Aldington, D., et al. (2017). Morphine for Chronic Neuropathic Pain in Adults. *Cochrane Database Syst. Rev.* 5, CD011669. doi:10.1002/14651858.CD011669.pub2

Cowan, C. S. M., Hoban, A. E., Ventura-Silva, A. P., Dinan, T. G., Clarke, G., and Cryan, J. F. (2018). Gutsy Moves: The Amygdala as a Critical Node in Microbiota to Brain Signaling. *Bioessays* 40 (1). doi:10.1002/bies.201700172

Dai, C. Q., Guo, Y., and Chu, X. Y. (2020). Neuropathic Pain: the Dysfunction of Drp1, Mitochondria, and ROS Homeostasis. *Neurotox. Res.* 38 (3), 553–563. doi:10.1007/s12640-020-00257-2

Donnelly, C. R., Andriessen, A. S., Chen, G., Wang, K., Jiang, C., Maixner, W., et al. (2020). Central Nervous System Targets: Glial Cell Mechanisms in Chronic Pain. *Neurotherapeutics* 17 (3), 846–860. doi:10.1007/s13311-020-00905-7

Elman, I., and Borsook, D. (2018). Threat Response System: Parallel Brain Processes in Pain Vis-À-Vis Fear and Anxiety. *Front. Psychiatry* 9, 29. doi:10.3389/fpsyt.2018.00029

Finnerup, N. B., Attal, N., Haroutounian, S., McNicol, E., Baron, R., Dworkin, R. H., et al. (2015). Pharmacotherapy for Neuropathic Pain in Adults: a Systematic Review and Meta-Analysis. *Lancet Neurol.* 14 (2), 162–173. doi:10.1016/S1474-4422(14)70251-0

Han, J. S., Bird, G. C., Li, W., Jones, J., and Neugebauer, V. (2005). Computerized Analysis of Audible and Ultrasonic Vocalizations of Rats as a Standardized Measure of Pain-Related Behavior. *J. Neurosci. Methods* 141 (2), 261–269. doi:10.1016/j.jneumeth.2004.07.005

Ji, G., and Neugebauer, V. (2019). Contribution of Corticotropin-Releasing Factor Receptor 1 (CRF1) to Serotonin Receptor 5-HT2CR Function in Amygdala Neurons in a Neuropathic Pain Model. *Int. J. Mol. Sci.* 20 (18). doi:10.3390/ijms20184380

Ji, G., Yakhnitsa, V., Kiritoshi, T., Presto, P., and Neugebauer, V. (2018). Fear Extinction Learning Ability Predicts Neuropathic Pain Behaviors and Amygdala Activity in Male Rats. *Mol. Pain* 14, 1744806918804441. doi:10.1177/1744806918804441

Ji, G., Zhang, W., Mahimainathan, L., Narasimhan, M., Kiritoshi, T., Fan, X., et al. (2017). 5-HT2C Receptor Knockdown in the Amygdala Inhibits Neuropathic-Pain-Related Plasticity and Behaviors. *J. Neurosci.* 37 (6), 1378–1393. doi:10.1523/JNEUROSCI.2468-16.2016

Kiritoshi, T., Ji, G., and Neugebauer, V. (2016). Rescue of Impaired mGluR5-Driven Endocannabinoid Signaling Restores Prefrontal Cortical Output to Inhibit Pain in Arthritic Rats. *J. Neurosci.* 36 (3), 837–850. doi:10.1523/JNEUROSCI.4047-15.2016

Li, X. H., McGrath, K. C., Nammi, S., Heather, A. K., and Roufogalis, B. D. (2012). Attenuation of Liver Pro-inflammatory Responses by Zingiber Officinale via Inhibition of NF-Kappa B Activation in High-Fat Diet-Fed Rats. *Basic Clin. Pharmacol. Toxicol.* 110 (3), 238–244. doi:10.1111/j.1742-7843.2011.00791.x

Lin, B., Wang, Y., Zhang, P., Yuan, Y., Zhang, Y., and Chen, G. (2020). Gut Microbiota Regulates Neuropathic Pain: Potential Mechanisms and Therapeutic Strategy. *J. Headache Pain* 21 (1), 103. doi:10.1186/s10194-020-01170-x

Liu, T., Zhang, L., Joo, D., and Sun, S. C. (2017). NF-κB Signaling in Inflammation. *Signal Transduct. Target Ther.* 2. doi:10.1038/sigtrans.2017.23

Mansour, D. F., Abdallah, H. M. I., Ibrahim, B. M. M., Hegazy, R. R., Esmail, R. S. E., and Abdel-Salam, L. O. (2019). The Carcinogenic Agent Diethylnitrosamine Induces Early Oxidative Stress, Inflammation and Proliferation in Rat Liver, Stomach and Colon: Protective Effect of Ginger Extract. *Asian Pac J. Cancer Prev.* 20 (8), 2551–2561. doi:10.31557/APJCP.2019.20.8.2551

Mazzitelli, M., and Neugebauer, V. (2019). Amygdala Group II mGluRs Mediate the Inhibitory Effects of Systemic Group II mGluR Activation on Behavior and Spinal Neurons in a Rat Model of Arthritis Pain. *Neuropharmacology* 158, 107706. doi:10.1016/j.neuropharm.2019.107706

Mazzitelli, M., Yakhnitsa, V., Neugebauer, B., and Neugebauer, V. (2022). Optogenetic Manipulations of CeA-CRF Neurons Modulate Pain- and Anxiety-like Behaviors in Neuropathic Pain and Control Rats. *Neuropharmacology* 210, 109031. doi:10.1016/j.neuropharm.2022.109031

Meier, M. L., Stämpfli, P., Humphreys, B. K., Vrana, A., Seifritz, E., and Schweinhardt, P. (2017). The Impact of Pain-Related Fear on Neural Pathways of Pain Modulation in Chronic Low Back Pain. *Pain Rep.* 2 (3), e601. doi:10.1097/PR9.0000000000000601

Navratilova, E., Ji, G., Phelps, C., Qu, C., Hein, M., Yakhnitsa, V., et al. (2019). Kappa Opioid Signaling in the Central Nucleus of the Amygdala Promotes Disinhibition and Aversiveness of Chronic Neuropathic Pain. *Pain* 160 (4), 824–832. doi:10.1097/j.pain.0000000000001458

Nees, F., and Becker, S. (2018). Psychological Processes in Chronic Pain: Influences of Reward and Fear Learning as Key Mechanisms - Behavioral Evidence, Neural Circuits, and Maladaptive Changes. *Neuroscience* 387, 72–84. doi:10.1016/j.neuroscience.2017.08.051

Neugebauer, V. (2020). Amygdala Physiology in Pain. *Handb. Behav. Neurosci.* 26, 101–113. doi:10.1016/b978-0-12-815134-1.00004-0

Neugebauer, V., Han, J. S., Adwanikar, H., Fu, Y., and Ji, G. (2007). Techniques for Assessing Knee Joint Pain in Arthritis. *Mol. Pain* 3, 8. doi:10.1186/1744-8069-3-8

Nguyen, T. D., Prykhodko, O., Hållenius, F. F., and Nyman, M. (2019). Monobutyrin Reduces Liver Cholesterol and Improves Intestinal Barrier Function in Rats Fed High-Fat Diets. *Nutrients* 11 (2). doi:10.3390/nu11020308

Portfors, C. V. (2007). Types and Functions of Ultrasonic Vocalizations in Laboratory Rats and Mice. *J. Am. Assoc. Lab. Anim. Sci.* 46 (1), 28–34.

Presto, P., Ji, G., Junell, R., Griffin, Z., and Neugebauer, V. (2021). Fear Extinction-Based Inter-individual and Sex Differences in Pain-Related Vocalizations and Anxiety-like Behaviors but Not Nocifensive Reflexes. *Brain Sci.* 11 (10). doi:10.3390/brainsci11101339

Rao, X., Huang, X., Zhou, Z., and Lin, X. (2013). An Improvement of the 2ˆ(-Delta Delta CT) Method for Quantitative Real-Time Polymerase Chain Reaction Data Analysis. *Biostat. Bioinforma. Biomath.* 3 (3), 71–85.

Schneider, L. E., Henley, K. Y., Turner, O. A., Pat, B., Niedzielko, T. L., and Floyd, C. L. (2017). Application of the Rat Grimace Scale as a Marker of Supraspinal Pain Sensation after Cervical Spinal Cord Injury. *J. Neurotrauma* 34 (21), 2982–2993. doi:10.1089/neu.2016.4665

Shen, C. L., Castro, L., Fang, C. Y., Castro, M., Sherali, S., White, S., et al. (2022a). Bioactive Compounds for Neuropathic Pain: An Update on Preclinical Studies and Future Perspectives. *J. Nutr. Biochem.* 104, 108979. doi:10.1016/j.jnutbio.2022.108979

Shen, C. L., Wang, R., Ji, G., Elmassry, M. M., Zabet-Moghaddam, M., Vellers, H., et al. (2022b). Dietary Supplementation of Gingerols- and Shogaols-Enriched Ginger Root Extract Attenuate Pain-Associated Behaviors while Modulating Gut Microbiota and Metabolites in Rats with Spinal Nerve Ligation. *J. Nutr. Biochem.* 100, 108904. doi:10.1016/j.jnutbio.2021.108904

Simon, A., Darcsi, A., Kéry, Á., and Riethmüller, E. (2020). Blood-brain Barrier Permeability Study of Ginger Constituents. *J. Pharm. Biomed. Anal.* 177, 112820. doi:10.1016/j.jpba.2019.112820

Sotocinal, S. G., Sorge, R. E., Zaloum, A., Tuttle, A. H., Martin, L. J., Wieskopf, J. S., et al. (2011). The Rat Grimace Scale: a Partially Automated Method for Quantifying Pain in the Laboratory Rat via Facial Expressions. *Mol. Pain* 7, 55. doi:10.1186/1744-8069-7-55

Sperry, M. M., Yu, Y. H., Welch, R. L., Granquist, E. J., and Winkelstein, B. A. (2018). Grading Facial Expression Is a Sensitive Means to Detect Grimace Differences in Orofacial Pain in a Rat Model. *Sci. Rep.* 8 (1), 13894. doi:10.1038/s41598-018-32297-2

Sud, R., Spengler, R. N., Nader, N. D., and Ignatowski, T. A. (2008). Antinociception Occurs with a Reversal in Alpha 2-adrenoceptor Regulation of TNF Production by Peripheral Monocytes/macrophages from Pro- to Anti-inflammatory. *Eur. J. Pharmacol.* 588 (2-3), 217–231. doi:10.1016/j.ejphar.2008.04.043

Tan, P. H., Ji, J., Yeh, C. C., and Ji, R. R. (2021). Interferons in Pain and Infections: Emerging Roles in Neuro-Immune and Neuro-Glial Interactions. *Front. Immunol.* 12, 783725. doi:10.3389/fimmu.2021.783725

Teixeira-Santos, L., Albino-Teixeira, A., and Pinho, D. (2020). Neuroinflammation, Oxidative Stress and Their Interplay in Neuropathic Pain: Focus on Specialized Pro-resolving Mediators and NADPH Oxidase Inhibitors as Potential Therapeutic Strategies. *Pharmacol. Res.* 162, 105280. doi:10.1016/j.phrs.2020.105280

Thompson, J. M., and Neugebauer, V. (2019). Cortico-limbic Pain Mechanisms. *Neurosci. Lett.* 702, 15–23. doi:10.1016/j.neulet.2018.11.037

Tjendraputra, E., Tran, V. H., Liu-Brennan, D., Roufogalis, B. D., and Duke, C. C. (2001). Effect of Ginger Constituents and Synthetic Analogues on Cyclooxygenase-2 Enzyme in Intact Cells. *Bioorg Chem.* 29 (3), 156–163. doi:10.1006/bioo.2001.1208

Veinante, P., Yalcin, I., and Barrot, M. (2013). The Amygdala between Sensation and Affect: a Role in Pain. *J. Mol. Psychiatry* 1 (1), 9. doi:10.1186/2049-9256-1-9

Yang, C., Fang, X., Zhan, G., Huang, N., Li, S., Bi, J., et al. (2019). Key Role of Gut Microbiota in Anhedonia-like Phenotype in Rodents with Neuropathic Pain. *Transl. Psychiatry* 9 (1), 57. doi:10.1038/s41398-019-0379-8

Conflict of Interest: The authors declare that the research was conducted in the absence of any commercial or financial relationships that could be construed as a potential conflict of interest.

Publisher's Note: All claims expressed in this article are solely those of the authors and do not necessarily represent those of their affiliated organizations, or those of the publisher, the editors and the reviewers. Any product that may be evaluated in this article, or claim that may be made by its manufacturer, is not guaranteed or endorsed by the publisher.

frontiers | Frontiers in Pharmacology

ORIGINAL RESEARCH
published: 19 July 2022
doi: 10.3389/fphar.2022.920201

Xiongshao Zhitong Recipe Attenuates Nitroglycerin-Induced Migraine-Like Behaviors *via* the Inhibition of Inflammation Mediated by Nitric Oxide Synthase

Song Yang[1,2,3†], *Cong Chen*[4†], *Xiaoyao Liu*[4], *Qianjun Kang*[4], *Quantao Ma*[4], *Pin Li*[1,2,3], *Yujie Hu*[4], *Jialin Li*[4], *Jian Gao*[1,2,3*], *Ting Wang*[1,2,3*] *and Weiling Wang*[1,2,3*]

[1]*Beijing Research Institute of Chinese Medicine, Beijing University of Chinese Medicine, Beijing, China,* [2]*State Administration of Traditional Chinese Medicine Key Laboratory of Famous Doctors and Famous Prescriptions, Beijing, China,* [3]*National Medical Products Administration Key Laboratory for Research and Evaluation of Traditional Chinese, Beijing University of Chinese Medicine, Beijing, China,* [4]*School of Traditional Chinese Medicine, Beijing University of Chinese Medicine, Beijing, China*

Migraine is a major cause of disability worldwide, particularly in young adults and middle-aged women. Xiongshao Zhitong Recipe (XZR) is a traditional Chinese medicine prescription used for treating migraine, but its bioactive components and therapeutic mechanisms remain unclear. We aimed to confirm the therapeutic effect of XZR on migraine and to determine the possible mechanism and bioactive components of XZR. Here, a sensitive UHPLC-LTQ-Orbitrap MS assay was carried out to analyze the ingredients of XZR, and a total of 62 components were identified, including coumarins, phenolic acids, phthalides, flavonoids, and terpenoids; among them, 15 components were identified in the serum samples after XZR treatment. We established a rat model of migraine *via* nitroglycerin (NTG) injection. The *in vivo* experiments demonstrated that XZR attenuated allodynia and photophobia in rats with NTG-induced migraine, and XZR also demonstrated analgesic effects. XZR reversed the abnormal levels of nitric oxide, 5-hydroxytryptamine (5-HT), calcitonin gene-related peptide (CGRP), and substance P (SP) to normal levels. XZR also downregulated inflammatory reactions, including mast cell degranulation and serum IL-1β, IL-6, and TNF-α levels. In terms of mechanism, we revealed that XZR treated NTG-induced migraine through the inhibition of neuronal nitric oxide synthase (nNOS) and inducible nitric oxide synthase (iNOS) expression in both the trigeminal nucleus caudalis (TNC) and periaqueductal gray matter (PAG), as well as the total NOS enzyme activity, which regulated the NF-κB signaling pathway. Additionally, imperatorin and xanthotoxin, two major ingredients of XZR, showed a high binding affinity to nNOS (Gly468-Leu616). *In vitro*, XZR, imperatorin, and xanthotoxin inhibited the nNOS expression and the NF-κB signaling pathway in lipopolysaccharide (LPS)-stimulated PC12 cells. In conclusion, we demonstrated the therapeutic effects of XZR and provided evidence that XZR played a critical anti-inflammatory role by suppressing NOS and NF-κB signaling pathway activation.

OPEN ACCESS

Edited by:
Gokhan Zengin,
Selcuk University, Turkey

Reviewed by:
Fereshteh Farajdokht,
Tabriz University of Medical Sciences, Iran
Sufang Liu,
Texas A&M University, United States

***Correspondence:**
Jian Gao
gaojian_5643@163.com
Ting Wang
wangting1973@sina.com
Weiling Wang
wangwl_1014@163.com

[†]*These authors have contributed equally to this work*

Specialty section:
This article was submitted to Ethnopharmacology, a section of the journal Frontiers in Pharmacology

Received: *14 April 2022*
Accepted: *13 June 2022*
Published: *19 July 2022*

Citation:
Yang S, Chen C, Liu X, Kang Q, Ma Q, Li P, Hu Y, Li J, Gao J, Wang T and Wang W (2022) Xiongshao Zhitong Recipe Attenuates Nitroglycerin-Induced Migraine-Like Behaviors via the Inhibition of Inflammation Mediated by Nitric Oxide Synthase. Front. Pharmacol. 13:920201. doi: 10.3389/fphar.2022.920201

Imperatorin and xanthotoxin were potential bioactive components of XZR. The findings from this study supported that XZR was a candidate herbal drug for migraine therapy.

Keywords: Xiongshao Zhitong Recipe (XZR), migraine, NOS, NF-κB, SPR

INTRODUCTION

Migraine is a complex disorder characterized by recurrent disabling attacks of headache accompanied by nausea, vomiting, and paroxysmal neurovascular dysfunction (Raggi et al., 2022). The Global Burden of Diseases, Injuries, and Risk Factors Study 2016 (GBD 2016) showed that migraine was one of the leading causes of disability worldwide, especially among young adults and middle-aged women (Collaborators, 2018). The average morbidity and lifetime prevalence of migraine were 13.2% and 19%, respectively (Victor et al., 2010; Arroyo-Quiroz et al., 2014).

Although the mechanisms underlying migraine remain poorly understood, several main potential mechanisms have been suggested by researchers, including the activation of meningeal afferents, neuropeptide release, abnormal cranial vasodilation, neurogenic inflammation, and central pain sensitization (Edvinsson and Haanes, 2021). Much evidence supports that nitric oxide (NO) plays an important role in triggering migraine (Thomsen and Olesen, 2001). The synthesis of NO is catalyzed by nitric oxide synthase (NOS), which oxidizes a nitrogen atom in the guanidine group at the end of L-arginine (L-Arg) (Yuan et al., 2021). Through the NO-cyclic guanosine monophosphate (cGMP) pathway, NO can induce the initial phase of migraine headache associated with cerebral vasodilation and then trigger the delayed phase of migraine pain by stimulating the release of inflammatory neuropeptides, which results in sterile neurogenic inflammation and the sensitization of the perivascular nociceptors in the trigeminovascular system that promote migraine attacks (Reuter et al., 2001; Guo, 2017). NO also induces neuronal NOS (nNOS), which can be considered a significant marker of the sensitization of the trigeminal system (Spekker et al., 2021). Studies have also shown that the nuclear factor-kappa B (NF-κB) pathway plays an important role in the neurogenic inflammation of migraines. Following inflammatory injury, the NF-κB p65 subunit can be transferred to the nucleus and bind to specific DNA sequences, thereby initiating gene transcription and inducing the expression of multiple cytokines, including tumor necrosis factor-α (TNF-α), interleukin-1β (IL-1β), and interleukin-6 (IL-6) (Lai et al., 2019; Moisset et al., 2021).

Current treatments for migraine include general analgesics, such as nonsteroidal anti-inflammatory drugs (NSAIDs); specific painkillers, such as serotonin receptor agonists (such as triptans and 5-HT1B and 5-HT1D inhibitors); calcitonin gene-related peptide (CGRP) receptor antagonists [anti-CGRP monoclonal antibodies (mAbs)]; and selective CGRP receptor inhibitors (Silberstein, 2004). However, the adverse reactions of NSAIDs and triptans, including dizziness, nasopharyngitis, medication-overuse headache, and vascular risks, increase the difficulties of migraine treatment (Syed, 2016). Although anti-CGRP monoclonal antibodies effectively control migraines, a case series of probable migraine-related stroke, systemic inflammatory disorders, polyarthralgia, and reversible cerebral vasoconstriction syndrome following CGRP inhibition have been reported (Assas, 2021). Therefore, it is necessary to seek potential therapeutics for migraine.

Traditional Chinese medicine (TCM) has been used in the clinical treatment of migraine for many years (Li et al., 2011; Huang et al., 2020). Xiongshao Zhitong Recipe (XZR) is often used in the clinic for treating headaches due to wind–phlegm–blood stasis. A clinical study revealed that XZR shows a variety of desirable pharmacological effects on migraines, for instance, supporting Qi, promoting blood circulation, dispelling wind, and relieving pain (Su et al., 2016). However, the active ingredients and mechanism of XZR in treating migraine remain unknown. In this study, we established a migraine model with nitroglycerin (NTG) and evaluated the effects of XZR on migraine. In addition, we developed a surface plasmon resonance (SPR)-based high-throughput screening platform. With this platform and UHPLC-LTQ-Orbitrap MS, Western blotting, and immunofluorescence, we eventually determined the chemical composition of XZR and its possible mechanism of action in the treatment of migraine, and we preliminarily confirmed the active components in XZR with the NOS inhibitory activity.

MATERIALS AND METHODS

Chemicals and Reagents

XZR comprises eight botanical drugs: Conioselinum anthriscoides "Chuanxiong" [*Apiaceae*] (No. 20200728), *Paeonia lactiflora* Pall. (No. 20200614), *Angelica dahurica* (Hoffm.) Benth. & Hook.f. ex Franch. & Sav. (No. 20200526), *Salvia miltiorrhiza* Bunge (No. 20200511), *Brassica juncea* (L.) Czern (No. 20200528), *Smilax glabra* Roxb (No. 20200611), *Beauveria bassiana* (Bals.) Vuillant (No. 20200212), and *Xanthium strumarium* subsp. strumarium (No. 20191128). Botanical drugs were provided by Bencao Fangyuan Group Co., Ltd. (Chongqing, China) and identified by Prof. Xiangri Li, Beijing University of Chinese Medicine. The samples of XZR (No. 20210111) were deposited in the Beijing Research Institute of Chinese Medicine, Beijing University of Chinese Medicine.

Rizatriptan was purchased from Hubei Ouly Pharmaceutical Co., Ltd. (Hubei, China). NTG injections were purchased from Beijing Yimin Pharmaceutical (China, 1 mg/ml). An NO assay kit (No. 13-2-1) and NOS activity assay kit (No. 14-1) were purchased from Nanjing Jiancheng Bioengineering Institute (Nanjing, China). 5-Hydroxytryptamine (5-HT) (No. CEA808Ge), TNF-α (No. SEA133Ra), and IL-1β (No. SEA563Ra) enzyme-linked immunosorbent assay (ELISA) kits

and recombinant nitric oxide synthase 1 (NOS1) (RPA815Ra02) were purchased from Cloud-Clone Corp. (Wuhan, China). The IL-6 ELISA kit was from BioLegend (San Diego, CA, No. 437107). The CGRP ELISA kit was purchased from Bertin Bioreagent (France, No. 5482). The substance P (SP) ELISA kit was purchased from Cayman (United States, No. 583751). nNOS (C7D7) rabbit mAb (No. 4231), NeuN (E4M5P) mouse mAb (No. 94403), and the NF-κB Pathway Sampler Kit (No. 9936) were purchased from Cell Signaling Technology (United States). The anti-iNOS antibody was purchased from Abcam (United States, No. 3523). Neutral balsam (No. G8590) and toluidine blue O (No. G3670) were purchased from Beijing Solarbio Science Technology Group Co., Ltd. (Beijing, China).

Preparation of Xiongshao Zhitong Recipe Samples

Botanical drugs were weighed in accordance with the proportions of XZR used in the clinic. Eight volumes of pure water were added. The extraction was performed 2 times for 1.5 h each time. After the first extraction, the filtrate was collected, and then six volumes of pure water were added for the second extraction. The combined extracts were filtered and concentrated at 80°C for 9 h under reduced pressure. After vacuum drying, 287.62 g of dry powder was obtained. The drug–extract ratio of XZR was 18.20%.

The intermediate dose of XZR (the equivalent clinical dose) used in rat experiments was calculated with the below formula: intermediate dose of XZR = 70.01 g/day × 18.20% × 6/70 kg.

The clinical raw drug dosage was 70.01 g/person/day, and the drug–extract ratio of XZR was 18.20%. On the basis of an average adult body weight of 70 kg, according to the body surface area (BSA) normalization method (Rockville et al., 2005; Nair and Jacob, 2016; Heinrich et al., 2020), the equivalent dose of human and rats was about 6.

The low dose was half of the equivalent clinical dose, while the high dose was twice the equivalent clinical dose. Accordingly, the three doses of XZR were 0.55, 1.09, and 2.18 g/kg/day, and the dose of rizatriptan was 0.857 mg/kg/day (the equivalent clinical dose).

UHPLC-LTQ-Orbitrap MS Analysis of the Main Xiongshao Zhitong Recipe Components and Serum Components

The dried extract (0.2 g, 65 mesh) was accurately weighed and extracted by infusion with 50 ml of 80% methanol for 30 min. The extracted solution was filtered through a 0.22 μm nylon membrane filter before injection for the analysis of XZR components.

A total of 12 Sprague–Dawley male rats, weighing 250 ± 20 g (age of 6 weeks), were maintained for 12 h with no food but freely available water before treatment administration. The rats were randomly divided into two groups: the normal control group and the XZR group (n = 6). The rats in the XZR group were administered the XZR water extract at a dose of 7.644 g/kg, 7 times the equivalent clinical dose. The same volume of water was administered to the rats in the normal control group. Blood samples were obtained by the retro-orbital puncture at 0, 15, 30, and 60 min after XZR administration. After centrifugation for 15 min at 3,500 rpm, serum samples were acquired, and the mixed serum samples from the same group were purified in solid phase extraction (SPE) microcolumns for further analysis.

The identification of chemical constituents in XZR and the serum was performed with the UHPLC-LTQ-Orbitrap MS method. Chromatographic separation was performed on a Dionex Ultimate 3000 UHPLC Plus Focused Ultra High-Performance Liquid Chromatography System (Thermo Scientific, Santa Clara, CA, United States) comprising a UPLC pump, a DAD detector, scanning from 200 to 800 nm, and a cooling autosampler. The chromatographic conditions were as follows: column: ACQUITY UPLC BEH C18 (1.7 μm, 2.1 mm × 100 mm); solvent system: acetonitrile (A) and water containing 0.1% formic acid (B); gradient elution: 0–30.0 min, 5%–85% A; 30.1–35.0 min, 5% A; flow rate: 0.3 ml/min; injection volume: 10 μl; column temperature: 30°C. MS analysis was performed using an LTQ-OrbitrapXL hybrid mass spectrometer (Thermo Fisher Scientific) fitted with a HESI source and operated in negative and positive ion modes, with a mass range of 150–1,500 and a high resolution set at 30,000 using the normal scan rate. The data-dependent MS/MS events were always performed on the most intense ions detected in full-scan MS. The MS/MS isolation width was 1 amu. Nitrogen was used as the sheath gas, and helium served as the collision gas. The key optimized ESI-MSP parameters were as follows: source temperature: 300.0°C; source voltage: 4 kV; sheath gas (nitrogen): 50 L/min; auxiliary gas flow: 10 arb; capillary voltage: 25 V; and tube lens: 110.0 V. Data were collected and analyzed with Xcalibur 2.1 software (Thermo Fisher Scientific). Three batches of XZR were used to identify the concentrations of paeoniflorin and salvianolic acid B (**Supplementary Material**).

Animals

The 60 specific pathogen-free (SPF) adult male Sprague-Dawley rats (200 ± 20 g) used in the study were provided by Beijing Vital River Laboratory Animal Technique Co., Ltd. (Beijing, China). The animals were kept in the Experimental Animal Center at the Beijing University of Chinese Medicine (Beijing, China) at 22 ± 2°C on a 12-h/12-h light/dark cycle. The animals were given regular feed and free access to water. All studies were strictly performed in accordance with the international ethical guidelines and related ethical regulations of the Beijing University of Chinese Medicine (No. BUCM-4-2021020101-1009).

Migraine Model Induced by Nitroglycerin

The rats were randomly divided into six groups: the control group, NTG control group (NTG group, 10 mg/kg), rizatriptan group (rizatriptan, 0.0857 mg/ml), XZR low-dose group (XZR-L group, 0.55 g/kg), XZR intermediate-dose group (XZR-M group, 1.09 g/kg), and XZR high-dose group (XZR-H group, 2.18 g/kg). Rats in the rizatriptan group, XZR-L group, XZR-M group, and XZR-H group were intragastrically administered the respective drugs once per day for seven consecutive days. All rats, except those in the control group, were subcutaneously injected with NTG 30 min after the last treatment (Zhang et al., 2017). Rats in

the control group were injected with an equivalent volume of distilled water.

Behavioral Test

The frequency of head scratching was measured with a video camera (DSC-WX9, China). Briefly, a video camera was placed away from the cubicle in positions facing the subject. Thirty minutes after NTG injection, all rats were acclimatized to the cubicles for 5 min, and then the scratching behaviors of the rats were recorded for 1.5 h. Scratching behaviors were quantified based on the observations of the defined events [for details, see Chanda et al. (2013)] in a blinded manner and counted by two colleagues from a digital video.

Mechanical Threshold Test

Thirty minutes after NTG injection, the mechanical threshold was tested as described previously (Gautam and Ramanathan, 2021). Briefly, the facial and plantar surfaces of the rat were stimulated with electronic von Frey filaments. A series of filaments (0–60 g) were applied on the facial and plantar surfaces with pressure causing the filament to buckle and held for approximately 6–8 s. The average withdrawal reading of three trials was recorded as the final value.

Light-Aversive Test

A light–dark test was used to evaluate light-aversive behavior 30 min after NTG injection (Bonnet et al., 2019). Briefly, rats were acclimatized for 5 min in a light-aversion chamber (25 cm × 25 cm × 40 cm) before testing. Light-aversive behavior was examined within 30 min after NTG injection. Rats were placed in the light zone of the light-aversion chamber, and data were collected for 30 min. Tests were administered at least 5 min apart.

Toluidine Blue O Dyeing of Dural Mast Cells

The dura mater was isolated at 1.5 h after NTG injection on the 7th day of XZR administration. The isolated dura mater was placed on a glass slide and stained with toluidine blue for 2 min. The dura mater was washed with PBS three times and then fixed with ethanol (95%, 85%, and 75%). Images were taken at ×20 magnification by an Evos FL Auto 2 (Thermo Fisher Scientific, America). Mast cells with inhomogeneous staining, pale cells, and cells with disfigured borders surrounding the positively stained granules were classified as degranulated (Loewendorf et al., 2016). The rate of degranulation was calculated as the number of degranulated cells to the total number of cells.

Biochemical Determination

All rats were anesthetized with 4% pentobarbital sodium at 1.5 h after model establishment. Blood samples were collected from the abdominal aorta to determine plasma 5-HT and serum IL-1β, IL-6, SP, and CGRP levels with the ELISA method, while the level of NO in serum was detected with an NO biochemical kit (Nanjing Jiancheng Institute of Biological Engineering, Nanjing, China) by the colorimetric method. The brain tissues of these rats were used to test the TNF-α level by ELISA.

Western Blot Analysis

The rat trigeminal nucleus caudalis (TNC) and periaqueductal gray matter (PAG) were collected at 1.5 h after model establishment. Tissues were lysed in the RIPA lysis buffer. The protein concentration was determined with a bicinchoninic acid (BCA) kit (Beyotime, China). The protein samples (50 μg) were separated on sodium dodecyl sulfate–polyacrylamide gel electrophoresis (SDS–PAGE) gels and transferred onto polyvinylidene fluoride (PVDF) membranes (Bio-Rad, United States). The membranes were blocked with 5% skim milk for 2 h at room temperature. Then, the membranes were incubated with primary antibodies, namely, anti-iNOS (1:500), anti-NF-κB (1:1,000), anti-nNOS (1:1,000), anti-Iκbα (1:1,000), and anti-Ikkβ (1:1,000), at 4°C overnight. The next day, the membranes were incubated with the secondary antibody for 1 h at room temperature. Then, the protein bands were detected with electrochemiluminescence (ECL) and analyzed with an Amersham Imager 680 (Cytiva, United States).

Immunofluorescence Staining

The rat TCN and PAG were fixed in 4% paraformaldehyde 1.5 h after model establishment, dehydrated with sucrose solution, and coated with ETC. Tissues were cut into 5 μm sections with a Leica CM1900 cryostat. The TCN and PAG sections were washed three times with PBS, blocked in 2% goat serum, and incubated with the following primary antibodies: anti-nNOS (1:50), anti-iNOS (1:50), and anti-NeuN (1:200) overnight at 4°C. On the next day, the samples were incubated with the corresponding secondary antibodies at room temperature for 1 h without light, and then DAPI (10 μg/ml) was added for 10 min to stain the nuclei. Images were obtained using Evos FL Auto2. The relative area and the mean fluorescence intensity were analyzed using ImageJ software.

Affinity Measurement

Biacore T200 was used to detect the specific binding between the main constituents of XZR absorbed in the blood and recombinant nNOS (Gly468-Leu616). Biacore T200 (GE Healthcare) was used to measure the binding affinities (Huang et al., 2021). nNOS (Gly468–Leu616) was diluted in sodium acetate solution (pH 5.0) to a final concentration of 50 μg/ml. The solution of nNOS (Gly468–Leu616) was immobilized on a CM5 sensor chip (GE Healthcare) by amine coupling to reach target densities of 12,000 resonance units (RUs). Immobilized nNOS (Gly468–Leu616) was used to capture the chemical compound. The running buffer contained PBS-T (10 mM sodium phosphate, 150 mM NaCl, 0.005% Tween-20, pH 7.4) and 1% DMSO. Then, eight concentrations of each molecule (0, 1.56, 3.125, 6.25, 12.5, 25, 50, and 100 μM) were injected at a flow rate of 30 μl/min and 25°C. Blank immobilization was performed on one of the sensor chip surfaces for the correction of the binding response. The protein binding time and dissociation time were both 120 s. Sensorgrams were analyzed using Biacore T200 Evaluation version 3.2.1 (Cytiva).

Cell Culture

PC12 cells were purchased from the Cell Resource Center of Shanghai Institutes for Biological Sciences, Chinese Academy of

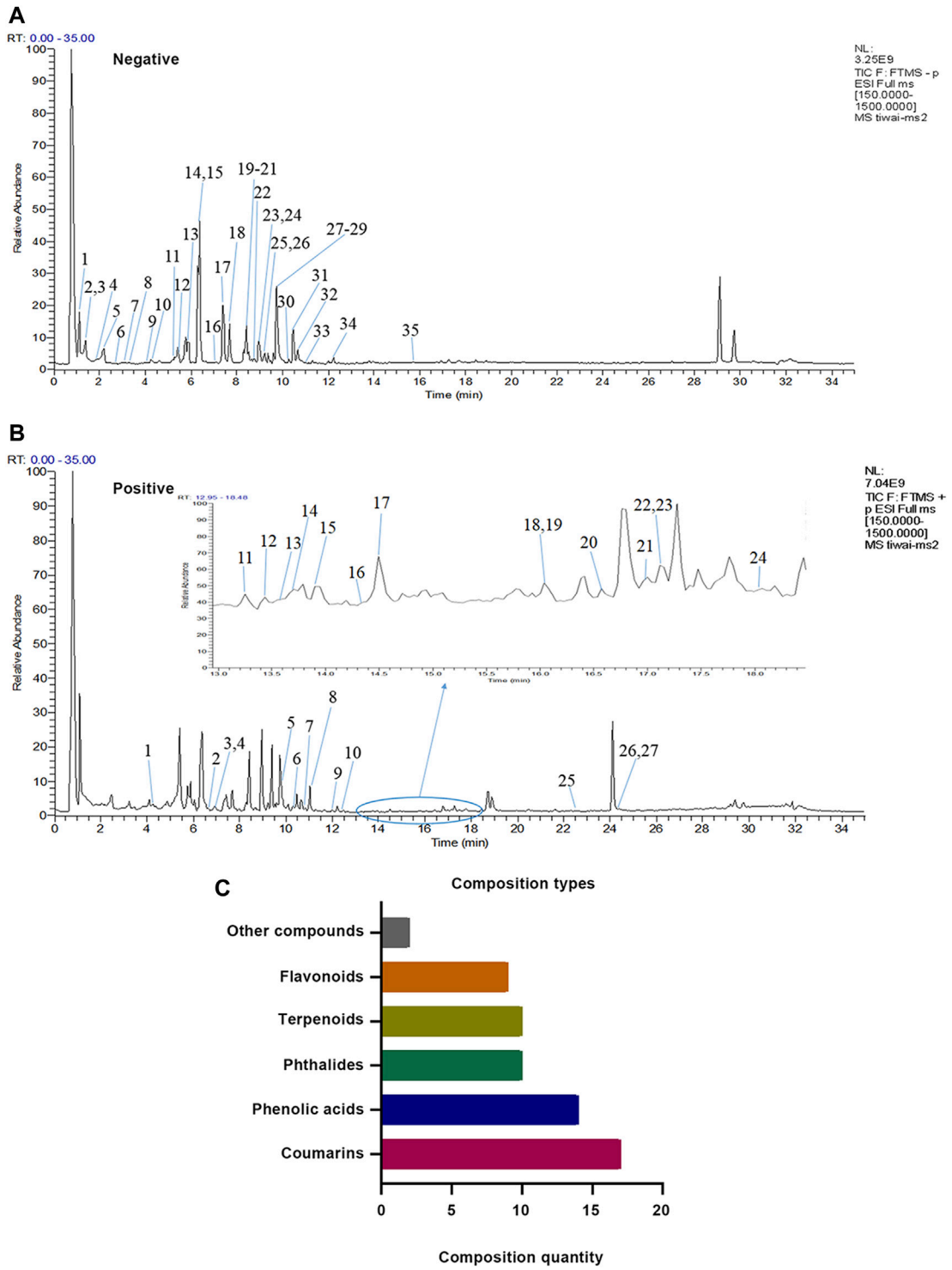

FIGURE 1 | Identification results of the main chemical components of XZR by UHPLC-LTQ-Orbitrap MS. **(A)** Total ion flow diagram of XZR in anion mode (details of Nos. 1–35 are listed in **Supplementary Table S1**). **(B)** Total ion flow diagram of XZR in the positive ion mode (details of Nos. 1–27 are listed in **Supplementary Table S2**). **(C)** Identification of the main components in XZR. XZR, Xiongshao Zhitong Recipe.

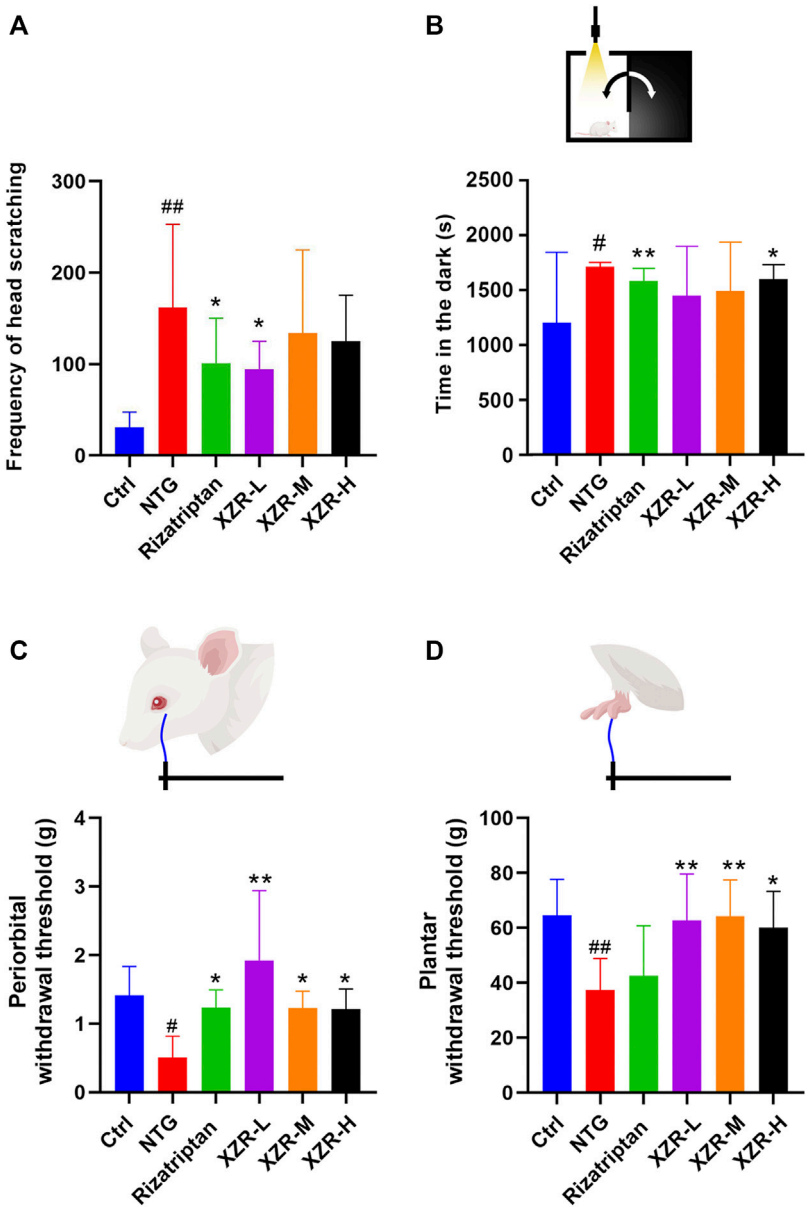

FIGURE 2 | XZR improved migraine-like behavior in the NTG-induced migraine rat model. **(A)** Frequency of head scratching. **(B)** Time in the dark chamber. **(C)** Periorbital withdrawal threshold. **(D)** Plantar withdrawal threshold. Data are presented as the mean ± standard deviation. $^{\#}p < 0.05$, $^{\#\#}p < 0.01$ versus control group, $^{*}p < 0.05$, $^{**}p < 0.01$ versus NTG group, $n = 7–10$. XZR, Xiongshao Zhitong Recipe; NTG, nitroglycerin.

Sciences (Shanghai, China), cultured in 1640 medium supplemented with 10% FBS and 1% penicillin/streptomycin and incubated at 37°C with 5% CO_2. PC12 cells were seeded into 6-well plates at a density of 2×10^4 cells/ml. After 24 h of culture, the culture medium was replaced with a serum-free medium and cultured for another 12 h. Then, the cells were treated with L-NAME (1 mM), XZR (25, 50 and 100 μg/ml), imperatorin (IMP) (12.5, 25, and 50 μM), and xanthotoxin (XAN) (12.5, 25, and 50 μM) for 48 h, and an *in vitro* inflammation model was induced by lipopolysaccharide (LPS) (1 μg/ml) intervention for 0.5 h. The PC12 cells were harvested for Western blot detection.

Statistical Analysis

All data are shown as the mean ± standard deviation (SD). All statistical analyses were performed by SPSS 20.0 statistical software. Statistical differences were determined with a one-way analysis of variance (ANOVA), and a least significant difference (LSD) post hoc test was used for comparing the mean values. The level of significant difference was set at $p < 0.05$.

RESULTS

Chemical Composition of Xiongshao Zhitong Recipe

A total of 62 compounds were identified in XZR, including 27 components in the positive ion mode and 35 components in the negative ion mode (**Figures 1A,B**; **Supplementary Tables S1, S2**). The 62 identified chemical components included 17 coumarins, 14 phenolic acids, 10 phthalides, 10 terpenoids, 9 flavonoids, and 2 other components (**Figure 1C**). The retention times, molecular formulas, and MS2 fragment ions of the identified components in XZR are summarized in **Supplementary Tables S1, S2**.

Xiongshao Zhitong Recipe Improved the Migraine-Like Behaviors of Rats With Nitroglycerin-Induced Migraine

Subcutaneous injection of NTG was used to establish a migraine rat model and evaluate the efficacy of XZR. After the subcutaneous injection of NTG, the typical behaviors of frequent head scratching, cage climbing, and photophobia began to appear in rats of the NTG group within 3–5 min and lasted for at least 2 h.

The behavioral characteristic of head scratching indicated successful establishment of a migraine rat model (Li, et al., 2011; Gao et al., 2014). As shown in **Figure 2A**, rats in the control group occasionally scratched their heads within 90 min of behavioral monitoring. The number of head scratches was nearly 30. Compared with that in the control group, the number of head scratches in the NTG group was markedly increased (161.80 ± 91.15, $p < 0.01$). The rizatriptan (101.00 ± 49.43, $p < 0.05$) and XZR-L (94.50 ± 30.61, $p < 0.05$) groups showed significantly fewer head scratches than the NTG group, while the XZR-M (134.00 ± 90.77) and XZR-H (124.90 ± 50.55) groups also showed fewer head scratches than the NTG group, but the difference was not significant.

In **Figures 2C,D**, NTG injection evoked strong extracephalic tactile allodynia, as the periorbital and plantar withdrawal thresholds (periorbital allodynia and plantar allodynia) were 0.51 ± 0.31 g and 37.37 ± 11.53 g, respectively, which were much lower than those in the control group. Rizatriptan and XZR administration significantly attenuated NTG-induced periorbital allodynia, as the animals had enhanced mean periorbital withdrawal thresholds (rizatriptan group 1.23 ± 0.26 g, $p < 0.05$; XZR-L group 1.92 ± 1.02 g, $p < 0.01$; XZR-M and XZR-H groups, 1.23 ± 0.25 g and 1.22 ± 0.29 g, respectively, $p < 0.05$). Furthermore, XZR treatments significantly attenuated NTG-induced plantar allodynia, as the mean plantar withdrawal thresholds in rats were enhanced (XZR-L and XZR-M groups 62.73 ± 16.88 g and 64.23 ± 13.26 g, respectively, $p < 0.01$; XZR-H group 60.07 ± 13.22 g, $p < 0.05$). XZR also exhibited an analgesic effect in the acetic-acid-induced writhing model, as represented by a significant decrease in the frequency of writhing (**Supplementary Figure S1**).

In addition to pain, the disabling symptoms of migraine often include photophobia (Bonnet, et al., 2019). The light-aversive behavior (photophobia) of rats after NTG injection was evaluated using the light–dark transition test. As shown in **Figure 2B**, 30 min after NTG injection, the rats in the NTG group spent 1.4-fold more time in the dark chamber than those in the control group. Rats in the rizatriptan (1584.00 ± 111.80 s) and XZR-H (1602 ± 126.50 s) groups showed no signs of photophobia, as the animals spent significantly less time in the dark chamber than those in the NTG group (1713.00 ± 38.42 s).

Altogether, these data indicated that XZR effectively attenuated NTG-induced cephalic and extracephalic tactile allodynia in rats with migraine.

Xiongshao Zhitong Recipe Regulated Migraine Mediators in the Nitroglycerin-Induced Migraine Rat Model

The pathological response of migraine is closely related to the release of related neuropeptides, such as CGRP and SP, and neurotransmitters, such as 5-HT. ELISA was performed to evaluate the levels of these migraine mediators in serum and plasma.

As shown in **Figure 3A**, the level of serum CGRP was significantly increased in the NTG group (127.66 ± 12.98 pg/ml) compared with that in the control group (104.93 ± 13.52 pg/ml), while compared with the NTG group, the levels of serum CGRP in the XZR groups (XZR-L group 124.53 ± 15.49 pg/ml, $p > 0.05$; XZR-M group 107.33 ± 12.75 pg/ml, $p < 0.05$; and XZR-H group 98.27 ± 9.93 pg/ml, $p < 0.01$) were significantly decreased in a dose-dependent manner. Rats in the XZR-H group even showed a return of the high level of serum CGRP to normal levels. Furthermore, there was a significant decrease in serum CGRP levels after rizatriptan treatment (89.50 ± 11.18, $p < 0.01$).

The plasma 5-HT concentration (36.19 ± 1.34 ng/ml, $p < 0.01$) was significantly decreased in the NTG group compared with that in the control group (64.25 ± 32.15 ng/ml). After XZR treatments, plasma 5-HT concentrations were increased, and the optimal effect was seen in the XZR-M group (57.71 ± 10.57 ng/ml, $p < 0.05$) (**Figure 3B**).

Although the levels of SP did not significantly change after the interventions, there was a clear downward trend in the XZR-L group (**Figure 3C**).

Xiongshao Zhitong Recipe Reduced Markers of Inflammation in the Nitroglycerin-Induced Migraine Rat Model

The degranulation of dural mast cells indicates local inflammation, nociceptive afferent activation of TG neurons, and vasodilation (Irmak et al., 2019), suggesting that activated dural mast cells may mediate headache. Mast cell degranulation of the dura was detected in our experiment. Toluidine blue staining showed that mast cells in the control group were long, spindle-shaped, and dark purple. Mast cells in the NTG group were irregular in shape, enlarged in volume, and released granular substances, which were significantly alleviated after XZR treatment (**Figure 4A**). As shown in **Figure 4B**, the percentage of degranulated mast cells in rats in the NTG group (47.73% ± 11.41%) was much higher than that in the control group (19.06% ±

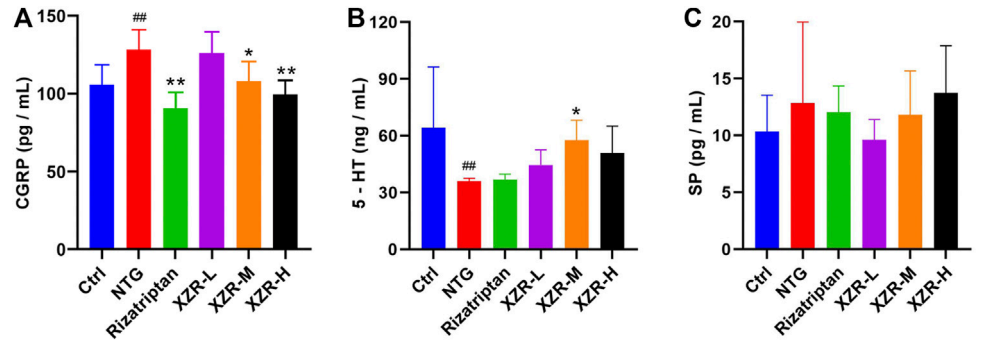

FIGURE 3 | XZR regulated neuropeptide and neurotransmitter levels in rats with NTG-induced migraine. **(A)** CGRP in serum, $n = 6$, **(B)** 5-HT in plasma, $n = 6$, and **(C)** SP in serum, $n = 5$. Data are presented as the mean ± standard deviation. $^{\#\#}p < 0.01$ versus the control group, $^{*}p < 0.05$, $^{**}p < 0.01$ versus the NTG group. XZR, Xiongshao Zhitong Recipe; CGRP, calcitonin gene-related peptide; 5-HT, 5-hydroxytryptamine; SP, substance P; NTG, nitroglycerin.

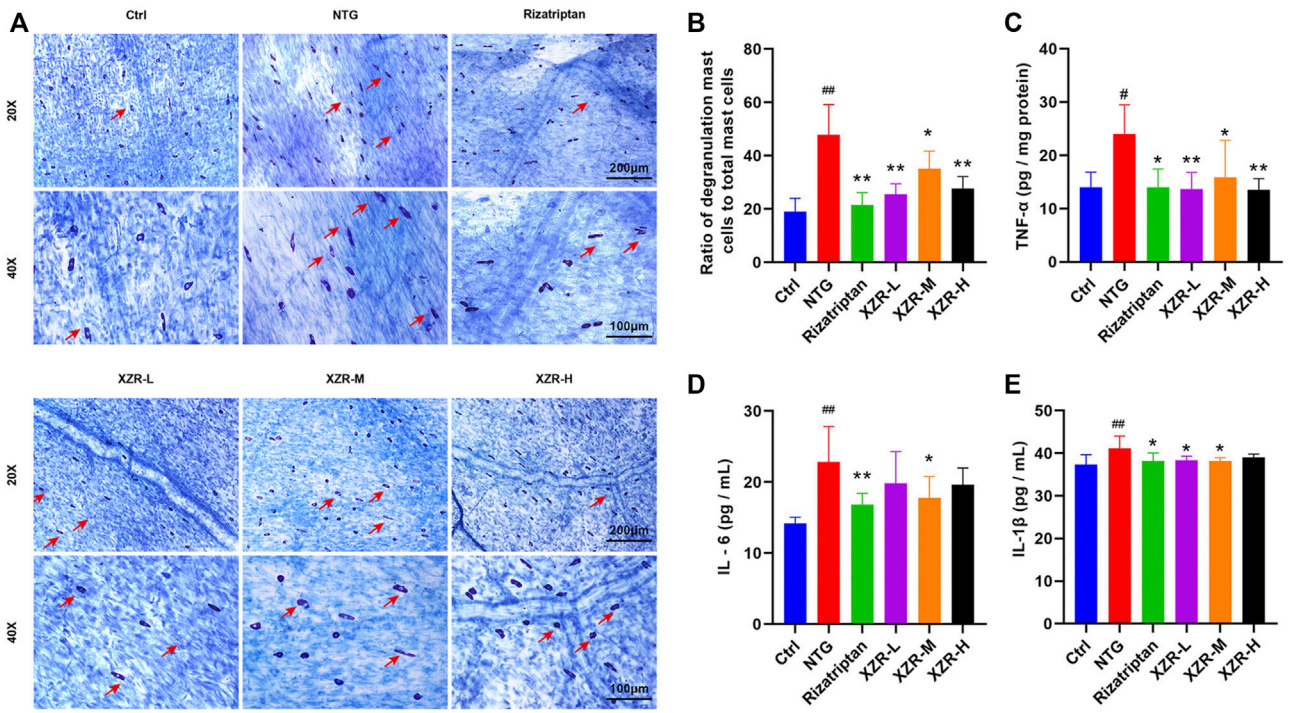

FIGURE 4 | XZR reduced the inflammation of rats with NTG-induced migraine. **(A)** Toluidine blue staining of mast cells in the dura (original magnification ×20 and ×40). Scale bars = 200 μm (×20) and 100 μm (×40). The arrow indicates degranulated mast cells. **(B)** Ratio of degranulated mast cells to total mast cells. **(C)** TNF-α in brain and **(D)** IL-6 and **(E)** IL-1β in serum. Data are presented as the mean ± standard deviation, $n = 5$–6. $^{\#}p < 0.05$, $^{\#\#}p < 0.01$ versus the control group, $^{*}p < 0.05$, $^{**}p < 0.01$ versus the NTG group. XZR, Xiongshao Zhitong Recipe; NTG, nitroglycerin.

4.97%, $p < 0.01$). Compared with the NTG group, the percentages of degranulated mast cells in the dura in the rizatriptan (21.52% ± 4.65%), XZR-L (25.52% ± 3.94%), and XZR-H groups (27.66% ± 4.48%) were obviously decreased ($p < 0.01$).

To further investigate the effect of XZR on inflammation, the secretion of cytokines, including TNF-α, IL-1β, and IL-6, was also detected. As shown in **Figures 4C–E**, compared with the control group, the level of TNF-α (24.05 ± 5.42 pg/mg protein) in the midbrain and the concentrations of IL-1β (41.11 ± 2.92 pg/ml) and IL-6 (22.80 ± 5.02 pg/ml) in serum were significantly increased in the NTG group ($p < 0.01$). Rizatriptan almost decreased the TNF-α (14.04 ± 3.41 pg/mg protein), IL-6 (16.83 ± 1.59 pg/ml), and IL-1β (38.21 ± 1.86 pg/ml) concentrations to normal levels. Moreover, intermediate-dose XZR had a similar beneficial effect, as it reversed the high levels of TNF-α (15.91 ± 6.93 pg/mg protein), IL-1β (38.20 ± 0.76 pg/ml), and IL-6 (17.76 ± 3.02 pg/ml) in rats with migraine

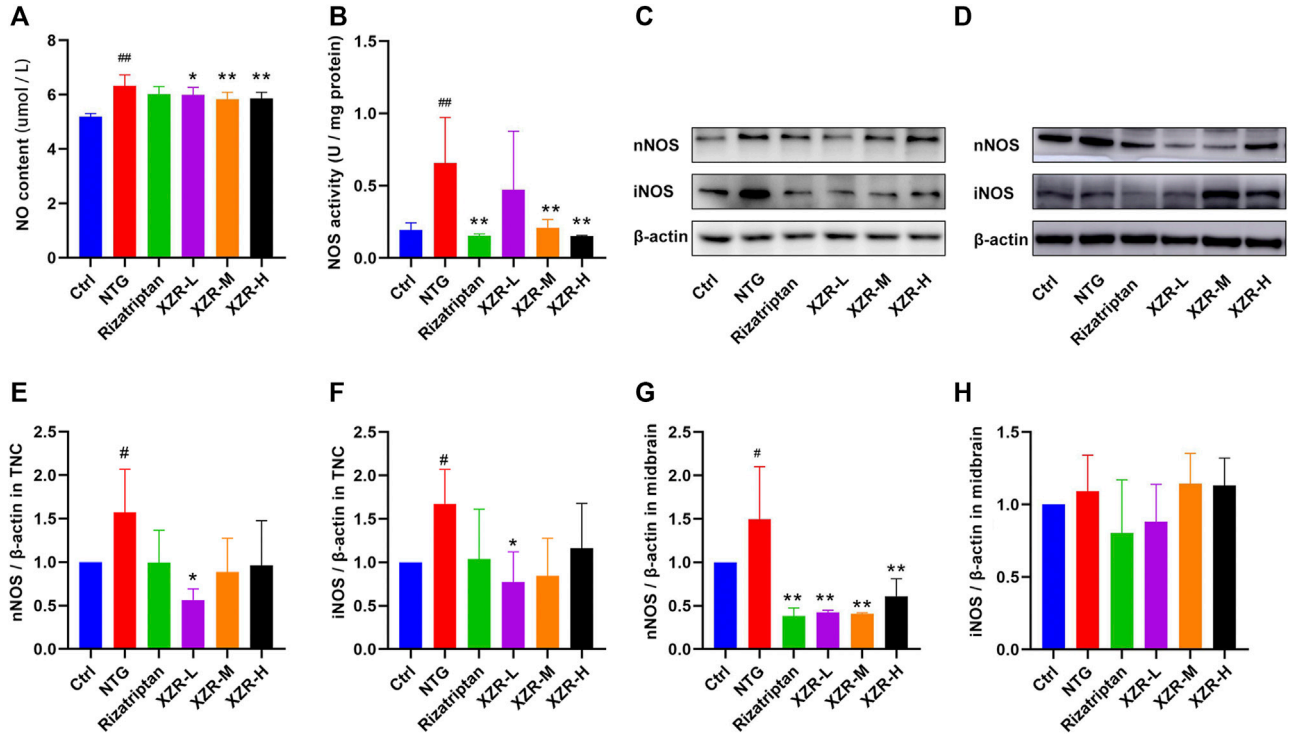

FIGURE 5 | XZR inhibited the NOS-mediated production of NO in rats with NTG-induced migraine. **(A)** NO level and **(B)** NOS activity in midbrain, $n = 6$. **(C,D)** Relative expression levels of nNOS and iNOS in the TNC and midbrain were determined by Western blotting. **(E,F)** Relative expression levels of nNOS and iNOS in the TNC. **(G,H)** Relative expression levels of nNOS and iNOS in the midbrain. Data are presented as the mean ± standard deviation, $n = 3$. $^{\#}p < 0.05$, $^{\#\#}p < 0.01$ versus control group, $^{*}p < 0.05$, $^{**}p < 0.01$ versus the NTG group. XZR, Xiongshao Zhitong Recipe; TNC, trigeminal nucleus caudalis; NTG, nitroglycerin.

($p < 0.05$). Both the XZR-L (13.73 ± 3.07 pg/mg protein) and XZR-H (13.57 ± 2.06 pg/mg protein) groups showed significantly decreased TNF-α levels ($p < 0.01$), and the XZR-L group (38.87 ± 0.93 pg/ml) showed obviously reduced levels of IL-1β, compared with the NTG group ($p < 0.05$).

Xiongshao Zhitong Recipe Inhibited Nitric Oxide Synthase-Mediated Nitric Oxide Production in Rats With Nitroglycerin-Induced Migraine

As an endogenous gaseous signaling molecule, NO regulation is altered in migraine pathogenesis, and NO is endogenously produced in the body by NOS. NO and NOS are clearly important regulators of migraine (Pradhan et al., 2018). ELISA was performed to evaluate the NO level and NOS activity in plasma. As shown in **Figure 5A**, the level of plasma NO in the NTG group (6.33 ± 0.40 μM) was significantly increased compared with that in the control group (5.19 ± 0.12 μM, $p < 0.01$), and XZR (XZR-L 5.99 ± 0.28 μM, $p < 0.05$; XZR-M 5.84 ± 0.25 μM, $p < 0.01$; XZR-H 5.86 ± 0.23 μM, $p < 0.01$) significantly reduced the NO levels. More importantly, the NOS activity in the NTG group (0.66 ± 0.32, $p < 0.01$) was much higher, nearly 3-fold, than that in the control group (0.19 ± 0.05) (**Figure 5B**). Compared with treatment with NTG, the NOS activity was obviously decreased after treatment with rizatriptan (0.15 ± 0.01, $p < 0.01$) and the intermediate (0.21 ± 0.06, $p < 0.01$) and high (0.15 ± 0.01, $p < 0.01$) doses of XZR, which was consistent with the NO results.

In addition, Western blot analysis was performed to observe the expression of nNOS and iNOS in the TNC and midbrain. In the TNC, the results showed a significantly increased expression of nNOS (1.57 ± 0.50, $p < 0.05$) and iNOS (1.67 ± 0.40, $p < 0.05$) in the NTG group (**Figures 5C,E,F**), reduced nNOS expression levels in the XZR-L group (0.56 ± 0.13, $p < 0.05$), and the return of iNOS expression to normal levels in the XZR-L group (0.77 ± 0.35, $p < 0.05$). In the midbrain, the abnormal expression of nNOS was observed only in the NTG group (1.50 ± 0.61), and all treatments, including rizatriptan (0.38 ± 0.09, $p < 0.01$) and low (0.43 ± 0.02, $p < 0.01$), intermediate (0.41 ± 0.01, $p < 0.01$) and high (0.61 ± 0.20, $p < 0.01$) doses of XZR, downregulated nNOS expression levels compared with those in the NTG group (**Figures 5D,G,H**).

For further confirmation, the expression and localization of nNOS and iNOS in the rat spinal TNC and PAG were observed by immunofluorescence. The results of the immunofluorescence double-label experiments were shown in **Figure 6**. In the TNC, the fluorescence intensities of nNOS (65.36 ± 12.97, $p < 0.01$; **Figures 6A,E**) and iNOS (135.30 ± 39.62, $p < 0.05$; **Figures 6B,F**) were significantly increased in the NTG group compared with those in the control group, and the fluorescence intensity of nNOS was

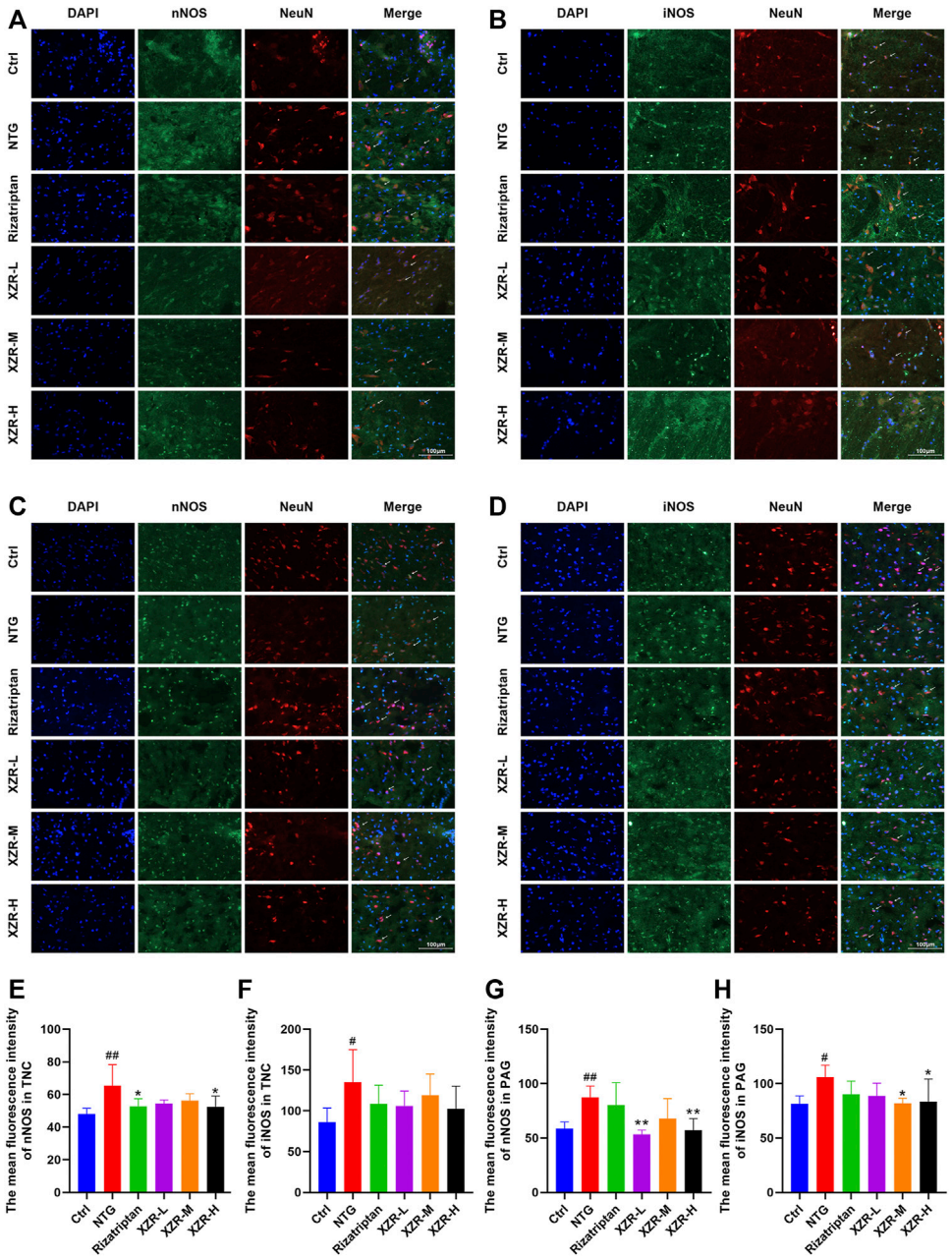

FIGURE 6 | XZR reduced the NOS expression in the TNC and PAG. **(A,B)** Immunofluorescence of nNOS and iNOS in the TNC and **(C,D)** PAG. Immunofluorescence double-label, DAPI (blue), nNOS and iNOS (green), and NeuN (red), scale bar = 100 μm. **(E,F)** The mean fluorescence intensity of nNOS and iNOS in the TNC. **(G,H)** The mean fluorescence intensity of nNOS and iNOS in the PAG. Data are presented as the mean ± standard deviation, $n = 6$. $^{\#}p < 0.05$, $^{\#\#}p < 0.01$ versus the control group, $^{*}p < 0.05$, $^{**}p < 0.01$ versus the NTG group. XZR, Xiongshao Zhitong Recipe; TNC, trigeminal nucleus caudalis; NTG, nitroglycerin; PAG, periaqueductal gray.

significantly decreased in the rizatriptan and XZR-H groups compared with that in the NTG group (52.83 ± 4.52 and 52.45 ± 6.56, respectively, $p < 0.05$). In the PAG, the fluorescence intensities of nNOS (87.26 ± 10.49, $p < 0.01$; **Figures 6C,G**) and iNOS (105.80 ± 11.16, $p < 0.05$; **Figures 6D,H**) were increased in the NTG group compared with those in the control group, while the fluorescence intensity of nNOS in the XZR-L and XZR-H groups (53.26 ± 4.06 and 57.01 ± 10.76, respectively, $p < 0.01$) was significantly decreased and the fluorescence intensity of iNOS in the XZR-M and XZR-H groups (81.86 ± 4.73 and 83.39 ± 20.85, respectively, $p < 0.05$) was decreased compared to that in the NTG group.

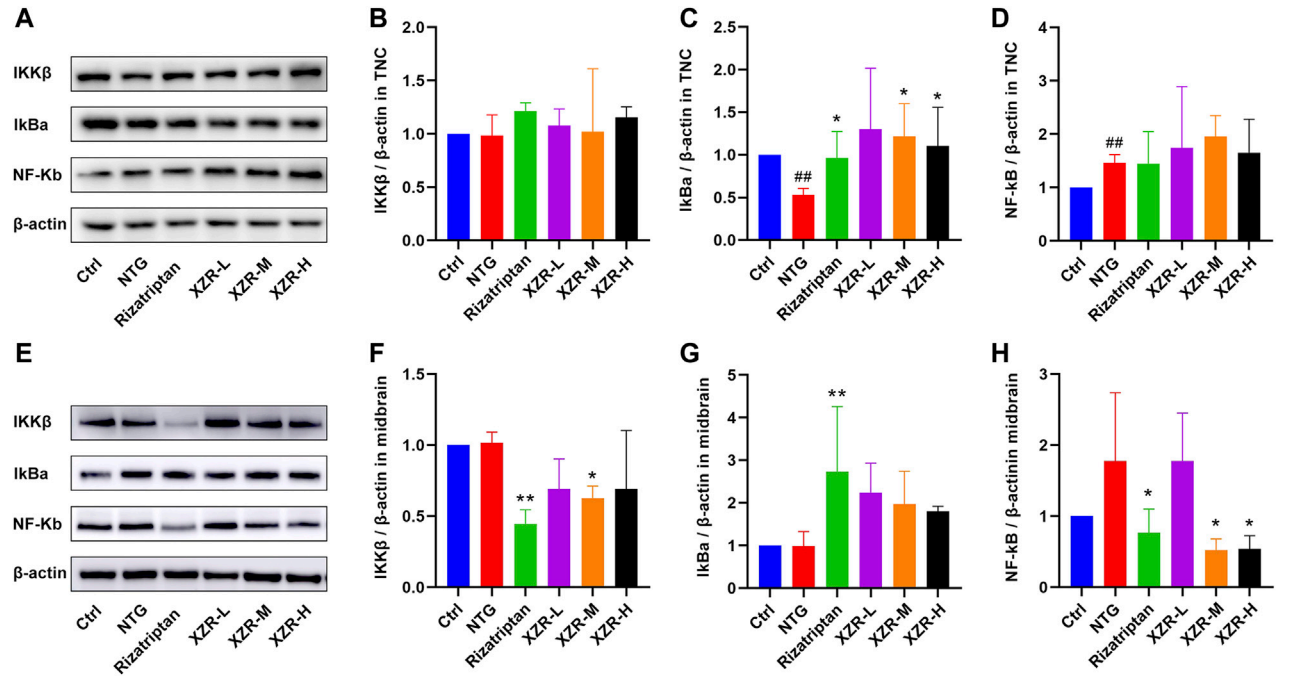

FIGURE 7 | XZR inhibited inflammation *via* the NF-κB signaling pathway. **(A)** Representative Western blot images of IKKβ, IκBα, and NF-κB expression in the TNC. **(B)** Relative expression of IKKβ in the TNC. **(C)** Relative expression of IκBα in the TNC. **(D)** Relative expression of NF-κB in the TNC. **(E)** Representative Western blot images of IKKβ, IκBα, and NF-κB expression in the midbrain. **(F)** Relative expression of IKKβ in the midbrain. **(G)** Relative expression of IκBα in the midbrain. **(H)** Relative expression of NF-κB in the midbrain. Data are presented as the mean ± standard deviation, $n = 3–5$. $^{\#\#}p < 0.01$ versus the control group, $^{*}p < 0.05$, $^{**}p < 0.01$ versus the NTG group. XZR, Xiongshao Zhitong Recipe; NTG, nitroglycerin.

Xiongshao Zhitong Recipe Inhibited Inflammation *via* the NF-κB Signaling Pathway

Accompanied by the abnormal expression of cytokines and NOS, the NF-κB signaling pathway is also involved in the neurogenic inflammation caused by NTG-induced migraine. Furthermore, Western blotting was performed to investigate the expression of proteins in the NF-κB signaling pathway, including IKKβ, IκBα, and NF-κB in the TNC and midbrain, and the effect of XZR.

As shown in **Figures 7A–D**, in the TNC, the expression level of IκBα (0.53 ± 0.08, $p < 0.01$) was obviously reduced and that of NF-κB (1.46 ± 0.15, $p < 0.01$) was increased in the NTG group compared with that in the control group, while rizatriptan (0.96 ± 0.31, $p < 0.05$) and intermediate (1.22 ± 0.38, $p < 0.05$) and high (1.10 ± 0.46, $p < 0.05$) doses of XZR markedly increased the expression of IκBα.

In the midbrain (**Figures 7E,F**), the expression level of IKKβ in the rizatriptan (0.45 ± 0.10, $p < 0.01$) and XZR-M (0.63 ± 0.09, $p < 0.05$) groups was obviously reduced after treatment compared with that in the NTG group (1.02 ± 0.08). **Figures 7E,G** show that the IκBα expression in the rizatriptan group (2.73 ± 1.53, $p < 0.01$) was significantly increased, and low (2.2 ± 0.69), intermediate (1.97 ± 0.78), and high (1.80 ± 0.12) doses of XZR showed a tendency to increase the IκBα expression compared with that in the NTG group (0.99 ± 0.34). **Figures 7E,H** show that NF-κB expression in the rizatriptan (0.77 ± 0.33), XZR-M (0.52 ± 0.16), and XZR-H (0.54 ± 0.19) groups was obviously reduced after treatment compared with that in the NTG group (1.78 ± 0.96, $p < 0.05$).

Potential Target Analysis of Xiongshao Zhitong Recipe in Treating Migraine

Based on the above results, we provide strong evidence for a role of XZR in the treatment of migraine. However, the pharmacodynamic basis and molecular mechanism of XZR in its effect on migraine remain unclear. TCM prescriptions are characterized by multiple components, multiple targets, and multiple pathways. Therefore, the main constituents of XZR dissolved in serum were detected by the UHPLC-LTQ-Orbitrap MS. As shown in **Figures 8A,B**, a total of 15 components of XZR (including 7 coumarins, 3 phthalides, 3 terpenoids, and 2 phenolic acids) were identified in serum samples after XZR treatment—9 in the positive ion mode and 6 in the negative ion mode. The retention times, molecular formulas, and MS2 fragment ions of the identified exogenous ingredients of XZR are summarized in **Supplementary Tables S3 and S4**.

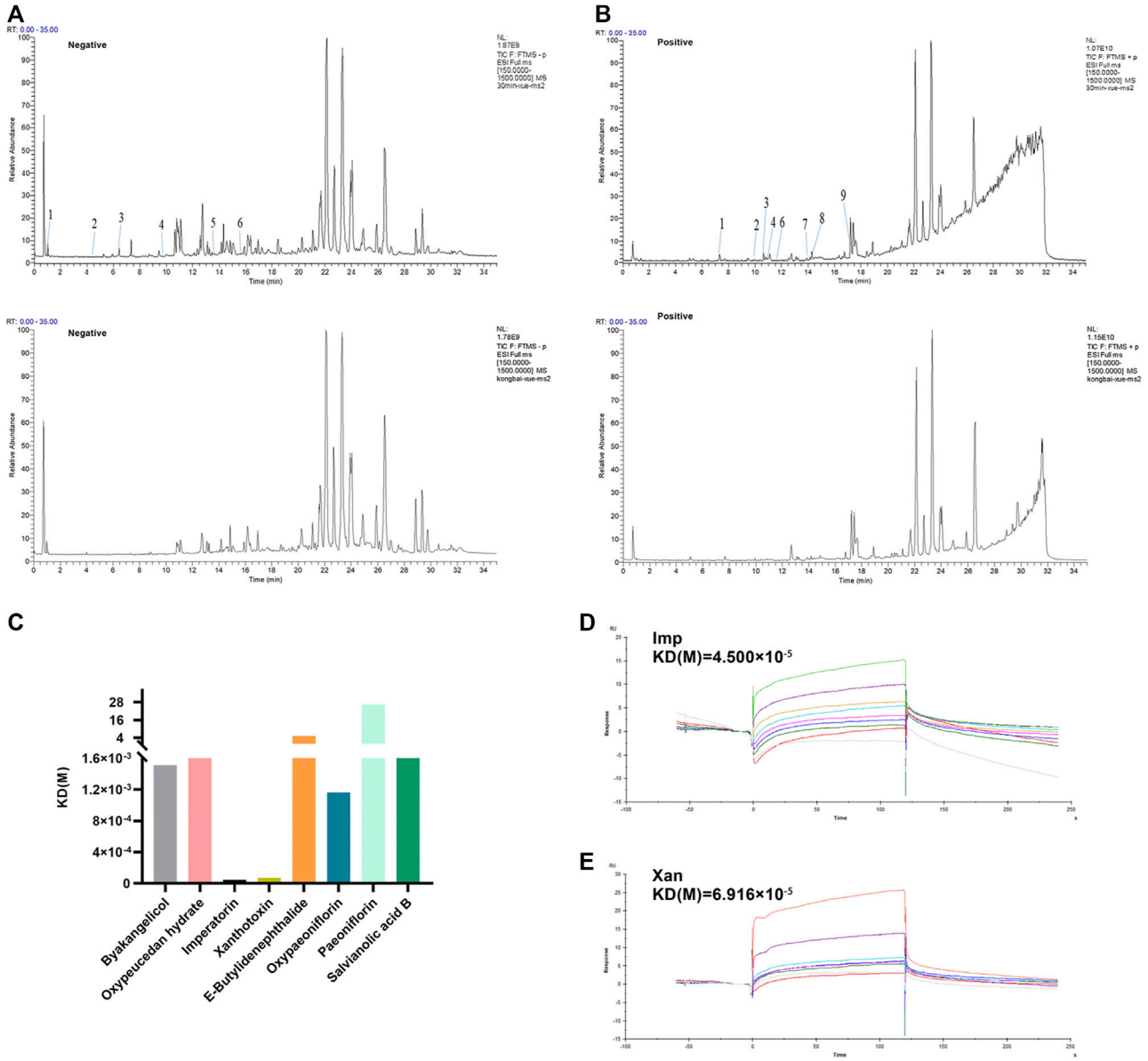

FIGURE 8 | Analysis of candidate targets of XZR against migraine. **(A)** Chromatographic and mass spectral data of the chemical compounds of XZR in the serum analyzed by UHPLC-LTQ-Orbitrap MS (negative mode) (top: serum sample acquired after XZR administration; bottom: blank serum sample. The details of Nos. 1–6 are listed in **Supplementary Tables S3**. **(B)** Chromatographic and mass spectral data of the chemical compounds of XZR in the serum analyzed by UHPLC-LTQ-Orbitrap MS (positive mode) (top: serum sample acquired after XZR administration; bottom: blank serum sample. The details of Nos. 1–9 are listed in **Supplementary Tables S4**. **(C)** Biacore analysis of eight compounds identified in serum bound to nNOS (Gly468–Leu616). **(D)** Biacore analysis of IMP bound to nNOS (Gly468–Leu616). **(E)** Biacore analysis of XAN bound to nNOS (Gly468–Leu616). XZR, Xiongshao Zhitong Recipe; Imp, imperatorin; Xan, xanthotoxin.

SPR is a novel and straightforward methodology used to study protein–compound interactions. Among the binding results between nNOS and the 15 constituents of XZR, imperatorin (Imp) and xanthotoxin (Xan) were found to directly bind to nNOS (Gly468–Leu616) in a concentration-dependent manner and showed a high affinity [K_D (Imp) = 0.45 μM, K_D (Xan) = 0.69 μM, respectively] (**Figures 8C–E**). However, the other components did not show such binding patterns.

Imperatorin and Xanthotoxin Inhibited the Nitric Oxide Synthase/NF-κB Signaling Pathway *In Vitro*

To validate the potential effect of imperatorin and xanthotoxin on the NOS/NF-κB signaling pathway, *in vitro* experiments were conducted. As shown in **Figures 9A,B**, nNOS expression was significantly higher in LPS-stimulated PC12 cells (1.68 ± 0.20) than in untreated cells ($p < 0.05$). Treatment with 25 μg/ml,

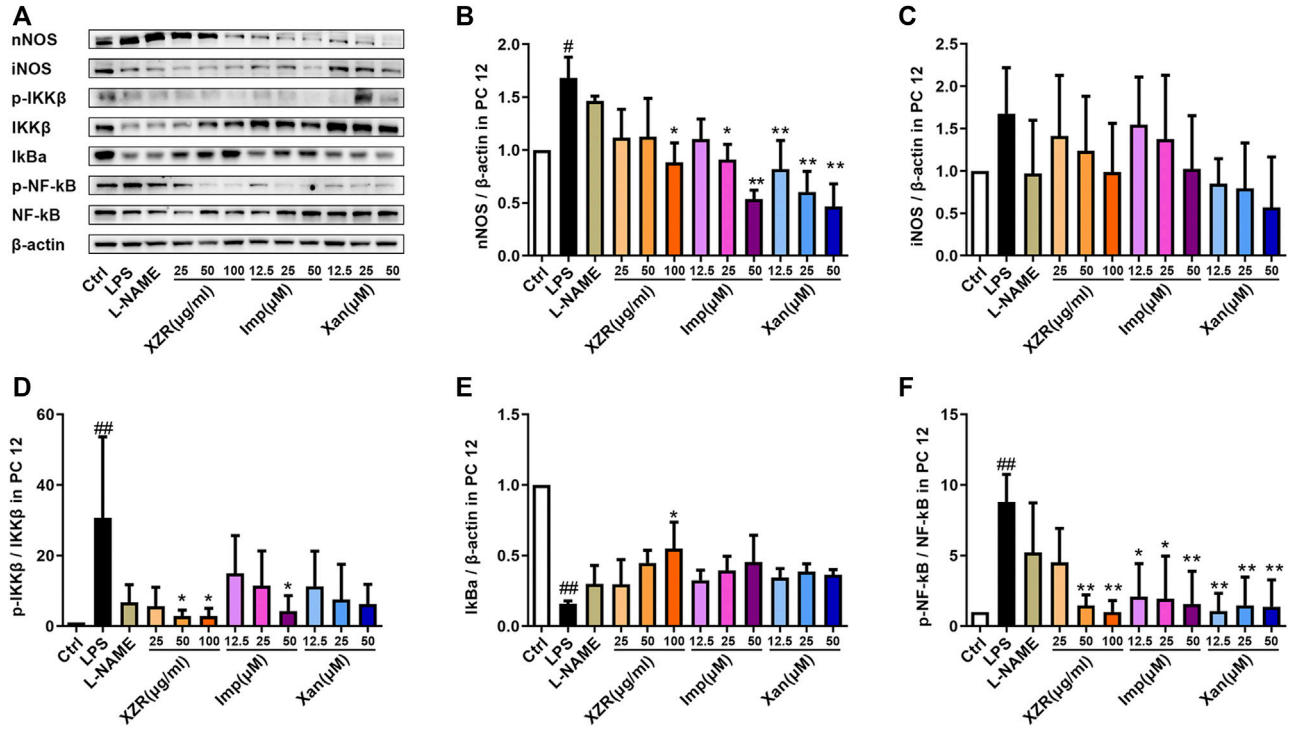

FIGURE 9 | IMP and xanthotoxin inhibited the NOS/NF-κB signaling pathway *in vitro*. **(A)** Representative Western blot images of nNOS, iNOS, IKKβ, IκBα, and NF-κB expression in LPS-treated PC12 cells. **(B)** Relative expression of nNOS. **(C)** Relative expression of iNOS. **(D)** Relative expression of IKKβ. **(E)** Relative expression of IκBα. **(F)** Relative expression of NF-κB. Data are presented as the mean ± standard deviation, $n = 3–5$. $^{\#}p < 0.05$, $^{\#\#}p < 0.01$ versus the control group, $^{*}p < 0.05$, $^{**}p < 0.01$ versus the LPS group. LPS: lipopolysaccharide. IMP: imperatorin.

50 μg/ml, and 100 μg/ml XZR reduced nNOS expression. However, the differences were statistically significant only at high doses of XZR (0.88 ± 0.32, $p < 0.05$). As expected, both imperatorin and xanthotoxin inhibited the nNOS expression in a dose-dependent manner. Imperatorin (25 μM 0.91 ± 0.29, $p < 0.05$; 50 μM 0.54 ± 0.08, $p < 0.01$) and xanthotoxin (12.5 μM 0.82 ± 0.27, $p < 0.01$; 25 μM 0.60 ± 0.34, $p < 0.01$; 50 μM 0.47 ± 0.21, $p < 0.01$) significantly reduced the nNOS expression compared with that in the LPS group. The iNOS expression in LPS-stimulated PC12 cells (1.68 ± 0.54, **Figures 9A,C**) was nearly 1.7-fold higher than that in untreated cells, and XZR (100 μg/ml 0.99 ± 0.58) almost reversed the high level of iNOS in LPS-stimulated PC12 cells to normal levels. Interestingly, there was little effect of imperatorin on the iNOS expression, while xanthotoxin inhibited the iNOS expression in a dose-dependent manner.

Similarly, markers of the activated NF-κB signaling pathway were observed in the supernatant of LPS-stimulated PC12 cells. The expression of *p*-IKKβ/IKKβ (30.71 ± 22.95, $p < 0.01$) and *p*-NF-κB/NF-κB (8.80 ± 1.95, $p < 0.01$) was significantly increased, and the expression of IκBα (0.16 ± 0.02, $p < 0.01$) was significantly reduced by LPS (**Figures 9D–F**).

In particular, XZR at 50 μg/ml and 100 μg/ml significantly inhibited the NF-κB signaling pathway in LPS-stimulated PC12 cells (**Figures 9D–F**). XZR (50 μg/ml and 100 μg/ml) treatment significantly reduced the expression of *p*-IKKβ/IKKβ (2.85 ± 1.71, $p < 0.05$; 2.86 ± 2.09, $p < 0.05$) and *p*-NF-κB/NF-κB (1.48 ± 0.74, $p < 0.01$; 1.00 ± 0.41, $p < 0.01$), and XZR (100 μg/ml) upregulated IκBα (0.55 ± 0.19, $p < 0.05$) expression. Different dosages of imperatorin and xanthotoxin inhibited the NF-κB signaling pathway to varying degrees. Imperatorin (50 μM) downregulated *p*-IKKβ/IKKβ (2.85 ± 1.71, $p < 0.05$), and all doses of imperatorin (12.5 μM 2.11 ± 2.32, $p < 0.05$; 25 μM 1.95 ± 3.05, $p < 0.05$; 50 μM 1.59 ± 2.31, $p < 0.01$) and xanthotoxin (12.5 μM 1.08 ± 1.25, $p < 0.01$; 25 μM 1.48 ± 1.99, $p < 0.01$; 50 μM 1.38 ± 1.90, $p < 0.01$) downregulated the expression of *p*-NF-κB/NF-κB.

DISCUSSION

Migraine is a widespread neurological disorder that affects nearly one billion people worldwide (Collaborators, 2018). According to GBD 2016, migraine is the second leading cause of disability, with a higher disability rate than all other neurological disorders combined (Disease, 2017). Migraine imposes a heavy financial burden on patients and countries due to high healthcare costs, work absences, and reduced productivity. Researchers are interested in developing therapies for migraine. XZR is one of the TCM recipes for treating headaches due to wind–phlegm–blood stasis. A clinical study revealed that XZR has a variety of desirable pharmacological effects on migraines (Su,

et al., 2016). However, the effective components and mechanism of action of XZR in the treatment of migraine remain unknown. Furthermore, due to the complex chemical components of XZR, it is difficult to elucidate the potential active compounds and precise pharmacological mechanisms involved in treating migraine and improving inflammatory conditions. We conducted a systemic study to evaluate the bioactive components and pharmacological mechanisms of XZR in the treatment of migraine.

This study has several highlights: 1) XZR, a Chinese herbal decoction, was effective in improving migraine-like behavior, including frequent head scratching, photophobia, and hyperalgesia; 2) XZR inhibited inflammation mediated by the NF-κB signaling pathway and the expression of CGRP in NTG-induced migraine; 3) XZR inhibited the NF-κB signaling pathway activation by inhibiting NOS in NTG-induced migraine; and 4) imperatorin and xanthotoxin interacted with nNOS and inhibited the NF-κB signaling pathway, suggesting that imperatorin and xanthotoxin might be effective substances in XZR.

Because of the complexity and variability in the botanical drugs of TCM, we strictly explored the process of extraction, purification, concentration, and granulation and carried out strict quality control at each step, including the property analysis, identification, and inspection of each herb and content determination of index components. As shown in **Supplementary Figures S2, Table S5**, the concentrations of paeoniflorin and salvianolic acid B in different batches of XZR were nearly 10.78 mg/g XZR extract and 16.46 mg/g XZR extract, respectively. More importantly, two batches of XZR were applied in animal experiments (**Figure 2**; **Supplementary Figure S3**), and the frequency of head scratching was similar. These data suggested that our extraction methods ensured that the different batches had good repeatability and reproducibility.

NTG, an NO donor compound, has been strongly implicated in the pathological mechanisms of migraine (Giesen et al., 2020). NTG administration was used to mimic the episodic migraine condition (Akerman et al., 2019). The reliability of the NTG-induced migraine model resides in its ability to reproduce headache attacks with features of spontaneous migraine attacks. In the present study, NTG (10 mg/kg) successfully provoked migraine that resulted in mechanical hyperalgesia and migraine-like behavior, including red ears, frequent head scratching, cage climbing, and photophobia, which was consistent with the clinical features of migraine, including head pain accompanied by nausea, vomiting, photophobia, and phonophobia (Dodick, 2018).

It was reported that women are three times more likely to suffer from migraines than men (Labastida-Ramirez et al., 2019). We evaluated the therapeutic effect of XZR on migraine in both sexes of animals in our previous experiment. The results showed that XZR showed a more obvious therapeutic effect on male rats than female rats (**Supplementary Figure S3**). Male rats showed fewer individual differences than female rats. Therefore, we chose male rats for this research. Utilizing an NTG-induced migraine model, we demonstrated that XZR could improve migraine symptoms. The number of head scratches and the time in the dark chamber were significantly decreased in XZR-treated rats compared with rats with NTG-induced migraine. XZR increased periorbital von Frey thresholds and paw sensory thresholds. Moreover, XZR reduced the writhing frequency in the acetic-acid-induced writhing model. All these data suggest that XZR exhibits excellent therapeutic effects on migraine.

The dose (e.g., g/day) per day and kg body weight used in the *in vivo* studies must be of therapeutic relevance. It is important to fully discuss the reason for using excessively high doses in the field of ethnopharmacology (Heinrich et al., 2020). As highlighted by Heinrich, medicinal plants require strict dose risk control to be of value in guiding clinical practice (Heinrich, 2013). XZR was a recipe of modified Sanpian decoction, which recorded in "Bian zheng lu" by Shiduo Chen in Qing dynasty. Conioselinum anthriscoides "Chuanxiong" [*Apiaceae*] (No. 20200728), *P. lactiflora* Pall. (No. 20200614), *A. dahurica* (Hoffm.) Benth. & Hook.f. ex Franch. & Sav. (No. 20200526), and *B. juncea* (L.) and Czern (No. 20200528) were the main drugs of Sanpian decoction. Sanpian decoction has a long history of therapy migraine (Xu et al., 2020). A meta-analysis has revealed the efficacy and safety of Sanpian decoction on migraine (Wu et al., 2020). The results showed that Sanpian decoction significantly improved the clinical efficacy [relative risk (RR) 4.19, 95% confidence intervals (CIs) 2.91–6.04, $p < 0.00001$; RR 1.29, 95% CI 1.09–1.54, $p = 0.003$ separately) and there were minor side effects related to Sanpian decoction, which were well tolerated. The dose of Sanpian decoction used in clinics was 94 g/per day for adult. According to the clinical practical experience of Sanpian decoction, XZR consisted of 15 g Conioselinum anthriscoides "Chuanxiong" [*Apiaceae*] (No. 20200728), 20 g *P. lactiflora* Pall. (No. 20200614), 10 g *A. dahurica* (Hoffm.) Benth. & Hook.f. ex Franch. & Sav. (No. 20200526), 15 g *S. miltiorrhiza* Bunge (No. 20200511), 10 g *B. juncea* (L.) Czern (No. 20200528), 20 g *S. glabra* Roxb (No. 20200611), 10 g *B. bassiana* (Bals.) Vuillant (No. 20200212), and 6 g *X. strumarium* subsp. strumarium (No. 20191128). The dosage of each herb in XZR complies with the provisions of Chinese Pharmacopoeia 2020. In clinics, the dose of XZR was 70 g/per day for adults. And the real-world research revealed that XZR improved migraine with little side effect (Su, et al., 2016). In summary, the effective dose of XZR was 70 g/per day for adults.

The rat dose in our study was calculated based on the body surface area and the corresponding clinically prescribed dose for a 70 kg human body [70.01 g (raw herbs)/70 kg/day] (Zhang et al., 2021). Therefore, the dosage of XZR-middle is almost equivalent to the human clinical dose, and the low dose is half of the equivalent clinical dose, while the high dose is double the equivalent clinical dose. The doses of XZR extract used in rats in this study were also consistent with that in most previous studies, that is, the dosage of decoction in rodents reached crude drug g/kg/day (Jiang et al., 2020; Zhang et al., 2021). It is worth emphasizing that the quantitative analysis of bioactive compounds in XZR and studies on the low dose levels assessing the therapeutic effect of XZR decoction warrant further exploration in the future.

In our study, XZR at a low concentration showed the optimal pharmacological effect on the frequency of head scratching as well as head and plantar withdrawal. The low dose of XZR was half of the equivalent clinical dose, while the high dose was double

the equivalent clinical dose. The intermediate dose of XZR was the equivalent clinical dose. Usually, the equivalent clinical dose of this TCM showed the best pharmacological effect. We also wondered why the low dose of XZR exhibited the best pharmacological effect. We considered that there are two possible reasons: 1) large individual differences. As shown in **Figure 2A**, the frequency of head scratching in rats in the NTG group was 161.80 ± 91.15, while the frequencies of head scratching were 134.00 ± 90.77 and 124.90 ± 50.55 after intermediate (XZR-M) and high (XZR-H) doses of XZR, respectively. The SD was high in these three groups. However, the XZR-M and XZR-H groups showed an obvious decreasing trend in the frequency of head scratching. Increasing the sample size and decreasing the standard deviation may be necessary in future research. 2) TCM prescriptions are characteristically multicomponent, multitarget, and multipath compounds for the comprehensive treatment of diseases. This phenomenon is commonly encountered in the efficacy evaluation of TCM prescriptions. In past decades, many efforts have been made to reveal the dose–effect relationships of TCM prescriptions. It was difficult to accurately evaluate the efficacy of TCM prescriptions because they are often mixtures of multiple components. In TCM, a prescription characteristically contains more than one herbal drug and multiple components for multiple treatment targets (Zha et al., 2015). TCM prescription dose–effect relationships cannot be described as simply as chemical drug dose–effect relationships (Huang et al., 2017). To date, no specific methods for exploring TCM prescription dose–effect relationships have been developed (Qiu et al., 2018). We will pay close attention to this phenomenon in our future research.

The mechanisms underlying migraine are unresolved; however, it has been demonstrated that inflammation plays crucial roles in headache attacks. Current studies have confirmed that inflammation is present in patients with migraine. It was reported that several major cytokines, such as TNF-α, IL-1β, and IL-6, were elevated in patients during migraine attacks (Yilmaz et al., 2010; Ramachandran, 2018; Edvinsson et al., 2019). The inflammatory response is particularly initiated by CGRP, pituitary adenylate cyclase-activating polypeptide (PACAP), NO, and SP and subsequently causes vasodilatation accompanied by meningeal mast cell degranulation (Irmak, et al., 2019; Cetinkaya et al., 2020; Kilinc et al., 2020). The degranulation of mast cells leads to the release of multiple proinflammatory substances, including enzymes, neurotrophic factors, proinflammatory cytokines, histamine, and serotonin (Koroleva et al., 2019), which activate meningeal nociceptors and induce peripheral and central sensitization (Levy, 2012; Conti et al., 2019). We demonstrated that the degranulation of mast cells in NTG-injected rats was almost 2.5-fold greater than that in control rats, which is consistent with other results (Guo et al., 2021). It was reported that NTG induces an increase in the NF-κB activity and the levels of cytokines, such as TNF-α, IL-6, and IL-1β (Edvinsson, et al., 2019). In our experiments, we also found that the levels of NO, CGRP, and cytokines, including TNF-α, IL-6, and IL-1β, were increased in NTG-treated rats. All these data suggested that NTG exerted a pharmacological effect by inducing neuroinflammation. XZR reduced the degranulation of mast cells as well as the levels of CGRP, SP, NO, and proinflammatory cytokines, including TNF-α, IL-1β, and IL-6, suggesting that XZR improved migraine by relieving the neurogenic inflammatory response.

The augmentation of inflammatory cytokines causes NF-κB dysfunction (Conti, et al., 2019). NF-κB is believed to be related to multiple signaling pathways in headache attacks. Selective inhibition of NF-κB offers a potential therapeutic approach for the treatment of headache (Reuter et al., 2002). Recently, it was discovered that three genes (NF-κBIA, TNFAIP3, and ILR2, closely related to the NF-κB family pathway) were abnormally expressed in chronic migraine patients, suggesting that the suppression of NF-κB activation was critical in resolving the upregulated inflammation and reducing the pain involved in the pathophysiology of the studied chronic migraine patients (Perry et al., 2016). Consistent with these results, we also found that NTG significantly activated the NF-κB signaling pathway, as indicated by the decreased IκB and increased p-IKK and p-NF-κB. XZR showed an inhibitory effect on the NF-κB signaling pathway in rats with NTG-induced migraine, suggesting that XZR could be an optimal therapeutic approach for the treatment of headache.

The activation of NF-κB signaling by NO has been commonly observed. NTG, as a donor of NO, always activates NF-kB phosphorylation and neuroinflammation (Chen et al., 2022). NO is involved in the activation of the dura mater and the subsequent activation of trigeminal fibers and the TNC (Giesen, et al., 2020). The synthesis of NO is catalyzed by nNOS, which can be found in dural mast cells, trigeminal nerve endings, and gasserian ganglion cells (Berger et al., 1994), suggesting its importance in trigeminal pain processing. It was reported that NOS activity was increased in patients with chronic tension-type headache (Sarchielli et al., 2002). A nonselective NOS inhibitor improved headache severity and accompanying symptoms in spontaneous migraine attack (Lassen et al., 1997). NO is involved in nociceptive processing in the central nervous system sensitization of pain pathways, and nNOS inhibition reduces central sensitization (Olesen, 2008). NO has been reported to augment the expression of cyclooxygenase-2 (COX-2), TNF-α, and glutathione-synthesizing enzymes and increase NF-κB activity (Umansky et al., 1998). It was also reported that NOS1-derived NO promoted oxidated low-density lipoprotein (OxLDL) uptake and enhanced the release of proinflammatory cytokines (Roy et al., 2020). In maternal inflammation-induced fetal brain injury, nNOS, NF-κB activation, and proinflammatory cytokine levels were found to be increased (Bandara et al., 2021). Furthermore, NTG was reported to increase the NOS activity and CGRP levels, which might promote inflammatory medium exudation synergistically, leading to the activation of the NF-κB pathway (Yao et al., 2020). However, some reports have suggested that NO has an inhibitory effect on the NF-κB activity. The mechanisms underlying this phenomenon are not clear, but it was supported that NO may be involved in the stabilization of IκBα or the nitrosation of the p50 subunit of NF-κB, leading to a decrease in its DNA-binding affinity (Matthews et al., 1996; delaTorre et al., 1998; delaTorre et al., 1999). Our study confirmed that NTG treatment increased both NO levels and NF-κB activation. L-NAME, a nonselective NOS inhibitor, could decrease p-IKK/IKK and p-NF-κB/NF-κB levels in PC12 cells. These

data suggested that NO, produced *via* NOS, could promote the NF-κB signaling pathway. As expected, XZR significantly reduced NO production by inhibiting both the expression and activity of NOS (nNOS and iNOS) and then inhibited the NF-κB signaling pathway. More research is needed to explore the relationship between NOS and NF-κB in XZR-treated migraine.

The trigeminovascular system is important in pain transmission in migraine attacks. Nociceptive transmission originates from the activation and sensitization of first-order trigeminovascular neurons (Ashina, 2020). The second-order trigeminovascular neurons are then activated by ascending nociceptive transmission, which is emitted from the trigeminal ganglion and projected to the brainstem. Ascending nociceptive transmission, in turn, activates and sensitizes third-order trigeminovascular neurons in the thalamus, which subsequently relay the nociceptive transmission to the somatosensory cortex and other cortical areas, ultimately resulting in migraine pain (Ashina, 2020). Our study confirmed that XZR treatment significantly reduced the expression of nNOS, iNOS, and NF-κB signaling pathway proteins in Sp5C cells, suggesting the important role of XZR in the ascending nociceptive transmission pathway.

Nociceptive transmission from the TNC is transmitted to higher brain structures, including the thalamus, brainstem nucleus, rostral ventromedial medulla, and PAG (Goadsby et al., 2009; Castro et al., 2017). In particular, PAG networks have been supposed to have an important role in the pathogenesis of migraine. XZR treatment also reduced the expression of the nNOS, iNOS, and NF-κB signaling pathway proteins in the PAG, suggesting the important role of XZR in the nociceptive transmission descending pathway.

We attempted to provide some substance basis for the pharmacological action of XZR. In the present study, the chemical components of XZR were determined by the UHPLC-LTQ-Orbitrap MS method for the first time. The results showed that coumarins, phenolic acids, flavonoids, phthalides, and terpenoids were the main components of XZR. It was reported that coumarins, such as auraptene, reduced NO production and COX-2, TNF-α, IL-1β, and iNOS expression in RAW 264.7 cells (Hsia et al., 2021) and the hippocampus (Amini-Khoei et al., 2022). Phenolic acids, such as gallic acid, decrease NO levels and exhibit antioxidant and anti-inflammatory effects (Awan et al., 2022). 5-O-Caffeoylshikimic acid suppressed not only the production of NO but also the expression of iNOS, TNF-α, and IL-1β (Lee et al., 2014). It was reported that the main flavonoids from a standardized *S. glabra* flavonoid extract, (-)-epicatechin, astilbin, neoastilbin, isoastilbin, and neoisoastilbin, which were present in the XZR extract, significantly inhibited the secretion of IL-1β, IL-6, NO, and NF-κB p-p65 (Zhao et al., 2020). The above evidence provides a potential role for XZR in anti-inflammatory reactions.

Increasing evidence suggests that iNOS does not show a decisive effect on migraine and that iNOS inhibitors fail to improve migraine (Hoffmann and Goadsby, 2012). Furthermore, it was reported that excessive NO is partly released by nNOS in migraine, and nNOS-specific inhibitors might effectively alleviate migraine (Greco et al., 2015). Therefore, we chose nNOS as a target to screen the effective components by Biacore T200. We revealed that imperatorin and xanthotoxin bound to nNOS (468-616). Xanthotoxin was reported to slow the release of IL-6 and TNF-α in RAW 264.7 cells by inhibiting the NF-κB signaling pathway (Lee et al., 2017). Xanthotoxin also exhibits multiple biological functions, such as the regulation of apoptosis and the proliferation of lymphocytes (Heshmati, 2014). These functions may have a synergistic effect with the functions of compounds that act on NOS/NF-κB in a direct or indirect manner.

CONCLUSION

The present study indicated that XZR alleviated NTG-induced migraines. The mechanism might be that XZR downregulated the NO production mediated by NOS, inhibited the NF-κB signaling pathway, and then decreased neurotransmitter and cytokine levels and exhibited an anti-inflammatory reaction. Imperatorin and xanthotoxin might be the effective components of XZR. The findings of this study provide insights into the clinical treatment of migraine with XZR.

DATA AVAILABILITY STATEMENT

The original contributions presented in the study are included in the article/**Supplementary Material**; further inquiries can be directed to the corresponding authors.

ETHICS STATEMENT

The animal study was reviewed and approved by the Beijing University of Chinese Medicine (No. BUCM-4-2021020101-1009).

AUTHOR CONTRIBUTIONS

WW, TW, and SY designed the experiments. CC, XL, QK, QM, and PL performed the experiments. YH and JL assisted the study. CC, WW, and JG drafted the article. All authors read and approved the final article.

FUNDING

This work was supported by the National Scientific and Technological Major Project for Significant New Drug Creation (No. 2017ZX09301011) and the National Natural Science Foundation for Youth of China (No. 81903766).

SUPPLEMENTARY MATERIAL

The Supplementary Material for this article can be found online at: https://www.frontiersin.org/articles/10.3389/fphar.2022.920201/full#supplementary-material

REFERENCES

Akerman, S., Karsan, N., Bose, P., Hoffmann, J. R., Holland, P. R., Romero-Reyes, M., et al. (2019). Nitroglycerine Triggers Triptan-Responsive Cranial Allodynia and Trigeminal Neuronal Hypersensitivity. *Brain* 142 (1), 103–119. doi:10.1093/brain/awy313

Amini-Khoei, H., Nasiri Boroujeni, S., Maghsoudi, F., Rahimi-Madiseh, M., Bijad, E., Moradi, M., et al. (2022). Possible Involvement of L-Arginine-Nitric Oxide Pathway in the Antidepressant Activity of Auraptene in Mice. *Behav. Brain Funct.* 18 (1), 4. doi:10.1186/s12993-022-00189-1

Arroyo-Quiroz, C., Kurth, T., Cantu-Brito, C., Lopez-Ridaura, R., Romieu, I., and Lajous, M. (2014). Lifetime Prevalence and Underdiagnosis of Migraine in a Population Sample of Mexican Women. *Cephalalgia* 34 (13), 1088–1092. doi:10.1177/0333102414529196

Ashina, M. (2020). Migraine. *N. Engl. J. Med.* 383 (19), 1866–1876. doi:10.1056/NEJMra1915327

Assas, M. B. (2021). Anti-migraine Agents from an Immunological Point of View. *J. Transl. Med.* 19 (1), 23. doi:10.1186/s12967-020-02681-6

Awan, A. M., Majeed, W., Muhammad, F., and Faisal, M. N. (2022). Acacia Jacquemontii Ethyl Acetate Extract Reduces Hyperglycemia and Pro-inflammatory Markers while Increasing Endogenous Antioxidant Potential in Alloxan-Induced Diabetic Rats. *Environ. Sci. Pollut. Res.* doi:10.1007/s11356-022-19493-4

Bandara, S. M. R., Samita, S., Kiridana, A. M., and Herath, H. M. M. T. B. (2021). Elevated Nitric Oxide and Carbon Monoxide Concentration in Nasal-Paranasal Sinus Air as a Diagnostic Tool of Migraine: a Case - Control Study. *Bmc Neurol.* 21 (1), 407. doi:10.1186/s12883-021-02434-y

Berger, R. J., Zuccarello, M., and Keller, J. T. (1994). Nitric Oxide Synthase Immunoreactivity in the Rat Dura Mater. *Neuroreport* 5 (4), 519–521. doi:10.1097/00001756-199401120-00039

Bonnet, C., Hao, J., Osorio, N., Donnet, A., Penalba, V., Ruel, J., et al. (2019). Maladaptive Activation of Nav1.9 Channels by Nitric Oxide Causes Triptan-Induced Medication Overuse Headache. *Nat. Commun.* 10 (1), 4253. doi:10.1038/s41467-019-12197-3

Castro, A., Raver, C., Li, Y., Uddin, O., Rubin, D., Ji, Y., et al. (2017). Cortical Regulation of Nociception of the Trigeminal Nucleus Caudalis. *J. Neurosci.* 37 (47), 11431–11440. doi:10.1523/JNEUROSCI.3897-16.2017

Cetinkaya, A., Kilinc, E., Camsari, C., and Ogun, M. N. (2020). Effects of Estrogen and Progesterone on the Neurogenic Inflammatory Neuropeptides: Implications for Gender Differences in Migraine. *Exp. Brain Res.* 238 (11), 2625–2639. doi:10.1007/s00221-020-05923-7

Chanda, M. L., Tuttle, A. H., Baran, I., Atlin, C., Guindi, D., Hathaway, G., et al. (2013). Behavioral Evidence for Photophobia and Stress-Related Ipsilateral Head Pain in Transgenic Cacna1a Mutant Mice. *Pain* 154 (8), 1254–1262. doi:10.1016/j.pain.2013.03.038

Chen, H., Tang, X., Li, J., Hu, B., Yang, W., Zhan, M., et al. (2022). IL-17 Crosses the Blood-Brain Barrier to Trigger Neuroinflammation: a Novel Mechanism in Nitroglycerin-Induced Chronic Migraine. *J. Headache Pain* 23 (1), 1. doi:10.1186/s10194-021-01374-9

Collaborators, G. B. D. H. (2018). Global, Regional, and National Burden of Migraine and Tension-type Headache, 1990-2016: a Systematic Analysis for the Global Burden of Disease Study 2016. *Lancet Neurol.* 17 (11), 954–976. doi:10.1016/S1474-4422(18)30322-3

Conti, P., D'Ovidio, C., Conti, C., Gallenga, C. E., Lauritano, D., Caraffa, A., et al. (2019). Progression in Migraine: Role of Mast Cells and Pro-inflammatory and Anti-inflammatory Cytokines. *Eur. J. Pharmacol.* 844, 87–94. doi:10.1016/j.ejphar.2018.12.004

DelaTorre, A., Schroeder, R. A., Bartlett, S. T., and Kuo, P. C. (1998). Differential Effects of Nitric Oxide-Mediated S-Nitrosylation on P50 and C-Jun DNA Binding. *Surgery* 124 (2), 137–41; discussion 141-2. doi:10.1016/s0039-6060(98)70113-8

DelaTorre, A., Schroeder, R. A., Punzalan, C., and Kuo, P. C. (1999). Endotoxin-mediated S-Nitrosylation of P50 Alters NF-Kappa B-dependent Gene Transcription in ANA-1 Murine Macrophages. *J. Immunol.* 162 (7), 4101–4108. doi:10.2202/1548-923X.1603

Disease, G. B. D. (2017). Injury I., Prevalence CGlobal, Regional, and National Incidence, Prevalence, and Years Lived with Disability for 328 Diseases and Injuries for 195 Countries, 1990-2016: a Systematic Analysis for the Global Burden of Disease Study 2016. *Lancet* 390 (10100), 1211–1259. doi:10.1016/S0140-6736(17)32154-2

Dodick, D. W. (2018). Migraine. *Lancet* 391 (10127), 1315–1330. doi:10.1016/S0140-6736(18)30478-1

Edvinsson, L., and Haanes, K. A. (2021). Identifying New Antimigraine Targets: Lessons from Molecular Biology. *Trends Pharmacol. Sci.* 42 (4), 217–225. doi:10.1016/j.tips.2021.01.002

Edvinsson, L., Haanes, K. A., and Warfvinge, K. (2019). Does Inflammation Have a Role in Migraine? *Nat. Rev. Neurol.* 15 (8), 483–490. doi:10.1038/s41582-019-0216-y

Gao, Z., Liu, X., Yu, S., Zhang, Q., Chen, Q., Wu, Q., et al. (2014). Electroacupuncture at Acupoints Reverses Plasma Glutamate, Lipid, and LDL/VLDL in an Acute Migraine Rat Model: A (1) H NMR-Based Metabolomic Study. *Evid. Based Complement. Altern. Med.* 2014, 659268. doi:10.1155/2014/659268

Gautam, M., and Ramanathan, M. (2021). Ameliorative Potential of Flavonoids of Aegle Marmelos in Vincristine-Induced Neuropathic Pain and Associated Excitotoxicity. *Nutr. Neurosci.* 24 (4), 296–306. doi:10.1080/1028415X.2019.1627768

Giesen, J., Füchtbauer, E. M., Füchtbauer, A., Funke, K., Koesling, D., and Russwurm, M. (2020). AMPA Induces NO-dependent cGMP Signals in Hippocampal and Cortical Neurons via L-type Voltage-Gated Calcium Channels. *Cereb. Cortex* 30 (4), 2128–2143. doi:10.1093/cercor/bhz227

Goadsby, P. J., Charbit, A. R., Andreou, A. P., Akerman, S., and Holland, P. R. (2009). Neurobiology of Migraine. *Neuroscience* 161 (2), 327–341. doi:10.1016/j.neuroscience.2009.03.019

Greco, R., Ferrigno, A., Demartini, C., Zanaboni, A., Mangione, A. S., Blandini, F., et al. (2015). Evaluation of ADMA-DDAH-NOS axis in Specific Brain Areas Following Nitroglycerin Administration: Study in an Animal Model of Migraine. *J. Headache Pain* 16, 560. doi:10.1186/s10194-015-0560-2

Guo, S. (2017). The Role of Genetics on Migraine Induction Triggered by CGRP and PACAP38. *Dan. Med. J.* 64 (3).

Guo, Z., Czerpaniak, K., Zhang, J., and Cao, Y. Q. (2021). Increase in Trigeminal Ganglion Neurons that Respond to Both Calcitonin Gene-Related Peptide and Pituitary Adenylate Cyclase-Activating Polypeptide in Mouse Models of Chronic Migraine and Posttraumatic Headache. *Pain* 162 (5), 1483–1499. doi:10.1097/j.pain.0000000000002147

Heinrich, M. (2013). *Phytotherapy*. New York.

Heinrich, M., Appendino, G., Efferth, T., Fürst, R., Izzo, A. A., Kayser, O., et al. (2020). Best Practice in Research - Overcoming Common Challenges in Phytopharmacological Research. *J. Ethnopharmacol.* 246, 112230. doi:10.1016/j.jep.2019.112230

Heshmati, F. (2014). Updating ECP Action Mechanisms. *Transfus. Apher. Sci.* 50 (3), 330–339. doi:10.1016/j.transci.2014.04.003

Hoffmann, J., and Goadsby, P. J. (2012). New Agents for Acute Treatment of Migraine: CGRP Receptor Antagonists, iNOS Inhibitors. *Curr. Treat. Options Neurol.* 14 (1), 50–59. doi:10.1007/s11940-011-0155-4

Hsia, C.-H., Jayakumar, T., Lu, W.-J., Sheu, J.-R., Hsia, C.-W., Saravana Bhavan, P., et al. (2021). Auraptene, a Monoterpene Coumarin, Inhibits LTA-Induced Inflammatory Mediators via Modulating NF-κB/MAPKs Signaling Pathways. *Evidence-Based Complementary Altern. Med.* 2021, 11. doi:10.1155/2021/5319584

Huang, Y., Ni, N., Hong, Y., Lin, X., Feng, Y., and Shen, L. (2020). Progress in Traditional Chinese Medicine for the Treatment of Migraine. *Am. J. Chin. Med.* 48 (8), 1731–1748. doi:10.1142/S0192415X2050086X

Huang, Y., Yu, S. H., Zhen, W. X., Cheng, T., Wang, D., Lin, J. B., et al. (2021). Tanshinone I, a New EZH2 Inhibitor Restricts Normal and Malignant Hematopoiesis through Upregulation of MMP9 and ABCG2. *Theranostics* 11 (14), 6891–6904. doi:10.7150/thno.53170

Huang, Z. Q., Fan, X. M., Wang, Y. M., Liang, Q. L., Tong, X. L., Bai, Y., et al. (2017). A New Method to Evaluate the Dose-Effect Relationship of a TCM Formula Gegen Qinlian Decoction: "Focus" Mode of Integrated Biomarkers. *Acta Pharmacol. Sin.* 38 (8), 1141–1149. doi:10.1038/aps.2016.165

Jiang, M., Wang, W., Zhang, J., Wang, C., Bi, Y., Li, P., et al. (2020). Protective Effects and Possible Mechanisms of Actions of Bushen Cuyun Recipe on Diminished Ovarian Reserve Induced by Cyclophosphamide in Rats. *Front. Pharmacol.* 11, 546. doi:10.3389/fphar.2020.00546

Kilinc, E., Tore, F., Dagistan, Y., and Bugdayci, G. (2020). Thymoquinone Inhibits Neurogenic Inflammation Underlying Migraine through Modulation of Calcitonin Gene-Related Peptide Release and Stabilization of Meningeal Mast Cells in Glyceryltrinitrate-Induced Migraine Model in Rats. *Inflammation* 43 (1), 264–273. doi:10.1007/s10753-019-01115-w

Koroleva, K., Gafurov, O., Guselnikova, V., Nurkhametova, D., Giniatullina, R., Sitdikova, G., et al. (2019). Meningeal Mast Cells Contribute to ATP-Induced Nociceptive Firing in Trigeminal Nerve Terminals: Direct and Indirect Purinergic Mechanisms Triggering Migraine Pain. *Front. Cell Neurosci.* 13, 195. doi:10.3389/fncel.2019.00195

Koyuncu Irmak, D., Kilinc, E., and Tore, F. (2019). Shared Fate of Meningeal Mast Cells and Sensory Neurons in Migraine. *Front. Cell Neurosci.* 13, 136. doi:10.3389/fncel.2019.00136

Labastida-Ramírez, A., Rubio-Beltrán, E., Villalón, C. M., and MaassenVanDenBrink, A. (2019). Gender Aspects of CGRP in Migraine. *Cephalalgia* 39 (3), 435–444. doi:10.1177/0333102417739584

Lai, T., Chen, L., Chen, X., He, J., Lv, P., and Ge, H. (2019). Rhynchophylline Attenuates Migraine in Trigeminal Nucleus Caudalis in Nitroglycerin-Induced Rat Model by Inhibiting MAPK/NF-κB Signaling. *Mol. Cell Biochem.* 461 (1-2), 205–212. doi:10.1007/s11010-019-03603-x

Lassen, L. H., Ashina, M., Christiansen, I., Ulrich, V., and Olesen, J. (1997). Nitric Oxide Synthase Inhibition in Migraine. *Lancet* 349 (9049), 401–402. doi:10.1016/s0140-6736(97)80021-9

Lee, D. S., Keo, S., Ko, W., Kim, K. S., Ivanova, E., Yim, J. H., et al. (2014). Secondary Metabolites Isolated from Castilleja Rubra Exert Anti-inflammatory Effects through NF-Kb Inactivation on Lipopolysaccharide-Induced RAW264.7 Macrophages. *Arch. Pharm. Res.* 37 (7), 947–954. doi:10.1007/s12272-013-0243-y

Lee, S. B., Lee, W. S., Shin, J. S., Jang, D. S., and Lee, K. T. (2017). Xanthotoxin Suppresses LPS-Induced Expression of iNOS, COX-2, TNF-α, and IL-6 via AP-1, NF-Kb, and JAK-STAT Inactivation in RAW 264.7 Macrophages. *Int. Immunopharmacol.* 49, 21–29. doi:10.1016/j.intimp.2017.05.021

Levy, D. (2012). Endogenous Mechanisms Underlying the Activation and Sensitization of Meningeal Nociceptors: The Role of Immuno-Vascular Interactions and Cortical Spreading Depression. *Curr. Pain Headache Rep.* 16 (3), 270–277. doi:10.1007/s11916-012-0255-1

Li, J. C., Shen, X. F., Meng, X. L., Zhang, Y., and Lai, X. R. (2011). Analgesic Effect and Mechanism of the Three TCM-Herbal Drug-Combination Tou Feng Yu Pill on Treatment of Migraine. *Phytomedicine* 18 (8-9), 788–794. doi:10.1016/j.phymed.2011.01.008

Loewendorf, A. I., Matynia, A., Saribekyan, H., Gross, N., Csete, M., and Harrington, M. (2016). Roads Less Traveled: Sexual Dimorphism and Mast Cell Contributions to Migraine Pathology. *Front. Immunol.* 7, 140. doi:10.3389/fimmu.2016.00140

Matthews, J. R., Botting, C. H., Panico, M., Morris, H. R., and Hay, R. T. (1996). Inhibition of NF-kappaB DNA Binding by Nitric Oxide. *Nucleic Acids Res.* 24 (12), 2236–2242. doi:10.1093/nar/24.12.2236

Moisset, X., Giraud, P., and Dallel, R. (2021). Migraine in Multiple Sclerosis and Other Chronic Inflammatory Diseases. *Rev. Neurol. Paris.* 177 (7), 816–820. doi:10.1016/j.neurol.2021.07.005

Nair, A. B., and Jacob, S. A. (2016). Simple Practice Guide for Dose Conversion between Animals and Human. *J. Basic Clin. Pharm.* 7 (2), 27–31. doi:10.4103/0976-0105.177703

Olesen, J. (2008). The Role of Nitric Oxide (NO) in Migraine, Tension-type Headache and Cluster Headache. *Pharmacol. Ther.* 120 (2), 157–171. doi:10.1016/j.pharmthera.2008.08.003

Perry, C. J., Blake, P., Buettner, C., Papavassiliou, E., Schain, A. J., Bhasin, M. K., et al. (2016). Upregulation of Inflammatory Gene Transcripts in Periosteum of Chronic Migraineurs: Implications for Extracranial Origin of Headache. *Ann. Neurol.* 79 (6), 1000–1013. doi:10.1002/ana.24665

Pradhan, A. A., Bertels, Z., and Akerman, S. (2018). Targeted Nitric Oxide Synthase Inhibitors for Migraine. *Neurotherapeutics* 15 (2), 391–401. doi:10.1007/s13311-018-0614-7

Qiu, Z., Yuan, H., Li, N., Yang, X., Hu, X., Su, F., et al. (2018). Bidirectional Effects of Moxifloxacin on the Pro-inflammatory R-esponse in L-ipopolysaccharide-stimulated M-ouse P-eritoneal M-acrophages. *Mol. Med. Rep.* 18 (6), 5399–5408. doi:10.3892/mmr.2018.9569

Raggi, A., Monasta, L., Beghi, E., Caso, V., Castelpietra, G., Mondello, S., et al. (2022). Incidence, Prevalence and Disability Associated with Neurological Disorders in Italy between 1990 and 2019: an Analysis Based on the Global Burden of Disease Study 2019. *J. Neurol.* 269 (4), 2080–2098. doi:10.1007/s00415-021-10774-5

Ramachandran, R. (2018). Neurogenic Inflammation and its Role in Migraine. *Semin. Immunopathol.* 40 (3), 301–314. doi:10.1007/s00281-018-0676-y

Reuter, U., Bolay, H., Jansen-Olesen, I., Chiarugi, A., Sanchez del Rio, M., Letourneau, R., et al. (2001). Delayed Inflammation in Rat Meninges: Implications for Migraine Pathophysiology. *Brain* 124 (Pt 12), 2490–2502. doi:10.1093/brain/124.12.2490

Reuter, U., Chiarugi, A., Bolay, H., and Moskowitz, M. A. (2002). Nuclear Factor-kappaB as a Molecular Target for Migraine Therapy. *Ann. Neurol.* 51 (4), 507–516. doi:10.1002/ana.10159

Rockville, M., Food, U., and Administration, D. (2005). USFDA. *Guidance for Industry: Estimating he Maximum Safe Starting Dose in Adult Healthy Volunteer.*

Roy, A., Saqib, U., Wary, K., and Baig, M. S. (2020). Macrophage Neuronal Nitric Oxide Synthase (NOS1) Controls the Inflammatory Response and Foam Cell Formation in Atherosclerosis. *Int. Immunopharmacol.* 83, 106382. doi:10.1016/j.intimp.2020.106382

Sarchielli, P., Alberti, A., Floridi, A., and Gallai, V. (2002). L-Arginine/nitric Oxide Pathway in Chronic Tension-type Headache: Relation with Serotonin Content and Secretion and Glutamate Content. *J. Neurol. Sci.* 198 (1-2), 9–15. doi:10.1016/s0022-510x(02)00035-7

Silberstein, S. D. (2004). Migraine. *Lancet* 363 (9406), 381–391. doi:10.1016/S0140-6736(04)15440-8

Spekker, E., Tanaka, M., Szabó, Á., and Vécsei, L. (2021). Neurogenic Inflammation: The Participant in Migraine and Recent Advancements in Translational Research. *Biomedicines* 10 (1). doi:10.3390/biomedicines10010076

Su, Z. Q., Chen, C., Li, P., and Wang, T. (2016). Summary of the Experience of QIN Yue-hao on the Treatment of Women's Migraine Based on Wind, Phlegm and Blood Stasis. *J. Basic Chin. Med.* 22 (12), 1702–1703.

Syed, Y. Y. (2016). Sumatriptan/Naproxen Sodium: A Review in Migraine. *Drugs* 76 (1), 111–121. doi:10.1007/s40265-015-0521-8

Thomsen, L. L., and Olesen, J. (2001). Nitric Oxide in Primary Headaches. *Curr. Opin. Neurol.* 14 (3), 315–321. doi:10.1097/00019052-200106000-00009

Umansky, V., Hehner, S. P., Dumont, A., Hofmann, T. G., Schirrmacher, V., Dröge, W., et al. (1998). Co-stimulatory Effect of Nitric Oxide on Endothelial NF-kappaB Implies a Physiological Self-Amplifying Mechanism. *Eur. J. Immunol.* 28 (8), 2276–2282. doi:10.1002/(SICI)1521-4141

Victor, T. W., Hu, X., Campbell, J. C., Buse, D. C., and Lipton, R. B. (2010). Migraine Prevalence by Age and Sex in the United States: a Life-Span Study. *Cephalalgia* 30 (9), 1065–1072. doi:10.1177/0333102409355601

Wu, B., Rao, H., Yang, S., Cai, S., Tan, L., Feng, Z., et al. (2020). Efficacy and Safety of the Classic Chinese Herbal Prescription Sanpian Decoction on Migraine: A Meta-Analysis. *Explore (NY)* 16 (5), 318–327. doi:10.1016/j.explore.2020.05.006

Xu, Z. M., Jia, M., Liang, X., Wei, J. J., Fu, Guo-Jing, Lei, Lin, et al. (2020). Clinical Practice Guideline for Migraine with Traditional Chinese Medicine(draft Version for Comments). *Zhongguo Zhong Yao Za Zhi* 21 (45), 5057–5067. doi:10.19540/j.cnki.cjcmm.20200903.502

Yao, G., Man, Y. H., Li, A. R., Guo, Y., Dai, Y., Wang, P., et al. (2020). NO Up-Regulates Migraine-Related CGRP via Activation of an Akt/GSK-3β/nf-Kb Signaling Cascade in Trigeminal Ganglion Neurons. *Aging (Albany NY)* 12 (7), 6370–6384. doi:10.18632/aging.103031

Yilmaz, I. A., Ozge, A., Erdal, M. E., Edgünlü, T. G., Cakmak, S. E., and Yalin, O. O. (2010). Cytokine Polymorphism in Patients with Migraine: Some Suggestive Clues of Migraine and Inflammation. *Pain Med.* 11 (4), 492–497. doi:10.1111/j.1526-4637.2009.00791.x

Yuan, R., Zhang, D., Yang, J., Wu, Z., Luo, C., Han, L., et al. (2021). Review of Aromatherapy Essential Oils and Their Mechanism of Action against Migraines. *J. Ethnopharmacol.* 265, 113326. doi:10.1016/j.jep.2020.113326

Zha, L. H., He, L. S., Lian, F. M., Zhen, Z., Ji, H. Y., Xu, L. P., et al. (2015). Clinical Strategy for Optimal Traditional Chinese Medicine (TCM) Herbal Dose Selection in Disease Therapeutics: Expert Consensus on Classic TCM Herbal Formula Dose Conversion. *Am. J. Chin. Med.* 43 (8), 1515–1524. doi:10.1142/S0192415x1550086x

Zhang, C., Wang, X., Wang, C., He, C., Ma, Q., Li, J., et al. (2021). Qingwenzhike Prescription Alleviates Acute Lung Injury Induced by LPS via Inhibiting TLR4/

NF-kB Pathway and NLRP3 Inflammasome Activation. *Front. Pharmacol.* 12, 790072. doi:10.3389/fphar.2021.790072

Zhang, X. F., Zhang, W. J., Dong, C. L., Hu, W. L., Sun, Y. Y., Bao, Y., et al. (2017). Analgesia Effect of Baicalein against NTG-Induced Migraine in Rats. *Biomed. Pharmacother.* 90, 116–121. doi:10.1016/j.biopha.2017.03.052

Zhao, X., Chen, R., Shi, Y., Zhang, X., Tian, C., and Xia, D. (2020). Antioxidant and Anti-inflammatory Activities of Six Flavonoids from Smilax Glabra Roxb. *Molecules* 25 (22). doi:10.3390/molecules25225295

Conflict of Interest: The authors declare that the research was conducted in the absence of any commercial or financial relationships that could be construed as a potential conflict of interest.

Publisher's Note: All claims expressed in this article are solely those of the authors and do not necessarily represent those of their affiliated organizations, or those of the publisher, the editors, and the reviewers. Any product that may be evaluated in this article, or claim that may be made by its manufacturer, is not guaranteed or endorsed by the publisher.

frontiers | Frontiers in Pharmacology

TYPE Original Research
PUBLISHED 09 August 2022
DOI 10.3389/fphar.2022.944502

OPEN ACCESS

EDITED BY
Rajeev K. Singla,
Sichuan University, China

REVIEWED BY
Temugin Berta,
University of Cincinnati, United States
Rohit Sharma,
Institute of Medical Sciences (Banaras Hindu University), India
G. N. S. Hema Sree,
M S Ramaiah University of Applied Sciences, India

*CORRESPONDENCE
Willias Masocha,
willias.masocha@ku.edu.kw

SPECIALTY SECTION
This article was submitted to Neuropharmacology, a section of the journal Frontiers in Pharmacology

RECEIVED 15 May 2022
ACCEPTED 05 July 2022
PUBLISHED 09 August 2022

CITATION
Al-Romaiyan A and Masocha W (2022), Pristimerin, a triterpene that inhibits monoacylglycerol lipase activity, prevents the development of paclitaxel-induced allodynia in mice. *Front. Pharmacol.* 13:944502. doi: 10.3389/fphar.2022.944502

Pristimerin, a triterpene that inhibits monoacylglycerol lipase activity, prevents the development of paclitaxel-induced allodynia in mice

Altaf Al-Romaiyan and Willias Masocha*

Department of Pharmacology and Therapeutics, Faculty of Pharmacy, Kuwait University, Safat, Kuwait

Background: Triterpenes such as euphol and pristimerin, which are plant secondary metabolites, were the first to be characterized as monoacylglycerol lipase (MAGL) inhibitors. MAGL inhibitors alleviate chemotherapy-induced neuropathic pain (CINP) in rodent models. Pristimerin has been shown to have additive anticancer activity with paclitaxel, a chemotherapeutic drug. However, the activity of pristimerin on CINP has not been evaluated.

Objectives: The aims of this study were to evaluate whether various triterpenes had activity against recombinant human MAGL and MAGL activity in mouse tissues, and whether pristimerin could prevent development of paclitaxel-induced mechanical allodynia.

Methods: The effects of four triterpenes betulinic acid, cucurbitacin B, euphol, and pristimerin on the activity human recombinant MAGL and MAGL activity of mice brain and paw skin tissues were evaluated using MAGL inhibitor screening and MAGL activity assay kits. The effects of treatment of female BALB/c mice with pristimerin intraperitoneally on the development of paclitaxel-induced mechanical allodynia were assessed using the dynamic plantar aesthesiometer and on nuclear factor-2 erythroid related factor-2 (*Nrf2*) gene expression in the paw skin were evaluated by real time polymerase chain reaction.

Results: Pristimerin inhibited the human recombinant MAGL activity in a concentration-dependent manner like JZL-195, a MAGL inhibitor. Betulinic acid, cucurbitacin B and euphol inhibited human recombinant MAGL activity but their effects were not concentration dependent and were less to that of pristimerin. Pristimerin inhibited both mouse brain and paw skin MAGL activity in a concentration-dependent manner. Paclitaxel induced mechanical allodynia and increase in MAGL activity in the paw skin. Treatment with pristimerin prevented the development of paclitaxel-induced mechanical allodynia and the paclitaxel-induced increase in MAGL activity. Pristimerin significantly upregulated mRNA expression of *Nrf2,* a regulator of endogenous antioxidant defense.

Conclusion: These results indicate that triterpenes inhibit human recombinant MAGL activity with varying degrees. Pristimerin inhibits both mouse brain and paw skin MAGL activity in a concentration-dependent manner, prevents both the development of paclitaxel-induced mechanical allodynia and the associated increase in MAGL activity in the paw skin, and might protect against paclitaxel-induced oxidative stress. Co-treatment with pristimerin and paclitaxel could be useful in the treatment of cancer and prevention of CINP.

KEYWORDS

triterpenes, monoacylglycerol lipase activity, chemotherapy-induced neuropathic pain, paclitaxel, mechanical allodynia, brain, paw skin

Introduction

Triterpenes are plant secondary metabolites, which contain about 30 carbon atoms, that have been isolated as active constituents of various plants (Jager et al., 2009; Parmar et al., 2013). They are classified into two main groups: tetracyclic and the pentacyclic triterpenes. Tetracyclic triterpenes include oleandrin, euphol and cucurbitacins (Jager et al., 2009; Parmar et al., 2013), of which euphol has been shown to inhibit recombinant rat monoacylglycerol lipase (MAGL) activity (King et al., 2009). Monoacylglycerol lipase is an enzyme that degrades the endocannabinoid 2-arachidonoylglycerol (2-AG) through hydrolysis to arachidonic acid and glycerol (Dinh et al., 2002; Saario et al., 2004). Endocannabinoids such as 2-AG and anandamide have analgesic activity (Rodriguez de Fonseca et al., 2005; Guindon and Hohmann, 2009; Munawar et al., 2017). Pentacyclic triterpenes are the largest group with compounds such as α-amyrin, β-amyrin, betulin, betulinic acid, pristimerin, lupeol, oleanolic acid, ursolic acid, maslinic acid, uvaol, and erythrodiol (Jager et al., 2009; Parmar et al., 2013), of which α-amyrin, β-amyrin and pristimerin have been shown to inhibit MAGL activity (King et al., 2009; Chicca et al., 2012). Various triterpenes such as lupeol, tormentic acid, betulin, betulinic acid and epibetulin have been reported to have antinociceptive and antiallodynic activities in acute pain, inflammatory pain and neuropathic pain caused by partial constriction of the sciatic nerve (Calixto et al., 2000; Bortalanza et al., 2002; Parmar et al., 2013). However, the effects of some of these triterpenes on MAGL activity and on chemotherapy-induced neuropathic pain (CINP) have not yet been evaluated.

Paclitaxel, a chemotherapeutic drug used in the treatment of breast cancer and other solid tumors causes dose-limiting CINP referred to as paclitaxel-induced neuropathic pain (PINP) (Polomano and Bennett, 2001; Cata et al., 2006; Wolf et al., 2008). Unfortunately, there is a scarcity of drugs to effectively alleviate or prevent the development of PINP. Currently, only duloxetine has moderate recommendation for the treatment of CINP, including PINP, while other agents useful in other types of neuropathic pain may also be used because of limited options for treating CINP (Hershman et al., 2014). Therefore, further research into both the pathophysiology of CINP and the search of novel, more efficacious and safer agents for the treatment of CINP is essential.

Recent data from our laboratory show that there is a decrease in the levels of 2-AG in the paw skin of mice with paclitaxel-induced mechanical allodynia, without a change in the protein levels of the enzyme MAGL (Thomas et al., 2020). Administration of 2-AG or a MAGL inhibitor JZL184 into the right hind paw skin of mice alleviated paclitaxel-induced mechanical allodynia in the injected right paw but did not affect the uninjected left paw (Thomas et al., 2020). These findings suggest that MAGL inhibitors could be useful for management of CINP.

Pristimerin has been reported to have anticancer activities against various types of cancer cell lines including those of breast cancer, cervical cancer, prostate cancer, gliomas, and fibrosarcoma (Yang et al., 2008; Byun et al., 2009; Lee et al., 2013; Yan et al., 2013; Hayashi et al., 2020). Pristimerin has also been shown to have additive anticancer activity with paclitaxel against breast cancer cell lines (Lee et al., 2018). This could lead to lower doses of paclitaxel being used for treating cancer and thus reduce the occurrence of the dose dependent PINP. However, the effects of pristimerin on the development of PINP or any CINP have not been evaluated.

The objectives of this study were to evaluate whether various triterpenes, including pristimerin had activity against recombinant human MAGL and MAGL activity in mouse brain and paw skin tissue, and whether pristimerin could prevent the development of mechanical allodynia induced by paclitaxel in mice. Other objectives were to evaluate if treatment with paclitaxel affects MAGL activity in the periphery at a time when female mice develop paclitaxel-induced mechanical allodynia, and also whether administration of pristimerin could reduce/prevent the effect of paclitaxel on MAGL activity.

Materials and methods

Animals

Female BALB/c mice (8–12 weeks old; $n = 54$) were used in this study and were supplied by the Animal Resources Centre at the Health Sciences Centre (HSC), Kuwait University. In the current study, female mice were used following the recommendation of the members of the Sex, Gender and Pain Special Interest Group of the International Association for the Study of Pain (IASP) that "all pain researchers consider testing their hypotheses in both sexes, or if restricted by practical considerations, only in females" (Greenspan et al., 2007). The strain was chosen based on availability and our previous studies with the same strain (Parvathy and Masocha, 2013; Masocha and Thomas, 2019; Thomas et al., 2020). The animals were handled in compliance with Directive 2010/63/EU of the European Parliament and of the Council on the protection of animals used for scientific purposes. All animal experiments were approved by the Ethical Committee for the use of Laboratory Animals in Teaching and in Research, HSC, Kuwait University (Ref: 23/VDR/EC/, Date 5/8/2020). They were kept in temperature controlled (24 ± 1°C) rooms with food and water *ad libitum*. All experiments were performed between 0800–1600 h to reduce the effects of circadian variations in pharmacological effects.

Evaluation of inhibitory potential of triterpenes on human monoacylglycerol lipase activity

The effects of four triterpenes, betulinic acid (Sigma–Aldrich, Germany), cucurbitacin B (Phytolab, Germany), euphol (TargetMol, United States) and pristimerin (Tocris, United Kingdom), on human recombinant MAGL activity was evaluated *in vitro* using the Monoacylglycerol lipase assay inhibitor screening colorimetry-based assay kit (Cayman Chemical, Ann Arbor, MI, United States) following the manufacturer's instructions. MAGL hydrolyses the substrate (4-nitrophenyl acetate) and generates 4-nitrophenol, whose absorbance was taken at 405 nm on microplate reader. JZL195, a dual inhibitor fatty acid amide hydrolase (FAAH) and MAGL, was used as a MAGL inhibitor reference standard for the assay.

Briefly, different concentrations of betulinic acid (0.1, 1, 10, 100 and 200 μM), cucurbitacin B (0.1, 1, 10, 100 and 200 μM), euphol (0.001, 0.01, 0.1 and 1 μM), pristimerin (0.001, 0.01, 0.1 and 1 μM) and JZL195 (0.001, 0.01, 0.1, 1 and 4.4 μM) were prepared in a solution made up of 50% dimethylsulfoxide (DMSO; Sigma-Aldrich) and 50% assay buffer. A mixture of assay buffer (150 μl), diluted human recombinant MAGL (10 μl), and solvent or inhibitor (10 μl) at different concentrations was incubated for 15 min at 25°C in a 96 well microplate. The reaction was initiated by adding 10 μl of MAGL substrate to all the wells being used and the plate incubated at 25°C in the microplate reader. The plate was shaken for 10 s to mix every time before taking absorbance at 405 nm for various time points (5, 10, 30, and 60 min) using a microplate reader (SpectraMax® iD3, Molecular Devices). The experiment was performed in triplicate.

%Activity was calculated as %Initial Activity = Inhibitor activity/Initial activity*100, following the manufacturer's protocol. Initial activity is the absorbance in the wells the reaction was run without inhibitor.

Evaluation of inhibitory potential of triterpenes on mouse brain and paw skin tissue monoacylglycerol lipase activity

The effects of pristimerin on mouse tissue MAGL activity was evaluated *in vitro* using the Monoacylglycerol Lipase (MAGL) Activity Assay Kit (Fluorometric) (ab273326; Abcam) following the manufacturer's instructions. MAGL cleaves a fluorescent substrate to generate arachidonic acid and fluorescent metabolite and the increased fluorescence is measured at Ex/Em 360/460 nm. A MAGL inhibitor (name not disclosed by company because it is proprietary information) is also used to differentiate MAGL activity from other sources of fluorescence. Pristimerin was selected because it was the one with best activity in inhibiting human recombinant MAGL amongst the triterpenes tested. JZL195, a dual inhibitor of FAAH and MAGL, was used as a MAGL inhibitor reference standard for the assay.

Briefly, mouse brain and paw skin tissues were dissected out and homogenized, 10 mg of tissue in 100 μl MAGL assay buffer, centrifuged at 10,000 g for 15 min (4°C), and the supernatant was collected, protein concentrations determined by the by Bicinchoninic acid (BCA) assay using bovine serum albumin (BSA) as standard, The supernatants were aliquoted and stored at −80°C until the time to measure MAGL activity using the assay kit (Abcam) at around 0.04–0.05 mg per reaction. Different concentrations (0.01, 0.1, 1, 4.4 and 10 μM) of pristimerin and JZL195 were prepared in a solution made up of 50% DMSO and 50% assay buffer. A mixture of assay buffer (60–75 μl), mouse brain or paw skin supernatant (5 or 20 μl, respectively), and solvent or inhibitor (10 μl) at different concentrations was incubated for 30 min at 37°C in a 96 well black microplate. The reaction was initiated by adding 10 μl of MAGL substrate to all the wells being used and the plate incubated at 37°C in the microplate reader (SpectraMax® iD3, Molecular Devices) set at low, 1 OD (optical density) and integration at 140 ms. The plate was shaken for 5 s to mix every time before measuring fluorescence at Ex/Em 360/460 in kinetic mode for 60 min reading every 10 min.

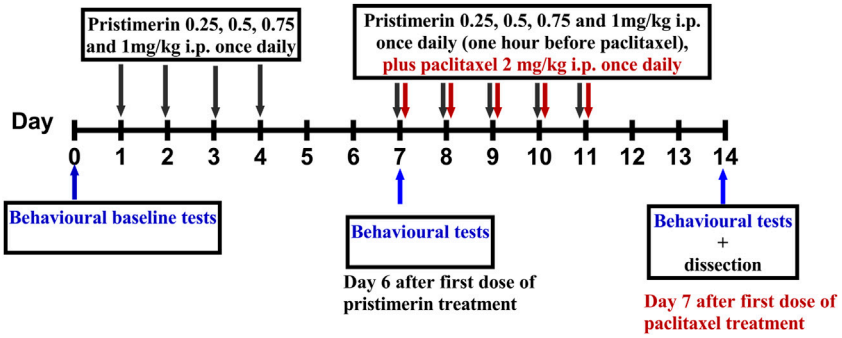

FIGURE 1
Drug administration schedule for treatment with pristimerin against paclitaxel-induced allodynia. The black arrows indicate the days pristimerin was administered, the maroon arrows indicate the days when paclitaxel was administered, while the blue arrows indicate when the behavioral tests were performed.

% MAGL activity was calculated as follows:
FS = Absorbance of well of interest—absorbance of well with vehicle plus kit inhibitor, following the manufacturer's protocol.
% MAGL activity = FS of drug/FS of vehicle*100

Administration of paclitaxel to induce mechanical allodynia

Paclitaxel (Tocris, United Kingdom) was dissolved in a solution made up of 50% Cremophor EL and 50% absolute ethanol to a concentration of 6 mg/ml and stored at − 20°C, for a maximum of 14 days, and diluted in normal saline (NaCl 0.9%), to a final concentration of 0.2 mg/ml just before administration. Paclitaxel 2 mg/kg was injected intraperitoneally (i.p.) in a volume of 10 ml/kg, once daily for 5 consecutive days as previously described (Parvathy and Masocha, 2013). The vehicle for pristimerin that consisted of 1.7% Cremophor EL and 1.7% ethanol in normal saline was injected to control animals. This treatment regimen produces mechanical allodynia in mice (Masocha and Thomas, 2019).

Drug administration

Pristimerin was dissolved in 100% DMSO to a concentration of 10 mg/ml and stored at −20°C and diluted in 2% DMSO in phosphate buffered saline (PBS) to a final concentration just before administration. Pristimerin 0.25, 0.5, 0.75, and 1 mg/kg was injected i.p. in a volume of 10 ml/kg, once daily for 4 consecutive days starting 6 days before the administration of paclitaxel. This was followed by administration of pristimerin 0.25, 0.5, 0.75 and 1 mg/kg for 5 days 1 h before paclitaxel injection (Figure 1). The vehicle for pristimerin that consisted of 3% DMSO in PBS was injected to control animals in the same pattern as pristimerin (Figure 1).

Assessment of mechanical allodynia

Mechanical allodynia was measured using the dynamic plantar aesthesiometer (Ugo Basile, Italy). Briefly, mice were left to habituate for 30–60 min inside plastic enclosures on top of a perforated platform. A microprocessor, which was programmed to automatically lift a metal filament that exerted a linearly increasing force (0.25 g/s with cut-off time of 20 s) on the hind paw, was pressed to start when the mice were settled. A stop signal was automatically attained, either when the animal removed the paw or at the cut-off force of 5 g. Withdrawal thresholds in response to the mechanical stimulus were automatically recorded in grams. The hind paws were tested at least 3 times. The baseline mechanical thresholds were assessed before initiation of treatment with pristimerin and before the induction of the neuropathic pain with paclitaxel.

Assessment of monoacylglycerol lipase activity in mice paw skin

Briefly, paw skin tissues were dissected out after treatment with pristimerin and paclitaxel (see Figure 1) on day 7 after paclitaxel treatment and homogenized, 10 mg of tissue in 100 µl MAGL assay buffer, centrifuged at 10,000 g for 15 min (4°C), and the supernatant was collected, protein concentrations determined by the by BCA assay using BSA as standard, The supernatants were aliquoted and stored at −80°C until the time to measure MAGL activity using the MAGL Activity Fluorometric assay kit (Abcam) at around 0.05 mg per reaction. A mixture of assay buffer (60 µl), paw skin supernatant (20 µl), and solvent or

inhibitor (10 µl) at different concentrations was incubated for 30 min at 37°C in a 96 well black microplate. The reaction was initiated by adding 10 µl of MAGL substrate to all the wells being used and the plate incubated at 37°C in the microplate reader (SpectraMax® iD3, Molecular Devices) set at low, 1 OD (optical density) and integration at 140 ms. The plate was shaken for 5 s to mix every time before measuring fluorescence at Ex/Em 360/460 in kinetic mode for 60 min reading every 10 min.

Relative fluorescence units (360/460 nm) of the MAGL-specific signal per mg of the samples was determined as follows: Firstly, the relative fluorescence units were corrected for weight of samples by dividing it by the amount of samples used in the reaction in mg. Secondly, the corrected relative fluorescence units of the wells with kit inhibitor were subtracted from that of well without inhibitor.

The area under the curve of the relative fluorescence units (360/460 nm) for each sample was calculated from zero to 60 min using GraphPad Prism 9.0.

Real time RT-PCR

Expression of *Nrf2* mRNA was quantified relative to the expression of the house keeping gene *18s* (18S ribosomal RNA) using real time PCR. Total RNA was extracted from fresh frozen paw skins, reverse-transcribed into cDNA and real time PCR performed using QuantStudio™ 7 Flex Real-Time PCR System (Applied Biosystems) as described previously (Masocha, 2009). The primers for Nrf2 and 18s rRNA, were purchased from Sigma-Aldrich. The sequences of the primers used were: *Nrf2* forward, 5′- CAGCATAGAGCAGGACATGGAG-3′ and reverse, 5′-GAACAGCGGTAGTATCAGCCAG-3′; *18s* forward, 5′-CGGCTACCACATCCAAGGAA-3′ and reverse, 5′-GCTGGAATTACCGCGGCT -3′. The threshold cycle (Ct) values for all cDNA samples were obtained and the level of mRNA for each sample were normalized to *18s* (housekeeping gene) ΔCt. The relative expression of the gene of interest was calculated using $-2^{-\Delta\Delta Ct}$ method (Livak and Schmittgen, 2001).

Statistical analyses

Data were tested for normality using the D'Agostino-Pearson normality test and if data passed the normality test parametric tests were used, however, if they failed the normality test non-parametric tests were used. Statistical analyses were performed using Student's *t* test, Mann-Whitney test, one-way analysis of variance (ANOVA) followed by Tukey's multiple comparisons test, Kruskal-Wallis test followed by Dunn's multiple comparisons test, or two-way repeated measures ANOVA followed by Dunnett's or Tukey's multiple comparisons test using GraphPad Prism software (version 9.0). The differences were considered significant at $p < 0.05$. The results in the text and figures are expressed as the Mean ± SEM.

Results

Inhibitory effects of triterpenes on recombinant human monoacylglycerol lipase activity

At 1 µM JZL195 and the triterpenes significantly inhibited the activity of recombinant human MAGL (Figure 2, $p < 0.05$). Two-way repeated ANOVA showed there was a significant effect of treatment with JZL195 [$F(1, 5) = 3094$, $p < 0.0001$], betulinic acid [$F(1, 5) = 15.54$, $p = 0.0109$], cucurbitacin B [$F(1, 5) = 13.49$, $p = 0.0144$] and pristimerin [$F(1, 5) = 243.2$ $p < 0.0001$], but not euphol [$F(1, 6) = 2.805$, $p = 0.1450$], on the activity of recombinant human MAGL compared to vehicle. The magnitude of inhibition (calculated at 10 min of incubation) was JZL195 (82% inhibition) > pristimerin (50% inhibition) > betulinic acid (30% inhibition) ≥ cucurbitacin B (25% inhibition) > euphol (16% inhibition). The inhibition of JZL195 and pristimerin on MAGL activity was maintained from 5 till 60 min, when the experiment was terminated, whereas the other triterpenes lost some activity with time (Figure 2).

JZL195 and pristimerin inhibited human recombinant MAGL activity in a concentration-dependent manner with median inhibitory concentrations (IC50s) of 113.9 and 130 nM, respectively (Figure 3D). Although betulinic acid, cucurbitacin B and euphol inhibited the activity of human recombinant MAGL their effects were not concentration-dependent, and thus could not calculate IC50 values (Figures 3A–C).

Inhibitory effects of triterpenes on mouse brain and paw skin

JZL195 and pristimerin inhibited both mouse brain and paw skin MAGL activity in a concentration-dependent manner with IC_{50}s of 0.869 and 1.6 µM in the brain, respectively and 1.726 and 0.596 µM in the paw skin, respectively (Figure 4).

Effects of pristimerin on the development of paclitaxel-induced mechanical allodynia in mice

Two-way repeated ANOVA showed that treatment of naïve mice with pristimerin 0.25, 0.5, 0.75, and 1 mg/kg i.p. daily for 4 consecutive days did not cause any significant changes to the withdrawal threshold of mice to the dynamic plantar

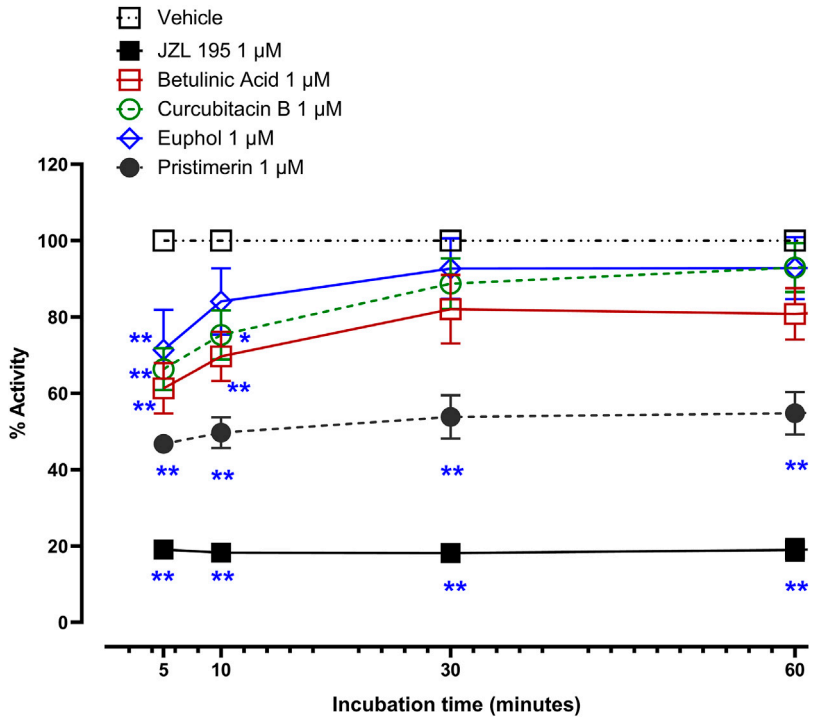

FIGURE 2
Inhibitory effects of 1 μM betulinic acid, cucurbitacin B, euphol, pristimerin and JZL195 on human recombinant MAGL activity over time. Each point represents the mean ± SEM of values obtained from 3 experiments. *$p < 0.05$, **$p < 0.01$ compared to drug vehicle at the same time after treatment (two-way repeated measures ANOVA followed by Dunnett's multiple comparisons test).

aesthesiometer on day 6 compared to pretreatment baseline values or vehicle treatment [Figure 5A, (4, 35) = 1.439, p = 0.2418].

Treatment with paclitaxel significantly reduced the withdrawal threshold of mice to the dynamic plantar aesthesiometer on day 7 compared to pretreatment values, with values of 2.46 ± 0.13 g versus 3.46 ± 0.24 g, respectively [t (16) = 3.691, p = 0.002], whereas vehicle only treated animals had similar values on day 7 compared to pretreatment values 3.68 ± 0.34 g versus 3.89 ± 0.32 g, respectively [t (16) = 0.4543, p = 0.6567]. On the other hand, mice treated with pristimerin 0.75 and 1 mg/kg plus paclitaxel had withdrawal threshold on day 7 similar to the pretreatment values, with values of 3.80 ± 0.20 g and 3.83 ± 0.21 g versus 4.45 ± 0.07 g and 3.55 ± 0.28 g, respectively [Figure 5B, U = 1.5, p = 0.0857, t (14) = 0.7815, p = 0.4475, respectively]. Kruskal-Wallis test showed that coadministration of pristimerin with paclitaxel significantly changed the withdrawal thresholds of mice compared to the paclitaxel plus vehicle group [H (5) = 18.75, p = 0.0009]. Post-hoc analysis showed that the lower doses of pristimerin 0.25 and 0.5 mg/kg did not significantly change withdrawal thresholds compared to paclitaxel plus vehicle-treated mice (Figure 5B, $p >$ 0.05), whereas the higher doses 0.75 and 1 mg/kg were significantly higher than those of the mice treated with paclitaxel plus vehicle (Figure 5B, $p < 0.05$). Treatment with pristimerin produced a dose-dependent protection against the development of paclitaxel-induced mechanical allodynia with an ED_{50} of 0.442 mg/kg (Figure 5B).

Effects of treatment with pristimerin on paclitaxel-induced monoacylglycerol lipase activity in the paw skin

Treatment with paclitaxel significantly increased the MAGL activity in the paw skin compared to vehicle-only-treated control mice (Figures 6A,B, $p < 0.05$). Two-way repeated ANOVA showed there was a significant effect of treatment with paclitaxel [F (1, 4) = 194.6, p = 0.0002] and paclitaxel plus pristimerin [F (1, 4) = 74.61, p = 0.0010] on the activity of MAGL compared to treatment with vehicle. Two-way repeated ANOVA showed there was a significant effect of treatment with pristimerin [F (1, 4) = 8.578, p = 0.0429] on the activity of MAGL from paw skins of mice with paclitaxel-induced allodynia compared to treatment with vehicle. The relative fluorescence units (360/460 nm) of the MAGL-specific signal per mg of the paw skin samples and AUC were higher in paclitaxel-treated mice compared to vehicle-only-treated control mice (Figures

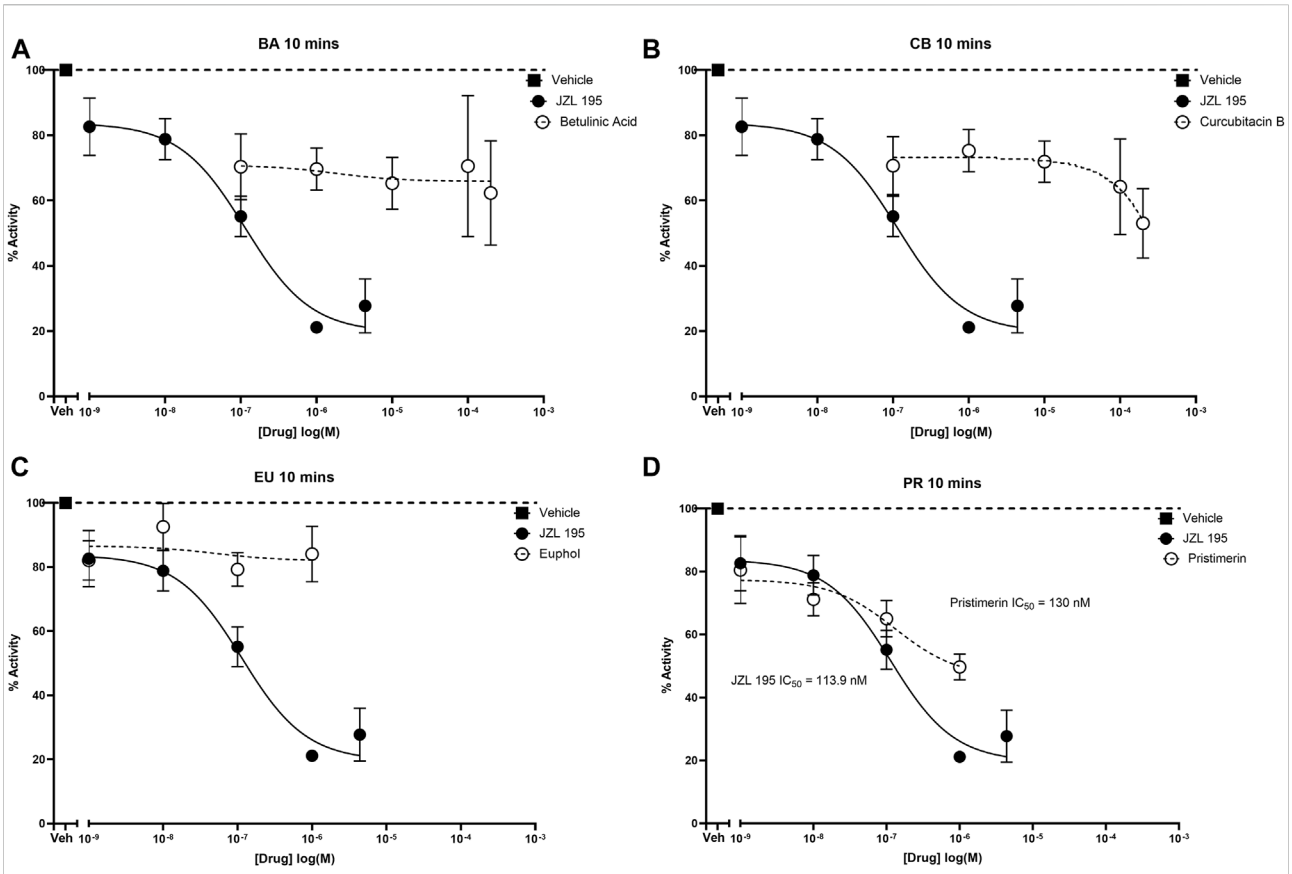

FIGURE 3
Inhibitory effects of various concentrations of betulinic acid, cucurbitacin B, euphol, pristimerin and JZL195 on human recombinant MAGL after 10 min of incubation. Each point represents the mean ± SEM of values obtained from 3 to 5 experiments.

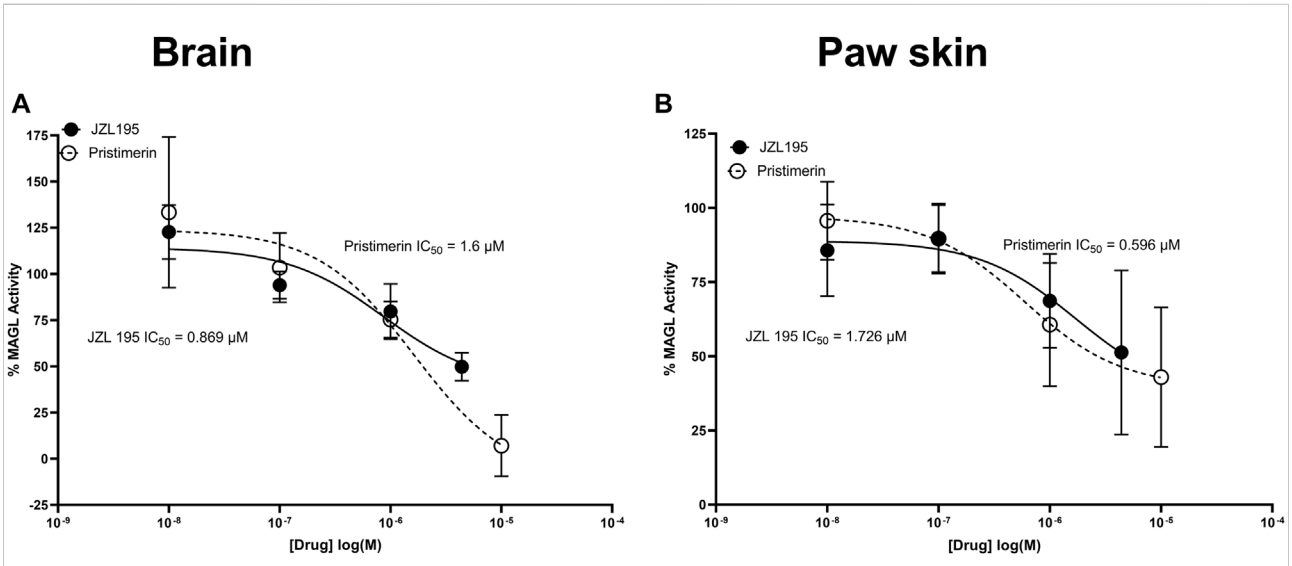

FIGURE 4
Inhibitory effects of various concentrations of pristimerin and JZL195 on mouse **(A)** brain and **(B)** paw skin MAGL after 10 min of incubation. Each point represents the mean ± SEM of values obtained from 3 experiments from samples pooled from 8 animals.

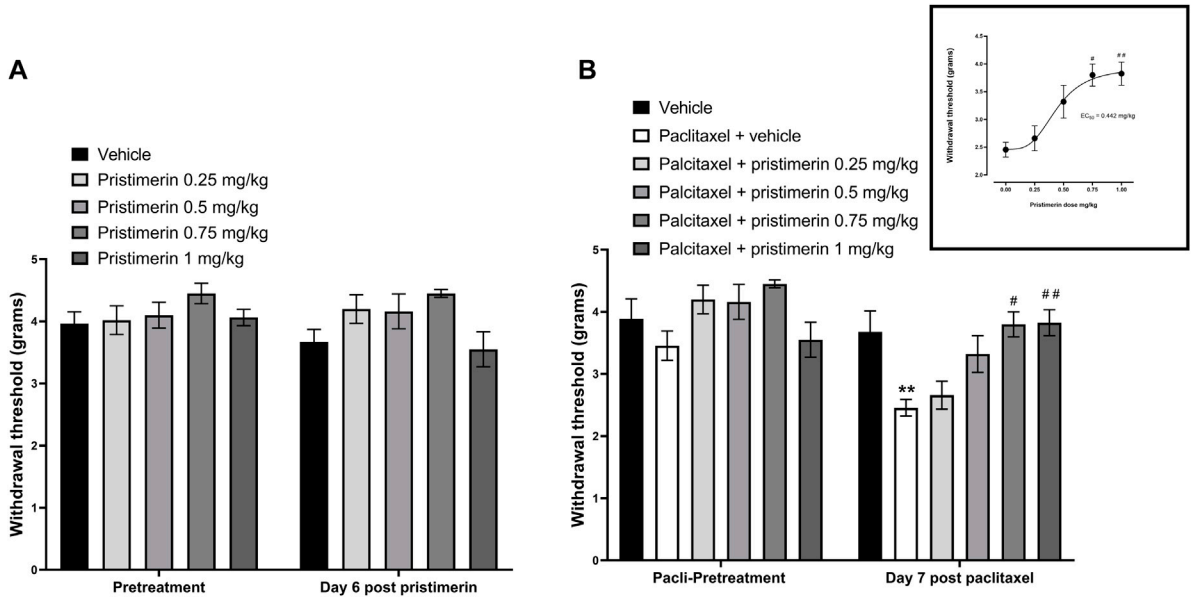

FIGURE 5
Pristimerin prevents the development of paclitaxel-induced mechanical allodynia in female BALB/c mice. **(A)** The effect of treatment of naïve mice with pristimerin on response to mechanical stimuli. Each bar represents the mean ± SEM of values obtained from four to eighteen animals. **(B)** The effect of treatment with pristimerin on the development of paclitaxel-induced mechanical allodynia at day 7 post-first injection (dpi) of paclitaxel. Each bar represents the mean ± SEM of values obtained from four to nine animals. $^{**}p < 0.01$ compared to pretreatment values (Mann-Whitney test), and $\#p < 0.05$, $\#\#p < 0.01$ compared to mice treated with paclitaxel + vehicle (two-way repeated measures ANOVA followed by Tukey's multiple comparisons test and for the insert Kruskal-Wallis test followed by Dunn's multiple comparisons test).

6A,B, $p < 0.05$). The AUC of relative fluorescence units was 1.48×10^{11} for paclitaxel-treated mice versus 3.35×10^{10} for vehicle-treated mice ($p < 0.05$).

One-way ANOVA showed that there were differences between treatment groups [$F(2, 6) = 252.9$, $p < 0.0001$]. Treatment with pristimerin significantly reduced the paclitaxel-induced increase in MAGL activity in the paw skin, i.e., the AUC of the relative fluorescence of the MAGL-specific signal per mg of the paw skin samples of mice treated with paclitaxel plus pristimerin were significantly lower than those of mice treated with paclitaxel plus vehicle (Figure 6B, $p < 0.01$), although still higher than the vehicle-only-treated control mice (Figure 6B, $p < 0.01$). The AUC of relative fluorescence units was 1.12×10^{11} for paclitaxel plus pristimerin-treated mice versus 1.48×10^{11} for paclitaxel plus vehicle-treated mice ($p < 0.05$).

Effects of treatment with pristimerin and paclitaxel on nuclear factor-2 erythroid related factor-2 gene expression in the paw skin

One-way ANOVA showed that there were differences between treatment groups in the *Nrf2* gene expression in the paw skin [$F(2, 13) = 7.741$, $p = 0.0061$]. Post-hoc analysis showed that treatment with paclitaxel did not significantly change the expression of *Nrf2* mRNA in the paw skin (Figure 7, $p > 0.05$). However, there was a trend towards reduction compared to vehicle-only-treated control mice i.e., the relative expression of *Nrf2* mRNA in vehicle-only-treated control mice was 1.066 ± 0.169 while that of paclitaxel-treated mice was 0.761 ± 0.080. Interestingly, coadministration of paclitaxel with pristimerin significantly upregulated the expression of *Nrf2* mRNA compared to vehicle-only-treated control mice and paclitaxel plus vehicle-treated mice (Figure 7, $p < 0.05$).

Discussion

This study shows all the four triterpenes (betulinic acid, cucurbitacin B, euphol and pristimerin) evaluated inhibited human recombinant MAGL activity, but only pristimerin did so in a concentration dependent manner. Pristimerin inhibited MAGL activity in mouse brain and paw skin tissues in a concentration dependent manner. Paclitaxel-induced mechanical allodynia was associated with increased MAGL activity in the paw skin. Treatment with pristimerin prevented the development of paclitaxel-induced mechanical allodynia and

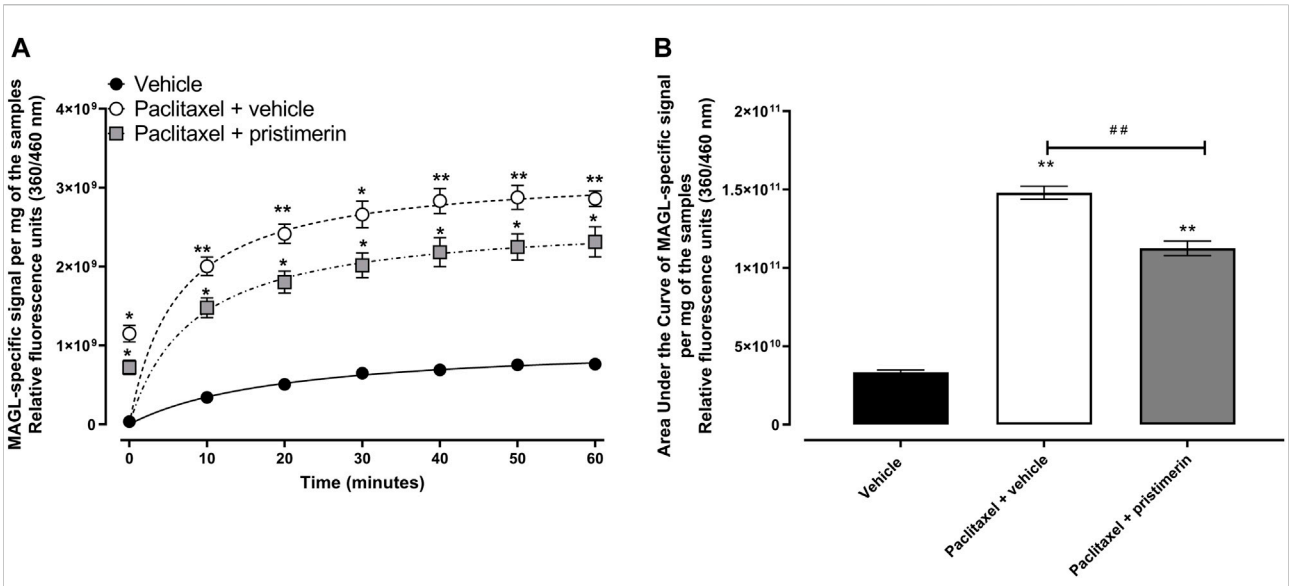

FIGURE 6
Pristimerin prevents the paclitaxel-induced increase in MAGL activity in the paw skin of female BALB/c mice. **(A)** Relative fluorescence units (360/460 nm) over time as a product of MAGL-specific signal per mg of the paw skin samples from vehicle-, paclitaxel plus vehicle- and paclitaxel plus pristimerin-treated mice at day 7 post-first injection (dpi) of paclitaxel. Each symbol represents the mean ± SEM of values obtained from 3 experiments from samples pooled from 4 animals. *$p < 0.05$, **$p < 0.01$ compared to mice treated with vehicle only (two-way repeated measures ANOVA followed by Tukey's multiple comparisons test). **(B)** Area under the curve of relative fluorescence of MAGL-specific signal per mg of the paw skin samples from vehicle-, paclitaxel plus vehicle- and paclitaxel plus pristimerin-treated mice at day 7 dpi of paclitaxel. Each symbol represents the mean ± SEM of values obtained from 3 experiments from samples pooled from 4 animals. **$p < 0.01$ compared to mice treated with vehicle only and ##$p < 0.01$ compared to mice treated with paclitaxel + vehicle (one-way ANOVA followed by Tukey's multiple comparisons test).

reduced the paclitaxel-induced increase in MAGL activity in the paw skin.

The first characterized MAGL inhibitors of plant origin are the triterpenes pristimerin and euphol using purified rat recombinant MAGL, with high IC_{50}s of 93 and 315 nM, respectively (King et al., 2009). In the current study, pristimerin inhibited human recombinant MAGL with IC_{50} of 130 nM, which was comparable to the values obtained by King et al. (2009) utilizing purified rat recombinant MAGL (King et al., 2009) and Chicca et al. utilizing human recombinant MAGL with IC_{50} of 204 nM (Chicca et al., 2012). On the other hand, although euphol inhibited human recombinant MAGL its effects were not concentration dependent and thus could not calculate IC_{50} values. We did not find any studies that evaluated the effects of euphol on human recombinant MAGL activity. Betulinic acid and cucurbitacin B, similar to euphol, inhibited MAGL activity but their effects were not concentration dependent. It was reported that betulinic acid "did not to hit," i.e., did not significantly inhibit, human MAGL although it inhibited human MAGL activity by about 23% at a concentration of 10 μM (Parkkari et al., 2014). In the current study betulinic acid at a concentration of 10 μM significantly inhibited human recombinant MAGL activity by about 35%. We did not find any studies that evaluated the effects of cucurbitacin B on human recombinant MAGL activity, however it effects on human recombinant MAGL was almost similar to that of betulinic acid. The magnitude of human recombinant MAGL inhibition by 1 μM of each of the triterpenes was pristimerin (50% inhibition) > betulinic acid (30% inhibition) ≥ cucurbitacin B (25% inhibition) > euphol (16% inhibition). Since pristimerin had a clear inhibitory effect on human recombinant MAGL, we evaluated its effects on mouse brain and paw skin MAGL activity. Pristimerin inhibited both mouse brain and paw skin MAGL activity in a concentration-dependent manner with IC_{50}s of 1.6 μM in the brain and 0.596 μM in the paw skin, respectively. The differences in the potencies of pristimerin between the human recombinant MAGL and the mouse tissues MAGL could be because of competing reactions, similar to what was described by King et al. (2009) because of the presence of other enzymes that pristimerin might bind to in the tissues.

In a recent study we observed that there was a decrease in the amount of 2-AG in the paw skin of mice with paclitaxel-induced mechanical allodynia (Thomas et al., 2020). However, the protein levels of MAGL, the enzyme that degrades 2-AG, were not significantly altered (Thomas et al., 2020). In the current study we found that mice treated with paclitaxel had increased MAGL activity in the paw skin compared to vehicle-treated animal. Thus, the increased MAGL activity

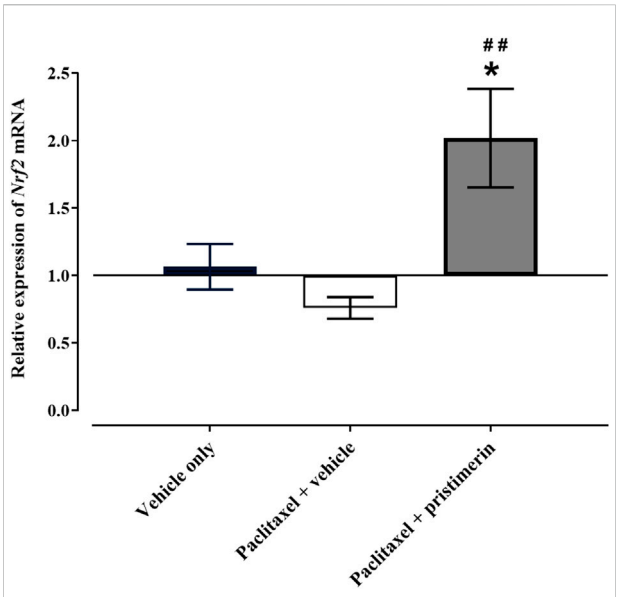

FIGURE 7
Effect of treatment with paclitaxel or paclitaxel + pristimerin on the relative expression of *Nrf2* mRNA in paw skins of female BALB/c mice at day 7 post first paclitaxel dose. Each bar represents the mean ± SEM of values obtained from 5-6 animals. *p < 0.05 compared to control mice (treated with vehicle only) at day 7 and ##p < 0.01 compared to mice treated with paclitaxel + vehicle (one-way ANOVA was followed by Tukey's multiple comparisons test).

most likely resulted in the decreased 2-AG level, which contributed to the paclitaxel-induced mechanical allodynia. Indeed, replacement of 2-AG by local administration of 2-AG or the MAGL inhibitor JZL184 alleviated paclitaxel-induced mechanical allodynia (Thomas et al., 2020). In other studies, systemic administration of MAGL inhibitors JZL184 and MJN110 reversed paclitaxel-induced allodynia (Curry et al., 2018; Slivicki et al., 2018). Thus, it was plausible that pristimerin, a MAGL inhibitor (King et al., 2009) could prevent the development of paclitaxel-induced allodynia. Indeed, treatment with pristimerin prevented the development of paclitaxel-induced allodynia and reduced the paclitaxel-induced increase in MAGL activity. Compared to other MAGL inhibitors such as JZL184 and MJN110, which did not alter the anticancer activities of paclitaxel (Curry et al., 2018), pristimerin might have an advantage because it had an additive effects on paclitaxel's anticancer activities against breast cancer cell lines (Lee et al., 2018). Thus, co-treatment with paclitaxel could have a dual advantage of reducing the dose of paclitaxel, PINP is a dose-dependent side effect, and also directly preventing PINP. This study evaluated the effects of pristimerin only on paclitaxel-induced mechanical allodynia, however, cold sensitivity is a pronounced side effect in CINP patients induced more by the platinum chemotherapeutic agents (Maihofner et al., 2021), thus further studies are needed to evaluate pristimerin effects on chemotherapy-induced cold hypersensitivity.

Oxidative stress and loss of epidermal nerve fibers are some of the major mechanisms involved in the pathogenesis of CINP (Han and Smith, 2013; Burgess et al., 2021). One of the major transcription factors involved in the regulation antioxidant response element–dependent genes is Nrf2 (Raghunath et al., 2018; He et al., 2020). It upregulates the expression of genes of molecules that protects against oxidative stress induced by xenobiotics and other stressors (Raghunath et al., 2018; He et al., 2020). Animals with paclitaxel-induced neuropathy and mechanical hypersensitivity had decreased expression of Nrf2 protein in the dorsal root ganglions (Zhao et al., 2019; Kumar Kalvala et al., 2022), which was reversed by treatment with drugs that have antihyperalgesic activity such as the cannabinoids cannabidiol and tetrahydrocannabivarin (Kumar Kalvala et al., 2022). In the current study, paclitaxel caused a tendency towards a decrease of *Nrf2* mRNA, and coadministration of pristimerin with paclitaxel significantly upregulated *Nrf2* mRNA. This suggests that pristimerin might prevent PINP also through upregulation of Nrf2 and having antioxidant activities. Further studies are warranted to explore whether pristimerin protects against PINP *via* upregulation and restoration of the antioxidant activities in tissues exposed to paclitaxel.

In conclusion the results of this study show that the triterpene pristimerin inhibits human recombinant MAGL activity as well as MAGL activity in mouse brain and paw skin tissues. Paclitaxel-induced mechanical allodynia is associated with increased MAGL activity in the paw skin, which most likely contributed to reduced 2-AG levels reported previously in animals with paclitaxel-induced mechanical allodynia (Thomas et al., 2020). Treatment with pristimerin, a triterpene with MAGL inhibitory activity prevented the development of paclitaxel-induced mechanical allodynia and reduced the paclitaxel-induced increase in MAGL activity, while increasing the expression of Nrf2, which controls antioxidant response element–dependent genes expression to protect against oxidative stress damage. Pristimerin has also been shown to have additive anticancer activity with paclitaxel against breast cancer cell lines (Lee et al., 2018). This could lead to lower doses of paclitaxel being used for treating cancer and thus reduce the occurrence of the dose dependent PINP. Therefore, pristimerin, and possibly other triterpenes, warrants further research as a potential candidate to be used in combination with paclitaxel for treatment of cancer and to prevent the development of PINP.

Data Availability Statement

The raw data supporting the conclusions of this article will be made available by the authors, without undue reservation.

Ethics statement

The animal study was reviewed and approved by the Ethical Committee for the use of Laboratory Animals in Teaching and in Research, Health Science Centre, Kuwait University.

Author contributions

AA-R: designed and performed the experiments, analyzed the data, revised the paper; WM: conceived, designed and performed the experiments, contributed reagents/materials/analysis tools, analyzed the data, wrote the paper. All authors read and approved the final manuscript.

Funding

This work was supported by grant PT01/20 from Kuwait University Research Sector.

Acknowledgments

We are grateful to Ahmad Barakat and Aisha Al-Baloushi for technical assistance with the experiments and to the staff from the Animal Resources Centre, HSC, Kuwait University for their support.

Conflict of interest

The authors declare that the research was conducted in the absence of any commercial or financial relationships that could be construed as a potential conflict of interest.

Publisher's note

References

Bortalanza, L. B., Ferreira, J., Hess, S. C., Delle Monache, F., Yunes, R. A., Calixto, J. B., et al. (2002). Anti-allodynic action of the tormentic acid, a triterpene isolated from plant, against neuropathic and inflammatory persistent pain in mice. *Eur. J. Pharmacol.* 453 (2-3), 203–208. doi:10.1016/s0014-2999(02)02428-7

Burgess, J., Ferdousi, M., Gosal, D., Boon, C., Matsumoto, K., Marshall, A., et al. (2021). Chemotherapy-induced peripheral neuropathy: Epidemiology, pathomechanisms and treatment. *Oncol. Ther.* 9 (2), 385–450. doi:10.1007/s40487-021-00168-y

Byun, J. Y., Kim, M. J., Eum, D. Y., Yoon, C. H., Seo, W. D., Park, K. H., et al. (2009). Reactive oxygen species-dependent activation of Bax and poly(ADP-ribose) polymerase-1 is required for mitochondrial cell death induced by triterpenoid pristimerin in human cervical cancer cells. *Mol. Pharmacol.* 76 (4), 734–744. doi:10.1124/mol.109.056259

Calixto, J. B., Beirith, A., Ferreira, J., Santos, A. R., Filho, V. C., and Yunes, R. A. (2000). Naturally occurring antinociceptive substances from plants. *Phytother. Res.* 14 (6), 401–418. doi:10.1002/1099-1573(200009)14:6<401::aid-ptr762>3.0.co;2-h

Cata, J. P., Weng, H. R., Lee, B. N., Reuben, J. M., and Dougherty, P. M. (2006). Clinical and experimental findings in humans and animals with chemotherapy-induced peripheral neuropathy. *Minerva Anestesiol.* 72 (3), 151–169.

Chicca, A., Marazzi, J., and Gertsch, J. (2012). The antinociceptive triterpene beta-amyrin inhibits 2-arachidonoylglycerol (2-AG) hydrolysis without directly targeting cannabinoid receptors. *Br. J. Pharmacol.* 167 (8), 1596–1608. doi:10.1111/j.1476-5381.2012.02059.x

Curry, Z. A., Wilkerson, J. L., Bagdas, D., Kyte, S. L., Patel, N., Donvito, G., et al. (2018). Monoacylglycerol lipase inhibitors reverse paclitaxel-induced nociceptive behavior and proinflammatory markers in a mouse model of chemotherapy-induced neuropathy. *J. Pharmacol. Exp. Ther.* 366 (1), 169–183. doi:10.1124/jpet.117.245704

Dinh, T. P., Carpenter, D., Leslie, F. M., Freund, T. F., Katona, I., Sensi, S. L., et al. (2002). Brain monoglyceride lipase participating in endocannabinoid inactivation. *Proc. Natl. Acad. Sci. U. S. A.* 99 (16), 10819–10824. doi:10.1073/pnas.152334899

Greenspan, J. D., Craft, R. M., LeResche, L., Arendt-Nielsen, L., Berkley, K. J., Fillingim, R. B., et al. (2007). Studying sex and gender differences in pain and analgesia: A consensus report. *Pain* 132 (1), S26–S45. doi:10.1016/j.pain.2007.10.014

Guindon, J., and Hohmann, A. G. (2009). The endocannabinoid system and pain. *CNS Neurol. Disord. Drug Targets* 8 (6), 403–421. doi:10.2174/187152709789824660

Han, Y., and Smith, M. T. (2013). Pathobiology of cancer chemotherapy-induced peripheral neuropathy (CIPN). *Front. Pharmacol.* 4, 156. doi:10.3389/fphar.2013.00156

Hayashi, D., Shirai, T., Terauchi, R., Tsuchida, S., Mizoshiri, N., Mori, Y., et al. (2020). Pristimerin inhibits the proliferation of HT1080 fibrosarcoma cells by inducing apoptosis. *Oncol. Lett.* 19 (4), 2963–2970. doi:10.3892/ol.2020.11405

He, F., Ru, X., and Wen, T. (2020). NRF2, a transcription factor for stress response and beyond. *Int. J. Mol. Sci.* 21 (13), E4777. doi:10.3390/ijms21134777

Hershman, D. L., Lacchetti, C., Dworkin, R. H., Lavoie Smith, E. M., Bleeker, J., Cavaletti, G., et al. (2014). Prevention and management of chemotherapy-induced peripheral neuropathy in survivors of adult cancers: American society of clinical oncology clinical practice guideline. *J. Clin. Oncol.* 32 (18), 1941–1967. doi:10.1200/JCO.2013.54.0914

Jager, S., Trojan, H., Kopp, T., Laszczyk, M. N., and Scheffler, A. (2009). Pentacyclic triterpene distribution in various plants - rich sources for a new group of multi-potent plant extracts. *Molecules* 14 (6), 2016–2031. doi:10.3390/molecules14062016

King, A. R., Dotsey, E. Y., Lodola, A., Jung, K. M., Ghomian, A., Qiu, Y., et al. (2009). Discovery of potent and reversible monoacylglycerol lipase inhibitors. *Chem. Biol.* 16 (10), 1045–1052. doi:10.1016/j.chembiol.2009.09.012

Kumar Kalvala, A., Bagde, A., Arthur, P., Kumar Surapaneni, S., Ramesh, N., Nathani, A., et al. (2022). Role of cannabidiol and tetrahydrocannabivarin on paclitaxel-induced neuropathic pain in rodents. *Int. Immunopharmacol.* 107, 108693. doi:10.1016/j.intimp.2022.108693

Lee, J. S., Yoon, I. S., Lee, M. S., Cha, E. Y., Thuong, P. T., Diep, T. T., et al. (2013). Anticancer activity of pristimerin in epidermal growth factor receptor 2-positive SKBR3 human breast cancer cells. *Biol. Pharm. Bull.* 36 (2), 316–325. doi:10.1248/bpb.b12-00685

Lee, Y., Na, J., Lee, M. S., Cha, E. Y., Sul, J. Y., Park, J. B., et al. (2018). Combination of pristimerin and paclitaxel additively induces autophagy in human breast cancer cells via ERK1/2 regulation. *Mol. Med. Rep.* 18 (5), 4281–4288. doi:10.3892/mmr.2018.9488

Livak, K. J., and Schmittgen, T. D. (2001). Analysis of relative gene expression data using real-time quantitative PCR and the 2(-Delta Delta C(T)) Method. *Methods* 25 (4), 402–408. doi:10.1006/meth.2001.1262

Maihofner, C., Diel, I., Tesch, H., Quandel, T., and Baron, R. (2021). Chemotherapy-induced peripheral neuropathy (CIPN): Current therapies and

topical treatment option with high-concentration capsaicin. *Support. Care Cancer* 29 (8), 4223–4238. doi:10.1007/s00520-021-06042-x

Masocha, W. (2009). Systemic lipopolysaccharide (LPS)-induced microglial activation results in different temporal reduction of CD200 and CD200 receptor gene expression in the brain. *J. Neuroimmunol.* 214 (1), 78–82. doi:10.1016/j.jneuroim.2009.06.022

Masocha, W., and Thomas, A. (2019). Indomethacin plus minocycline coadministration relieves chemotherapy and antiretroviral drug-induced neuropathic pain in a cannabinoid receptors-dependent manner. *J. Pharmacol. Sci.* 139 (4), 325–332. doi:10.1016/j.jphs.2019.02.007

Munawar, N., Oriowo, M. A., and Masocha, W. (2017). Antihyperalgesic activities of endocannabinoids in a mouse model of antiretroviral-induced neuropathic pain. *Front. Pharmacol.* 8, 136. doi:10.3389/fphar.2017.00136

Parkkari, T., Haavikko, R., Laitinen, T., Navia-Paldanius, D., Rytilahti, R., Vaara, M., et al. (2014). Discovery of triterpenoids as reversible inhibitors of α/β-hydrolase domain containing 12 (ABHD12). *PLoS One* 9 (5), e98286. doi:10.1371/journal.pone.0098286

Parmar, S. K., Sharma, T. P., Airao, V. B., Bhatt, R., Aghara, R., Surekha, C., et al. (2013). Neuropharmacological effects of triterpenoids. *Phytopharmacology* 4 (2), 354–372. http://inforesights.com/phytopharmacology/files/pp4v2i11.pdf.

Parvathy, S. S., and Masocha, W. (2013). Matrix metalloproteinase inhibitor COL-3 prevents the development of paclitaxel-induced hyperalgesia in mice. *Med. Princ. Pract.* 22 (1), 35–41. doi:10.1159/000341710

Polomano, R. C., and Bennett, G. J. (2001). Chemotherapy-evoked painful peripheral neuropathy. *Pain Med.* 2 (1), 8–14. doi:10.1046/j.1526-4637.2001.002001008.x

Raghunath, A., Sundarraj, K., Nagarajan, R., Arfuso, F., Bian, J., Kumar, A. P., et al. (2018). Antioxidant response elements: Discovery, classes, regulation and potential applications. *Redox Biol.* 17, 297–314. doi:10.1016/j.redox.2018.05.002

Rodriguez de Fonseca, F., Del Arco, I., Bermudez-Silva, F. J., Bilbao, A., Cippitelli, A., Navarro, M., et al. (2005). The endocannabinoid system: Physiology and pharmacology. *Alcohol Alcohol* 40 (1), 2–14. doi:10.1093/alcalc/agh110

Saario, S. M., Savinainen, J. R., Laitinen, J. T., Jarvinen, T., and Niemi, R. (2004). Monoglyceride lipase-like enzymatic activity is responsible for hydrolysis of 2-arachidonoylglycerol in rat cerebellar membranes. *Biochem. Pharmacol.* 67 (7), 1381–1387. doi:10.1016/j.bcp.2003.12.003

Slivicki, R. A., Xu, Z., Kulkarni, P. M., Pertwee, R. G., Mackie, K., Thakur, G. A., et al. (2018). Positive allosteric modulation of cannabinoid receptor type 1 suppresses pathological pain without producing tolerance or dependence. *Biol. Psychiatry* 84 (10), 722–733. doi:10.1016/j.biopsych.2017.06.032

Thomas, A., Okine, B. N., Finn, D. P., and Masocha, W. (2020). Peripheral deficiency and antiallodynic effects of 2-arachidonoyl glycerol in a mouse model of paclitaxel-induced neuropathic pain. *Biomed. Pharmacother.* 129, 110456. doi:10.1016/j.biopha.2020.110456

Wolf, S., Barton, D., Kottschade, L., Grothey, A., and Loprinzi, C. (2008). Chemotherapy-induced peripheral neuropathy: Prevention and treatment strategies. *Eur. J. Cancer* 44 (11), 1507–1515. doi:10.1016/j.ejca.2008.04.018

Yang, H., Landis-Piwowar, K. R., Lu, D., Yuan, P., Li, L., Reddy, G. P., et al. (2008). Pristimerin induces apoptosis by targeting the proteasome in prostate cancer cells. *J. Cell. Biochem.* 103 (1), 234–244. doi:10.1002/jcb.21399

Yan, Y. Y., Bai, J. P., Xie, Y., Yu, J. Z., and Ma, C. G. (2013). The triterpenoid pristimerin induces U87 glioma cell apoptosis through reactive oxygen species-mediated mitochondrial dysfunction. *Oncol. Lett.* 5 (1), 242–248. doi:10.3892/ol.2012.982

Zhao, X., Liu, L., Wang, Y., Wang, G., Zhao, Y., Zhang, Y., et al. (2019). Electroacupuncture enhances antioxidative signal pathway and attenuates neuropathic pain induced by chemotherapeutic paclitaxel. *Physiol. Res.* 68 (3), 501–510. doi:10.33549/physiolres.934084

Advantages of publishing in Frontiers

OPEN ACCESS
Articles are free to read for greatest visibility and readership

FAST PUBLICATION
Around 90 days from submission to decision

HIGH QUALITY PEER-REVIEW
Rigorous, collaborative, and constructive peer-review

TRANSPARENT PEER-REVIEW
Editors and reviewers acknowledged by name on published articles

Frontiers
Avenue du Tribunal-Fédéral 34
1005 Lausanne | Switzerland

Visit us: www.frontiersin.org
Contact us: frontiersin.org/about/contact

REPRODUCIBILITY OF RESEARCH
Support open data and methods to enhance research reproducibility

DIGITAL PUBLISHING
Articles designed for optimal readership across devices

FOLLOW US
@frontiersin

IMPACT METRICS
Advanced article metrics track visibility across digital media

EXTENSIVE PROMOTION
Marketing and promotion of impactful research

LOOP RESEARCH NETWORK
Our network increases your article's readership